Investigations of the conserved deubiquitinase Ubp12 in *Saccharomyces cerevisiae* and *Candida albicans* in response to oxidative stress

Katherine Addison

Thesis submitted for Doctor of Philosophy

Newcastle University

Faculty of Medical Sciences

Biosciences Institute

October 2023

Declaration

I certify that this thesis is my own work, except where acknowledged. Work in this thesis has not been previously submitted for another degree or qualification at this or any other university.

Dedication

For OI, you were, are, and will always be, so loved.

Covid-19 Impact Statement

My PhD project progress was considerably affected by the Covid-19 pandemic and subsequent lockdown/isolation periods. My project was a lab-based project, and thus losing 3 months of lab time from the March 2020 lockdown period and then the subsequent half occupancy restrictions adhered to in the following months when lab access was partially restored meant that I lost a substantial amount of time in the lab. Even when every member of the lab could return to work, there were still occupancy restrictions imposed on rooms, which had an impact for example on attempts to learn some new techniques. In addition to this, I had to self-isolate three times during my PhD (twice contracting Covid-19, once for contact with a positive case) essentially losing another month in the lab. I was awarded a 2-month extension by the BBSRC which has helped make up some of this time, however it did not fully compensate for all of the time lost at the bench or the disruption in the continuity of my research.

Abstract

Ubiquitination is a dynamic post-translational modification that regulates many cellular processes. Ubiquitin is attached to proteins using conjugation machinery and removed by deubiquitinases (DUBs), and the coordination of the activities of conjugation/deconjugation proteins determines the effects of ubiquitination on the functions of substrates. Many of the ubiquitin conjugation/deconjugation enzymes utilise catalytic cysteine residues, which renders them potentially susceptible to oxidation by reactive oxygen species (ROS). Low levels of ROS play essential functions in intracellular signalling processes, however high levels of ROS can cause oxidative damage to cellular components. Hence, ROS-induced damage is linked with numerous common age-related diseases. It is therefore essential that cells can recognise the specific ROS present in the cell, and distinguish between low levels and high levels of ROS, in order to elicit an appropriate response. Work from our lab and others revealed that ubiquitin and ubiquitin-like (UBL) conjugation and deconjugation proteins can be regulated by ROS, which consequently influences ubiquitin and UBL regulation of substrates. For example, our lab found that a conserved DUB in the model eukaryote *Saccharomyces cerevisiae,* Ubp12, forms a H_2O_2-specific intramolecular disulphide complex in a H_2O_2 concentration dependent manner. Interestingly, further work showed that the catalytic cysteine residue of Ubp12 is essential for the formation of this complex and that the cytosolic thioredoxin reductase, Trr1, may influence the cellular abundance of Ubp12. To gain insights into the regulation and functions of Ubp12 in *S. cerevisiae* a main aim of this study was to assess whether other cysteine residues present in Ubp12 are involved in the oxidation of the DUB and, moreover, to examine whether the thioredoxin system regulates the formation and/or reduction of the Ubp12 intramolecular disulphide complex. In addition, very little is known about the regulation and functions of the Ubp12 homologue present in the human fungal pathogen *Candida albicans* and hence studies were initiated to investigate the functions and regulation of this uncharacterised DUB. Excitingly, this study is the first to establish a role for the thioredoxin system in the oxidation of ubiquitin/UBL conjugation/deconjugation enzymes. For example, the cytosolic thioredoxins, Trx1 and Trx2, were found to regulate the previously identified Ubp12 disulphide complex, and other previously unidentified modified Ubp12 complexes. In addition, Trr1, Trx1 and Trx2 were shown

to influence the abundance of Ubp12. This study also revealed that specific conserved cysteine residues, in addition to the catalytic cysteine residue, present in homologues of Ubp12 are important in the oxidation of Ubp12 in *S. cerevisiae*. Interestingly, the cysteine residues in conserved CXXC motifs present in Ubp12 are important for oxidation of Ubp12 and raises the possibility, together with the analyses of the effects of other cysteine mutations and mutations of the thioredoxin system components, that disulphide shuffling may occur within Ubp12 in response to H_2O_2. Previous studies from our lab and others revealed that different H_2O_2 signalling pathways regulate H_2O_2 responses in two different strain backgrounds of *S. cerevisiae*. The results presented here revealed that, although Ubp12 is important for ROS responses in both of these strain backgrounds, Ubp12 may also have different functions and be regulated differently in each strain. Finally, studies to investigate the regulation and functions of the Ubp12 homologue in *C. albicans*, revealed that, like Ubp12 in *S. cerevisiae*, Ubp12 in *C. albicans* is important for oxidative stress responses. Moreover, oxidative stress induces the formation of an oxidised Ubp12 complex(es) which appeared similar in mobility to the oxidised Ubp12 complex observed in *S. cerevisiae*. However, interestingly, loss of Ubp12 had different effects on the sensitivity of *C. albicans* and *S. cerevisiae* cells to oxidative stress suggesting different functions for the DUB in each yeast. Thus, Ubp12 is important in oxidative stress responses in both *S. cerevisiae* and *C. albicans*, but specific roles and regulation appear to be different. Consistent with these observations, cells lacking Ubp12 displayed significantly reduced levels of HMW ubiquitinated proteins in *C. albicans* but not *S. cerevisiae*, and Ubp12 was found to be important for cell responses to DNA damage and DNA replication stress in *C. albicans* which but not in *S. cerevisiae*. Finally, this work also suggested that Ubp12 may have roles in morphological changes of *C. albicans* cells in response to environmental signals including H_2O_2. Given the potential roles of Ubp12 in processes linked to pathogenicity in *C. albicans* it is possible that Ubp12 is important for virulence. Collectively, this thesis provides new insights into the functions and regulation of Ubp12 in *S. cerevisiae* and in *C. albicans*. Dysregulation of the human homologue of Ubp12, USP15, is linked to several diseases and hence these studies may further understanding of the normal functions of USP15 an important step in the development of drug treatments for the benefit of human health.

Acknowledgements

I would firstly like to thank my supervisor, Professor Brian Morgan. His continuous advice, support and enthusiasm has been invaluable during this project, and has kept me motivated and focused during even the toughest moments. I would also like to thank the BBSRC for funding this research project.

Secondly, I would also like to thank Professor Janet Quinn, Dr Simon Whitehall, Dr Elizabeth Veal and Dr Julian Rutherford for their advice and suggestions during this project, and Professor Zofia Chrzanowska-Lightowlers and Dr Viktor Korolchuk for their expertise and guidance during my annual review meetings.

I would also like to thank past and current members of the yeast lab (Faye, Clement, Grace, Yasmin, Callum, Katharina, Alison, Martin, Ashleigh, Zoe, Elise, Min, Suki, Maisie, Emilia, Raphaela, Olga, Chloe and Tom) for helpful scientific conversation, but maybe more so, for making the 4 years so fun and enjoyable. I've been very lucky to work within a team of such great people, and can safely say we found a reason every day to laugh. A big thank you goes to BAM lab members Grace, my 'lab big sister', and Suki, my 'lab little sister' – your help and friendship is massively appreciated. A special thanks also goes to members of the Quinn lab, for their suggestions and experimental advice when working with *C. albicans*.

I would also like to thank my friends outside of the lab for their encouragement, and for making time outside of the lab so much fun. A special thanks goes to Eilidh, for technical help using Pymol, but more so for making my time in Newcastle so enjoyable and each evening after work so positive and happy.

Finally, I would also like to thank my parents, siblings and grandparents for all of their love and support. Mam, Dad, Rich and Alex, you have been a constant source of encouragement, during this PhD project and always, and I appreciate that a lot.

Table of Contents

List of abbreviations

•OH	Hydroxyl radical
ATP	Adenosine triphosphate
BCA	Bicinchoninic acid
bp	Base pair
BSA	Bovine serum albumin
BSO	Buthionine sulphoximine
C. albicans	*Candida albicans*
CDK	Cyclin dependent kinase
CGD	Chronic granulomatous disease
COPI	Coat protein complex I
COPII	Coat protein complex II
CRL	Cullin-RING ligases
CSN	COP9/signalosome
DAMP	Damage-associated molecular pattern
DDR	DNA damage response
DIC	Differential interference contrast
DNA	Deoxyribonucleic acid
DTT	Dithiothreitol
DUB	Deubiquitinase
E. coli	*Escherichia coli*
EDTA	Ethylenediaminetetraacetic acid
EGF	Epidermal growth factor
ER	Endoplasmic Reticulum
ERAD	Endoplasmic-reticulum-associated protein degradation
Glr	Glutathione reductase
Gpx	Glutathione peroxidases
Grx	Glutaredoxins
GSH	Reduced glutathione

GSSG	Oxidised glutathione
H_2O_2	Hydrogen peroxide
HECT	Homologous to the E6AP carboxyl terminus
HMW	High molecular weight
HRP	Horseradish Peroxidase
HU	Hydroxyurea
H. sapiens	*Homo sapiens*
IR	Infrared
JAMM	JAB1/MPN/Mov34 metalloenzyme
kDa	Kilodalton
MINDY	Motif interacting with Ub-containing novel DUB family
MMP	Matrix metalloprotease
MOM	Mitochondrial outer membrane
MW	Molecular weight
NADPH	Nicotinamide adenine dinucleotide phosphate
NEM	N-Ethylmaleimide
NF-kB	Nuclear factor kappa light chain enhancer of activated B cells
nH_2O	Nano H_2O
NLR	Nod-like receptor
NOX2	NADPH-dependent phagocytic oxidase
$\bullet O_2^-$	Superoxide
OD	Optical density
OTU	Ovarian tumour-related
PAMP	Pathogen-associated molecular patterns
PBS	Phosphate-buffered saline
PCNA	Proliferating cell nuclear antigen
PCR	Polymerase chain reaction
PDGF	Platelet derived growth factor
PEG	Polyethylene glycol
PHGpx	Phospholipid hydroperoxide Gpx

Prx	Peroxiredoxins
PTM	Post translational modification
RBR	Ring-between-Ring
RING	Really interesting new gene
RNA	Ribonucleic acid
ROS	Reactive oxygen species
Rpm	Revolutions per minute
RT-QPCR	Reverse transcriptase quantitative polymerase chain reaction
RTK	Receptor tyrosine kinase
SAGA	Spt-Ada-Gcn5 acetyltransferase
SCF	Skp, Cullin, F-box containing complex
S. cerevisiae	*Saccharomyces cerevisiae*
S. pombe	*Schizosaccharomyces pombe*
SD	Synthetic dextrose
SDS	Sodium dodecyl sulphate
SOD	Superoxide dismutase
STING	Stimulator of Interferon Genes
SUMO	Small Ubiquitin-like modifier
TBS	Tris-buffered saline
TBST	Tris-buffered saline tween
TCA	Trichloroacetic acid
TE	Tris EDTA
TGN	Trans-Golgi network
Tpx	Thioredoxin peroxidases
Trr	Thioredoxin reductase
Trx	Thioredoxins
Ub	Ubiquitin
UBD	Ubiquitin binding domain
UBL	Ubiquitin-like
UCH	Ubiquitin carboxy-terminal hydrolases

USP	Ubiquitin specific protease
UV	Ultra violet
WT	Wild Type
YAP	Yeast activator protein
YPD	Yeast extract peptone dextrose
YRE	Yap response element
ZnF	Zinc finger

List of Figures

List of Tables

Chapter One: Introduction

1.1 The ubiquitin system

1.1.1 Ubiquitin

Ubiquitin is a small, 76 amino acid (8.6 kDa) protein found ubiquitously in eukaryotic organisms and is a common post-translational modification (PTM) (Goldstein et al., 1975). Lysine residues are the primary target of ubiquitination within substrate proteins, although it is important to note that non-canonical ubiquitination on other amino acids residues does occur, such as serine, threonine and cysteine ubiquitination (McDowell and Philpott, 2013). Upon first identification ~forty years ago, it was hypothesised that ubiquitin's only function was to target proteins for proteasomal degradation (Pickart, 2004). However, further work has elucidated a wide variety of functions for ubiquitin in signal transduction mechanisms. Ubiquitin is covalently attached to target proteins and fulfils a range of functions such as altering cell signalling pathways, modulating protein-protein interactions and regulating protein localisation (Yau and Rape, 2016). Via these mechanisms, ubiquitination regulates various cellular processes such as protein degradation, DNA repair, the immune response and the cell cycle (Sun and Chen, 2004, Thrower et al., 2000, Suresh et al., 2016). In the model yeast *Saccharomyces cerevisiae*, ubiquitin is expressed by four genes, *UBI1, UBI2, UBI3* and *UBI4* (Jentsch and Pyrowolakis, 2000). *UBI1*, *UBI2* and *UBI3* encode a single ubiquitin protein fused to unrelated sequences whereas *UBI4* encodes five ubiquitin proteins, generating a poly-ubiquitin precursor (Finley et al., 1987). It is estimated that thousands of proteins are able to be ubiquitinated within the cell, and hence it is probable that most proteins will become ubiquitinated at some point (Kim et al., 2011).

1.1.2 Ubiquitin-like modifications (UBLs)

UBLs, named due to their similarities in sequence to ubiquitin, are a class of proteins added as post-translational modifications to target proteins. Perhaps the two most characterised UBLs, SUMO and Nedd, are encoded for by the genes *SMT3* and *RUB1* in *S. cerevisiae* respectively (Hochstrasser, 2009a). Smt3 and Rub1 proteins contain 18% and 55% amino acid sequence identity respectively with ubiquitin (Hochstrasser,

2009b). Other UBLs in *S. cerevisiae* include Urm1, Atg8 and Atg12, encoded by the *URM1, ATG8* and *ATG12* genes, respectively (Jentsch and Pyrowolakis, 2000). These UBLs are well conserved across eukaryotes, and additional UBL modifications have been identified that are not present in *S. cerevisiae* (Cajee et al., 2012). UBLs have a plethora of functions and influence many cellular processes, for example, sumoylation regulates chromatin remodelling, nuclear import and export, DNA repair and ribosome biogenesis (Gareau and Lima, 2010, Wilkinson and Henley, 2010). Members of the UBL family are characterised by the presence of a β-grasp fold (also present in ubiquitin, shown in Figure 1.1), and although they display variation in primary sequence, the tertiary structures of ubiquitin and UBLs are strikingly similar (Hochstrasser, 2000).

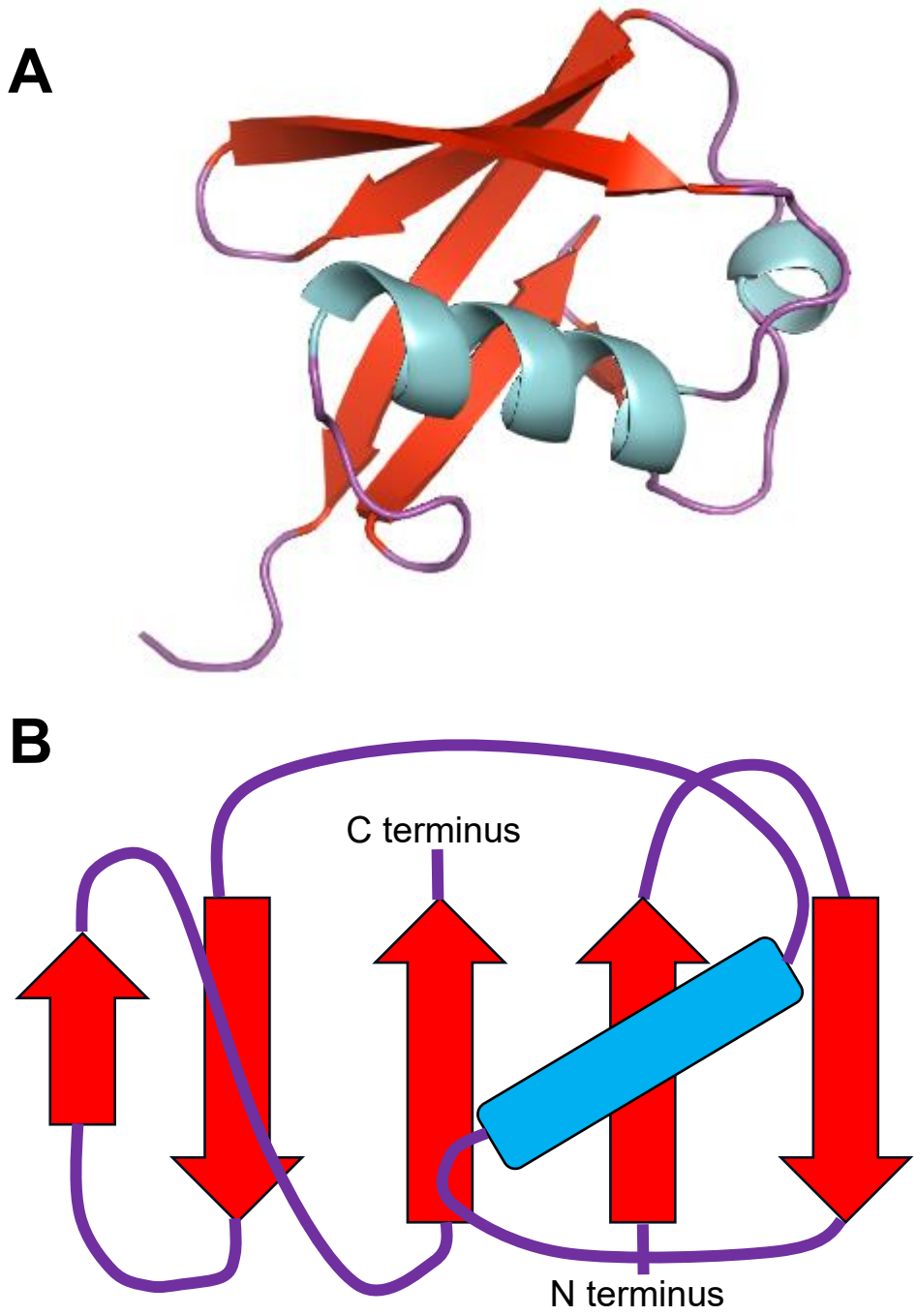

Figure 1.1. The β-grasp fold of ubiquitin.

β-sheets are denoted in red, α-helices in blue and loops in purple. The β- grasp fold of ubiquitin and UBLs consists of 4 core β-sheets 'cradling' a core α-helix. An additional β-sheet is present (short β-sheet in (B)) in ubiquitin and UBL β-grasp folds. (A) Cartoon ribbon representation of the β-grasp fold of ubiquitin created using PyMOL Molecular Graphics System (Schrödinger, 2015). (B) Diagram showing the topology of the β-grasp fold of ubiquitin (Burroughs et al., 2007).

1.1.3 Ubiquitin and UBL conjugation

The addition of ubiquitin and UBL moieties to substrates is a dynamic process whereby ubiquitin/UBL can be either attached or removed from the substrate. Interestingly, ubiquitin and most UBLs are conjugated to target proteins via very similar mechanisms which utilise an E1/E2/E3 enzyme cascade (Figure 1.2; (Streich and Lima, 2014)). The only exception in *S. cerevisiae* is the conjugation of Urm1, which is conjugated in an E2/E3 independent manner (Ravichandran et al., 2022). Ubiquitin/UBLs can also be removed from substrates by enzymes; for example, ubiquitin is removed by deubiquitinase enzymes (DUBs) and SUMO is removed by SENPs (Finley et al., 2012, Nayak and Müller, 2014). For reviews on conjugation/deconjugation and functions of other UBLs not specifically discussed below, see (Cajee et al., 2012, Hochstrasser, 2009b).

Before conjugation to substrates, ubiquitin and most UBLs are synthesised as inactive pre-cursors that require processing in order to expose the C-terminal glycine carboxylate (the residue that is conjugated to target proteins) (Kerscher et al., 2006). Three of the four genes encoding ubiquitin in *S. cerevisiae* (*UBI1, UBI2* and *UBI3*) produce ubiquitin with an additional unrelated tail peptide, however *UBI4* encodes poly-ubiquitin, where five ubiquitin moieties are expressed as one polypeptide (Ozkaynak et al., 1987). All of the ubiquitin precursors require processing, either by removal of the tail peptide or by separation of ubiquitin moieties, to allow for ubiquitin activation. The proteolytic processing of ubiquitin/UBLs before conjugation can proceed is performed by DUBs in the case of ubiquitin and other UBL-specific proteases (Kerscher et al., 2006).

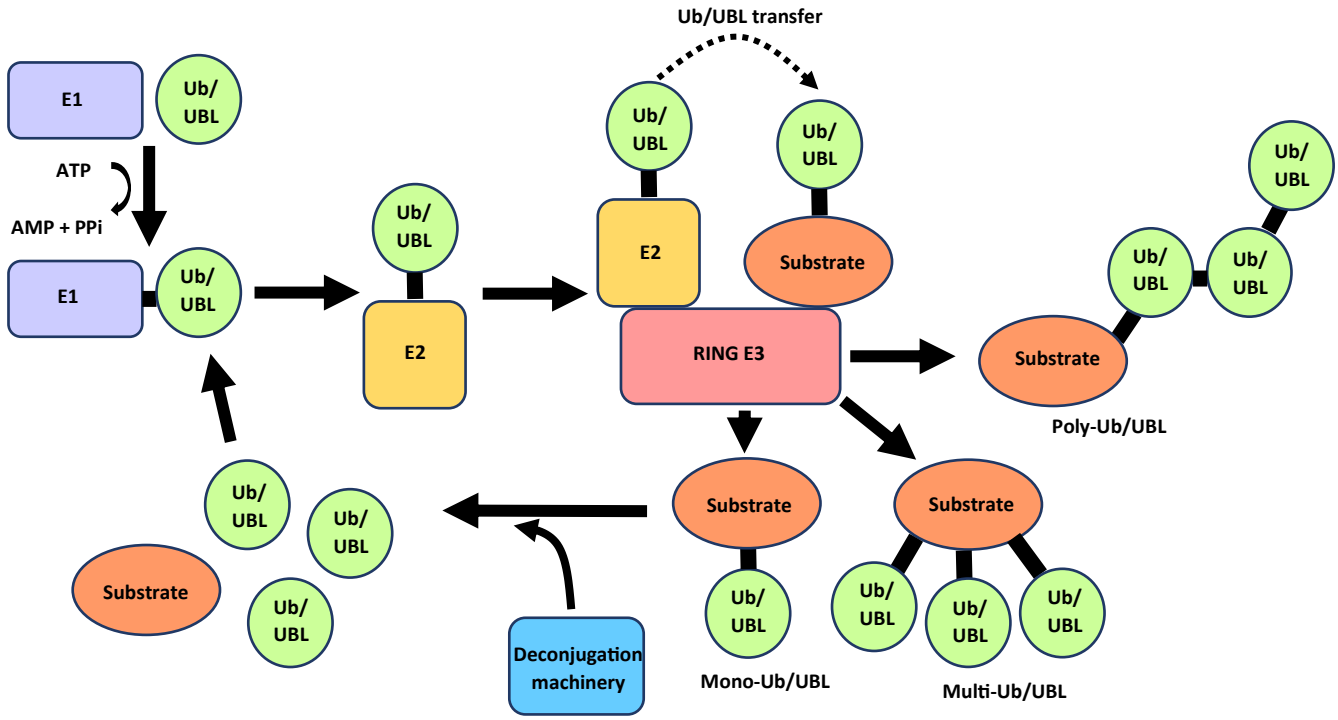

Figure 1.2. The ubiquitin (Ub)/ubiquitin-like (UBL) conjugation/deconjugation cycle.

The E1 activating enzyme binds the ubiquitin (Ub)/UBL through a thiol-esterification reaction hydrolysing ATP, allowing nucleophilic attack of the C terminus of Ub/UBL. The E2 conjugating enzyme then binds the activated Ub/UBL, before interacting with a specific E3 ligase which attaches the Ub/UBL to the target substrate (Pickart, 2001). In this diagram, the E3 ligase mechanism shown is that of a RING E3 ligase. Target proteins can be modified with one Ub/UBL (mono-ub/UBL), numerous, single Ub/UBLs (multi-Ub/UBL) or numerous, branched Ub/UBLs (poly-Ub/UBL). Substrates can also be deconjugated by the deconjugation machinery. All conjugation and deconjugation machinery proteins in the ubiquitination pathway utilise a catalytic cysteine except for the RING E3 ligases, which never actually interact with the ubiquitin, and the JAMM family of DUBs, which are metalloproteases. Adapted from (Rudnicka and Yamauchi, 2016).

The first step in the conjugation of ubiquitin or UBLs to substrates is activation, utilising an E1 ubiquitin/UBL activating enzyme (Haas et al., 1982). Firstly, E1 enzymes function to activate ubiquitin/UBLs via adenylation at the C-terminus in an ATP-dependent reaction (Huang et al., 2004, Ciechanover et al., 1981). This ubiquitin/UBL-AMP forms a thioester linkage with the catalytic cysteine of the E1 enzyme, allowing the E1 enzyme to bind and adenylate a second ubiquitin moiety. The E1 is then bound to two ubiquitin/UBL moieties, one at the T (thioester) site, and one at the A (adenylation) site (Haas and Rose, 1982, Haas et al., 1982). The E1 enzyme then

physically interacts with the E2-conjugating enzyme, transferring the UBL to the catalytic cysteine of the E2 via a thioester transfer reaction (discussed later) (Hershko et al., 1983, Haas et al., 1982). The double loading of ubiquitin/UBLs allows for an accelerated transfer of the UBL(T) monomer to the E2-conjugating enzyme, whilst also causing the general activation reaction to be conformationally and energetically favourable (Pickart et al., 1994, Schulman and Harper, 2009). *S. cerevisiae* cells express only one ubiquitin-specific E1-activating enzyme, Uba1 (encoded by the essential *UBA1* gene), whilst humans express two ubiquitin E1 enzymes, UBA1 and UBA6 (Schulman and Harper, 2009).

Once the ubiquitin/UBL monomer has been transferred to the E2-conjugating enzyme from the E1-activating enzyme, the ubiquitin/UBL monomers can be covalently attached to the target proteins by utilising E3 ligase enzymes. The E2 enzymes interact selectively with E1 activating enzymes and E3 ligases, and consequently dictate the direction of the conjugation reaction (Finley et al., 2012). E1 enzymes display specificity towards E2 enzymes unbound to ubiquitin/UBL substrates whereas E3 ligases preferentially bind to ubiquitin/UBL loaded E2 enzymes (Finley et al., 2012). Thus, E2 enzymes provide a critical step to ensure that ubiquitin/UBL cycling progresses unidirectionally. *S. cerevisiae* cells express eleven ubiquitin-specific E2-conjugating enzymes, all with distinct functions, which allows for substrate specificity in the modification reaction (Finley et al., 2012). Interestingly, of the ubiquitin E2 enzymes in *S. cerevisiae* only Cdc34 is essential, with functions in the regulation of the cell cycle and histone functions (Schwob et al., 1994, Finley et al., 2012). Interestingly, the SUMO-specific E2 enzyme Ubc9 and the Rub1-specific E2 enzyme Ubc12 were both initially classified as ubiquitin E2 enzymes, which highlights the similarities in structure between these enzymes.

E3 ligases catalyse the final step of ubiquitin/UBL conjugation, resulting in an isopeptide linkage from the C-terminus of the ubiquitin/UBL onto the ε-amino group of the target lysine residue within the substrate (Kerscher et al., 2006). There are three main classes of E3 ligases which function via different mechanisms in the ubiquitin family; RING (Really Interesting New Gene) ligases, HECT (Homologous to the E6-AP Carboxyl Terminus) ligases and RBR (Ring between Ring) ligases (Buetow and Huang, 2016). Some UBLs utilise non-canonical E3 ligases, such as Atg5, and no E3 ligases have been identified for the conjugation of Atg12, for more information on these

modifications see (Cappadocia and Lima, 2018). RING ligases are the most common and function by directly transferring the ubiquitin/UBL moiety from the E2 to the substrate. Both the E2-ubiquitin/UBL and the substrate for modification are bound to the E3 ligase simultaneously, allowing for nucleophilic attack of the E2-ubiquitn/UBL thioester bond by the target lysine residue (Ozkan et al., 2005). HECT-domain ligases function by transiently binding ubiquitin/UBL via the catalytic cysteine residue located in the HECT domain, before transferring it to the substrate (Metzger et al., 2012). HECT ligases have two distinct lobes, one containing the binding site for the E2 enzyme and one containing the catalytic cysteine residue of the E3 ligase. As a result, conformational change of approximately 50 Å is necessary to allow ubiquitin/UBL transfer to the catalytic cysteine residue of the E3 ligase (Ogunjimi et al., 2005). Thus, mutations in the region necessary for this conformational change notably decreases the catalytic activity of these enzymes (Verdecia et al., 2003). RBR ligases function somewhat as a hybrid of RING and HECT ligases, containing two RING domains joined by an In Between Rings (IBR) domain but also transiently bind the ubiquitin/UBL protein (Wenzel et al., 2011). In *S. cerevisiae* there are 5 ubiquitin-specific HECT-domain ligases and 40 ubiquitin-specific RING ligases (including RBR ligases) identified, making it the biggest group of proteins of the ubiquitination machinery (Finley et al., 2012).

In the case of ubiquitination, ubiquitin is typically attached to the lysine residue on the substrate protein by the C-terminal glycine residue of ubiquitin. However, there is evidence that non-canonical ubiquitination can occur on other amino acids in the substrate, such as serine, threonine or cysteine residues, or at the N-terminus of the substrate protein (Wang et al., 2007, Bloom et al., 2003, Cadwell and Coscoy, 2005). There are three main types of ubiquitination that occurs on substrates; mono-ubiquitination where one ubiquitin is added to the substrate, multi-ubiquitination where multiple ubiquitin moieties are added singly to the substrate, or poly-ubiquitination whereby chains of ubiquitin are covalently attached to the substrate (discussed in detail in section 1.1.4) (Swatek and Komander, 2016).

In the ubiquitin conjugation machinery, organisms tend to have very few E1 enzymes (*S. cerevisiae* 1, humans 2), more E2 enzymes (*S. cerevisiae* 11, humans ~40) and many E3 enzymes (*S. cerevisiae* 45, humans 500 - 1000) (Lee et al., 2008, Groettrup et al., 2008, Stewart et al., 2016, Nakayama and Nakayama, 2006, Finley et al., 2012).

In contrast, the SUMO conjugation pathway is more limited in the number of enzymes (2 E1 enzyme, 1 E2 enzyme, 4 E3 enzymes in *S. cerevisiae*). However similar to the ubiquitin conjugation machinery there are more E3 enzymes than E1 and E2 enzymes (Novatchkova et al., 2012). The specificity of substrate targeting is dictated by the specific enzymes that function in a particular E1, E2, E3 pathway. Therefore, the specific E1/E2/E3 enzyme cascade used to attach ubiquitin/UBL determines a highly orchestrated and specific ubiquitination/UBL signal.

In *S. cerevisiae*, SUMO is encoded by the *SMT3* gene while in human cells, SUMO is encoded by four genes, *SUMO1, SUMO2, SUMO3* and *SUMO4* (van der Veen and Ploegh, 2012). In *S. cerevisiae*, the conjugation of SUMO is achieved using an E1 activating enzyme, Aos1 or Uba2, one E2 conjugating enzyme Ubc9, and four E3 ligase enzymes Siz1, Siz2, Mms21 and Zip3 (Novatchkova et al., 2012). SUMO, like ubiquitin, requires pre-processing, utilising the desumoylase Ulp1 which cleaves the C-terminal amino acids and reveals a di-glycine motif (Li and Hochstrasser, 1999). Once activated, SUMO then binds to and is adenylated by an E1 activating enzyme (hence like ubiquitin, this is also an ATP-dependent reaction), forming a thioester bond with the catalytic cysteine residue located of the E1 enzyme. SUMO is then transferred onto the E2 conjugating enzyme, Ubc9, forming a thioester bond with the catalytic cysteine residue, before covalent attachment to a lysine residue in the target substrate by utilising one of the E3 ligase enzymes (Cajee et al., 2012). This process is remarkably similar to the ubiquitin conjugation pathway (Figure 1.2). Indeed, analysis of the crystal structures of the ubiquitin and SUMO E1 activating enzymes suggests that the enzymes function by very similar mechanisms (Lois and Lima, 2005).

Despite the striking similarities between ubiquitin and SUMO conjugation, there are also some notable differences. Interestingly, Ubc9, the sole SUMO E2 enzyme, is able to sumoylate target substrates without the aid of an E3 ligase, a phenomenon that is not observed with ubiquitination (Bernier-Villamor et al., 2002). The affinity of Ubc9 for target proteins may be increased by post-translational modifications. For example, the N-terminal sumoylation of Ubc9 results in an increased affinity for its substrate, Sp100 (Knipscheer et al., 2008). In *S. cerevisiae*, there are 45 E3 ubiquitin ligase enzymes, however for SUMO conjugation, there are only 4 E3 ligases. E3 ligases are primarily responsible for sumoylation of specific substrates, however the small number of these proteins raises the possibility that there may be some functional overlap in sumoylation

conjugation. Interestingly, analysis of global sumoylation in the double *siz1*Δ*siz2*Δ mutant of *S. cerevisiae* revealed that over 90% of sumoylation in the cell is dependent on these two enzymes, with apparently little specificity for the substrate proteins (Reindle et al., 2006). Ultimately, the conjugation of ubiquitin and SUMO to substrates are very similar, highly conserved processes, but do have some notable differences in the mechanisms for ubiquitination versus sumoylation.

1.1.4 Types of ubiquitin conjugation

As mentioned in Section 1.1.3, there are three main forms of ubiquitination; mono-ubiquitination, multi-ubiquitination and poly-ubiquitination (Figure 1.2). The type of ubiquitination and the ubiquitination pattern on a target protein can be very varied, impacting in many different ways on the fate of the substrate. Thus, the functionality of ubiquitination is very wide and depends on both the site(s) of modification on the target protein and the type of ubiquitination events.

1.1.4.1 Monoubiquitination and multiubiquitination

Monoubiquitination is the simplest form of ubiquitination, where one lysine of the target protein is ubiquitinated by one copy of ubiquitin. Monoubiquitination has a variety of functions and this is discussed in Section 1.1.5.1. Given the many different forms of ubiquitination it is interesting to note that proteomic analysis has suggested that there are higher levels of monoubiquitination within the cell than polyubiquitination (Kaiser et al., 2011).

Multiubiquitination is a form of monoubiquitination where numerous, single ubiquitin monomers are attached to multiple lysine residues in target proteins. Of the different forms of ubiquitination, perhaps due its complexity involving multiple sites on proteins, there is still much to learn regarding the functions of this form of ubiquitination. The structure and function of protein monoubiquitination and multiubiquitination, and examples of cellular processes that are influenced by these modifications, are shown in Figure 1.3.

1.1.4.2 Polyubiquitination

Poly-ubiquitination occurs as ubiquitin itself can become ubiquitinated on one of seven lysine residues present in the ubiquitin protein (K6, K11, K27, K29, K33, K48, K63) or at the N-terminal methionine of ubiquitin (Komander and Rape, 2012). This allows the synthesis of different structural forms of polyubiquitin chains which provides alternative functions for this protein modification. The different polyubiquitin structures, and examples of cellular processes that are influenced by these different polyubiquitin chains, are shown in Figure 1.3. Polyubiquitin chains can be homotypic, whereby the same ubiquitin lysine linkage, such as K48, is used throughout the whole chain, or heterotypic where the ubiquitin lysine linkages differ throughout the chain, forming either linear or branched chains, where one ubiquitin monomer can be ubiquitinated twice (Akutsu et al., 2016, Kulathu and Komander, 2012). They can also accommodate different physical shapes and conformations, such as the linear K63 polyubiquitin chains with minimal contact between monomers, and the globular K48 polyubiquitin chains which have high levels of interaction between each ubiquitin monomer (Eddins et al., 2007, Komander et al., 2009). At each stage of the process of constructing a polyubiquitin chain, there are various lysine residues available for modification on the previous ubiquitin monomer, hence cells also need to regulate which lysine residue becomes ubiquitinated. This regulation requires interaction between the E2 conjugating enzyme, the E3 ligase and the ubiquitin monomer itself, which dictate a specific orientation of the three proteins, only allowing ubiquitination of one target lysine residue (Li and Ye, 2008). Interestingly, some E2 enzymes, such as Ubc7 in *S. cerevisiae*, have been shown to conjugate polyubiquitin chains *en bloc*, i.e., adding a polyubiquitin chain rather than ubiquitin monomers sequentially (Finley et al., 2012). Thus, polyubiquitination is a complex and varied post-translational modification that requires specific regulation to form the different polyubiquitin chains. It is the type of chain and the linkages present within the chain that coordinate the fate and regulation of the substrate (see Section 1.1.5).

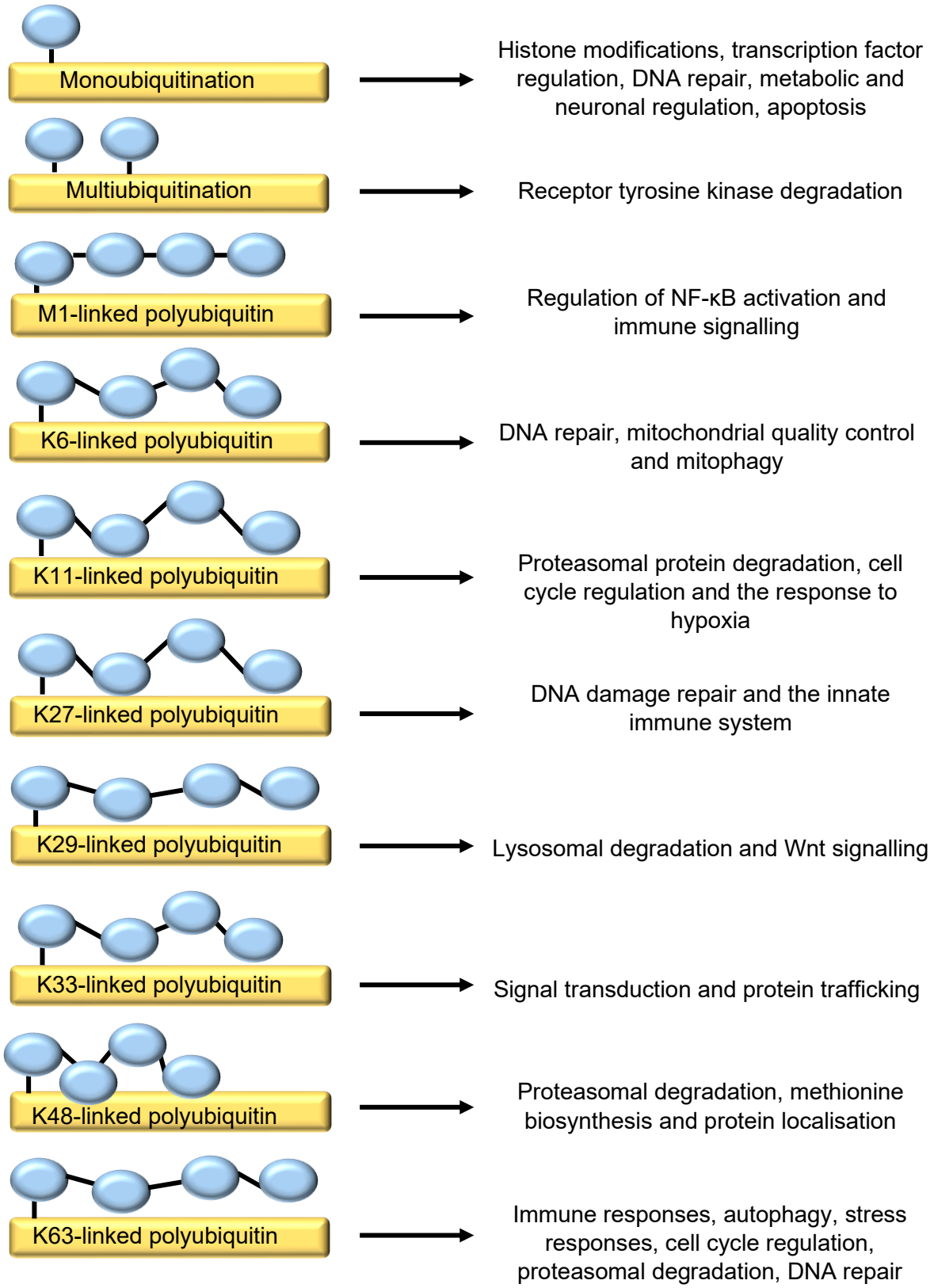

Figure 1.3. Types of ubiquitin linkages and their known functions.

The three types of ubiquitination, monoubiquitination, multiubiquitination and polyubiquitination, and the known functions of these types of ubiquitination, are shown. Ubiquitin monomers are displayed in blue, target proteins in yellow. Adapted from (Komander, 2009, Klein et al., 2016, Lafont et al., 2018).

1.1.5 Functions of ubiquitination

Since ubiquitination was first identified as a signal to mediate protein degradation at the proteosome, other roles for this protein modification have been identified (see summary Figure 1.3). Some of these roles will be discussed in this section, for detailed reviews see (Tracz and Bialek, 2021, Li and Ye, 2008, French et al., 2021, Swatek and Komander, 2016).

1.1.5.1 Functions of monoubiquitination and multiubiquitination

The most well-studied forms of ubiquitination are polyubiquitin chains. However, monoubiquitination is known to have diverse functions within the cell. For example, one main function of monoubiquitination is associated with the modification of histones. Indeed, *S. cerevisiae* cells that cannot monoubiquitinate histone H2B cannot successfully enter meiosis (Robzyk et al., 2000). There are also examples of non-histone proteins that are monoubiquitinated, such as NF-κB (see 1.1.5.9), the tumour suppressor p53 and FOX transcription factors, where monoubiquitination affects their function and downstream signalling (Nakagawa and Nakayama, 2015). Additionally, monoubiquitination is important in DNA repair and replication, the regulation of membrane associated processes such as protein secretion and endocytosis, the regulation of metabolic and neuronal proteins and the induction of apoptosis (Nakagawa and Nakayama, 2015). Multiubiquitination, a form of monoubiquitination (Figure 1.3), is not well characterised. However, one function of multiubiquitination has been well documented, where it has been shown to be important for the internalisation and lysosomal degradation of epidermal growth factor and platelet-derived growth factor receptors, both types of receptor tyrosine kinases (RTKs) (Haglund et al., 2003). Thus, monoubiquitination is a crucial modification in numerous important cellular processes.

1.1.5.2 K48 polyubiquitination functions

As discussed above polyubiquitination allows for the formation of homotypic or heterotypic ubiquitin chains (section 1.1.4.2), providing a large amount of potential diversity in the structures of polyubiquitin chains. The functions of polyubiquitin chains are specified by the lysine residue(s) of the ubiquitin monomer(s) in the chain that have

been ubiquitinated. The best characterised form of polyubiquitination is K48 polyubiquitination, initially identified as a signal for protein degradation at the 26S proteasome (Chau et al., 1989). In *S. cerevisiae*, K48 is the only essential lysine residue of ubiquitin indicating the importance of this type of protein modification (Chau et al., 1989). Importantly, it has been found that the threshold for successful proteasomal degradation of a modified substrate protein via K48 polyubiquitination is a minimum of 4 ubiquitin moieties, presented either as two dimers or as a tetramer, with cells exhibiting a preference for two diubiquitin chains (Thrower et al., 2000, Chau et al., 1989). Many well-studied E3 ligases specifically ubiquitinate proteins to target them for degradation by synthesising K48-linked chains, hence K48 linkages are the most abundant ubiquitin linkage in all organisms analysed (Peng et al., 2003, Xu et al., 2009). One of the best characterised E3 ligases, the SCF (SKP1, CUL1, F-box protein) complex, is an example of the E3 ligases noted to generate K48 polyubiquitin chains (for a review of SCF see (Willems et al., 2004)). In *S. cerevisiae*, the E2 enzyme Cdc34 with an SCF E3 ligase ubiquitinate Sic1, a cyclin-dependent kinase (CDK) inhibitor, ultimately causing its degradation allowing progression through the cell cycle (Schwob et al., 1994). Interestingly, Cdc34 is the only essential E2 enzyme in *S. cerevisiae*, and *cdc34* temperature-sensitive mutants arrest at the G1 phase to S phase boundary (Schwob et al., 1994). Thus, K48 linkages are essential for protein degradation, which in turn, regulates many cellular processes, such as cell cycle progression.

More recently, K48 ubiquitination has been shown to regulate other, non-proteolytic processes. For example, the Met4 transcription factor that regulates methionine biosynthesis in *S. cerevisiae*, is regulated by K48 polyubiquitination. In particular, when cells are exposed to an excess of methionine in media, Met4 becomes K48 polyubiquitinated and Met4 transcriptional activity is significantly reduced. However, this modification does not lead to degradation of Met4 at the proteasome. Instead, an intrinsic UBD (ubiquitin binding domain) of Met4 binds the ubiquitin, reducing the essential tetrameric chain length, thus blocking its degradation (Flick et al., 2006). Thus, K48 linkages inactivate Met4. Another example of a non-proteolytic function of K48-linked polyubiquitin is the regulation of the ubiquitin chaperone p97 (Cdc48 in *S. cerevisiae*). The p97 protein can selectively interact with various K48 polyubiquitinated proteins, with various consequences. Generally, p97 binding to K48-linked

polyubiquitin activates the ATPase activity of p97 and ultimately removes ubiquitinated substrates from their cellular compartments or protein complexes, functioning as a segregase (Li and Ye, 2008). Thus, K48 polyubiquitination can also regulate protein function, without targeting the protein for degradation.

1.1.5.3 K63 polyubiquitination functions

After K48-linked polyubiquitination, the next most characterised form of poly-ubiquitination is K63 polyubiquitination. The K63 polyubiquitination protein modification has been associated with various processes such as immune responses, autophagy regulation and stress response signalling (Komander and Rape, 2012). For example, gene ablation of the K63 specific E2 enzyme Ubc13, which interacts with various E3 ligases to catalyse K63 polyubiquitination (Madiraju et al., 2022), in mouse models revealed roles for Ubc13, and hence K63 polyubiquitination, in various immunological processes such as autoimmunity and inflammatory diseases (Yamamoto et al., 2006a, Yamamoto et al., 2006b). Several studies have further developed the link between K63 ubiquitination and immune responses, with K63 polyubiquitination shown to be critical in T cell regulation, Nod-like receptor (NLR) signalling and hence inflammasome formation, and viral responses via the regulation of STING (Stimulator of Interferon Genes) (Ni et al., 2019, Bednash and Mallampalli, 2016, Ni et al., 2017). Recent work has also linked K63 polyubiquitination in the immune response to SARS-CoV-2 via its regulation of STING, but further work is necessary to clarify this role (Madiraju et al., 2022). K63-linked polyubiquitination has also been shown to promote autophagy in stress-responses. For example, the K63 specific E3 ligase TRAF6 polyubiquitinates the autophagosome inducer ULK1, increasing its stability and hence its function (Nazio et al., 2013). K63-linked polyubiquitin chains have also been implicated in mitophagy via the E3 ligase Parkin, which ubiquitinates PINK1 (a serine threonine protein kinase), ultimately resulting in mitophagy (Ordureau et al., 2014). In addition, there is some evidence that K63 polyubiquitination regulates the cell cycle, where K63 polyubiquitination builds at sites of DNA damage and prevents the G2 phase to M phase transition (Mocciaro and Rape, 2012). Finally, K63 polyubiquitination has been shown to also fulfil proteolytic roles at the proteasome, despite initial findings which suggested that this modification was only involved in non-proteolytic roles such as cell signalling. For example, troponin I, an

inhibitor of the tropomyosin complex, was degraded when ubiquitinated with K63 linked chains (Kim et al., 2007).

1.1.5.4 K6 polyubiquitination functions

The remaining polyubiquitin linkages are not as well characterised or studied as K48 and K63 linkages. However, there is some data that provides possible roles for these other types of polyubiquitin chains. Although the role of K6-linked polyubiquitination still remains relatively unclear, it has been indirectly linked to DNA repair mechanisms via the E3 ligase BRCA1-BARD1, a tumour suppressor that forms K6-linked chains on substrates which includes the E3 ligase (Morris and Solomon, 2004). K6 linkages have also been found on mitochondrial outer membrane (MOM) proteins when the organelle is depolarised (Ordureau et al., 2014). Moreover, data suggests that K6 linkages are important for mitochondrial quality control, and mitophagy is delayed when K6 chains are blocked using a K6R mutant version of ubiquitin (Ordureau et al., 2015). However, despite these studies the exact role(s) of K6 linkages remains to be clarified.

1.1.5.5 K11 polyubiquitination functions

K11-linked polyubiquitination has been linked to proteasomal protein degradation, cell cycle regulation and the response to hypoxia. Experiments revealed that when the APC/C complex (anaphase-promoting complex) is activated during mitosis, K11-linked chains are assembled resulting in termination of mitosis and protein degradation via the proteasome (Akutsu et al., 2016). K11-linked polyubiquitin chains have also been linked to the cellular response to hypoxia. However, although the K11-specific DUB Cezanne has been linked with the regulation of the HIF1α and HIF2α (Hypoxia-inducible factor 1/2α) transcription factors, further characterised is required (Bremm et al., 2014, Moniz et al., 2015).

1.1.5.6 K27 polyubiquitination functions

Currently, K27-linked polyubiquitination is thought to act as a specific cell signalling cue, involved in DNA damage repair and in the innate immune system. For example, it has been shown that upon DNA damage histone 2A is ubiquitinated using K27-linked chains which are recognised by mediators and initiate the DNA damage response (DDR) (Gatti et al., 2015). In response to exogenous DNA from invading pathogens, STING, a major mediator of immune-related genes, becomes ubiquitinated with K27-linked polyubiquitin (Wang et al., 2014). These ubiquitin chains function as a platform for the binding of TANK-binding kinase 1 (TBK1), activating TBK1 and subsequently activating IRF3, a transcription factor that regulates genes involved in the immune response (Wang et al., 2014).

1.1.5.7 K29 polyubiquitination functions

K29-linked polyubiquitin is known to target cells for lysosomal degradation (Kim et al., 2011). However more recently these linkages have been observed to act as inhibitors of signalling via the Wnt pathway, a signalling pathway that when dysregulated is implicated in tumorigenesis and other diseases (Clevers and Nusse, 2012). In canonical Wnt signalling, β-catenin is degraded via a complex containing two kinases, and two scaffold proteins, one of which is Axin. When Wnt binds the receptor, this complex is destroyed and β-catenin is able to translocate to the nucleus and regulate target genes. Axin can be ubiquitinated via K29-linked polyubiquitin chains, which prevents interaction with Wnt coreceptors and ultimately inhibits canonical Wnt signalling (Fei et al., 2013).

1.1.5.8 K33 polyubiquitination functions

K33-linked polyubiquitination has been associated with AMPK-related kinases, NUAK1 and MARK4, where K33 (and K29)-linked chains are suggested to inhibit their activity (Al-Hakim et al., 2008), and T-cell receptor zeta (TCR-ζ) regulation, where the K33 linkage prevents phosphorylation of and hence association with the accessory protein Zap-70 (Huang et al., 2010). More recently, Crn7 has been shown to be ubiquitinated via K33 linkages. Upon binding Eps15, a clathrin adaptor protein, Crn7

is transported to the trans-Golgi network (TGN) and ultimately aids the elongation of TGN tubules (Yuan et al., 2014). K33-linked polyubiquitin chains on Crn7 are important for the interaction with Eps15, and the thus the translocation of Crn7 to the TGN (Yuan et al., 2014). Thus, K33 linkages are implicated in signal transduction and in protein trafficking processes.

1.1.5.9 N-terminal M1 polyubiquitination functions

Ubiquitin can also be added to the N-terminal methionine of ubiquitin (M1). One well-characterised example of M1-linked polyubiquitin is in the activation of NF-κB. NF-κB (nuclear factor-κB) is a transcription factor that regulates many cellular processes, including immune responses, inflammation and cell growth (Park and Hong, 2016). As a result, aberrant NF-κB signalling has been linked to many diseases, such as various types of cancer and inflammatory conditions (Oeckinghaus and Ghosh, 2009). Canonical activation of NF-κB is achieved by the I kappa B kinase (IKK) complex, which phosphorylates IκBα, an NF-κB inhibitor. Phosphorylation of IκBα causes downstream ubiquitination events on IκBα, targeting it for degradation and allowing NF-κB to translocate to the nucleus (Hoffmann et al., 2002). M1-linked polyubiquitin chains regulate NF-κB activation, as NEMO, the regulatory subunit of the IKK complex, is M1-polyubiquitinated. This is necessary for IKK complex activation via TAK1 (TGF-β activated kinase 1) which causes activation of NF-κB regulated genes (Emmerich et al., 2013, Gilmore, 2006).

In summary, ubiquitination therefore influences a diverse range of cellular functions by utilising different types of linkages and attachments to alter protein function/activity. Furthermore, ubiquitin can itself be modified by different post-translational modifications such as acetylation, phosphorylation, or conjugation of another UBL, further increasing the diversity of ubiquitin functions. These other post translational modifications and their functions in ubiquitin biology will not be discussed here (for a review, see (Swatek and Komander, 2016)) but demonstrates the complexity of ubiquitination signals and their roles in cellular processes.

1.1.5.10 Recognition of ubiquitination

The presence of different functions for different ubiquitination signals indicates the presence of proteins able to recognise and respond to these different signals. One method of interaction with ubiquitination involves ubiquitin binding domains (UBDs) which are small domains that are incorporated into interacting proteins. UBDs bind ubiquitin non-covalently, and transmit the function of ubiquitination to affect the relevant cellular processes (Hicke et al., 2005). A hydrophobic region of ubiquitin (Leu8, Ile44, Val70) is essential for UBD binding, and some polyubiquitin chains, such as K48 chains, have to undergo conformational changes to expose this hydrophobic region (Mueller et al., 2004). Some data suggests that UBDs can function quite promiscuously, and that other domains of the interacting protein restricts the conformational form of ubiquitination that can interact with the UBD (Raasi et al., 2005, Li and Ye, 2008). However, there is some evidence of linkage-specific UBD binding. Polyubiquitin chains exist in different three-dimensional conformations dependent upon the lysine linkage, for examples, K48 chains are globular, compact forms of polyubiquitin whereas K63 polyubiquitin chains form a linear structure, with no contact between neighbouring ubiquitin monomers (Eddins et al., 2007, Komander et al., 2009), which can dictate UBD specificity. Interestingly, some UBDs can differentiate between polyubiquitin chains exhibiting similar three-dimensional conformations. For example, NEMO, the regulatory subunit of the IKK complex (see 1.1.5.9), can differentiate between structurally similar polyubiquitin chains (Komander and Rape, 2012). Thus, UBDs can utilise the proximity of ubiquitin monomers within a ubiquitin chain and the flexibility of the chain to recognise different forms of polyubiquitination.

1.1.6 Ubiquitin and UBL deconjugation

Ubiquitination and UBL modifications are dynamic protein modifications involving discrete conjugation and deconjugation mechanisms. The ‘off’ mechanism is achieved using deconjugation enzymes such as DUBs for ubiquitin deconjugation and SENPs for SUMO deconjugation, for reviews see (Nayak and Müller, 2014, Harrigan et al., 2018, Amerik and Hochstrasser, 2004). DUBs have two main functions; to remove or modify the ubiquitination signal and consequently alter the fate/regulation of the

substrate protein, and to recycle ubiquitin for further conjugation (Clague and Urbe, 2006). DUBs remove ubiquitin from substrates by breaking the isopeptide linkage between the C-terminal glycine of ubiquitin, and the residue (normally lysine) ubiquitinated on target proteins. DUBs are also important in the pre-processing of immature ubiquitin, allowing it to be activated and conjugated to target proteins (Kerscher et al., 2006). DUBs can also display preference for cleaving an entire ubiquitin chain *en bloc* (base cleavage), cleaving the chain in the middle (endo-cleavage), or by cleaving single ubiquitin monomers (exo-cleavage; discussed in Section 1.1.6.2.2). Hence, DUBs can function as an 'off' switch, by removing the whole ubiquitin chain, or as a modifier of the signal, by removing ubiquitin monomers and hence changing the role of the ubiquitination signal (Lange et al., 2022). Given the wide range of functions of various ubiquitination signals (discussed in Section 1.1.5), DUBs can regulate these same functions by reversing or altering the ubiquitination signal. Analysis of DUB function has been notoriously difficult due to the large numbers found in cells (human cells >100, *S. cerevisiae* >20) and the large degree of redundancy in function that is displayed by the different DUBs (Schaefer and Morgan, 2011). However, although there is still much to be elucidated, the functions of many DUBs have been associated with specific cellular processes (Table 1.1).

DUBs have been classified into two main groups depending on their catalytic mechanism; cysteine proteases, which utilise a catalytic cysteine residue to remove ubiquitin, and zinc metalloproteases, which co-ordinate a zinc ion in order to deconjugate ubiquitin (Komander, 2010). Generally, the cysteine proteases work via a catalytic triad or diad, where a histidine functions to lower the pKa of the catalytic cysteine to allow it to hydrolyse the isopeptide linkage between ubiquitin and the substrate protein. The third amino acid in the catalytic triad is either an asparagine or an aspartate residue which functions to align the histidine. These residues are situated in close proximity in the structure of the DUB, allowing deprotonation of the catalytic cysteine which then can deubiquitinate substrates (Amerik and Hochstrasser, 2004). However, some DUBs align their histidine via other mechanisms and hence only require a catalytic diad (Storer and Menard, 1994).

1.1.6.1 Families of deubiquitinases (DUBs)

As mentioned above to date, >100 DUBs have been identified in humans and *S. cerevisiae* contains >20 (Finley et al., 2012, Reyes-Turcu et al., 2009). Until recently, there was thought to be 5 main DUB families – 4 cysteine protease families, the USP family (ubiquitin-specific proteases), the UCH family (ubiquitin C-terminal hydrolases), the OTU family (ovarian tumour proteases), and the Josephin family, and one family of zinc metalloproteases, the JAMM family (Jab1/MPN/MOV34) (Mevissen and Komander, 2017). However, two new DUB families have recently been discovered which also utilise a catalytic cysteine residue, the MINDY family (motif interacting with Ub-containing novel DUB family) and the Zup1 family (zinc-finger-containing Ub peptidase) (Abdul Rehman et al., 2016, Kwasna et al., 2018). All the DUB families except the Josephin and Zup1 DUB families, are found in *S. cerevisiae*. In *S. cerevisiae*, 16 of the 22 DUBs are homologues of the USP family (Ubp1 – Ubp16), one is a homologue of the UCH family (Yuh1), two are homologues of the OTU family (Otu1 and Otu2), two are homologues of MINDY DUBs (Miy1 and Miy2), and the JAMM family has one homologue (Rpn11) (Table 1.1) (Huseinovic et al., 2018). Therefore, 21 out of 22 possible DUBs in *S. cerevisiae* utilise a catalytic cysteine residue to deconjugate ubiquitin. Table 1.1 displays these DUBs in *S. cerevisiae*, their mammalian homologues and any identified functions in *S. cerevisiae*.

Family	***S. cerevisiae* DUB**	**Mammalian homologue**	**Function in yeast**
USP	Ubp1	USP19	Endocytosis (Schmitz et al., 2005).
USP	Ubp2	USP28	Regulates mitochondrial fusion, membrane protein sorting and oxidative stress, and deubiquitinates Rsp5 (Anton et al., 2013, Lam et al., 2009, Silva et al., 2015, Kee et al., 2006).

USP	Ubp3	USP10	Regulates gene silencing, osmotic stress, autophagy and ribophagy, protein trafficking and protein degradation upon heat stress (Baker et al., 1992, Cohen et al., 2003, Kraft et al., 2008, Moazed and Johnson, 1996, Fang et al., 2016).
USP	Ubp4/Doa4	USP4/8	Paralogue of Ubp5. Maintains levels of free, monomeric ubiquitin and recycles ubiquitin from proteasome and vacuole targeted proteins (Nikko and Andre, 2007, Swaminathan et al., 1999).
USP	Ubp5	USP4/8	Paralogue of Ubp4. Regulates cytokinesis (Wolters and Amerik, 2015).
USP	**Ubp6**	**USP14**	**Degrades ubiquitin chains at the proteasome (Hanna et al., 2006).**
USP	Ubp7	USP21	Paralogue of Ubp11. Involved in S-phase progression (Bohm et al., 2016).
USP	Ubp8	USP22	Deubiquitinates histone H2B and Cse4 (Henry et al., 2003, Canzonetta et al., 2015).
USP	Ubp9	USP12/1	Paralogue of Ubp13. Involved in mitochondrial biogenesis (Kanga et al., 2012).
USP	Ubp10	USP20/36	Regulates ribosomal biogenesis, PCNA and histone H2BK123 deubiquitination, endocytosis of Gap1p and gene silencing (Richardson et al., 2012, Gallego-Sánchez et al., 2012, Schulze et al.,

			2011, Kahana, 2001, Kahana and Gottschling, 1999).
USP	Ubp11	USP21	Paralogue of Ubp7.
USP	**Ubp12**	**USP15**	**Regulates mitochondrial fusion, genomic stability, proteasomal degradation and DNA damage responses (Anton et al., 2013, Ang et al., 2016, Gödderz et al., 2017, Álvarez et al., 2019).**
USP	Ubp13	USP46	Paralogue of Ubp9. Regulates mitochondrial biogenesis and sensitivity to cold temperatures (Kanga et al., 2012, Hernández-López et al., 2011).
USP	Ubp14	USP5	Disassembles unanchored ubiquitin chains and degrades fructose-1,6-bisphosphate (Amerik et al., 1997, Regelmann et al., 2003).
USP	Ubp15	USP7	Regulates G1 to S phase progression, peroxisome biogenesis and methionine synthesis (Ostapenko et al., 2015, Debelyy et al., 2011, Benschop et al., 2010).
USP	Ubp16	USP16	Localised to the mitochondrial membrane yet no known function (Kinner and Kolling, 2003).
OTU	Otu1	OTU1	Degradation of ER-associated proteins (Stein et al., 2014).
OTU	**Otu2**	**OTUD6B**	**Uncharacterised.**
UCH	Yuh1	UCHL3	Rub1 ubiquitin-like protein processing but also cleaves ubiquitin (Linghu et al., 2002).

JAMM	Rpn1	POH1	Bound to the 26S proteasome lid, cleaves whole ubiquitin chains (Mevissen and Komander, 2017).
MINDY	Mindy1	MINDY-1	Uncharacterised, preferentially cleaves K48 linkages (Abdul Rehman et al., 2016).
MINDY	Mindy2	MINDY-2	Uncharacterised.

Table 1.1. DUBs in *S. cerevisiae.*

The 22 putative DUBs in *S. cerevisiae*, their mammalian homologues and their functions in *S. cerevisiae* (Huseinovic et al., 2018).

1.1.6.1.1 USP family

The biggest and best characterised family of DUBs is the USP family (Nijman et al., 2005). The catalytic domain of USP DUBs contains two motifs, Cys and His boxes, which accommodate the catalytic triad (cysteine, histidine and aspartic acid) in the folded protein. As previously described, the histidine residue lowers the pKa of the catalytic cysteine, which can then hydrolyse the isopeptide bond between ubiquitin and substrate. The third residue (Asp) is necessary for stabilisation. The size of USP DUBs differ hugely due to the variable region, whose function is unknown, that lies between the catalytic Cys and His boxes (Nijman et al., 2005). Analysis of crystal structures revealed that USP DUBs exhibit a specific tertiary structure comprising of a palm, a thumb and finger-like motifs, where the palm and the thumb create a groove where the catalytic cysteine is located (Hu et al., 2002). Only one USP DUB, CYLD, is known to differ from this structure, lacking the finger domain (Komander et al., 2008). USP DUBs have also been found to have no catalytic activity when unbound to a substrate. However, upon substrate binding, conformational changes are induced which bring the catalytic triad into proximity with each other (Komander, 2009). There is also evidence that substrate binding can omit proteins that were previously blocking catalysis (Amerik and Hochstrasser, 2004).

In human cells, there are 56 known USP DUBs making it by far the largest family of DUBS. This is mirrored in *S. cerevisiae*, which express 16 USP DUBs (Finley et al., 2012). As predicted for a large family of DUBs, the individual DUB functions regulate many cellular processes (see Table 1.1 for known functions in *S. cerevisiae*, for the functions of mammalian USPs see the reviews of (Nijman et al., 2005, Reyes-Turcu et al., 2009).

1.1.6.1.2 UCH family

The UCH family of DUBs exhibit very similar folding to USP DUBs, and indeed their catalytic triads are superimposable (Amerik and Hochstrasser, 2004). In the case of UCH DUBs, the catalytic triad consists of cysteine, histidine and aspartate residues, and deubiquitinate proteins via the same mechanism as USPs. However, evidence suggests that UCH DUBs preferentially deubiquitinate small proteins due to the presence of a peptide arc which partially blocks access of the active site to large proteins (Amerik and Hochstrasser, 2004). The catalytic site of UCH DUBs also lies in a deep groove which accommodates only the C-terminal glycine of ubiquitin and therefore offers a level of specificity (Amerik and Hochstrasser, 2004).

S. cerevisiae cells express one known UCH DUB, Yuh1, whilst 4 have been identified in human cells (Table 1.1) (Finley et al., 2012). Interestingly however Yuh1, although a putative deubiquitinase, preferentially binds the UBL Rub1 (Linghu et al., 2002). Due to the presence of a small binding pocket in UCH DUBs, it is speculated that these DUBs cleave monoubiquitin and are involved in ubiquitin processing (Larsen et al., 1998).

1.1.6.1.3 OTU family

The OTU DUB family use a catalytic triad of cysteine, histidine and asparagine residues (Mevissen et al., 2013). These function as other cysteine protease DUBs, where the histidine lowers the pKa of the catalytic cysteine, allowing nucleophilic attack on the isopeptide linkage, and stability is provided by the asparagine residue (Du et al., 2020). With catalytic diads, the catalytic cysteine is stabilised by a hydrogen bond network (Nanao et al., 2004). OTU DUBs were originally identified using

bioinformatics, where sequence similarity was observed between the *otu* gene in *Drosophila* and cysteine proteases (Makarova et al., 2000). Since then, numerous OTU DUBs have been identified and now comprise the second largest class of DUBs in humans and *S. cerevisiae*.

The human genome has been found to encode 18 OTU DUBs whilst *S. cerevisiae* genome contains only 2 genes encoding Otu1 and Otu2 (Table 1.1). Functional analysis of Otu1 has revealed that it binds to polyubiquitin preferentially, but does have weak interactions with monoubiquitinated substrates (Messick et al., 2008). Moreover, Otu1 has a preference for K48-linked chains over K29- or K63-lnked polyubiquitin, and kinetic data suggests that it functions as an endo DUB, releasing diubiquitin moieties from polyubiquitin chains (Messick et al., 2008). Although the functions of Otu1 are not well characterised, it is shown to interact with Cdc48, an important component of the ERAD (endoplasmic-reticulum-associated protein degradation) pathway (Messick et al., 2008). The function and specificity of Otu2 has not been well studied, but some evidence has linked this DUB to the ribosome (Huseinovic et al., 2018).

1.1.6.1.4 MINDY family

The MINDY DUBs are the most recently discovered family that are present in *S. cerevisiae*. Although they also utilise a catalytic triad, in this case it is comprised of cysteine, histidine and threonine residues. Interestingly, the catalytic domain of MINDY DUBs is a protein fold not seen in any other family of DUBs (Abdul Rehman et al., 2016). Despite the identification of a novel residue involved in DUB catalysis (threonine), it is predicted that deubiquitination occurs in a similar manner to other DUBs that utilise a catalytic triad, with histidine lowering the pKa of the catalytic cysteine, allowing hydrolysis of the isopeptide bond, and the threonine residue functioning to stabilise the interaction (Abdul Rehman et al., 2021).

Interestingly, the two validated mammalian MINDY DUBs, MINDY-1/FAM63A and MINDY-2/FAM188A can function as exo-DUBs or endo-DUBs, depending on the ubiquitin chain length (Abdul Rehman et al., 2021). Both exhibit selectivity for K48 polyubiquitin chains, however there is evidence that MINDY-2 may be able to cleave mixed/branched polyubiquitin chains, which is not suggested for MINDY-1 (Abdul Rehman et al., 2021). The MINDY-1 homologue in *S. cerevisiae*, Miy1, also

preferentially cleaves K48 polyubiquitin, however the MINDY-2 homologue, Miy2, does not show any deubiquitinating activity despite the conservation of catalytic residues (Abdul Rehman et al., 2016). At present, there are no known substrates or functions of these DUBs, hence more work is necessary to validate their *in vivo* functions.

1.1.6.1.5 JAMM family

The JAMM family of DUBs are zinc metalloproteases which function via a different mechanism to those outlined above. In this case, they utilise histidine and serine residues, and either an aspartate or a glutamate residue, to coordinate two Zn^{2+} ions (Shrestha et al., 2014). The first Zn^{2+} ion interacts with the Asp/Glu residue, generating a hydroxide ion from a water molecule which nucleophillically attacks the isopeptide linkage (Maytal-Kivity et al., 2002, Tran et al., 2003). The second Zn^{2+} ion is responsible for stabilising the complex (Maytal-Kivity et al., 2002).

Humans encode 12 JAMM DUBs, whereas *S. cerevisiae* encode only one, Rpn11 (Pan et al., 2022). Interestingly, Rpn11 is the only essential DUB expressed in *S. cerevisiae*, with non-lethal mutants displaying increased levels of ubiquitinated proteins, growth impairments and problems with the DNA replication machinery (Finley et al., 2012, Gallery et al., 2007). Furthermore, knock-down experiments exploring the role of Poh1, the human homologue of Rpn11, revealed growth defects, an increase in ubiquitinated proteins and defects in substrate degradation and proteasomal activity (Gallery et al., 2007). In accordance with this, Rpn11 has been associated with the 26S proteasome, deubiquitinating polyubiquitin chains *en bloc* with some preference for K48 and K63 linked chains, signals both known for targeting proteins for proteasomal degradation (Mevissen and Komander, 2017, Pan et al., 2022).

1.1.6.2 DUB specificity

As with the ubiquitin conjugation enzymes, DUBs also exhibit preferences for the substrates from which ubiquitin is to be removed. However, studying the functions and substrates of DUBs *in vivo* is particularly challenging due to the functional redundancy which is displayed by these proteins. Consequently, it is very hard to identify specific targets of DUBs. However, DUBs exhibit some preference based on ubiquitin chain

length, the type of chain linkage, the substrate itself and the presence of other proteins in complex with the ubiquitinated protein. In most cases, DUB specificity is likely to be dictated by a combination of these preferences, which together ultimately fine-tune the catalytic targeting of DUBs.

1.1.6.2.1 Substrate specificity

One level of specificity utilised by DUBs is direct recognition of the ubiquitinated substrate. Deubiquitination of monoubiquitin signals specifically requires interaction of the DUB with the substrate protein, although currently substrates of monoubiquitination are not well-characterised. As a consequence, direct substrate recognition by DUBs which remove monoubiquitination is not well understood. Interaction with the ubiquitinated substrate is also important for *en bloc* removal of polyubiquitin. It is thought that non-catalytic domains of the DUBs involved in this process are responsible for this interaction, allowing catalytic regions to function whilst also binding the substrate (Nijman et al., 2005). Indeed, many USP DUBs contain various other protein binding motifs in their structure, predicted to be important for substrate binding (Clague et al., 2013). One example of direct substrate recognition has been clarified. Studies of the deubiquitinating function of Ubp6 revealed direct interactions with the histone monomer H2B in the SAGA complex via electrostatic interactions using conserved tyrosine and arginine residues of Ubp6, whilst removing the monoubiquitination signal (Morgan et al., 2016).

1.1.6.2.2 Chain-linkage specificity

Ubiquitin cleavage is also regulated by the linkage(s) in the ubiquitin chain. DUBs can function as ‘endo-DUBs’ which cleave ubiquitin within a chain, or ‘exo-DUBs’ which cleave ubiquitin from the end of the chain (Heride et al., 2014). Endo-DUBs generate ubiquitin chains that then need processed further into monoubiquitin by DUBs, whereas exo-DUBs cleave single ubiquitin monomers. These cleavages allow the modification of ubiquitin chains by DUBs to alter the ubiquitin signal and/or to recycle ubiquitin monomers. Processing of unanchored ubiquitin chains is performed by a distinct type of exo-DUB, namely USP5 and USP13 in mammalian cells, that require a zinc finger motif to recognise the exposed diglycine motif at the C-terminus of ubiquitin (Reyes-Turcu et al., 2006). In *S. cerevisiae* Ubp14 (the homologue of USP5)

recognises unanchored ubiquitin, and reviewed computational analysis suggests that this DUB may bind zinc however no metal analysis has been performed (Amerik et al., 1997). Some DUBs seem to display a primary preference for chain length, for example Ubp8 and Rpn11 in *S. cerevisiae*. Ubp8 preferentially cleaves monoubiquitin from the histone monomer H2B in the SAGA complex, while Rpn11 can cleave a whole ubiquitin chain *en bloc* (Ingvarsdottir et al., 2005, Mevissen and Komander, 2017).

Often it is the tertiary shape of the ubiquitination signal that dictates which DUBs can deubiquitinate it. The tertiary conformation of ubiquitination is controlled by the lysine modifications within the chain, for example K48 chains exist as globular structures whereas K63 chains are linear structures (Ronau et al., 2016). Thus, the 'endo' or 'exo' activity of DUBs can also be dictated by the polyubiquitin linkages present in the substrate protein. For example, in human cells USP21 can function as an endo-DUB with K63-linkages but only as an exo-DUB with K6-linkages (Mevissen and Komander, 2017). Importantly, to function as an endo-DUB the DUB must be able to accommodate the C-terminal ubiquitin chain. In this respect some DUBs such as the OTU family members OTUD2 and OTUD3 actually employ a second ubiquitin binding site (S2) to aid endo processing (Mevissen et al., 2013).

1.1.6.2.3 DUB partners

Proteins in complex with the DUB can also regulate and enhance DUB activity. Many DUBs have a relatively low binding affinity for ubiquitin and hence their specificity for substrates may be regulated through interaction with partner proteins (Ventii and Wilkinson, 2008). Hence, similar to E3 ligase enzymes, it is likely that many DUBs utilise scaffold and adaptor proteins to aid specific deubiquitination (Amerik and Hochstrasser, 2004). There has been a large number of potential binding partners identified for many mammalian DUBs (reviewed in (Ventii and Wilkinson, 2008). In *S. cerevisiae* for example, Bre5, which is in complex with Ubp3, is necessary for the subsequent deubiquitination and degradation of the Ubp3 target proteins, vesicle forming complexes COPI and COPII (Cohen et al., 2003, Li et al., 2007). Additionally, Rpn11, an OTU DUB associated with the 26S proteasome, only displays catalytic activity when physically associated with the proteasome suggesting that this interaction is important for deubiquitination (Koulich et al., 2008). Interestingly, the proteasome also cannot function efficiently without its associated DUBs, hence they

are mutually reliable on each other. OTU1B, a mammalian OTU DUB, has significantly increased enzymatic activity when associated with E2 enzymes, such as UBE2N or UBE2D (Wiener et al., 2013). These E2 enzymes stabilise the DUB, which has an intrinsically disordered N-terminal region. Interestingly, there is evidence that this interaction is important for the specific preference of OTU1B to deubiquitinate K48-linked chains (Wiener et al., 2013). A final example is USP1, which utilises a cofactor, UAF1 (USP1 associated factor 1). UAF1 functions as an activator, increasing the catalytic turnover of USP1, but does not alter ubiquitin binding affinity (Cohn et al., 2007). Despite some well characterised examples, there are still many proteins found in complex with DUBs where their function remains unclear. Further studies of these proteins have the potential to reveal drug targets for clinical treatments to allow the modulation of DUB activity in specific contexts, without removing the global function of the DUB.

1.1.6.2.4 Ub vs. UBL specificity

Given the similar tertiary structures of ubiquitin and UBLs, it is essential that the deconjugation machinery can differentiate between these different proteins. Despite very similar tertiary structures, the primary structures of these proteins vary which generates different surface properties such as charge and hydrophobicity (Ronau et al., 2016). These differences provide the deconjugation machinery with a route to differentiate between ubiquitin and the different UBLs. For example, when DUBs interact with ubiquitin, there are several ubiquitin residues that are crucial for recognition. The primary recognition site (S1) of the DUB binds approximately 20% - 40% of ubiquitin, triggering the C-terminus of ubiquitin to extend and become engulfed by the DUB, which also allows ubiquitin recognition (Komander, 2009, Schaefer and Morgan, 2011). Several key residues (L71, R72, L73, R74, G75, G76) differentiate the C-terminus of ubiquitin from other UBLs, and R74 and G75 are particularly important for DUB recognition (Komander, 2009).

Some DUBs cleave other UBL modifications in preference to ubiquitin, for example Yuh1 cleavage of Rub1 in *S. cerevisiae*, and hence there can be some overlap between deconjugase enzymes (Linghu et al., 2002). In mammalian cells USP21 can cleave ISG15 (a UBL modification), although kinetic data revealed that USP21has a 80-fold higher preference for ubiquitin (Ye et al., 2011). Although structural differences

between ubiquitin and NEDD8 prevent most USP DUBs deconjugating NEDD8, there is also some data that suggests USP DUBs can cleave NEDD8 (Ye et al., 2011).

1.1.6.2.5 Outstanding questions about DUB specificity

There remain many unanswered questions regarding how DUBs specifically target and fine tune ubiquitination signals. Currently, there are examples of ubiquitination with no identified DUB, suggesting the potential to discover new roles and classes of DUBs in the future (Mevissen and Komander, 2017). Indeed, for a long time only five families of DUBs (USP, UCH, OTU, JAMM and Joesephin) were validated. However, recently two new DUB families have been identified (MINDY and Zup1) (Li and Reverter, 2021). The development of more efficient DUB probing mechanisms, such as those that were used to identify these two new families, there is a potential to identify further members of these families and even new families of DUBs. Currently, there is also very little evidence of DUBs that function on specific, branched forms of polyubiquitin and whether the branched nature could delay or hinder DUB activity. Indeed, the function of many endo-DUBs may be inhibited in these circumstances because the ubiquitin binding in the S1 site is modified at multiple positions. Although some *in vitro* studies have described no inhibitory effect of branched polyubiquitin on DUB action, this has yet to be replicated *in vivo* (Mevissen et al., 2016). Other post-translational modifications of ubiquitin also have potential implications for the DUB specificity. For example, phosphorylation of polyubiquitin at several serine residues significantly decreases the ability of DUBs to bind ubiquitin (Wauer et al., 2015). However, to date no phosphoubiquitin-specific DUB has been identified that is linked to the effect of this ubiquitin modification (Wauer et al., 2015, Huguenin-Dezot et al., 2016). This observation is physiologically relevant with respect to the DUB-mediated process of mitochondrial turnover, where ubiquitin is phosphorylated on S65. Interestingly, USP30, a DUB involved in mitochondrial turnover, displays a lower binding affinity for phosphoubiquitin (Wauer et al., 2015). Thus, despite extensive studies of DUBs, the complexity of the structures and modifications of polyubiquitin chains, together with the balance between redundancy and specificity exhibited by the different DUBs, leaves many unanswered questions regarding how DUBs target specific forms of ubiquitination.

1.1.6.3 Regulation of DUBs

Given the number of DUBs within cells and their diversity and specificity, it is not surprising that these proteins are regulated by a variety of mechanisms, including several post translational modifications (for a review see (Wang and Wang, 2021)). These modifications can influence the activity of the DUB in several ways, for example by directly altering the catalytic function of the DUB or indirectly by influencing the subcellular location of the protein. Phosphorylation is one post translational modification that regulates DUBs. DUBs can be phosphorylated on serine, threonine or tyrosine residues at 11 potential sites (Swatek and Komander, 2016). For example, proteomic analysis revealed that several DUBs, including USP15, the homologue of Ubp12 in *S. cerevisiae*, are phosphorylated in response to DNA damage (Matsuoka et al., 2007). For example, activation of ABL1/c-Abl (ABL proto-oncogene 1) in response to DNA damage causes the phosphorylation of the DUB OTULIN, enhancing its interaction with β-catenin (Wang et al., 2020b). This stabilises β-catenin and enhances Wnt signalling. Interestingly, the A20 DUB influences inflammatory responses by regulating the NF-κB pathway (see 1.1.5.9), and can also be phosphorylated at position S381 (Hutti et al., 2007). Although unphosphorylated A20 down-regulates the NF-κB response, when A20 becomes phosphorylated, the inflammatory response is reduced to a much greater extent (Hutti et al., 2007). Consequently, phosphorylation of DUBs can directly alter their activity. In addition to these effects on activity, phosphorylation influences the cellular location of DUBs. For example, when phosphorylated, cytosolic USP10 is translocated to the nucleus where it deubiquitinates a target substrate, p53 (Yuan et al., 2010). Phosphorylation of USP15 also regulates its subcellular localisation and its deubiquitination of PRP31, regulating spliceosome dynamics (Das et al., 2019b).

Interestingly, DUBs can also become ubiquitinated and sumoylated (Swatek and Komander, 2016). In most cases of these cases, ubiquitination is predicted to signal the proteasomal degradation of the DUB. For example, USP4, which is in a complex with the E3 ligase Rho52, deubiquitinates Rho52 whilst Rho52 ubiquitinates USP4 (Wada and Kamitani, 2006). Hence, USP4 and Rho52 regulate the ubiquitin modification status of each other. However, they also exhibit auto-ubiquitination and auto-deubiquitination. Indeed, a mutant form of USP4 was ubiquitinated in cells but

was not deubiquitinated, suggesting that the mutant USP4 protein could not auto-deubiquitinate (Wada and Kamitani, 2006). It has also been observed that USP25 can become sumoylated. This sumoylation decreased the binding affinity of USP25 to substrate polyubiquitin, significantly reducing the catalytic ability of the DUB (Meulmeester et al., 2008).

The transcription of genes that encode DUBs is also regulated to fine-tune the activity of DUBs in a temporal manner. An excellent example is the observation that cytokine induction triggered the upregulation of genes encoding several DUBs, catalytically similar to the USP family, in murine lymphocytes due to the presence of cytokine responsive elements within the DUB genes (Baek et al., 2004). When the cytokines are degraded, these DUBs are also efficiently degraded, limiting their presence to cytokine induction (Baek et al., 2004).

Enzymes of the conjugation/deconjugation pathways of ubiquitin and UBLs are also regulated by oxidation. Given that the majority of the main enzymes in these pathways utilise a catalytic cysteine residue, it is perhaps not surprising that these pathways are regulated in this way. This form of regulation of will be discussed in detail in Section 1.3.

1.1.6.4 DUBs in disease and health

Dysregulation of DUB activity has been implicated in numerous diseases, such as cancers and neurodegenerative disorders, and hence they are attractive targets for therapeutic intervention (Popovic et al., 2014). Indeed, understanding the biology underpinning DUB regulation and function is attracting huge interest and is an essential step in the future development of clinical approaches to target DUBs with drugs for the benefit of human health. For an extensive review that discusses links between DUBs and disease, see (Harrigan et al., 2018).

Analysis of mammalian cells has revealed important links with DUBs in the progression of multiple cancers. For example, USP7 regulates the tumour suppressor, p53. Mdm30, an E3 ligase, ubiquitinates p53 and targets the protein for proteasomal degradation (Harris and Levine, 2005). USP7 removes this ubiquitination, and as consequence p53 is stabilised and retains its function as a tumour-suppressor (Li et

al., 2002). The mammalian DUB USP15 (Ubp12 in *S. cerevisiae*) positively regulates the transforming growth factor-β (TGFβ) pathway, which ultimately influences the growth of glioblastoma cells (Eichhorn et al., 2012). USP15, in complex with the SMURF2 E3 ligase complex, deubiquitinates and stabilises the type I TGFβ receptor, which enhances TGFβ signalling. Furthermore, USP15 is upregulated in ovarian and breast cancers, which suggest that development of drugs to target this DUB may have wide therapeutic potential (Eichhorn et al., 2012). In addition to these examples, many other mammalian DUBs (for example USP8, USP20, USP28, USP22, UCHL1) have been implicated in cancer progression (Lai et al., 2020).

Many mammalian DUBs have also been linked to various neurological disorders, such as Parkinson's disease and Alzheimer's (Lim et al., 2020). For example, USP15 and USP8 have been implicated in the progression of Parkinson's disease through their involvement in the regulation of mitochondrial dynamics (Lim et al., 2020). Mutations in Parkin, an E3 ligase enzyme translocated to mitochondria to induce mitophagy, is the second most common cause of Parkinson's disease. Significantly, USP8 has been shown to deubiquitinate Parkin itself and α-synuclein, a protein whose accumulation in the ubiquitinated form can aggregate in Lewy bodies, a key biomarker in Parkinson's and other neurodegenerative diseases such as Alzheimer's (Durcan et al., 2014, Alexopoulou et al., 2016). USP15 co-localises with Parkin at mitochondria and, although there is no evidence that it deubiquitinates Parkin, there is evidence that USP15 can inhibit Parkin-mediated ubiquitination (Cornelissen et al., 2014). Other DUBs, including USP14 and ATXN3, have also been shown to regulate Parkinson's disease. Interestingly, the congenital condition Down's Syndrome caused by trisomy of chromosome 21, is linked to the activity of USP16, a DUB that is also expressed from chromosome 21. In particular, in a mouse model of Down's syndrome, defects in stem cell renewal were rescued by modifying the expression of USP16 to mirror the expression of USP16 that occurs in control mice (Adorno et al., 2013). Thus, several DUBs are important in the progression of certain neurological and neurodegenerative disorders.

There are many examples of DUBs that regulate inflammatory processes. The DUB A20, the most well studied example, deubiquitinates several regulators of the NF-κB pathway, specifically NF-κB essential modulator (NEMO), receptor-interacting

serine/threonine-protein kinase 1 (RIPK1) and tumour necrosis factor (TNF) receptor-associated factor 6 (TRAF6) (Wertz et al., 2004). A zinc-finger motif of A20 can also bind to ubiquitinated NEMO, which prevents NF-κB activation (Skaug et al., 2011). As a consequence of these mechanisms, A20 regulates toll-like receptor signalling and hence innate immune responses.

Finally, there are many studies that link DUBs to the regulation of infectious diseases. Interestingly, certain viruses' express cysteine proteases that act like DUBs to counteract the beneficial ubiquitination that aids the host immune responses. For example, the SARS-CoV and MERS-CoV viruses have the intrinsic ability to deubiquitinate key proteins in host immune responses (Sun et al., 2012). Many pathogenic bacteria also express DUBs which aid pathogenicity and, moreover, some of these DUBs exhibit an ability to remove the NEDD8 UBL (Pruneda et al., 2016). It has also been observed that certain parasitic infections utilise DUBs to regulate host responses in a similar manner (Artavanis-Tsakonas et al., 2006).

In summary, given the extensive roles of DUBs in the progression of the pathologies of common diseases and infections, studies of the underlying links between DUBs and human health are important for the potential development of drugs that target these DUBs to provide new and improved clinical treatments.

1.2 Reactive oxygen species (ROS)

Reactive oxygen species (ROS) are unstable, oxygen-containing molecules that can readily react with other compounds. Within the cell there are three main species of ROS; H_2O_2, hydroxyl radicals (•OH) and superoxide anions ($•^-O_2$), which are either produced endogenously or are introduced into the cell from exogenous sources (see Section 1.2.1). High levels of ROS can cause oxidative stress, resulting in intracellular damage to proteins, DNA and lipids and consequently has been linked with the possible onset of numerous age-related diseases (Figure 1.4). In an attempt to prevent oxidative stress, as ROS levels become higher, the cell induces the transcription of genes that encode antioxidants and repair proteins to restore homeostasis and to repair damage (Figure 1.4). However, oxidative stress occurs if the levels of ROS continue to rise and antioxidant mechanisms are overwhelmed. Oxidative stress is

defined as an imbalance between ROS production and antioxidant capabilities and results in damage to intracellular components (discussed in Section 1.2.2). In contrast to these damaging effects of oxidative stress, lower levels of ROS have been found to play important roles in signal transduction in various cellular processes (see Section 1.3). Hence, as a consequence of the inevitable production and exposure of cells to ROS, it is vital that cells can distinguish the type and the levels of the ROS within the cell in order to respond in an appropriate manner.

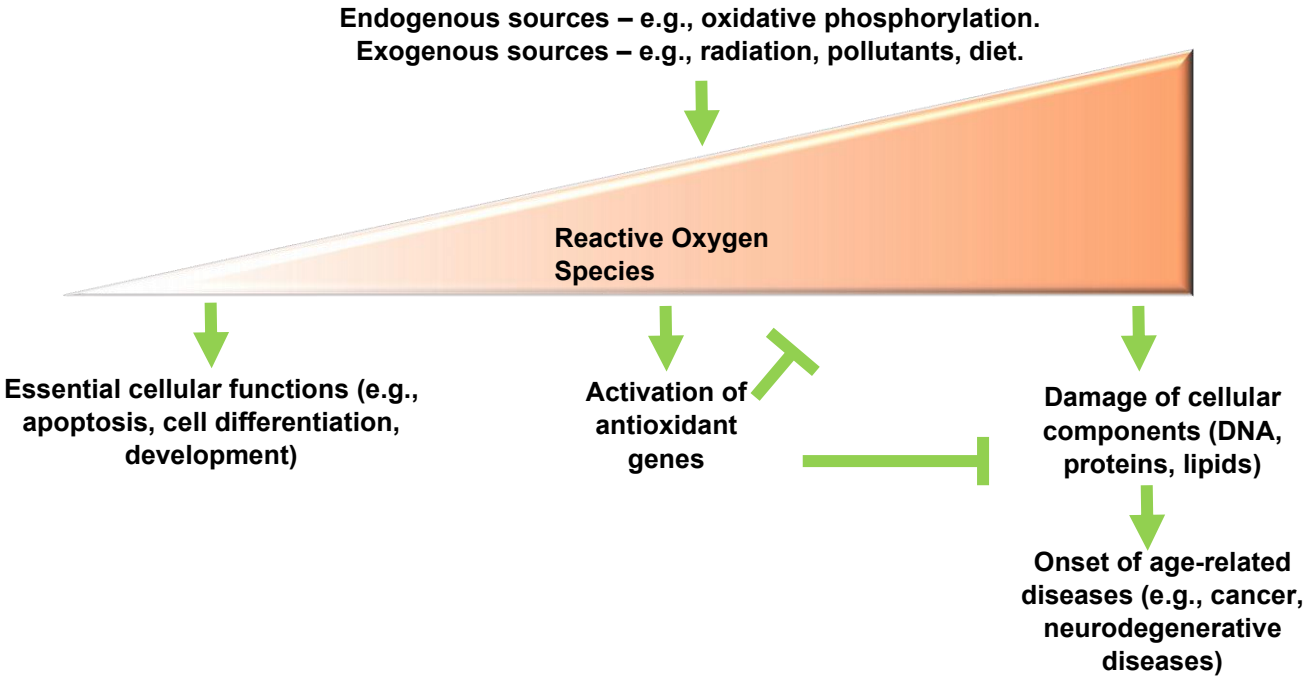

Figure 1.4. The cellular effects of different concentrations of ROS.

ROS can accumulate in cells from endogenous or exogenous sources and can have a multitude of effects on cells, dependent on the concentration and the type of ROS. At low levels, ROS have important roles in signalling cascades that modulate a variety of different processes, such as apoptosis, cell differentiation, and development. As the levels of ROS increase, this activates the expression of genes that encode antioxidants as a defence mechanism to resolve homeostasis and repair damage. However, if antioxidant mechanisms are overwhelmed this leads to oxidative stress and the damage of cellular components which has been linked to the onset of common age-related pathologies. It is therefore essential that cells can distinguish the types and levels of ROS to respond in an appropriate manner (Mittler, 2017, Brieger et al., 2012).

1.2.1 Types & sources of ROS

The three main ROS found in the cell are H_2O_2, hydroxyl radicals (•OH) and superoxide anions ($•^-O_2$). The hydroxyl radicals are the most reactive and damaging form of these ROS. As a result of their reactivity, hydroxyl radicals have a very short half-life of approximately 1 ns, and hence the damaging action of hydroxyl radicals occurs proximal to the site of their production (Cheeseman and Slater, 1993). However, despite this short half-life and hence restricted activity, hydroxyl radicals can react with many biomolecules and need to be tightly controlled. Although superoxide anions are not as reactive as hydroxyl radicals, they can cause some intracellular damage. At a low pH, superoxide anions can become protonated, forming another, more reactive radical $HO_2•$. However, it is estimated only 1% of superoxide anions are converted to this more damaging form within the cell (Cheeseman and Slater, 1993). The main significance of superoxide anions as a form of ROS is their conversion into H_2O_2. H_2O_2 displays weak oxidising abilities but can be readily broken down within the cell, so does not pose a big threat to cells. However, H_2O_2 can be further processed into hydroxyl radicals in the presence of transition metals and as a consequence can indirectly cause much intracellular damage. H_2O_2 is a relatively stable form of ROS that can travel relatively easily throughout cells because it possesses an ability to easily diffuse through hydrophobic membranes (Kohen and Nyska, 2002). Thus, although these three ROS are all capable of oxidation, the biggest threat is posed by their potential to produce the highly reactive hydroxyl radical.

As mentioned, cells are exposed to ROS from both endogenous and exogenous sources. ROS are produced within the cell as a by-product of several biological processes, such as oxidative phosphorylation. In some cases, they are also produced intentionally, for example during phagocytosis (Cheeseman and Slater, 1993). Cells also can be exposed to ROS from exogenous sources, such as exposure to UV radiation. The main sources of cellular ROS are discussed below.

1.2.1.1 Electron transport chain

The major source of intracellular ROS is from the action of electron transport chains, utilised in mitochondria during oxidative phosphorylation. Indeed, it is estimated that mitochondria generate 90% of all intracellular ROS (Balaban et al., 2005). Superoxide radicals are generated at two sites, complex I (NADH dehydrogenase) and complex III (ubiquinone cytochrome c reductase), through leaked electrons interacting with O_2 (Hirst et al., 2008, Tahara et al., 2009). In *S. cerevisiae*, oxidative phosphorylation does not utilise complex I and instead utilises three rotenone insensitive NADH dehydrogenase enzymes (Bakker et al., 2001). These enzymes also cause electron leakage through the oxidation of NADH, which then causes the production of superoxide anions by interaction with molecular oxygen (Fang and Beattie, 2003). Thus, mitochondria (mammalian cells and *S. cerevisiae*) possess specific antioxidant mechanisms, such as superoxide dismutase enzymes (SODs), catalase enzymes and the mitochondrial thioredoxin system, which attempt to counteract the production of ROS (Tirichen et al., 2021). These will be discussed in detail in Section 1.2.3, but briefly, SOD enzymes catalyse the conversion of superoxide anions into H_2O_2, which is then processed by the mitochondrial thioredoxin system and catalase enzymes (Jastroch et al., 2010). Efficient removal of H_2O_2 is essential to prevent the formation of the highly reactive hydroxyl radicals.

1.2.1.2 Transition metals

Numerous transition metals, such as copper, iron, zinc, cobalt and manganese, are utilised in many cellular processes. For example, iron is an essential nutrient, in humans the majority of all iron is incorporated into haemoglobin or myoglobin (Shikama, 2006). Transition metals are also crucial in providing stability to protein complexes, in protein folding, and in DNA/RNA binding, for example in the structure of the zinc finger (ZnF) motif (Palm-Espling et al., 2012, Iannuzzi et al., 2014, Cassandri et al., 2017). Iron is also a crucial nutrient in the formation of iron-sulphur (Fe-S) clusters which are involved in many cellular processes, perhaps most notably, in electron transfer systems for example during oxidative phosphorylation (Rouault and Tong, 2008). The ability of transition metals to function as cofactors in redox biology

also gives them key roles in metalloenzymes, which include SODs (Younus, 2018). For example, Mn-SODs contain a manganese ion that cycles between Mn^{3+} and Mn^{2+} to allow the detoxification of superoxide anions (Hassan and Schrum, 1994). Although the roles of transition metals in redox biology are important in many cellular processes, they can also react inappropriately producing ROS. Free iron ions participate in the Fenton reaction, a two-step process by which iron ions interact with superoxide anions and H_2O_2 to produce a hydroxyl radical (see Figure 1.5) (Winterbourn, 1995). Iron ions can then also participate in the Haber-Weiss reaction, which also generates hydroxyl radicals (Figure 1.5) (Kehrer, 2000). Consequently, the levels of metal within the cell requires tight regulation.

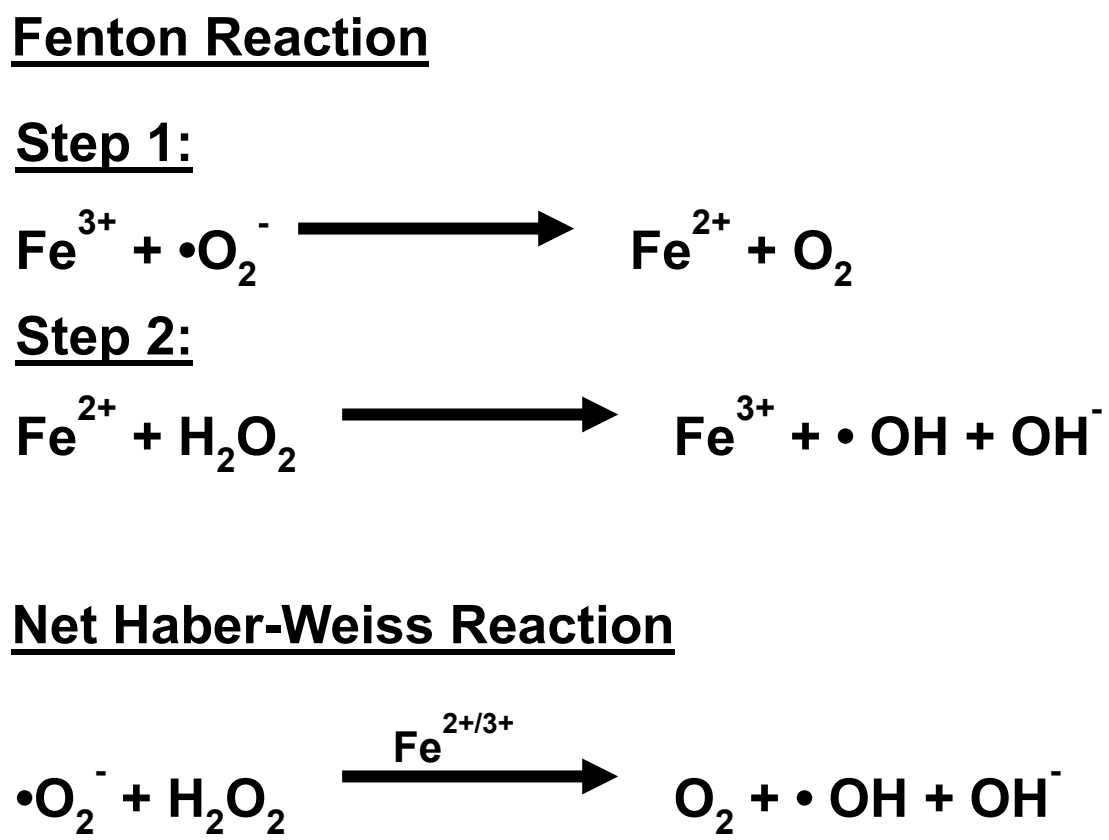

Figure 1.5. The Fenton reaction and the net Haber-Weiss reaction.

The Fenton reaction: Fe^{3+} reacts with a superoxide anion to generate molecular oxygen and Fe^{2+}. Fe^{2+} can then react with H_2O_2 to generate a hydroxyl radical and a hydroxide ion. **The net Haber-Weiss reaction:** In a multi-step process which redox cycles iron, superoxide anions interact with H_2O_2 to generate molecular oxygen, a hydroxyl radical and a hydroxide ion. Adapted from (Kehrer, 2000).

1.2.1.3 The immune response

The immune system is an important example of ROS production, where the ROS acts as a defence mechanism against pathogens. A well-studied example is the process of phagocytosis. When macrophage recognition of a pathogen occurs, it is engulfed and the macrophage begins to form the phagolysosome, an acidic compartment to kill the invading pathogen (Slauch, 2011). Formation of the phagolysosome relies on the delivery of various antimicrobial proteins, such as proteases and lysozyme (Garin et al., 2001). When the pathogen is sequestered into the phagolysosome, ROS (and reactive nitrogen species) are employed to degrade the pathogen. NOX2 (NADPH-dependent phagocytic oxidase) is assembled on the membrane of the phagolysosome and pumps free electrons into the compartment, allowing the conversion of oxygen molecules into superoxide anions, which are then processed into H_2O_2 and other forms of ROS (Slauch, 2011, Dupre-Crochet et al., 2013). This process, also termed the 'respiratory burst', is crucial for the efficient removal of pathogens by macrophages. CGD (chronic granulomatous disease) is a condition characterised by the inability of neutrophils to efficiently kill pathogens and is caused by defective NOX2 (Dinauer, 1993). The important roles of NOX2 and the respiratory burst in the generation of ROS in the immune response is demonstrated by the life expectancy of CGD patients being only 40 years (Arnold and Heimall, 2017). More recently, ROS have been shown to also contribute to adaptive immunity. For example, when T-cell receptors are activated, both H_2O_2 and superoxide anions are produced, which then regulate the action of various effector proteins (such as protein kinase C, PKC), altering cell metabolism (Cemerski et al., 2002). Thus, in certain contexts such as phagocytosis, the production of high levels of ROS is beneficial.

1.2.1.4 Radiation

Exogenous sources of ROS are mainly from radiation and xenobiotics. Radiation is encountered by cells from exposure to natural sources (e.g., the sun) or during medical procedures which include radiotherapy. Studies of the potential harm that can be caused by radiotherapy found that infrared (IR) radiation can easily penetrate cells

and cause the radiolysis of water molecules, ultimately generating ROS (Cui et al., 2019). Interestingly, x-rays can also produce the free radicals •H and •OH from water (Halliwell, 2006). Additionally, UVB radiation has been shown to generate intracellular ROS through catalase enzymes, whereby UVB is absorbed by the enzyme and converted into ROS which can then be detoxified by antioxidant mechanisms (see 1.2.3) (Heck et al., 2003).

1.2.1.5 Xenobiotics

Xenobiotics, a substance foreign to the cell such as drugs and food additives, can also result in the production of ROS. Exposure to certain xenobiotics and their derivatives (e.g., quinones) can directly generate ROS or increase levels of ROS by interfering with antioxidant mechanisms (Steffensen et al., 2020). Xenobiotics can also indirectly generate ROS. When exposed to xenobiotics, cells employ various mechanisms to digest or react to the foreign chemical, producing xenobiotic metabolism machinery (Klotz and Steinbrenner, 2017). The generation of this machinery, and the resultant metabolism of xenobiotics, can both generate ROS (Kehrer, 1993). Quinones are reactive compounds derived from aromatic molecules that are formed as metabolites of various xenobiotics, such as drugs and food (Bolton and Dunlap, 2017). Quinones are able to participate in redox cycling to generate semiquinone radicals, which can then in turn generate ROS (Bolton et al., 2000). An example is Vitamin K, an important nutrient in the production of proteins necessary for building bones and blood clotting. Vitamin K is metabolised into vitamin K hydroquinone through the action of two enzymes; NQO1 (NADPH Quinone Oxidoreductase 1) and NQR2 (NRH quinone oxidoreductase 2) (Gong et al., 2008). Vitamin K undergoes redox cycling reactions between its semiquinone form and quinone form, utilising O_2 and hence generating superoxide anions (Gong et al., 2008). Finally, it is estimated that up to 90% of Alzheimer's and Parkinson's disease cases are caused by some environmental factor, such as xenobiotics, rather than the genetics of the patient (Hofer et al., 2021). Interestingly, post-mortem analysis of the brains of Parkinson's disease revealed that they had been exposed to high levels of oxidative-stress (Dias et al., 2013). This oxidative stress is hypothesised to be due to the inhibition of neuromelanin, a pigment that is responsible for sequestering harmful molecules in the brain, such as xenobiotics

and excess levels of metals. Current models (under investigation) suggest that xenobiotics disturb the action of neuromelanin, which results in the release of various metal ions and xenobiotics into the brain, generating high levels of ROS and oxidative stress (Capucciati et al., 2021). Although further studies are required, it suggests a role for xenobiotic-induced ROS production in the onset of certain neurodegenerative diseases.

1.2.2 Effects of ROS

The presence of reactive ROS within the cell can damage many cellular components, predominantly proteins, DNA and lipids. The ways in which these biomolecules are affected by ROS are discussed below.

1.2.2.1 Proteins

Oxidation of proteins is an important modification that influences normal structures and functions (see Section 1.3). However, proteins can also be inappropriately oxidised and damaged by oxidation. Protein oxidation includes oxidation of amino acid side chains, oxidation of the peptide backbone or protein-protein cross-linking (Berlett and Stadtman, 1997). The high oxidising potential of ROS renders numerous amino acid side chains susceptible to oxidation which can inactivate protein function. Sulphur-containing residues, cysteine and methionine, are readily oxidised (Bin et al., 2017). Reversible methionine oxidation appears to have little effect on protein function, and has been hypothesised to function as a ROS-scavenging mechanism rather than to change protein function (Luo and Levine, 2009). Cysteine residues on the other hand can form disulphide bonds in response to ROS (Mythri et al., 2013). Disulphide bonds are reversible protein modifications, however irreversible oxidation of sulphur residues can also occur. The first oxidation reaction generates a sulphenic acid (-SOH) version of cysteine, which can be resolved into a disulphide or reduced back to the thiol state (Finkel, 2011). However, further oxidation can produce sulphinic ($-SO_2H$) and sulphonic ($-SO_3H$) acid forms, which are generally irreversible (Finkel, 2011). Interestingly, the sulphinic form can be reduced by the action of sulphiredoxin (Srx) proteins (Biteau et al., 2003). Srx proteins reduce cysteine under specific conditions,

such as under oxidative stress conditions, where Srx is translocated to the nucleus to reduce peroxidase enzymes (Noh et al., 2009). However, the formation of sulphonic acid is always irreversible (Biteau et al., 2003). Thus, the oxidation of cysteine residues in proteins can induce the formation of disulphide bonds, which can fulfil many regulatory roles, or inactivate the protein through irreversible oxidation.

Proteins can also become carbonylated on the side chains of threonine, proline, lysine and arginine residues in response to ROS (Weng et al., 2017). Carbonylation of these residues is irreversible and can affect other post-translational modifications of the protein, for example lysine residues can be modified with ubiquitin and UBLs and threonine can be phosphorylated. Consequently, carbonylation can have many effects on protein functions. The carbonylation of protein side chains in response to ROS is also used as a marker of oxidative stress, and has therefore been linked with various pathologies (Stadtman, 2006).

Alterations to the protein backbone can also be induced by ROS. Primarily hydroxyl radicals stimulate a series of reactions where the peptide backbone forms a carbon-centred radical which is then oxidised to form alkyl, alkylperoxyl, and alkoxyl radical intermediates (Berlett and Stadtman, 1997). These reactive intermediates are capable of reacting with and oxidising amino acid side chains (Berlett and Stadtman, 1997). However, in anaerobic or oxygen-limiting conditions, these reactions cannot proceed and in this case the carbon-centred radical can actually cross-link to different proteins (Berlett and Stadtman, 1997). Formation of alkyl radicals can also result in the fragmentation of the protein backbone by either the diamide or α-amidation pathways (Berlett and Stadtman, 1997). Finally, peptide chain cleavage can also be induced when ROS directly attack the side chains of proline, glutamate and aspartate residues (Garrison, 1987). Hydroxyl radicals interact with a hydrogen atom at the γ-carbon of the residue, which through a series of redox events causes the eventual cleavage of the peptide bond (Garrison, 1987).

1.2.2.2 DNA

DNA can also be damaged by ROS. In humans, it is estimated that 10^5 damage events occur to DNA each day/cell, including single-stranded breaks, double-stranded breaks, DNA cross-linking, or damage to a nucleotide/the DNA backbone (Bridge et

al., 2014). Notably, chemotherapeutic drugs, such as doxorubicin, elevate ROS levels within the cell as a mechanism of genotoxicity (Conklin, 2004).

ROS, primarily hydroxyl radicals, are known to induce single- and double-stranded breaks in the DNA backbone by hydrogen abstraction, creating a carbon-centred radical, which can then react to form numerous products (Juan et al., 2021). Oxidation can also cause mutations within the DNA code. The oxidation of guanine at the C8-position is a well-studied form of DNA oxidation, where guanine becomes hydroxylated by a hydroxyl radical forming the product 8-hydroxyguanine (Juan et al., 2021). Incorporation of 8-hydroxyguanine into DNA causes missense mutations, whereby the guanine nucleotide now functions as thymine, bonding to adjacent adenine bases (Kamiya et al., 1992). Other research also found that the incorporation of 8-hydroxyguanine can stimulate G – C and G – A transversions, although the primary mutation is G – T (Suzuki and Kamiya, 2016). The abundance of 8-hydroxyguanine in DNA is utilised as a key marker of oxidative stress, and has also been noted to be a major cause of cancer (Nakabeppu et al., 2006). As a result of the damaging effects of modified guanine, cells have evolved mechanisms to reverse this type of damage, but these are unable to repair all the mutations (Nakabeppu, 2014).

Interestingly, mitochondrial DNA (mtDNA) undergoes more DNA damage by ROS due to the proximal nature of the oxidative phosphorylation process and the lack of histones to protect the DNA (Richter et al., 1988). Many mutations that cause neuronal diseases, such as Parkinson's disease and ALS, are presumed to be introduced by the oxidation of mtDNA by ROS (Lawless et al., 2020). Interestingly, and perhaps unsurprisingly, the rate of 8-hydroxyguanine formation in mtDNA is approximately 16 times higher when compared to nuclear DNA (Richter et al., 1988).

It is clear that DNA damage is an extremely detrimental consequence of elevated ROS levels within the cell. These harmful effects of ROS are linked to age-related diseases which involve the accumulation of mutations, such as cancer and neurodegenerative diseases, and hence it is crucial for human health that ROS-related DNA damage is minimised.

1.2.2.3 Lipids

Lipids are hydrophobic biomolecules and hence are also susceptible to attack from hydroxyl radicals. Lipid peroxidation is induced when phospholipids, the predominant component of cellular membranes, are exposed to ROS (Juan et al., 2021). Hydroxyl radicals attack unsaturated fatty acids, generating a hydroperoxidised lipid and an alkyl radical (Juan et al., 2021). This oxidation can then stimulate further oxidation of proximal lipids. The effect of this lipid peroxidation is a decrease in bilayer thickness and alterations to membrane fluidity and integrity, consequently allowing easier movement of substances across the membrane (Yadav et al., 2019). In addition to perturbing membrane dynamics and integrity, lipid peroxidation can also affect the binding and function of membrane-bound proteins (Buettner, 1993). Membrane function is integral to many cellular processes and hence ROS-induced damage of these structures can have many harmful effects.

1.2.2.4 ROS in health and disease

Due to the ability of ROS to oxidise the key fundamental cellular components (proteins, DNA and lipids), the physiological consequences of these oxidation events have been linked with many aspects of human health and disease. Exposure of cells to ROS has been shown to regulate the process of aging, where exposure of macromolecules to ROS over time causes oxidative damage and the eventual loss of the macromolecules' functions (Liguori et al., 2018). Previously termed the free-radical theory of aging, this process is now referred to as the oxidative stress theory of aging (Beckman and Ames, 1998). Although the exact ways in which ROS promote cellular aging are not fully understood, the primary hypothesis is that ROS-induced damage ultimately induces cellular senescence. Indeed, there are numerous ways in which ROS can stimulate senescence. For example, ROS can reduce the action of Ca^{2+}-ATPase enzymes in the endoplasmic reticulum which induces cardiac senescence (Ureshino et al., 2014). ROS can also regulate the mTOR pathway in a variety of ways (Chandrasekaran et al., 2017). The mTOR pathway is an important signalling pathway involved in the regulation of various processes, including autophagy, cell growth and cell survival (Zoncu et al., 2011). Inhibition of the mTOR pathway, using the drug rapamycin, has increased the lifespan of various model organisms (Chung et al., 2013). ROS regulate

the mTOR pathway at various points, for example, certain ROS destabilise the interaction between mTOR and Raptor (Regulatory-associated protein of mTOR, an adaptor protein), modulating the mTOR pathway (Yoshida et al., 2011). ROS are also known to regulate matrix metalloproteases (MMPs), which are linked with cellular senescence and are found in high quantities in affected tissues of age-related diseases (Kar et al., 2010). For example, ROS are shown to regulate the activation of MMP1, an MMP that cleaves collagen, increasing cellular senescence (Kar et al., 2010). Indeed, treatment of cells with ROS or antioxidant inhibitors significantly increases the expression of MMPs (Wenk et al., 1999). Many studies have also linked oxidative damage to the shortening of chromosome telomeres, a crucial structure that determines cell senescence (von Zglinicki, 2000). For example, ROS can attack telomeres, causing the removal of POT1, a protein that aids telomere lengthening (Kawanishi and Oikawa, 2004). The specific mechanisms of how ROS regulate these processes, and other examples, are described in more detail in (Chandrasekaran et al., 2017).

As a result of these studies and many others, increased levels of ROS have been linked to the aging process and decreased life span in various model systems, for a review see (Santos et al., 2018). For example, increased levels of ROS were observed in the brains of older rats compared to the brains of younger rats (Driver et al., 2000). In addition, the exposure of *Caenorhabditis elegans* to mimetics of antioxidants increased their life span (Melov et al., 2000). Furthermore, several age-related pathologies have been attributed to oxidative stress (Stohs, 1995). However, despite the extensive links between elevated levels of ROS and decreased life span, there is also data that supports the hypothesis that ROS can have a positive role in the aging process. For example, work in insect cells revealed that ROS were crucial for the regulation of the insulin-signalling pathway, which increased the diapause process, a period of developmental rest necessary to increase life span (Zhang et al., 2017). Additionally, reverse electron transport by respiratory complex I generates ROS, a process that was found to increase the life span of *Drosophila* (Scialò et al., 2016). Thus, the functions of ROS in the aging process are complex and suggest both harmful and beneficial roles.

As a result of the links of ROS in lifespan, they have been implicated in the progression of many age-related pathologies. For example, in the progression of diabetes, long-

term exposure to ROS affects the expression of genes that reduce glucose secretion, and results in the secretion of defective insulin (Sha et al., 2020). ROS have also been linked to neurodegenerative diseases, such as Parkinson's disease and Alzheimer's disease. Post-mortem analysis of Parkinson's disease sufferers revealed high levels of 4-hydroxyl-2-nonenal (a by-product of lipid peroxidation) and 8-hydroxyguanine in the brain, thus lipid peroxidation and DNA oxidation may play a crucial role in disease progression (Anik et al., 2022). There are numerous ways in which ROS are thought to cause the onset of Alzheimer's disease. For example, build-up of lipid-based ROS causes an iron-dependent form of cell death (Ferroptosis), a process which has been cited as one of the key contributors of cell death in patients with Alzheimer's disease (Reichert et al., 2020). Moreover, amyloid-β is a peptide that accumulates in mitochondria of Alzheimer's disease patients, ultimately causing ROS generation (with the aid of transition metals such as Fe^{2+}), further damaging the brain. Finally, ROS have been linked to the progression of many cancers. Indeed, the oxidative switch is a process that increases the intracellular levels of ROS in cancer cells, and is considered a hallmark of essentially all cancers (Liou and Storz, 2010). There has been a very large numbers of studies that have investigated the relationships between ROS and cancers and hence only a few examples will be mentioned here. For a detailed review, see (Liou and Storz, 2010). It is notable that ROS-sensitive signalling pathways such as the MAP/Erk pathway, the PI3k/Akt pathway and IKK/ NF-κB signalling regulate several key processes in cancer progression (such as cell proliferation and differentiation, protein synthesis, glucose metabolism and cell survival) (Storz, 2005). One example of this type of regulation is the observation that exposure of cells to H_2O_2 and superoxide anions increases cell proliferation in various cancer cell lines (Storz, 2005). Indeed, consistent with this finding, treatment of cancer cells with antioxidants has been shown to inhibit proliferation (Behrend et al., 2003). These findings, together with many others, have established influential effects of ROS on cancer progression.

Hence, the links between ROS, the aging process and age-related diseases highlights the importance of understanding the mechanisms underlying how cells detect and respond to ROS within the cell.

1.2.3 Cellular defences against ROS

The cell has evolved various mechanisms which act to restore redox homeostasis when cells are exposed to oxidative stress. These include superoxide dismutases (SODs), catalase enzymes, peroxidases, the thioredoxin system and the glutathione system. Additionally, cells respond to high levels of ROS by inducing the expression of genes encoding components of these responses. This section will focus on these defences in *S. cerevisiae*.

Certain enzymatic responses (SODs, catalase enzymes and peroxidase enzymes) are considered the first line of defence against ROS in the cell and are reviewed below. The actions of these enzymes are summarised in Figure 1.6.

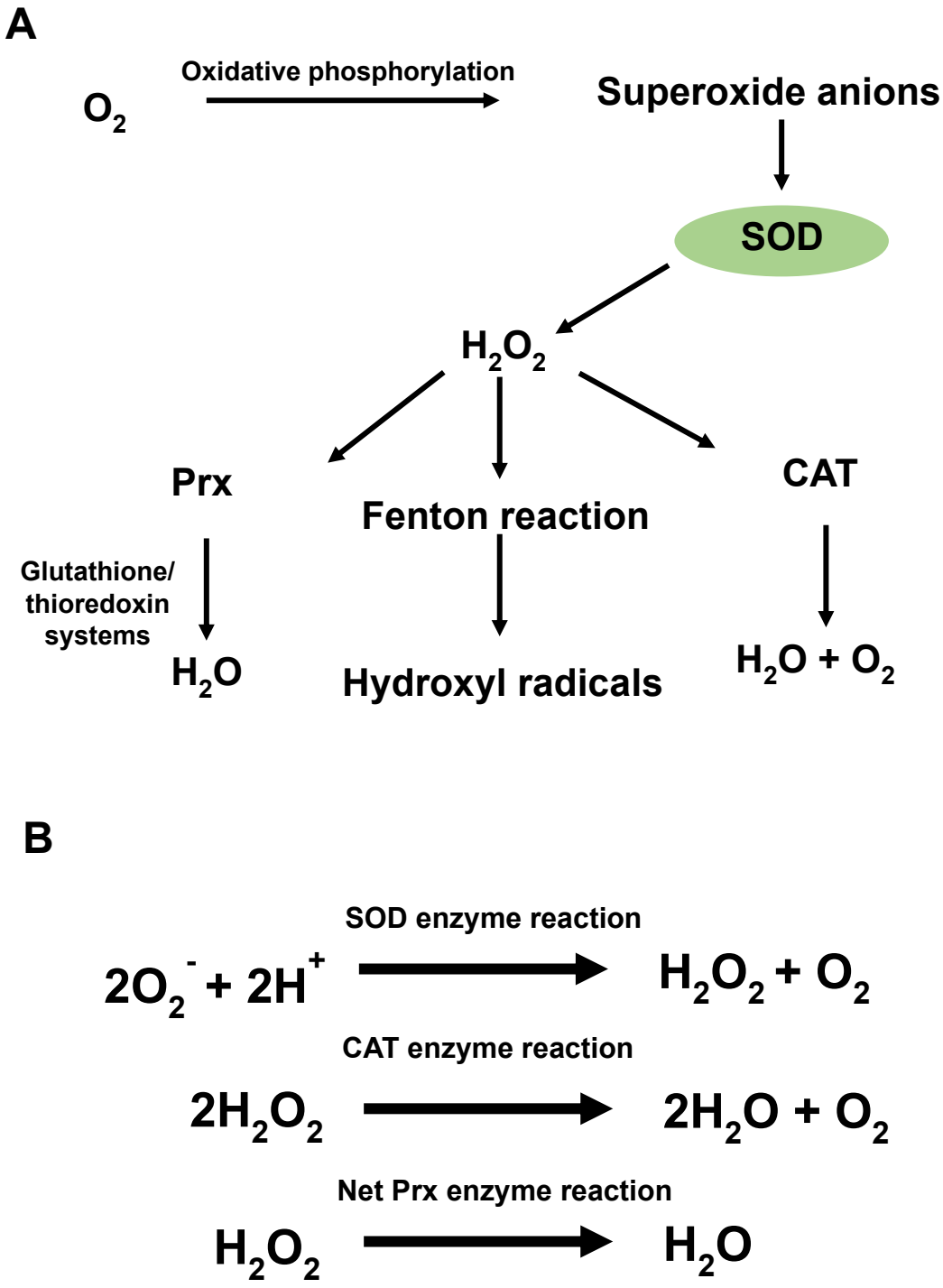

Figure 1.6. Summary of enzymatic defences against ROS.

(A) Superoxide anions are generated from molecular oxygen during oxidative phosphorylation (see 1.2.1.1). These superoxide anions are then metabolised to H_2O_2 by SODs, which can then be converted into H_2O and O_2 by catalase (CAT) enzymes, H_2O by peroxidase (Prx) enzymes (with the aid of the glutathione/thioredoxin system, see 1.2.3), or into damaging hydroxyl radical via the Fenton reaction (see 1.2.1.2). The diagram is adapted from (Nandi et al., 2019). (B) The reaction mechanisms for SODs, catalase enzymes and Prx enzymes.

1.2.3.1 Superoxide dismutase enzymes

Superoxide dismutase enzymes (SODs) are metalloenzymes that utilise their metal ion to reduce superoxide anions into H_2O_2 and water (Figure 1.6). There are four types of SODs which are classified by the metal ion utilised in the redox reaction; Mn-SODs, Cu-Zn-SODs, Fe-SODs and Ni-SODs (Younus, 2018). *S. cerevisiae* cells contain 2 SODs, Sod1, a cytosolic Cu-Zn-SOD, and Sod2, a mitochondrial Mn-SOD (Rattanawong et al., 2015). The immature form of Sod1 binds the copper-containing chaperone, Ccs1, which promotes the binding of the stabilising zinc ion. Ccs1 also induces the formation of a disulphide bond in Sod1, which allow the transfer of the catalytic copper ion to Sod1 and activates the protein (Boyd et al., 2019). Interestingly, a small amount of Sod1 has also been found to localise to the mitochondrial membrane (Sturtz et al., 2001) and movement of Sod1 into the mitochondria is also facilitated by the Ccs1 chaperone (Field et al., 2003).

In contrast to Sod1, Sod2 can only bind manganese, and hence become active, within the mitochondria. Smf2, a manganese transporter, and Mtm1, a mitochondrial carrier protein, are required for this activation (Luk et al., 2005). Given the mitochondrial location of Sod2, its primary role is scavenging superoxide produced by oxidative phosphorylation. The mitochondrially localised fraction of Sod1 also contributes to this process (Field et al., 2003). Furthermore, *sod2*Δ cells display hypersensitivity to hyperoxia and cannot grow under respiratory conditions (van Loon et al., 1986, Guidot et al., 1993). Thus, Sod2 is important for the detoxification of endogenous ROS but does not seem to respond to exogenous ROS. This is in contrast to *sod1*Δ mutants which are hypersensitive to exogenous ROS (such as the superoxide generator menadione), in addition to exhibiting poor growth under respiratory conditions (Gralla and Valentine, 1991, Longo et al., 1996). The action of SODs is conserved in eukaryotes, and interestingly, the SOD2 human homologue (and the SOD1 human homologue when targeted to mitochondria) can rescue the phenotypes observed in *sod2*Δ cells (Whittaker and Whittaker, 2012).

1.2.3.2 Catalase enzymes

Catalase enzymes play important roles in the detoxification of H_2O_2. In a two-step reaction, two molecules of H_2O_2 are metabolised into two H_2O molecules and one O_2 molecule (Figure 1.6) (Deisseroth and Dounce, 1970). Two catalase enzymes, Cta1 and Ctt1, have been identified in *S. cerevisiae* which are encoded by the *CTA1* and *CTT1* genes, respectively (Traczyk et al., 1985, Skoneczny and Rytka, 2000). These catalase enzymes are located in different cellular compartments, Cta1 is localised to the peroxisomes and mitochondria whilst Ctt1 is localised to the cytoplasm (Lapinskas et al., 1993). Although Cta1 and Ctt1 are functionally similar, Cta1 displays more structural similarity to the catalase enzymes expressed in *C. tropicalis* (Hörtner et al., 1982). Both Cta1 and Ctt1 can be removed simultaneously from cells without loss of viability, suggesting possible redundancy between catalase enzymes and other antioxidant mechanisms (Izawa et al., 1996). Interestingly, however, analysis of the single mutants has revealed that each protein has specific roles. Cta1 functions to reduce H_2O_2 in the peroxisomes that are produced during fatty acid β-oxidation (Cohen et al., 1985). In mitochondria, Cta1 reduces the H_2O_2 produced by the action of SOD enzymes that have catalysed the breakdown of superoxide anions produced during oxidative phosphorylation (Sturtz et al., 2001). On the other hand Ctt1, localised in the cytoplasm, is important in the general oxidative stress response by protecting proteins from harmful oxidation (Jamieson, 1998). Interestingly, *ctt1*Δ cells are hyper-sensitive to H_2O_2 but this is not observed in *cta1*Δ cells (Martins and English, 2014). Thus, Ctt1 and Cta1 have distinct roles within the oxidative stress response.

1.2.3.3 Peroxidase enzymes

Peroxidases are a class of isoenzymes that catalyse, in a series of redox reactions, the metabolism of H_2O_2 into water (Figure 1.6) (Khan et al., 2014). In *S. cerevisiae* there are three classes of peroxidase enzymes, Prx enzymes (peroxiredoxins) and Gpx enzymes (glutathione peroxidases) that utilise catalytic cysteine residues to reduce H_2O_2, and Ccp1, a peroxidase that utilises a heme group (Avery and Avery, 2001, Rhee et al., 2005, Charizanis et al., 1999). In *S. cerevisiae* there are 5 Prx enzymes (Tsa1, Tsa2, Dot5, Ahp1, Prx1), 3 Gpx enzymes (Gpx1, Gpx2, Gpx3) and

one heme peroxidase, Ccp1. These enzymes have different subcellular localisations; Tsa1 and Tsa2 are found in the cytosol, Ahp1 is found in the cytosol and tethered to the plasma membrane, Dot5 is a nuclear protein, Prx1 is present in mitochondria, Gpx1 is found in the cytosol and the peroxisomal matrix, Gpx2 is cytosolic and nuclear, Gpx3 is cytosolic and mitochondrial, and Ccp1 is found in mitochondria (Wong et al., 2004, Erman and Vitello, 2002). Prx and Gpx enzymes were initially classified by the protein that they primarily use as their reductant; Prx enzymes primarily utilise thioredoxin as their reductant, and Gpx enzymes typically utilise glutathione as their reductant. However, all three Gpx enzymes in *S. cerevisiae* are classified as phospholipid hydroperoxide Gpx enzymes (PHGpx), which means that they primarily rely on molecules, such as thioredoxin, as electron donors instead of utilising glutathione as an electron donor (as observed with classical Gpx enzymes (cGpx)) (Avery and Avery, 2001).

Prx enzymes are classified by whether one cysteine residue (1-Cys) or two cysteine residues (2-Cys) is involved in catalysis, and 2-Cys Prx enzymes can be further classified into typical or atypical 2-Cys enzymes (Poole, 2007). However, all Prx enzymes utilise a conserved cysteine residue, the peroxidatic cysteine (C_P), that becomes oxidised upon the reduction of H_2O_2. 2-Cys Prx enzymes utilise a second cysteine, the resolving cysteine (C_R), that forms a disulphide with the C_P residue to complete catalysis; the C_P residue of typical 2-Cys Prx enzymes binds to a C_R residue of another Prx, whilst the C_P residue of atypical Prx bind to a C_R residue within the same Prx enzyme (Zhu et al., 2012). 1-Cys enzymes do not utilise another cysteine residue, but instead rely on an electron donor (Rhee, 2016). In *S. cerevisiae*, this electron donor was actually found to be glutathione for 1-Cys Prx enzymes (Greetham and Grant, 2009). All Gpx enzymes in *S. cerevisiae* function as atypical 2-Cys peroxidase enzymes; Gpx2 and Gpx3 preferentially use thioredoxin as an electron donor, whereas Gpx1 uses both thioredoxin and glutathione (Delaunay et al., 2002, Tanaka et al., 2005, Ohdate et al., 2010). Conversely, Ccp1 (cytochrome c peroxidase) uses iron in a series of redox reactions to reduce H_2O_2 to water (Charizanis et al., 1999).

Interestingly, *S. cerevisiae* cells which lack all 5 Prx enzymes are still viable, suggesting that there may be functional overlap between Prx enzymes and other antioxidant mechanisms (Wong et al., 2004). Indeed, proteins of other antioxidant

pathways, including Gpx and Glr enzymes (discussed later), were upregulated in cells lacking the 5 Prx (Wong et al., 2004). However, despite retaining viability, cells lacking all 5 Prx did display increased sensitivity to peroxide stress revealing an important role for Prx enzymes in peroxide detoxification. Of the five Prx enzymes in *S. cerevisiae*, Tsa1 and Tsa2, which have very similar protein sequences, have been the most extensively studied. For example, *tsa2*Δ cells display a greater sensitivity to H_2O_2 when compared with sensitivity associated with *tsa1*Δ cells, however the double *tsa1*Δ*tsa2*Δ mutant confers an even greater H_2O_2-sensitive phenotype (Wong et al., 2002). This suggests that these proteins, despite their high degree of similarity of protein sequences and mechanism of action, have both overlapping and distinct functions in the response of cells to H_2O_2. There is also evidence of distinct roles for the different Gpx enzymes in *S. cerevisiae*. For example, *gpx3*Δ cells, but not cells lacking either Gpx1 or Gpx2, display increased sensitivity to H_2O_2 stress (Inoue et al., 1999). However, the expression of *GPX2*, but not *GPX3*, was upregulated in response to oxidative stress (Inoue et al., 1999). Interestingly, expression of *TSA1* was not induced in *gpx3*Δ strains, whilst the Gpx proteins are upregulated in *tsa1*Δ cells (Inoue et al., 1999). Together, these data suggest significant functional overlap between individual Prx/Gpx enzymes, and also functional interactions between the two enzyme families.

Prx and Gpx enzymes have also been shown to have roles outside of their functions in peroxide detoxification. For example, Gpx3 and Tsa1 are known regulators of responses to H_2O_2 in certain strain backgrounds of *S. cerevisiae* (discussed in Section 1.2.3.3). In addition, Tsa1 can function as a protein chaperone in response to oxidative stress by binding unfolded proteins to prevent their aggregation (MacDiarmid et al., 2013). *In vitro* studies have suggested this chaperone function is important in heat tolerance and in protection of ribosomal subunits in response to DTT (Jang et al., 2004, Rand and Grant, 2006). *In vivo* studies have also shown that this chaperone activity is important in protein homeostasis in low-zinc conditions (MacDiarmid et al., 2013). Tsa1 and Tsa2 have both also been linked to protection from nitrosative stress (Wong et al., 2002).

1.2.3.4 The thioredoxin system

The thioredoxin system involves thioredoxins (Trx), small, heat-stable enzymes which can reduce disulphides within other proteins (Lee et al., 2013b). Trx proteins, and other proteins involved in redox cycling such as Grxs, utilise a thioredoxin fold structure, composed of 4/5 β-sheets flanked by 3 α-helices (Martin, 1995). Trx proteins utilise two catalytic cysteine residues in the highly conserved CXXC motif, where one cysteine initially forms a disulphide with a thiol group of the target protein. The second cysteine of the CXXC motif then forms an intramolecular disulphide with the first cysteine of the CXXC, effectively reducing the target protein. Thioredoxin reductase proteins (Trr) then reduce Trx using NADPH as an electron donor, recycling thioredoxin for further use (Nagarajan et al., 2017). *S. cerevisiae* cells contain three Trx proteins (Trx1, Trx2, Trx3) and two Trr proteins (Trr1, Trr2); Trx1, Trx2 and Trr1 are localised in the cytoplasm, and Trx3 and Trr2 are localised in mitochondria (Pedrajas et al., 1999). Trx proteins react slowly and hence inefficiently with H_2O_2 (Chae et al., 1994). Instead, Trx proteins often modulate cellular levels of ROS indirectly through their interactions with oxidised peroxiredoxins (Netto and Antunes, 2016). The relationship between Trx, Trr and Prx proteins is summarised in Figure 1.7.

Interestingly, individual deletion of the genes encoding Trx1, Trx2, Trr1 and Trr2 all increased the sensitivity of cells to H_2O_2 (Garrido and Grant, 2002). Indeed, further studies of the roles of the cytoplasmic thioredoxins, Trx1 and Trx2, revealed that Trx2 is more important for defence against exogenous H_2O_2 than Trx1 and, moreover, that the expression of *TRX2* is increased relative to the induction of *TRX1* in response to H_2O_2 (Garrido and Grant, 2002). In contrast to these thioredoxin system proteins, *trx3*Δ cells did not exhibit this increased sensitivity to H_2O_2 (Trotter and Grant, 2005). These results suggest that Trr2 has a secondary role in addition to that associated with interaction with Trx3. It was also observed that the glutathione reductase Glr1 (see 1.2.3.2.2) and Trr2 both influenced the oxidation state of Trx3, indicating that Trx3 is regulated by Glr1 as well as Trr2 (Trotter and Grant, 2005). Furthermore, these results revealed that there is functional overlap between the glutathione and the thioredoxin systems (Trotter and Grant, 2005). These data suggesting functional overlap is consistent with the finding that the inviability of *S. cerevisiae* cells simultaneously lacking thioredoxins and glutaredoxins can be rescued when either one thioredoxin or

one glutaredoxin was expressed in these mutant cells (Draculic et al., 2000). Despite evidence of functional overlap between the thioredoxin system and the glutathione system, each system displays a certain degree of specificity and, moreover, are activated in response to different types of ROS. For example, in *S. cerevisiae* the thioredoxin system is activated in response to H_2O_2 but not diamide whilst in contrast the glutathione system is activated in response to both of these oxidising agents (Wheeler et al., 2003, Garrido and Grant, 2002).

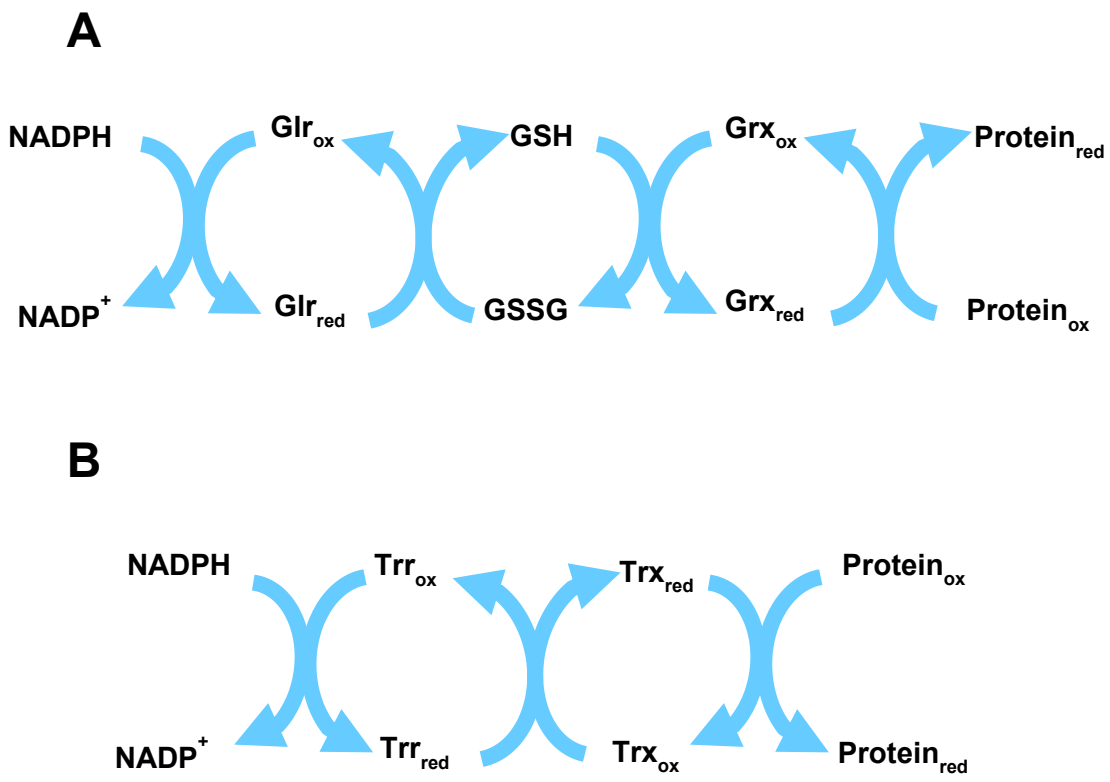

Figure 1.7. Redox cycling in the glutaredoxin and the thioredoxin systems.

(A) The glutaredoxin system. Proteins are oxidised by ROS, which are then reduced by Grx proteins. These oxidised Grx proteins are subsequently reduced by glutathione, and oxidised glutathione is in turn reduced by Glr proteins. Finally, Glr proteins are reduced by NADPH. (B) The thioredoxin system. Proteins are oxidised by ROS, which are then reduced by Trx proteins. These oxidised Trx proteins are subsequently reduced by Trr proteins, which are then finally reduced by NADPH. In many cases within the cell, the oxidised protein in both of these systems are the respective peroxidase enzymes.

1.2.3.5 The glutathione system

The glutathione system utilises a class of proteins, glutaredoxins (Grx) which, similarly to thioredoxins, can reduce proteins and in the process become oxidised (Figure 1.7) (Ogata et al., 2021). Grx is then reduced by glutathione, which in turn is reduced by glutathione reductase (Glr) which is finally reduced by NADPH (Figure 1.7) (Harlan et al., 1984). *S. cerevisiae* cells express 8 Grx proteins (Grx1 – Grx8) and one Glr protein, Glr1. There are 3 cytoplasmic di-thiol Grx proteins, Grx1, Grx2 and Grx8, which exhibit overlapping abilities to reduce proteins utilising two cysteine residues in the Grx protein (Herrero and de la Torre-Ruiz, 2007). The other Grx proteins are mono-thiol, and are localised to either the nucleus (Grx3 and Grx4), mitochondria (Grx5) or the endoplasmic reticulum/Golgi apparatus (Grx6 and Grx7) (Luo et al., 2010). Grx proteins appear to have different roles in ROS responses. For example, Grx1 and Grx5 are important for cellular responses to menadione (superoxide generator) and H_2O_2, whereas Grx2 only functions in response to H_2O_2 (Rodríguez-Manzaneque et al., 1999, Luikenhuis et al., 1998). Unlike the thioredoxin system in *S. cerevisiae* there is only one glutathione reductase, Glr1, which is localised to the cytosol and mitochondria (Collinson and Dawes, 1995).

The key molecule in the glutathione system is glutathione, an abundant protein that functions as a cellular buffer to ROS (Forman et al., 2009). Glutathione is a tripeptide consisting of cysteine, glutamate and glycine residues that is synthesised via a two-step reaction; the first step is catalysed by γ-glutamylcysteine synthetase (*GSH1*), the second is catalysed by glutathione synthetase (*GSH2*) (Tang et al., 2015). Interestingly, *gsh1*Δ cells are inviable in minimal media that does not contain glutathione, and *gsh1*Δ cells grown in media containing glutathione display hypersensitivity to H_2O_2 and superoxide (Stephen and Jamieson, 1996). The cysteine residue of glutathione is able to become oxidised and glutathione has a low redox potential. The oxidation status of glutathione is tightly maintained by NADPH and hence it is often found in the reduced state (GSH) within the cell (Penninckx, 2002). Glutathione can directly reduce ROS within the cell, and in the process becomes oxidised to GSSG, or can bind other cysteine-containing proteins by forming a disulphide bond with the protein to protect them from irreversible oxidation (Xiong et

al., 2011). Glr1 can reduce GSSG to GSH (Figure 1.7), a process that is vital to maintain redox homeostasis.

1.2.3.6 Regulation of gene expression in ROS responses

Another defence mechanism in response to ROS is the activation of the expression of genes whose encoded proteins are involved in restoring homeostasis and in damage repair. In *S. cerevisiae*, Yap1 and Skn7 are the main transcription factors that are important for the response of cells to oxidants (Taymaz-Nikerel et al., 2016, Herrero et al., 2008).

Yap1 is a member of the yeast activator protein (YAP) family, a family of bZIP transcription factors that contains 7 other members (Yap2 – Yap8) (Rodrigues-Pousada et al., 2019). Yap transcription factors are a member of the wider AP-1 family of transcription factors and were originally identified by their ability to bind to the AP-1 recognition element in promoters (Yan et al., 1998). Yap proteins are activated in response to various stress conditions; for example, Yap2 is activated in response to elevated levels of cadmium, Yap4 and Yap6 are activated in response to osmotic shock, and importantly, Yap1 is activated in response to oxidative stress (Rodrigues-Pousada et al., 2019). Yap transcription factors modulate gene expression by binding the promoters of target genes in the Yap response element (YRE) (Tan et al., 2008). Early studies revealed that Yap1 induces the expression of *TRX2* in response to various oxidising agents (including H_2O_2 and diamide) (Kuge and Jones, 1994). However, since then, Yap1 has been shown to regulate the expression of approximately 70 genes, including the antioxidant encoding genes *GPX3*, *TSA1*, *TRR1* and *TRX2* (Yan et al., 1998, Mulford and Fassler, 2011).

The activity of Yap1 is regulated by the nuclear exportin Crm1 and the nuclear importin Pse1 (Yan et al., 1998, Isoyama et al., 2001). Yap1 contains a nuclear export signal (NES) and the protein is exported from the nucleus to the cytosol in unstressed conditions in a Crm1-dependent manner (Yan et al., 1998). Furthermore, Yap1 is maintained in a reduced state by the thioredoxin system (Izawa et al., 1999). When oxidative stress occurs the Crm1-Yap1 interaction is disrupted by oxidation events, and consequently, the NES of Yap1 is inhibited and Yap1 accumulates in the nucleus

through the action of Pse1 to regulate gene expression (Isoyama et al., 2001). The oxidation of Yap1 in response to H_2O_2 is reliant on different proteins depending on the strain background. In the BY4741 strain background Ybp1 and Gpx3, a peroxidase that is regulated by the thioredoxin system, are essential for Yap1 activation in response to H_2O_2 (Delaunay et al., 2002). Gpx3 is firstly oxidised at its C36 residue, and the signal is transduced to Yap1 by forming an intermolecular disulphide between C36 of Gpx3 and C598 of Yap1. The disulphide is then resolved into an intramolecular disulphide which involves C598 and C303 of Yap1. This oxidation of Yap1 blocks the NES and activates the protein (Wood et al., 2003). As a by-product of Yap1 oxidation Gpx3 forms an intramolecular disulphide, which is reduced by the thioredoxin system. Ybp1 forms a complex with Yap1 and Gpx3 and functions to chaperone disulphide bridge formation between Yap1 and Gpx3 (Veal et al., 2003, Bersweiler et al., 2017). The Gpx3/Ybp1-dependent activation of Yap1 is summarised in Figure 1.8. Interestingly, in *C. albicans* Cap1, which is the homologue of Yap1 in *S. cerevisiae*, is activated in response to H_2O_2 using the homologues of Gpx3 and Ybp1 (same names in *C. albicans*) indicating that this activation mechanism is conserved in closely related yeast (Patterson et al., 2013). However, Ybp1 is mutated in the W303 strain background of *S. cerevisiae* and in this case Yap1 oxidation, nuclear localisation and activation in response to H_2O_2 is regulated by Tsa1 (Figure 1.8) (Ross et al., 2000). Intriguingly, the distantly related yeast *S. pombe* Pap1, the homologue of Yap1 in *S. cerevisiae*, is activated in response to H_2O_2 using Tpx1 the homologue of Tsa1 (Calvo et al., 2013). Hence, different mechanisms regulate the activation of Yap1 and its homologues in response to H_2O_2, dependent on the genetic background of the yeast.

Interestingly, other oxidising agents activate Yap1 by different mechanisms. For example, disulphide bridges are formed in the C-terminal end of Yap1 in response to diamide. Indeed, cysteine residues essential for Yap1 activation in response to H_2O_2 are not necessary for Yap1 activation in response to diamide (Delaunay et al., 2000). Interestingly, Yap1 can be activated by menadione (superoxide generator) by both of the mechanisms described above (Azevedo et al., 2003). Regulation of Yap1 activity is also linked to Trx1, Trx2 and Trr1 activity in the thioredoxin system, which act to reduce oxidise Yap1 (Izawa et al., 1999, Delaunay et al., 2000). Yap1 therefore demonstrates that proteins (Gpx3, Tsa1, Trx1, Trx2, Trr1) which act to restore redox

homeostasis and repair damage are also involved in the regulation of ROS-sensing mechanisms.

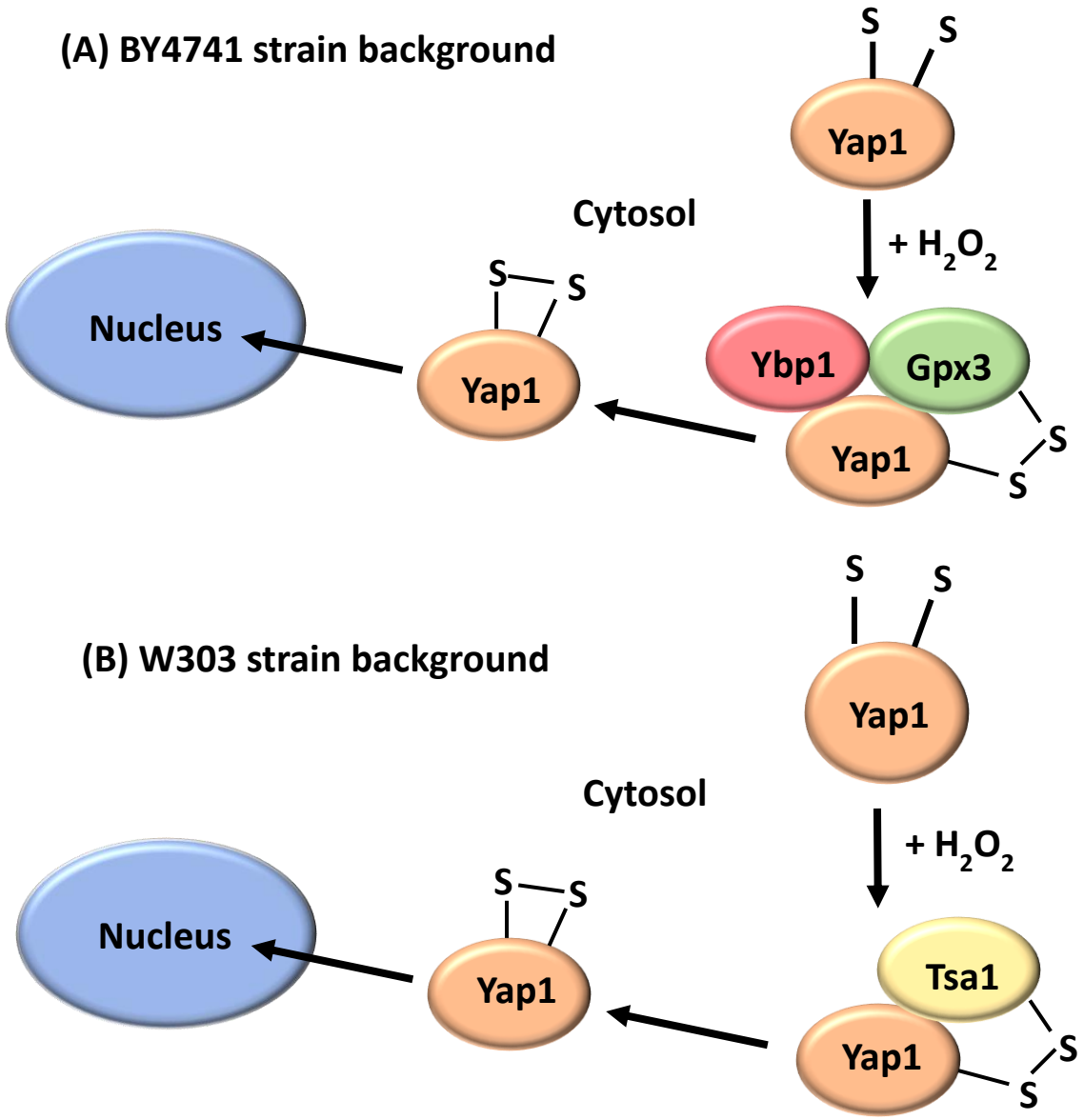

Figure 1.8. Yap1 activation in different *S. cerevisiae* strain backgrounds.

In all *S. cerevisiae* strain backgrounds, in unstressed cells reduced Yap1 is exported from the nucleus to the cytoplasm in a Crm1-dependent manner. However, H_2O_2 exposure results in Yap1 oxidation which disrupts the Crm1/Yap1 interaction. (A) In BY4741 cells Ybp1 promotes the formation of a Yap1 intermolecular disulphide complex with Gpx3, which is then resolved to an intramolecular Yap1 disulphide. (B) In W303 cells which lacks a wild-type Ybp1 protein, Tsa1, rather than Gpx3, forms an intermolecular disulphide complex with Yap1. This is then also resolved to an intramolecular Yap1 disulphide. (A & B) In both strain backgrounds, formation of the Yap1 intramolecular disulphide promotes the activation and the nuclear accumulation of Yap1 and consequently transcription of Yap1 target genes.

Skn7 is another transcription factor with important roles in the oxidative stress response in *S. cerevisiae*. Indeed, *skn7*Δ cells exhibit increased sensitivity to H_2O_2 stress (Krems et al., 1996). Skn7 is also important in other cellular processes, such as cell wall biosynthesis and the regulation of G1 cyclin genes (Brown et al., 1993, Morgan et al., 1995). Interestingly, the activity of Skn7 in the regulation of gene expression in response to oxidative stress is mediated through interaction with Yap1 (Mulford and Fassler, 2011). Indeed, antioxidant encoding genes which are activated by both Yap1 and Skn7 contain adjacent binding sites for each transcription factor in their promoters, suggesting that the two proteins cooperate to induce the expression of target genes (Mulford and Fassler, 2011). Consistent with this, coimmunoprecipitation experiments provided evidence that supports the interaction of Yap1 and Skn7 (Mulford and Fassler, 2011). Interestingly, when Yap1 translocates to the nucleus in response to oxidative stress, Yap1 can bind Skn7 which is always present in the nucleus. Moreover, specific cysteine residues of Yap1 (C303, C598 and C629) are essential for Yap1 and Skn7 interactions (Mulford and Fassler, 2011). Acting together, Yap1 and Skn7 induce the expression of a number of genes encoding antioxidants (such as *CCP1, TSA1* and *CTT1*) which are important for responses to oxidative stress (Charizanis et al., 1999, He and Fassler, 2005).

1.3 ROS sensing and intracellular signalling

As discussed previously in this chapter, high levels of ROS can damage intracellular components (Section 1.2.2), but lower levels of ROS are also essential as signalling molecules (Figure 1.4). For example, ROS function as second messengers in the immune response. The innate immune system relies on the recognition of PAMPs (pathogen-associated molecular patterns) and DAMPs (damage-associated molecular patterns) to stimulate a response (Schieber and Chandel, 2014). ROS have been shown to be vital for this recognition, and also function in inflammasome activation, which detects pathogens, initiates pro-inflammatory cytokines and stimulates cell death (Allen et al., 2009). Amongst the different types of ROS, H_2O_2 is particularly suitable for a role as a signalling molecule. H_2O_2 is stable when compared to reactive radicals and its physiochemical properties allow easy transport within a cell, for example through the action of membrane transporter aquaporin (Wang et al., 2020a).

Furthermore, the production and degradation of H_2O_2 by specific enzymes allows temporal and spatial control over its action (Forman et al., 2004). For example, H_2O_2 is produced in response to the EGF and PDGF growth factors to regulate cell proliferation (Bae et al., 1997). H_2O_2 inactivates the phosphatase 1B and PTEN phosphatases, altering downstream signalling which increases proliferation (Bae et al., 1997, Lee et al., 2002). Hence, if antioxidant mechanisms were activated in response to any concentration or type of ROS, then important cellular processes would be affected. It is therefore essential that cells can distinguish both the type and the concentration of the ROS present in order to respond in an appropriate manner.

As described above (1.2.3.3) *S. cerevisiae* cells respond to the presence of different oxidising agents (such as H_2O_2 and diamide) using different signalling mechanisms that regulate the Yap1 transcription factor. Cells can also detect and respond to different concentrations of ROS in an appropriate manner. For example, in *S. pombe* oxidised Tpx1 activates the Yap1 homologue, Pap1, at low levels of H_2O_2 (Quinn et al., 2002). However, at higher levels of H_2O_2, Tpx1 becomes inactivated by oxidation which inhibits activation of Pap1 but promotes the activation of the Sty1 stress-activated MAPK and the Atf1 transcription factor (Quinn et al., 2002). This alters the patterns of induced gene expression as the concentration of H_2O_2 increases (Quinn et al., 2002). Interestingly, increasing evidence suggests that the oxidation of ubiquitin/UBL conjugation/deconjugation enzymes is also utilised as mechanisms to sense and respond to both the type and the concentration of ROS present in the cell (discussed below).

1.3.1 Regulation of sumoylation by ROS

Many of the enzymes involved in the conjugation and deconjugation of ubiquitin and UBL proteins utilise a catalytic cysteine residue (see 1.1). This raises the possibility that the relative sensitivity of these catalytic cysteine residues to oxidation may be involved in ROS sensing and signal transduction. Indeed, when mammalian cells are exposed to low levels of H_2O_2, the SUMO E1 Uba2 and E2 Ubc9 form a disulphide complex which prevents further sumoylation (Figure 1.9) (Bossis and Melchior, 2006). However, the SENPs, which remove sumoylation, remain active at low H_2O_2 resulting in the desumoylation of many substrates (Bossis and Melchior, 2006). However, in

contrast, at high levels of H_2O_2, although the Uba2 and Ubc9 disulphide complex is retained, and the SENP SENP1 is inactivated via an intermolecular disulphide at its catalytic cysteine residue, C603, and C613 of another SENP1 monomer (Figure 1.9) (Xu et al., 2008). Consequently, although new sumoylation is prevented by inactivation of Uba2 and Ubc9, protein sumoylation present prior to the addition of high levels of H_2O_2 is retained as SENP1 can no longer desumoylate substrates (Bossis and Melchior, 2006, Xu et al., 2008). The *S. cerevisiae* SENP, Ulp1, was also found to be oxidised in this manner (Xu et al., 2008). Importantly, these oxidation events were found to be reversible and are suggested to be important in the prevention of irreversible sulfhydryl oxidation. This differential sensitivity of the E1/E2 enzymes and the SENPs to inactivation by different levels of H_2O_2 determines specific substrate sumoylation patterns depending on the level of H_2O_2 detected. Interestingly, this differential oxidation of the sumoylation machinery regulates the ATM–Chk2 DNA damage response pathway and hence cell survival (Stankovic-Valentin et al., 2016). These data highlight the significance of the regulation of SUMO modification in responses to ROS.

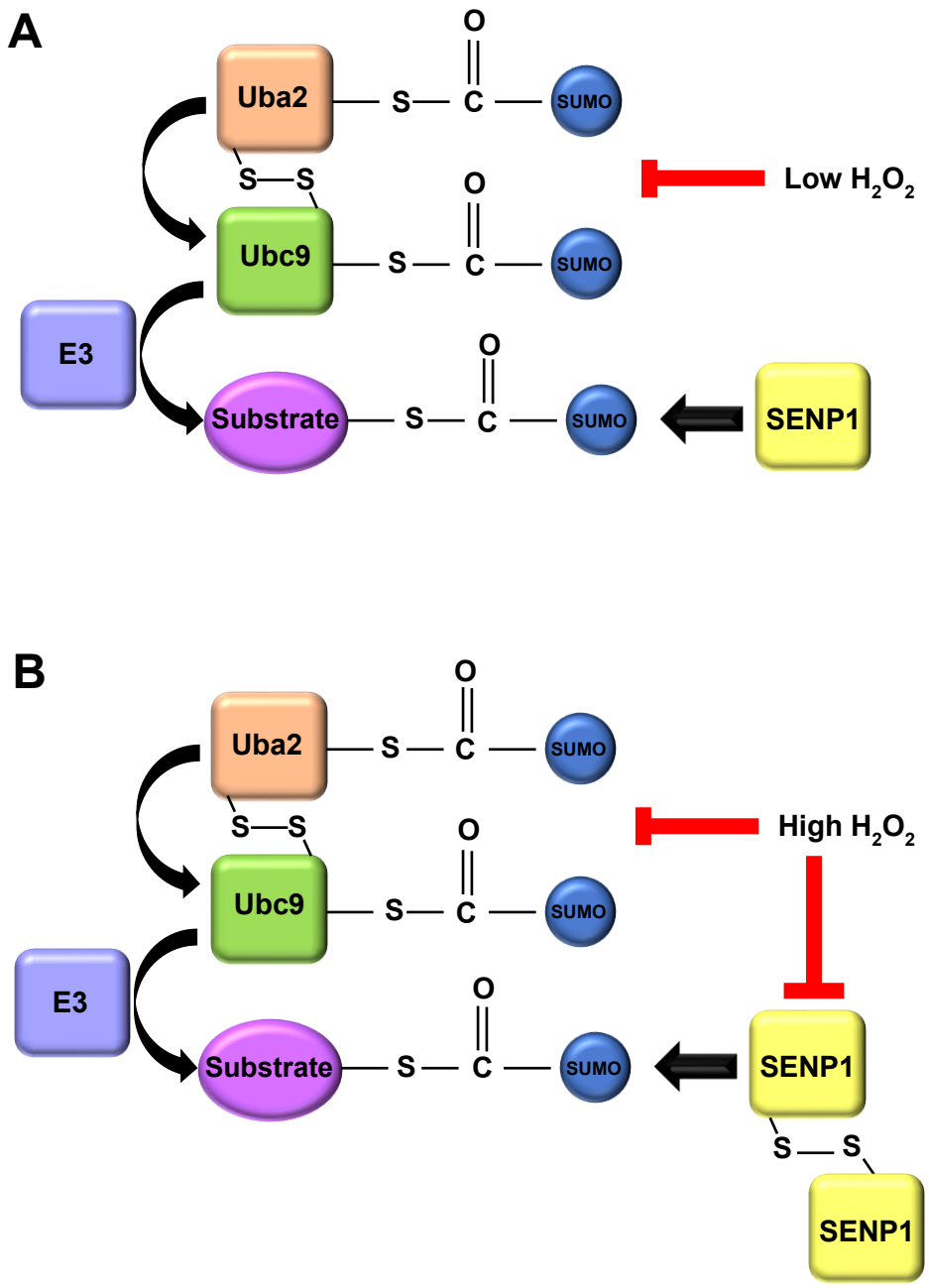

Figure 1.9. Differential H_2O_2 regulation of SUMO machinery.

(A) When mammalian cells are exposed to low levels of H_2O_2, an inhibitory disulphide bond forms between the catalytic cysteine residues of Uba2 and Ubc9. This inhibits sumoylation, however SUMO can still be deconjugated by SENP enzymes. (B) When mammalian cells are exposed to high levels of H_2O2, in addition to the formation of the Uba1/Ubc9 disulphide, SENP1 also becomes inhibited through the formation of an intermolecular disulphide bond with another SENP1, using its catalytic cysteine residue rendering it inactive. In these high-level ROS conditions SUMO can neither be conjugated or deconjugated to/from target proteins (Bossis and Melchior, 2006, Xu et al., 2008).

1.3.2 Regulation of ubiquitination by ROS

In contrast to the effects of low and high levels of H_2O_2 on sumoylation, global ubiquitination did not appear to be affected in mammalian cells by the same conditions that influenced sumoylation (Bossis and Melchior, 2006). However, ubiquitin conjugation/deconjugation pathways utilise many more enzymes than those used in sumoylation/desumoylation pathways and hence it was possible that a limited number of enzymes in ubiquitination/deubiquitination pathways were actually affected by exposure of cells to H_2O_2 which did not have a detectable effect on global ubiquitination. Indeed, consistent with this hypothesis, studies in *S. cerevisiae*, which have much fewer ubiquitination/deubiquitination pathway enzymes than mammalian cells and hence is easier to study, revealed that the ubiquitin pathway E1 enzyme Uba1 forms a disulphide complex with the E2 enzyme Cdc34, but not with several other ubiquitin pathway E2 enzymes, in response to ROS (Doris et al., 2012). Furthermore, similar to the disulphide complex formed between Uba2 and Ubc9 in mammalian cells, the Uba1-Cdc34 disulphide is formed between the individual catalytic cysteine residues of Uba1 and Cdc34, which inactivates both proteins. Indeed, similar to the studies in mammalian cells (Bossis and Melchior, 2006), ROS exposure of S. cerevisiae cells did not have major effects on global ubiquitination (Doris et al., 2012). Interestingly, formation of the Uba1-Cdc34 disulphide complex was induced in response to both H_2O_2 and diamide and, moreover, was found to be influenced by the glutathione system (Doris et al., 2012), which also responds to H_2O_2 and diamide stress (see section 1.2.3). Significantly, Cdc34 is an essential conserved E2 enzyme that regulates cell cycle progression and studies revealed that formation of the Uba1-Cdc34 disulphide complex is important for the regulation of the cell cycle in response to oxidative stress (Doris et al., 2012). Under physiological levels of ROS, Uba1 and Cdc34 ubiquitinate the Sic1 cyclin-dependent kinase (CDK) inhibitor, targeting it for proteasomal degradation (Figure 1.10) (Cocklin et al., 2011). Sic1 inhibits CDK complexes (specifically the Cdc28-Clb5 complex) and the timing of the degradation of Sic1 determines the timing of the G1 phase to S phase transition in the cell cycle (Doris et al., 2012). Hence, inhibition of the reduction in Sic1 levels by the formation of the Uba1/Cdc34 disulphide inhibits cell cycle progression from G1 phase to S phase (Figure 1.10) (Doris et al., 2012). Thus, similar to the regulation of sumoylation in mammalian cells, oxidation of related ubiquitin pathway enzymes in *S.*

cerevisiae acts as a redox sensing mechanism that regulates cell cycle progression to prevent damage to the cell.

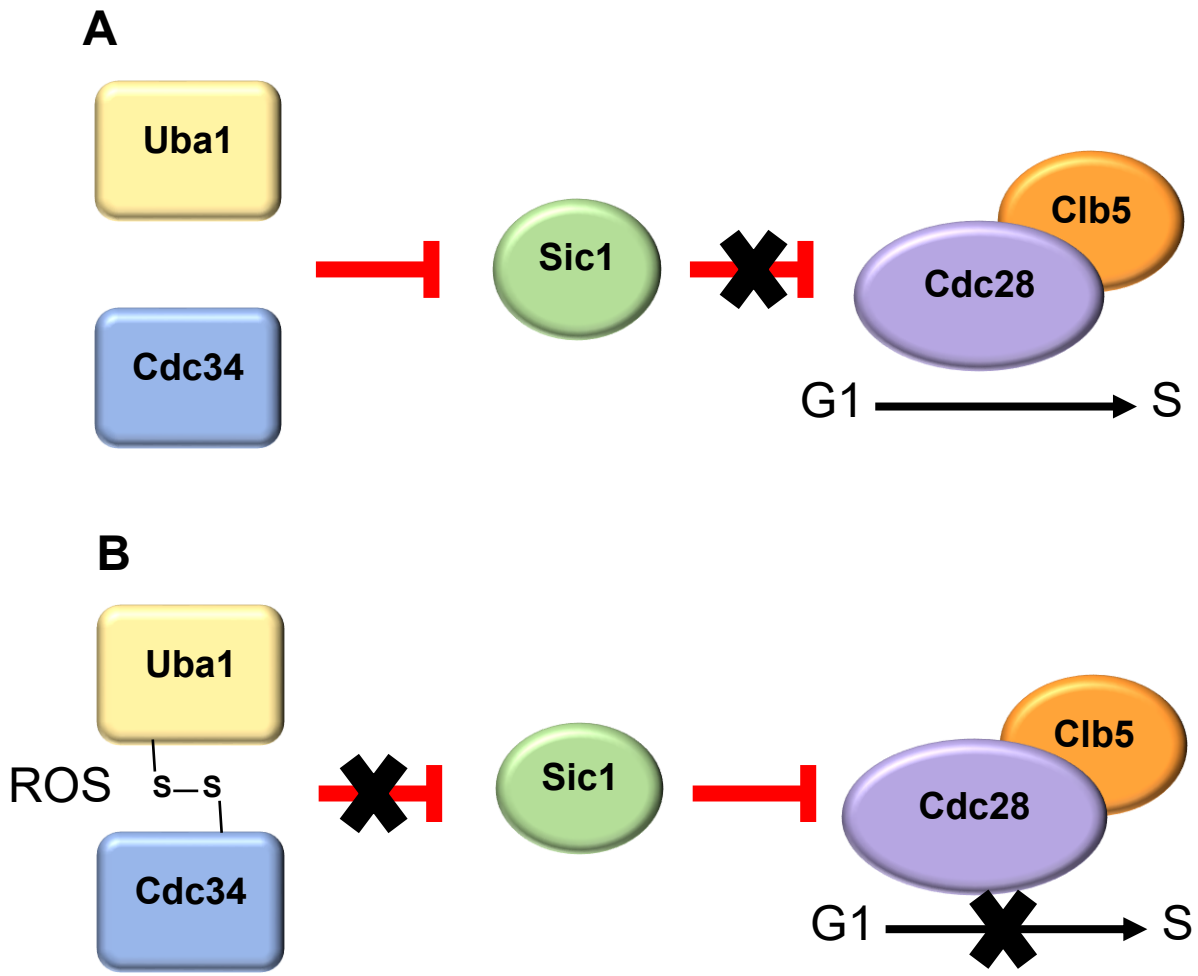

Figure 1.10. Oxidation of Uba1 and Cdc34 in *S. cerevisiae* regulates Sic1.

(A) Under physiological levels of ROS, Uba1 and Cdc34 ubiquitinate Sic1, a Cdc28-Clb5 CDK complex inhibitor, targeting it for proteasomal degradation and allowing progression from G1 to S phase. (B) Under oxidative stress conditions, the Uba1-Cdc34 disulphide is formed, preventing the ubiquitination and degradation of Sic1. Thus, Sic1 inhibits the Cdc28-Clb5 CDK complex and prevents transition into S phase (Doris et al., 2012).

1.3.3 Regulation of DUBs by ROS

The studies of Uba1 and Cdc34 oxidation in *S. cerevisiae* suggests the possibility that, similar to the regulation of SENPs in mammalian cells (Xu et al., 2008), DUB functions might also be regulated by oxidation. Previous work in mammalian cells and in *S. cerevisiae* are discussed below.

1.3.3.1 DUBs and ROS responses in mammalian cells

Initial studies in mammalian cells revealed that DUB activity can be regulated by ROS. For example, USP1 is reversibly inactivated by H_2O_2 (Cotto-Rios et al., 2012). USP1 has been shown to have crucial roles in the maintenance of genome stability (Jones et al., 2012), and interestingly one substrate of USP1 is PCNA (proliferating cell nuclear antigen), with deletion of USP1 causing an elevated level of monoubiquitinated PCNA (Cotto-Rios et al., 2012). PCNA is a highly conserved homotrimer that functions as a DNA clamp, working as a co-factor with DNA polymerase to regulate various processes at the replication fork, such as DNA replication and DNA damage responses (Moldovan et al., 2007). It was therefore suggested that the inactivation of USP1 by ROS may regulate DNA replication and the DNA damage response via its action on PCNA. Furthermore, the two DUBs, USP7 and USP19, were also found to be regulated by ROS, whereby H_2O_2 reversibly oxidises their catalytic cysteine residue inactivating DUB activity (Cotto-Rios et al., 2012, Lee et al., 2013a). Another example in mammalian cells is the OTU DUB Cezanne which was found to be susceptible to inactivation of the catalytic cysteine residue by H_2O_2 (Yin et al., 2019). This oxidation event results in increased activity of the NF-κB pathway (Yin et al., 2019). In all of these DUB cases described above, addition of the reducing agent DTT reversed DUB oxidation and restored the cellular functions of the enzymes (Cotto-Rios et al., 2012, Lee et al., 2013a, Yin et al., 2019).

1.3.3.2 DUBs and ROS in S. cerevisiae

Previous work in *S. cerevisiae* revealed that the Ubp2 DUB is also regulated by ROS (Silva et al., 2015). In particular, H_2O_2 was found to reversibly inactivate Ubp2, although the underlying mechanism is not fully understood (Silva et al., 2015). However, given that Ubp2 utilises a catalytic cysteine residue it is possible that

inactivation of Ubp2 could be linked to the formation of a disulphide which involves the catalytic cysteine, perhaps analogous to the regulation of SENP1 (Xu et al., 2008). Significantly, this inactivation of Ubp2 was shown to be involved the stimulation of K63 polyubiquitination in response to H_2O_2 (Silva et al., 2015). Furthermore, the data suggested that H_2O_2-induced K63 ubiquitination was important for the regulation of protein expression in response to the ROS (Silva et al., 2015). Given the large number of DUBs present in mammalian cells (>100 DUBs) our lab has begun to investigate the relationships between all of the DUBs present in the model yeast *S. cerevisiae* (22 DUBs) and ROS responses in an attempt to obtain a more complete picture of how an organism responds to ROS through the regulation of these enzymes. Interestingly, these initial studies have revealed striking specific effects of different oxidising agents on specific DUBs in *S. cerevisiae* (Curtis, 2019). For example, the Ubp12 DUB was found to form a high molecular weight (HMW) disulphide complex specifically in response to H_2O_2 but not in response to either diamide or the superoxide generator menadione (Curtis, 2019). Furthermore, the kinetics of formation of this HMW disulphide complex was shown to be influenced by the concentration of H_2O_2. In particular, higher levels of H_2O_2 induced increased amounts of the HMW disulphide complex which also were maintained for longer times frame after H_2O_2 exposure (Curtis, 2019). Furthermore, similarly to the oxidation of Uba1 and Cdc34 (Doris et al., 2012), the oxidation of Ubp12 is dependent on the catalytic cysteine residue suggesting that DUB function is altered by H_2O_2 (Curtis, 2019). Analysis of the Ubp12 disulphide complex by mass spectrometry together with other experiments suggested that, in contrast to the mixed disulphide complex of Uba1 and Cdc34, the Ubp12 HMW oxidation complex appears to involve formation of an intramolecular disulphide(s) (Curtis, 2019). Interestingly, in contrast to Uba1 and Cdc34, preliminary work also identified a role for the cytosolic thioredoxin reductase Trr1 in the regulation of Ubp12 regulation (Curtis, 2019). However, the potential links between the H_2O_2-induced oxidation of Ubp12 were not further explored. Hence, despite these exciting initial findings, there is still much to learn about the regulatory mechanisms underlying the regulation of Ubp12 oxidation and about the functions and potential conservation of this oxidation.

1.3.4 Functions of Ubp12 in yeast and USP15 in mammals

The Ubp12 DUB is highly conserved from yeast to mammals. For example, Ubp12 homologues are found in yeast, such as *C. albicans* (named Ubp12) and the very distantly related *S. pombe* (named Ubp12), and in mammalian cells (named USP15, see Table 1.1). This section will describe knowledge about the functions of Ubp12 in yeast and about the functions and disease links of USP15 in humans.

1.3.4.1 Ubp12 in yeast

Although the functions and substrates of Ubp12 in *S. cerevisiae* have not been well characterised some studies have been performed. For example, Ubp12 and Ubp2 were found to act in opposition to each other in the process of mitochondrial dynamics (Anton et al., 2013). Specifically, Ubp2 was shown to promote mitochondrial fusion, whereas Ubp12 promotes mitochondrial fission. These effects of Ubp2 and Ubp12 appeared to be linked to the different functions of the DUBs in influencing the ubiquitination state of the mitofusin, Fzo1, which functions to regulate mitochondrial fission and fusion (Anton et al., 2013). More recent work has also linked the Ubp3 DUB with mitochondrial activity through Cdc48 regulation (Chowdhury et al., 2018). Significantly, Cdc48 regulates the activity of Ubp12 and Ubp2; Cdc48 regulates the ubiquitination and proteasomal degradation of Ubp12, which stabilises Ubp2, as Ubp12 regulates the ubiquitination of Ubp2 (Simões et al., 2018). This therefore promotes mitochondrial fusion via the action of Ubp2 on Fzo1 (Simões et al., 2018). Interestingly, Ubp12 has also been implicated with genome stability in *S. cerevisiae*. In particular, the *UBP12* gene was found to be one of the top five mutator genes when assessing the effect of overexpressing ~85% of open reading frames in *S. cerevisiae* and, moreover, overexpression of *UBP12* increased the mutation rate ~38-fold when compared to a control vector (Ang et al., 2016). It is intriguing to note that H_2O_2-induced DNA damage also affects genome stability (Qi et al., 2019). With respect to these links with genome stability it is interesting to note that Ubp12, and another DUB Ubp10, have been shown to regulate PCNA (Álvarez et al., 2019). In this case, both Ubp12 and Ubp10 associate with PCNA at replication forks and deubiquitinate PCNA (Álvarez et al., 2019). Deletion of the *UBP12* and *UBP10* genes (both as single deletions and a double mutant) resulted in elevated levels of DNA repair mechanisms,

including template switching and translesion synthesis. Hence, deubiquitination of PCNA by Ubp12 and Ubp10 regulates DNA repair and maintenance (Álvarez et al., 2019). Ubp12 has also been found to regulate the proteasomal degradation of Rad23-dependent substrates via deubiquitination of Rad23 (Gödderz et al., 2017). Cdc48, a ubiquitin-selective segregase, and Rad23, a ubiquitin shuttle factor, cooperate to translocate ubiquitinated proteins to the proteasome. Overexpression of *UBP12* stabilises Rad23-dependent substrates, which is consistent with the observation that mutation of Rad23 to prevent ubiquitination of the protein also stabilises Rad23-dependent substrates (Gödderz et al., 2017). Hence, Ubp12 has a role in the regulation of Rad23 and therefore the degradation of proteins targeted for degradation by Rad23. Finally, Ubp12 has been found to regulate Gpa1, a G protein alpha subunit (Wang et al., 2005). Deletion of Ubp12 causes an accumulation of both mono- and poly-ubiquitinated Gpa1, which causes the movement of Gpa1 to the cytoplasm and vacuole from the plasma membrane (Wang et al., 2005). Gpa1 is involved in pheromone sensing, and thus it is suggested that Ubp12 may influence pheromone sensing in *S. cerevisiae* (Wang et al., 2005).

Ubp12 in *S. pombe*, a distantly-related yeast to *S. cerevisiae*, has not been widely studied, however some papers have revealed some specific roles for this DUB. Firstly, Ubp12 has been found to regulate the ubiquitination of PCNA, alongside Ubp2, Ubp15 and Ubp16, with accumulated levels of ubiquitinated PCNA observed in the quadruple mutant (Álvarez et al., 2016). It is suggested that Ubp12 functions redundantly with Ubp15 in this context, as mutation of Ubp12 alone did not confer a phenotype however it did greatly enhance phenotypes observed in Ubp15 mutant strains (Álvarez et al., 2016). The data suggests that the role of these DUBs in regulating the ubiquitination of PCNA is important for the proper replication of DNA during S phase (Álvarez et al., 2016). Ubp12 has also been shown to function with the COP9/signalosome (CSN) to regulate cullin-RING ubiquitin ligases (CRLs) (Zhou et al., 2003, Wee et al., 2005). The CSN is a protein complex with isopeptidase activity, catalysing deneddylation from CRLs (Liakopoulos et al., 1998). *In vitro* studies have suggested that the CSN inhibits CRLs (Zhou et al., 2003), however *in vivo* studies have shown that the CSN actually activates CRLs (Cope and Deshaies, 2003). Interestingly, Ubp12 deubiquitination, alongside Csn5-catalysed cullin deneddylation, has been found to maintain the stability of CRL substrate adapter proteins, facilitating the function of CRL *in vivo* (Wee

et al., 2005). Indeed, *UBP12* is a non-essential gene in *S. pombe*, yet becomes essential in cells with defective adapter recruitment to CRLs (Wee et al., 2005). Thus, in *S. pombe*, Ubp12 has roles in regulating DNA replication during S phase via deubiquitination of PCNA, and in regulating the function of CRLs *in vivo* through stabilising deubiquitination of CRL adapter proteins.

In *C. albicans*, a more closely-related yeast species to *S. cerevisiae*, very little is known about Ubp12, despite conservation with *S. cerevisiae* Ubp12. There is only one paper in the published literature that gives any insight into Ubp12 function in *C. albicans*, which showed that *UBP12* is one of 23 genes where polymorphisms arise in particularly virulent strains from patient-derived samples (Zhang et al., 2009). Thus, despite the absence of known substrates or functions of Ubp12 in *C. albicans*, there is a link between Ubp12 and the virulence of *C. albicans*.

In summary, despite these studies, there is much to learn about the regulation and functions of Ubp12 in *S. cerevisiae* and particularly about homologues of Ubp12 in other yeast. However, given the results from our lab regarding the links between Ubp12 and H_2O_2 it is tempting to speculate that Ubp12 may have conserved roles in responses to ROS in yeast.

1.3.4.2 USP15 in humans

USP15, the mammalian homologue of Ubp12, is a zinc-binding DUB that has been implicated in the pathologies of several human diseases. Zinc binding occurs at conserved CXXC motifs of USP15, and is found to aid conformational stability (Ye et al., 2009). Upregulation of USP15 has been implicated with the progression of various cancers, such as glioblastoma, breast cancer and ovarian cancer (Chou et al., 2017). Interestingly however, USP15 has been found to function both as an oncogene and as a tumour suppressor. For example, USP15 was shown to stabilise the oncoproteins MDM2 (an E3 ligase) and HPV type-16 E6, which reduces the tumour-supressing activity of p53 (Zou et al., 2014, Vos et al., 2009). Conversely, USP15 is known to function with the COP9 signalosome complex (CSN) to stabilise IκBα and APC, negative regulators of oncogenic NF-κB and Wnt pathway signalling respectively, thus functioning as a tumour suppressor (Huang et al., 2009, Schweitzer et al., 2007). Thus, the role of USP15 in cancer progression is complex and is likely to vary dependent on

the type of cancer. USP15 has also been linked to Parkinson's disease through regulation of the E3 ligase, Parkin (Cornelissen et al., 2014). Normally, Parkin is translocated to depolarised mitochondria to induce mitophagy by the ubiquitination of mitochondrial membrane proteins (Corti et al., 2011). This process is disrupted by loss-of-function mutations of the gene encoding Parkin and these mutations are one of the main causes for the onset of Parkinson's disease (Corti et al., 2011). Interestingly, inhibition of USP15 partially rescued the defective mitophagy phenotype associated with mutated Parkin, indicating a role for USP15 in the regulation of mitophagy (Cornelissen et al., 2014). It is interesting to note here that Ubp12 in *S. cerevisiae* also has a role in regulating mitochondrial dynamics (see 1.3.4.1) (Anton et al., 2013). Finally, USP15 is an important regulator of the response of cells to viral infection. Upon viral infection, RIG1 (retinoic acid-inducible gene-I) functions as a viral sensor, binding to the phosphate groups of RNA within the virus (Pichlmair et al., 2006). Significantly, activation of RIG1 relies on ubiquitination by the E3 ligase TRIM25 and, importantly, USP15 deubiquitinates TRIM25 to stabilise the protein (Inn et al., 2011). Thus, USP15 has an important role in maintaining cellular responses to viral infections.

Given these connections between USP15 and common human diseases there is significant potential in developing drugs that target the activity of this DUB in certain contexts for the benefit of human health. It is possible from the studies in *S. cerevisiae* to date that USP15 is linked to ROS responses in human cells which may provide insight that will aid the development of drugs that specifically target this DUB.

1.4 Aims and objectives of this thesis

The deubiquitination of substrates is a crucial mechanism in the regulation of many cellular processes. Hence, it is important to understand the regulation of DUBs as this determines the activities of these cellular processes. As described above, protein oxidation is a post translational modification of DUBs that alters their activity. Previous work from this laboratory demonstrated that the *S. cerevisiae* DUB, Ubp12, forms an intramolecular disulphide complex specifically in response to H_2O_2. Furthermore, the catalytic cysteine residue of Ubp12 was shown to be essential for the formation of this complex, suggesting that this cysteine residue became oxidised in response to H_2O_2. Some preliminary analysis suggested a possible role for thioredoxin reductase in the regulation of Ubp12 but the potential role of the thioredoxin system in Ubp12 oxidation was not investigated. Therefore, the aim of this thesis was to further characterise the regulation and functions of oxidation of Ubp12 in *S. cerevisiae* and, moreover, to investigate the conservation of regulation and functions of Ubp12 in *C. albicans*, a clinically important and closely related yeast species.

Specific objectives of this thesis were to:

1) Explore the potential regulation of Ubp12 by the thioredoxin system.

2) Investigate the mechanism of oxidation of Ubp12 in response to H_2O_2.

3) Assess the conservation of regulation and functions of Ubp12 in *C. albicans* and initiate studies of the potential role of Ubp12 in the morphology of *C. albicans*.

Chapter Two: Materials and Methods

2.1 Yeast strains and growth conditions

2.1.1 *S. cerevisiae*

The *S. cerevisiae* strains used in this study (Appendix A) were derived from either the W303 strain background (*ade2-1, can1-100, his3-11,15, leu2-3,112, trp1-1, ura3-1*) or the BY4741 strain background (*his3Δ1, leu2Δ0, met15Δ0, ura3Δ0*) which was originally derived from the S288C strain background.

S. cerevisiae cells were grown at 30°C unless stated otherwise, in either rich, complete YPD media (YPD, 1% w/v Bacto-yeast extract, 2% w/v Bacto-peptone, 2% w/v glucose, +/- 2% w/v agar) or SD minimal media (0.67% w/v Bacto-yeast nitrogen base without amino acids, 2% w/v glucose, +/- 2% w/v agar). Minimal media was supplemented with adenine sulphate (25 mg/l), L-histidine (12.5 mg/l), L-leucine (25 mg/l), L-tryptophan (12.5 mg/l), uracil (10 mg/l), L-methionine (12.5 mg/l) and L-lysine (37.5 mg/l) as appropriate. Selection for kanamycin resistance was achieved by supplementing YPD with G418 (400 µg/ml).

2.1.2 *C. albicans*

The *C. albicans* strains used in this study (Appendix B) were derived from the SN148 strain background (*arg4Δ/arg4Δ, leu2Δ/leu2Δ, his1Δ/his1Δ, ura3Δ::imm434/ura3Δ::imm434, iro1Δ::imm434/iro1Δ::imm434*).

C. albicans cells were grown at 30°C in either rich, complete YPD media (YPD, 1% w/v Bacto-yeast extract, 2% w/v Bacto-peptone, 2% w/v glucose, +/- 2% w/v agar) or SD minimal media (0.67% w/v Bacto-yeast nitrogen base without amino acids, 2% w/v glucose, +/- 2% w/v agar). Minimal media was supplemented with adenine sulphate (25 mg/l), L-histidine (12.5 mg/l), L-leucine (25 mg/l), L-tryptophan (12.5 mg/l), L-methionine (12.5 mg/l), L-lysine (37.5 mg/l), L-arginine (12.5 mg/l) and uridine (57.5 mg/l) as appropriate.

2.2 Yeast techniques

2.2.1 Yeast transformation

2.2.1.1 S. cerevisiae transformation

S. cerevisiae cells were transformed with DNA following the high efficiency lithium acetate method (Schiestl and Gietz, 1989). Briefly, 50 ml of mid-log-phase growing cells were pelleted (2 minutes, 3000 rpm), washed twice in dH_2O and resuspended in 1 ml of LiAc/TE (0.1 M LiAc/ 10 mM Tris-HCl pH 7.4, 1 mM EDTA pH8). Per transformation, 200 µl of cells, 5 µg of boiled salmon sperm DNA and 0.1 – 10 µg of the DNA to be transformed were mixed. 1 ml of LiAc/TE/PEG (0.1 M LiAc, 10 mM Tris-HCl pH 7.4, 1 mM EDTA pH8, 40% w/v PEG-4000) was added, mixed, and then incubated at 30°C (shaking) for 30 minutes. After heat-shock at 42°C for 15 minutes, cells were pelleted (7000 rpm, 30 seconds) and resuspended in 150 µl nH_2O. Cells were then spread onto appropriate, selective plates and incubated at 30°C for 3 – 5 days.

2.2.1.2 C. albicans transformation

C. albicans cells were transformed with DNA following the high efficiency lithium acetate method (Schiestl and Gietz, 1989). 200 ml of cells (OD_{660nm} 1-3) were pelleted (2 minutes, 2500 rpm), washed in 20 ml of LiAc/TE and resuspended in 1 – 2 ml of LiAc/TE. Per transformation, 100 µl of cells, 5 µg of boiled salmon sperm DNA and 0.1 – 5 µg DNA to be transformed were mixed. 700 µl of LiAc/TE/PEG were added, mixed, and then incubated at 30°C (shaking) for 3 hours. After heat-shock for 45 minutes at 42°C, cells were pelleted (8000 rpm, 1 minute) and resuspended in 100 µl of nH_2O. Cells were then spread onto appropriate, selective plates and incubated at 30°C for 3 – 5 days.

2.2.2 Yeast strain construction

2.2.2.1 S. cerevisiae mating and dissections

Strains of opposite mating type were crossed on YPD agar and sporulated on sporulation agar (1% w/v potassium acetate, 0.1% w/v yeast extract, 0.05% w/v glucose) at 30°C for 2-3 days. Cells were resuspended in 100 µl 5% v/v glusulase (PerkinElmer) and incubated for 30 minutes at 30°C. The cells were then gently mixed

with 900 µl of nH_2O. 100 µl of this solution were then pipetted onto YPD agar and tetrads were dissected using the tetrad dissector (Singer Instruments). The resultant spores were incubated at 30°C for 3 days.

2.2.3 Plasmid extraction from *S. cerevisiae*

Plasmids were extracted from *S. cerevisiae* using the STET method (Robzyk and Kassir, 1992). Briefly, overnight cultures were pelleted (5000 rpm, 3 minutes), washed twice with TE buffer, and resuspended in 100 µl STET buffer (8% w/v sucrose, 50 mM Tris-HCl pH 8, 50 mM EDTA, 5% v/v Triton X-100). Cells were lysed using 0.2 g of 0.45 mm glass beads and vortexed vigorously. 100 µl of STET buffer were added and lysates were incubated at 100°C for 4 minutes. Lysates were then cooled on ice and centrifuged (13000 rpm, 10 minutes, 4°C). 100 µl of supernatant were added to 50 µl of 7.5 M ammonium acetate and DNA was precipitated at -20°C for 1 hour. Samples were then centrifuged (13000 rpm, 10 minutes, 4°C), and 100 µl of supernatant added to 200 µl ice-cold ethanol. Plasmid DNA was pelleted (13000 rpm, 10 minutes), washed using 70% v/v ethanol and finally resuspended in 10 – 20 µl nH_2O. Plasmid DNA was then transformed into *E. coli* (Section 2.3.4).

Plasmid Name	Comments	Reference
pRS426	2-micron plasmid containing a *URA3* marker	Lab stock
pRS426-Ubp12-3HA	2-micron plasmid with a *URA3* marker expressing wild-type Ubp12 tagged with 3HA	(Curtis, 2019)
pRS426-Ubp12-3HA-C373S	2-micron plasmid with a *URA3* marker expressing Ubp12 where C373 is mutated to serine, tagged with 3HA	(Curtis, 2019)
pRS426-Ubp12-3HA-Group1C-S	2-micron plasmid with a *URA3* marker expressing Ubp12 where C519, C536 and C539 are mutated to serine, tagged with 3HA	This study

pRS426-Ubp12-3HA-Group2C-S	2-micron plasmid with a *URA3* marker expressing Ubp12 where C967, C985 and C988 are mutated to serine, tagged with 3HA	This study
pFA-HA-*HIS1*	Epitope tagging vector with a *HIS1* marker	(Lavoie et al., 2008)
pFA-HA-*URA3*	Epitope tagging vector with a *URA3* marker	(Lavoie et al., 2008)
loxP-*HIS1*-loxP (LHL)	Plasmid contains a disruption cassette with a selectable *HIS1* marker	(Shahana et al., 2014)
loxP-*ARG4*-loxP (LAL)	Plasmid contains a disruption cassette with a selectable *ARG4* marker	(Shahana et al., 2014)
CIp10	Vector for integrating *URA3* in *C. albicans*	Lab stock

Table 2.1. Plasmids used in this study.

2.2.4 Stress sensitivity spot tests

S. cerevisiae and *C. albicans* cells were grown to mid-log phase in appropriate media and cultures diluted to the same OD_{660nm}. 5-fold serial dilutions in the appropriate media were then spotted onto agar plates containing the indicated stress agents using a 48-pin tool (Sigma). Plates assessing UV sensitivity were irradiated for the indicated dose using a Stratalinker. All plates were incubated at 30°C unless stated otherwise for 2 – 3 days. Plates exposed to UV light were incubated in the dark.

2.2.5 Growth curves

S. cerevisiae cells were grown in the appropriate media to mid-log phase and cultures diluted to the same OD_{660nm}. Cells were then exposed to the indicated oxidising agent and the OD_{660nm} of the cultures was monitored at the indicated time points using a spectrophotometer for 6 – 8 hours. Doubling time was calculated using the following equation:

$$Doubling\ time = \frac{\ln(2)}{exponent\ of\ growth}$$

2.2.6 *C. albicans* yeast-hyphae switch analysis

C. albicans cells were grown to stationary phase in YPD media. Hyphae formation was induced by diluting these cultures 1:10 with fresh YPD media containing 10% v/v fetal calf serum (Invitrogen). Cells were then incubated at 37°C for 6 hours shaking at 180 rpm. Cells were fixed and imaged as described in 2.2.11.

2.2.7 Protein extraction

S. cerevisiae and *C. albicans* cells were grown to mid-log-phase in the appropriate media (see earlier in the text) at 30˚C and treated with oxidising agents as indicated. Cells were pelleted (3000 rpm, 1 minute) in an equal volume of 20% w/v TCA and snap frozen in liquid nitrogen for protein extraction. Next, pellets were thawed on ice and resuspended in 200 µl 10% w/v TCA and 1 ml of chilled glass beads. Samples were then lysed in a bead-beater (Biospec Products). Lysates were then pelleted (13000 rpm, 15 minutes, 4°C) and pellets were washed 3 times with 200 µl acetone. Pellets were air-dried and solubilised with TCA buffer (100 mM Tris-HCl pH 8, 1% w/v SDS, 1 mM EDTA, 12.5 mM NEM) and incubated at 25°C for 30 minutes. After incubation at 37°C for 5 minutes, and centrifugation at 13000 rpm for 5 minutes, the supernatant was retained and protein concentration obtained using a BCA protein assay kit (ThermoScientific) according to the manufacturer's instructions.

2.2.8 Western blotting

Protein samples were mixed with sufficient 4 x loading dye (0.5% w/v bromophenol blue, 10% w/v SDS, 625 mM Tris-HCl pH 6.8, 50% v/v glycerol) and denatured at 100°C for 3 minutes. Proteins were then resolved on 8% - 15% SDS-polyacrylamide gels using PageRuler Pre-stained Protein Ladder (ThermoScientific) for molecular weight reference. After electrophoresis proteins were transferred to a Protran nitrocellulose membrane (Amersham) for 2 hours at 400 mA. For quantification using the LI-COR system, membranes were incubated shaking at room temperature in the dark with Revert 700 Total Protein Stain (LI-COR) for 5 – 10 minutes, and washed twice for 30 seconds with the Revert 700 Wash Solution (LI-COR). These membranes were imaged on the Odyssey CLx Infrared Imaging System (LI-COR) for analysis of total protein loaded. Membranes were blocked using 10% w/v BSA in TBS-T (1 mM Tris-HCl pH 8, 15 mM NaCl, 0.01% v/v Tween-20) for 30 minutes, with shaking. Next,

membranes were incubated with primary antibodies (Table 2.2) diluted in 5% w/v BSA shaking overnight at 4°C. Membranes were washed 3 times for 5 minutes with TBS-T and incubated for 1 hour, with shaking, with the appropriate secondary antibodies in the dark (Table 2.2). Blots were then imaged on the Odyssey CLx Infrared Imaging System (LI-COR). Western blot quantification was obtained using the LI-COR system, quantifying levels of protein relative to the total protein signal for each lane.

Some western blots were developed alternatively. The membrane was treated identically however it was not treated with the Revert 700 Total Protein Stain and secondary antibody incubation did not require darkness. After secondary antibody incubation, membranes were washed with TBS-T a further 3 times for 5 minutes and treated with ECL Chemiluminescent kit (GE Healthcare) for scanning on a Typhoon FLA 9500 (GE Healthcare).

Antibody and Manufacturer	Type	Working concentration	Raised In
Anti-HA (ThermoScientific)	Primary	1:1000	Mouse
Anti-PαP (Sigma)	Primary	1:1000	Rabbit
Anti-ubiquitin (Santa-Cruz)	Primary	1:500	Mouse
Anti-Mouse HRP (Sigma)	Secondary	1:2000	Mouse
IRDye® 800CW anti-Mouse (LI-COR)	Secondary	1:15000	Goat
IRDye® 800CW anti-Rabbit (LI-COR)	Secondary	1:15000	Goat

Table 2.2. Antibodies used in this study.

2.2.9 RNA extraction

25 ml of mid—log phase growing *S. cerevisiae* cells, treated as described in the text, were pelleted (3000 rpm, 2 minutes). Cells were then washed in 1 ml nH_2O, transferred to a ribolyser tube, and pelleted again (3000 rpm, 2 minutes) before being snap frozen. Pellets were thawed on ice and resuspended in 750 µl TES (0.1M Tris-HCl pH 7, 0.5% w/v SDS, 100 mM EDTA) and 750 µl acidic phenol-chloroform. After cell suspensions were vortexed and incubated at 65°C for 1 hour, vortexing every 10 minutes for 10 seconds, samples were placed on ice for 1 minute, vortexed for 20 seconds, and

centrifuged (4°C, 6000 rpm, 15 minutes). 700 µl of the aqueous phase for each sample were added to 700 µl acidic phenol-chloroform and the samples centrifuged (4°C, 14000 rpm, 5 minutes). After repeating this step 500 µl of the aqueous phase were added to a 2 ml Eppendorf tube, containing 1.5 ml 100% v/v ethanol and 50 µl of 3 M NaAc (pH 5.2), and the samples vortexed for 10 seconds. Following precipitation of the RNA at – 20°C overnight, tubes were centrifuged for 10 minutes, 14000 rpm (room temperature) and the supernatant discarded. Pellets were resuspended in 500 µl 70% v/v ethanol and centrifuged for 1 minute, 14000 rpm. Supernatant was discarded and samples were centrifuged again for 5 seconds, 14000 rpm. RNA pellets were air-dried for 5 – 10 minutes and 100 µl nH_2O were added. Pellets were resuspended by incubation at 65°C for 1 minute with vortexing. Finally, the RNA concentration was quantified using a Nanodrop spectrophotometer.

2.2.10 Quantitative reverse transcriptase qPCR (RT-qPCR)

Prior to RT-qPCR, 5 µg of RNA were DNase–treated, using a Turbo DNA-free kit (Fisher Scientific) according to the manufacturer's instructions, and stored at -80°C. RT-qPCR was performed using the One Step qPCR Master Mix with SYBR Green (Primer Design) with the primers described below (Table 2.3). Reactions contained 165 ng of RNA (1 µl of the DNase-treated 5 µg), 5 µl Master Mix, 300 nM forward primer, 300 nM reverse primer, with nH_2O to a total volume of 10 µl.

The following steps were used:

Step 1 (reverse transcriptase): 10 minutes, 55°C

Step 2 (Taq activation): 2 minutes, 95°C

Step 3 (denaturation): 30 seconds, 95°C

Step 4 (data collection): 1 minute, 60°C

Steps 3 – 4 were cycled 50 times

RT-qPCR data were collected using a Rotor-gene 6000 real time PCR cycler (Corbett) where SYBR Green signal detection was recorded. Enrichment for each target was calculated using the comparative C_T method (Livak and Schmittgen, 2001), using actin for normalisation. RT-qPCR reactions were performed in biological triplicate and technical duplicate.

Primer Name	Sequence (5' –> 3')
Actin Fw sc	GCCTTCTACGTTTCCATCCA
Actin Rev sc	GGCCAAATCGATTCTCAAAA
Ubp12 Fw sc	TGCAATGCCTGGTACACATT
Ubp12 Rev sc	AGTGCCCGATAGTGGATTTG

Table 2.3. qPCR oligonucleotide primers used in this study.

The oligonucleotide primers were obtained from Sigma-Aldrich.

2.2.11 Fixing cells and microscopy

C. albicans cells were grown to mid log phase (OD_{660nm}) as described in the text, pelleted and fixed using paraformaldehyde as described previously (Enjalbert et al., 2006). Briefly, 10% of the final cell volume of 3.7% w/v paraformaldehyde in PEM (1 mM EGTA pH 8, 100 mM piperazine-1, 4-bis (2-ethanesulfonic acid) (PIPES) pH 6.8, 1 mM $MgSO_4$) were added to cells and mixed for 30 minutes at room temperature. Cells were washed three times in PEM and resuspended in 1 ml of PEM. Cells suspensions were then stored in the fridge until imaged.

10 µl of fixed cells were fixed onto microscope slides using poly-L-lysine and left at room temperature for 20 minutes. 5 µl of Vectashield mounting medium (Vector laboratories) was then added and the coverslip placed on top. Coverslips were sealed with nail varnish and slides were imaged on a Zeiss Axioimager microscope (63X oil immersion objective). Images were captured and analysed using Axiovision software.

2.3 Molecular biology techniques

2.3.1 PCR

All oligonucleotide primers used in PCR reactions in this study are detailed in Appendix C.

2.3.1.1 Phusion High-Fidelity Polymerase (NEB)

Phusion High-Fidelity Polymerase (NEB) was used to amplify products, which required proof-reading, for further use in cloning or sequencing. Reaction mixtures consisted of 0.5 µl Phusion Polymerase (0.02 U), 0.1-1 ng template DNA, 0.5 µl each of forward and reverse primer (10 µM each), 0.5 µl dNTP mix (10 mM), 1.5 µl $MgCl_2$ (1.5 mM),

10 µl 5x Phusion HF or GC buffer (supplied by manufacturer), made up to 50 µl with sterile nH_2O. Reactions were performed using the following conditions in a thermocycler:

Step 1 (initial denaturation): 2 minutes, 94°C

Step 2 (denaturation): 30 seconds, 94°C

Step 3 (annealing): 30 seconds, 50 – 65°C *

Step 4 (extension): 0.5 – 6 minutes **, 72°C

Step 5 (final extension): 10 minutes, 72°C

Steps 2 – 4 were cycled 35 times

* Annealing temperatures were determined from the melting temperatures of the specific oligonucleotide primers used in the reaction.

** Extension times were determined by the length of the product: 1 minute per 1kb DNA.

Primers pairs and annealing temperatures used in Phusion PCR reactions for this thesis are below in Table 2.4.

Forward Primer	Reverse Primer	Annealing Temperature (°C)
Gpx3-Deletion Frag fw	Gpx3-Deletion Frag rev	58
M13F	426-12-3HA-1-rev	63
426-12-3HA-2-fw	M13R	61
M13F	426-12-3HA-2-rev	63
426-12-3HA-3-fw	M13R	61
M13F	Ubp12-C536S-frag-1-rev	63
Ubp12-C536S-frag-2-fw	M13R	61
ubp12ChkDelF	ubp12ChkTagR	50
Ubp12-Del-Fw-CA	Ubp12-Del-Rev-CA	65
Ubp12-HA-F	Ubp12-HA-R	50

Table 2.4. Primer pairs and annealing temperatures used in Phusion reactions.

2.3.1.2 DreamTaq Green DNA Polymerase (ThermoScientific)

For non-proof-reading PCR, DreamTaq Green DNA Polymerase (ThermoScientific) was used. Reaction mixtures consisted of 0.25 µl DreamTaq Green DNA Polymerase (0.1 U), 5 µl DreamTaq Green buffer (supplied by manufacturer), 0.1-1 ng template DNA, 0.5 µl each of forward and reverse primer (10 µM each), 0.5 µl dNTP mix (10 mM), made up to 50 µl with sterile nH_2O. Reactions were performed using the following conditions in a thermocycler:

Step 1 (initial denaturation): 10 minutes, 94°C

Step 2 (denaturation): 30 seconds, 94°C

Step 3 (annealing): 30 seconds, 50 – 62°C *

Step 4 (extension): 0.5 – 6 minutes **, 72°C

Step 5 (final extension): 10 minutes, 72°C

Steps 2 – 4 were cycled 35 times

* Annealing temperatures were determined from the melting temperatures of the specific oligonucleotide primers used in the reaction.

** Extension times were determined by the length of the product: 1 minute per 1kb DNA.

Primers pairs and annealing temperatures used in DreamTaq PCR reactions for this thesis are below in Table 2.5.

Forward Primer	Reverse Primer	Annealing Temperature (°C)
Trr2 Del Chk Fw	Trr2 Del Chk Rev	56
Tsa1 Del Chk Fw	Tsa1 Del Chk Rev	56
Tsa2 Del Chk Fw	Tsa2 Del Chk Rev	56
Trx1 Del Chk Fw	Trx1 Del Chk Rev	56
Trx2 Del Chk Fw	Trx2 Del Chk Rev	56
Gpx3-Deletion Frag fw	Gpx3-Deletion Frag rev	58
M13F	M13R	58
ubp12ChkDelF	ubp12ChkTagR	50

Ubp12-DelChk-Fw-CA	Arg4-Chk-EarlyRev-CA	56
Ubp12-DelChk-Fw-CA	His1-Chk-EarlyRev-CA	58
Ubp12-DelChk-Fw-CA	Ubp12-DelChk-Rev-CA	58
Ubp12-check-fw-CA-internal	Ubp12-check-rev-CA-internal	55
Ubp12-HA-check-fw	HA-check-rev	60

Table 2.5. Primer pairs and annealing temperatures used in DreamTaq reactions.

2.3.2 Restriction enzyme digestion

Plasmid DNA was digested using the appropriate restriction enzymes and buffers as per the manufacturer's instructions. The digested products were visualised on an agarose gel (2.3.3).

2.3.3 Agarose gel electrophoresis, DNA purification and DNA sequencing

Plasmid digests and PCR products were separated and analysed using 1% w/v agarose gels, using TAE buffer (40 mM Tris acetate, 1 mM EDTA pH8) containing 5 µg/ml ethidium bromide. DNA was extracted from agarose gels using a QIAquick Gel Extraction kit (QIAGEN) according to manufacturer's instructions. DNA in solution was isolated using either ethanol precipitation or the GeneJET PCR Purification kit as per the manufacturer's instructions. DNA concentrations were calculated using a Nanodrop spectrophotometer. DNA sequencing reactions were completed by Eurofins Genomics.

2.3.4 *E. coli* transformation and plasmid purification

Plasmids were transformed into Subcloning Efficiency™ DH5α Competent Cells (Invitrogen) via the $CaCl_2$ method (Maniatis, 1985). Cells were plated onto LB agar plates (2% w/v Bacto-tryptone, 1% w/v Bacto-yeast extract, 1% w/v NaCl pH 7.2, 2% w/v agar) containing 0.1 mg/ml ampicillin (Sigma-Aldrich) and then incubated at 37°C overnight. Resultant colonies were grown in LB liquid media (2% w/v Bacto-tryptone, 1% w/v Bacto-yeast extract, 1% w/v NaCl pH 7.2) containing 0.1 mg/ml ampicillin at 37°C overnight. Plasmids were isolated from these overnight cultures using the GenElute Plasmid Miniprep kit (Sigma-Aldrich) according to the manufacturer's instructions.

2.4 Statistical analysis

All statistical tests were performed in GraphPad Prism (GraphPad Prism software). P values were calculated using unpaired T tests using Welch's correlation where appropriate, where (*) indicates $p<0.05$, (**) indicates $p<0.01$ and (***) indicates $p<0.001$.

Chapter Three: Regulation of Ubp12 by the thioredoxin and glutathione systems

3.1 Introduction

The thioredoxin and glutathione systems are two major antioxidant mechanisms employed by cells to defend against elevated levels of ROS (see 1.2.3.2). These systems are crucially important in maintaining redox homeostasis and are conserved from bacteria up to single cell eukaryotes such as yeast, and complex multicellular organisms such as humans (Laurent et al., 1964, Aslund et al., 1994). Despite being two separately characterised systems, the thioredoxin system and the glutathione system do display some overlap in activity and function (see 1.2.3.2). However, it is also clear that the two systems are regulated differently and respond to different oxidising agents. Importantly, the glutathione system responds to both H_2O_2 and diamide in *S. cerevisiae*, while in contrast the thioredoxin system responds only to H_2O_2 (Wheeler et al., 2003, Garrido and Grant, 2002, Kosower and Kosower, 1995).

As described in Chapter 1 of this thesis, Ubp12 is regulated by oxidation, forming an intramolecular disulphide complex specifically in response to H_2O_2 (Curtis, 2019). Ubp12 may be directly oxidised by H_2O_2, however it is likely it could involve some intermediary protein as seen with the H_2O_2-induced activation of Yap1 and the roles of Gpx3/Tsa1 (see 1.2.3.3). Even if the oxidation of Ubp12 by H_2O_2 is a direct oxidation event, it is possible at least one of the antioxidant pathways within the cell are responsible for reducing it. Given the specificity of Ubp12 oxidation to H_2O_2, it is possible that the H_2O_2-specific antioxidant system, the thioredoxin system, is involved in the regulation of Ubp12 (either directly in forming the disulphide and/or in reducing oxidised Ubp12). In support of this hypothesis, the Uba1-Cdc34 disulphide is induced by both H_2O_2 and diamide, and is exclusively regulated by the glutathione system which also responds to both H_2O_2 and diamide (see section 1.3.2) (Doris et al., 2012). Excitingly, previous work from this laboratory established a preliminary link between the thioredoxin system and Ubp12 (Curtis, 2019). In particular, there was a significant decrease in the levels of Ubp12 in a *trr1*Δ mutant. However, no other investigations of the potential role of thioredoxin system proteins were performed. Therefore, the aim of this chapter is to explore the potential connections between the thioredoxin system

proteins and the regulation of Ubp12, and to explore whether the glutathione system has any role in the regulation of Ubp12.

3.2 Results

3.2.1 Thioredoxin system proteins regulate Ubp12

3.2.1.1 Construction of thioredoxin system mutants expressing epitope-tagged Ubp12

As described above, previous unpublished work from our lab identified a role for the cytosolic thioredoxin reductase, Trr1, in the regulation of Ubp12 (Curtis, 2019). However, potential roles of other members of the thioredoxin system on Ubp12 were not explored. In addition, thioredoxin system proteins have previously been shown to have important roles in the regulation of cellular responses to H_2O_2 in *S. cerevisiae* (see section 1.2.3.3) (Delaunay et al., 2002, Ross et al., 2000). Hence, it was possible that thioredoxin system proteins regulate the oxidation and/or reduction of Ubp12. To begin to investigate these possibilities the first step was to construct strains where the various genes encoding members of the thioredoxin system were deleted in cells that also express 3HA epitope-tagged Ubp12 from the normal genomic locus. To create the required strains extensive genetic crosses were performed using *MATa* (KA10) and *MAT*α (KA32) haploid cells expressing 3HA epitope-tagged Ubp12 (Ubp12-3HA) and haploid cells of the opposite mating type containing the gene deletions of the various members of the cytoplasmic thioredoxin system (*tsa1*Δ (SR9), *tsa2*Δ (SR48), *trx1*Δ*trx2*Δ (KD467)). In addition, a cross was set up between KA32 expressing Ubp12-3HA and KA26, a *MATa* strain containing a deletion of the gene encoding the mitochondrial thioredoxin reductase Trr2 (*trr2*Δ), to allow investigations of the potential role of the mitochondrial thioredoxin system in the regulation of Ubp12. Potential *tsa1*ΔUbp12-3HA, *tsa2*ΔUbp12-3HA, *trx1*Δ*trx2*ΔUbp12-3HA and *trr2*ΔUbp12-3HA strains were identified from the genetic crosses by testing on appropriate selective media for the presence of the selectable marker associated with each gene deletion and the expression of Ubp12-3HA (see Appendix A). Candidates representing potential successful strain constructions were analysed by PCR to check the presence of the correct gene deletion (Figure 3.2).

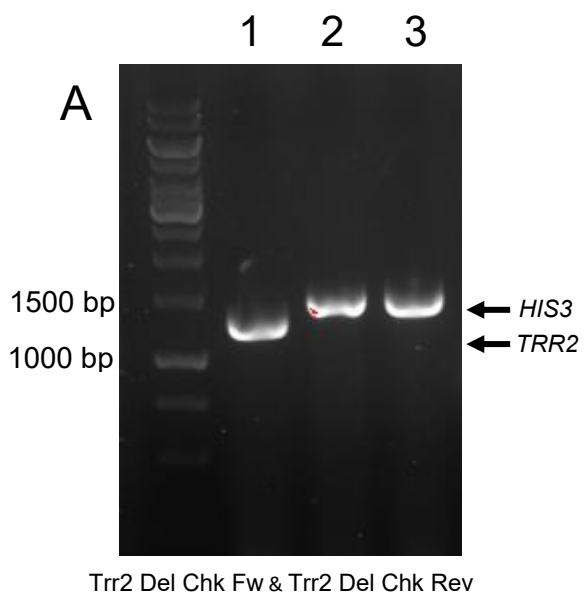

Trr2 Del Chk Fw & Trr2 Del Chk Rev

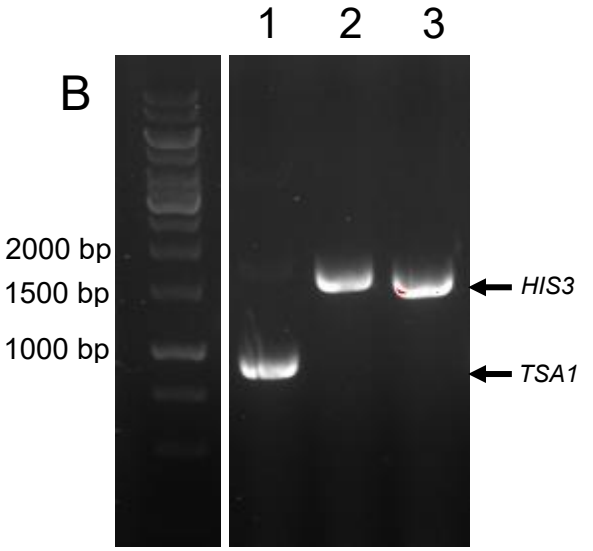

Tsa1 Del Chk Fw & Tsa1 Del Chk Rev

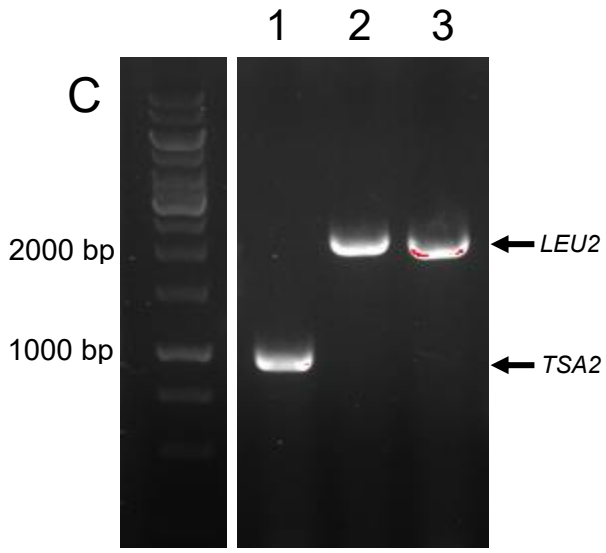

Tsa2 Del Chk Fw & Tsa2 Del Chk Rev

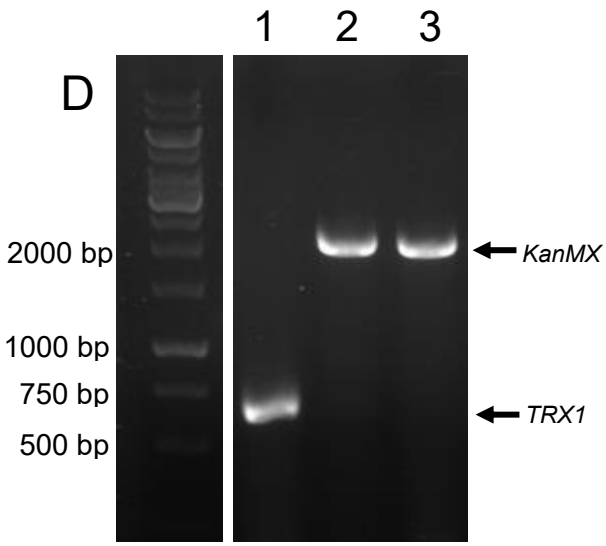

Trx1 Del Chk Fw & Trx1 Del Chk Rev

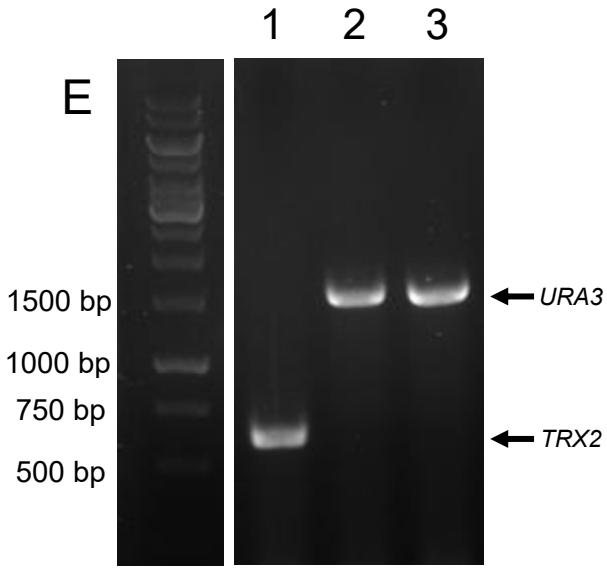

Trx2 Del Chk Fw & Trx2 Del Chk Rev

Figure 3.1. PCR analyses to confirm deletion of the *TSA1*, *TSA2*, *TRX1*, *TRX2* and *TRR2* genes in Ubp12-3HA expressing strains.

A-E) Agarose gel analysis of the Phusion PCR reactions (see section 2.3.1.1) to check the deletion of the indicated thioredoxin system genes. For PCR conditions see Table 2.4. Primers used for each reaction are indicated below each gel (Appendix C). For each gel, lane 1 is the negative control (W303-1a), lane 2 is the positive control (the gene delete strain prior to the genetic cross), and lane 3 is the potential deletion strain expressing Ubp12-3HA. The primers used to check the presence of the wild type gene or the gene deletion were predicted to generate a PCR product of (A) either 1295 bp (*TRR2*) or approximately 1500 bp (*trr2*Δ) if the *TRR2* gene is deleted with *HIS3*, (B) either 930 bp (*TSA1*) or approximately 1600 bp (*tsa1*Δ) if the *TSA1* gene is deleted with *HIS3*, (C) either 976 bp (*TSA2*) or approximately 2000 bp (*tsa2*Δ) if the *TSA2* gene is deleted with *LEU2*, (D) either 664 bp (*TRX1*) or approximately 2000 bp (*trx1*Δ) if the *TRX1* gene is deleted with a kanamycin resistance cassette, and (E) either 619 bp (*TRX2*) or approximately 1600 bp (*trx2*Δ) if the *TRX2* gene is deleted with *URA3.* GeneRuler 1 kb DNA Ladder (ThermoScientific) was use.

As can be seen, all of the genetic crosses were successful (Figure 3.1). Hence the following strains expressing Ubp12-3HA were obtained: *trr2*ΔUbp12-3HA (KA52), *tsa1*ΔUbp12-3HA (KA65), *tsa2*ΔUbp12-3HA (KA64) and *trx1*Δ/*trx2*ΔUbp12-3HA (KA81).

3.2.1.2 Analyses of the Ubp12 protein in thioredoxin system mutants

To investigate the potential effects of the thioredoxin system mutants on the levels of Ubp12 levels and on the H_2O_2-induced oxidation of Ubp12, protein extracts from cells of *trr1*ΔUbp12-3HA (KA77), *trr2*ΔUbp12-3HA (KA52), *tsa1*ΔUbp12-3HA (KA65), *tsa2*ΔUbp12-3HA (KA64) and *trx1*Δ/*trx2*ΔUbp12-3HA (KA81) cells exposed to 2 mM H_2O_2 for 0 or 10 minutes were analysed by western blotting (Figure 3.2).

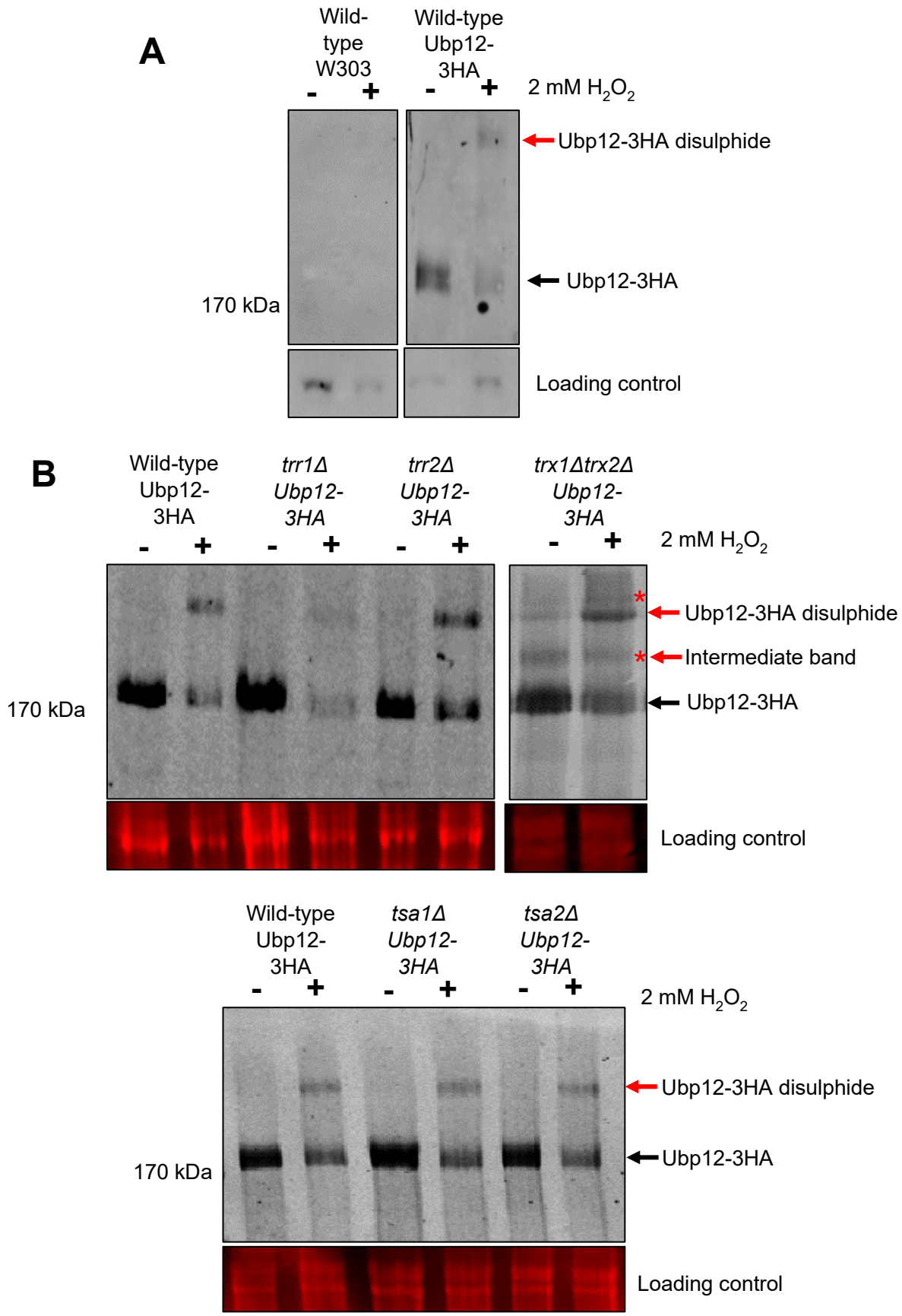
A
Wild-type W303
Wild-type Ubp12-3HA
- + - +
2 mM H_2O_2
Ubp12-3HA disulphide
Ubp12-3HA
170 kDa
Loading control
B
Wild-type Ubp12-3HA
trr1Δ Ubp12-3HA
trr2Δ Ubp12-3HA
trx1Δtrx2Δ Ubp12-3HA
- + - + - + - +
2 mM H_2O_2
Ubp12-3HA disulphide
Intermediate band
Ubp12-3HA
170 kDa
Loading control
Wild-type Ubp12-3HA
tsa1Δ Ubp12-3HA
tsa2Δ Ubp12-3HA
- + - + - +
2 mM H_2O_2
Ubp12-3HA disulphide
Ubp12-3HA
170 kDa
Loading control

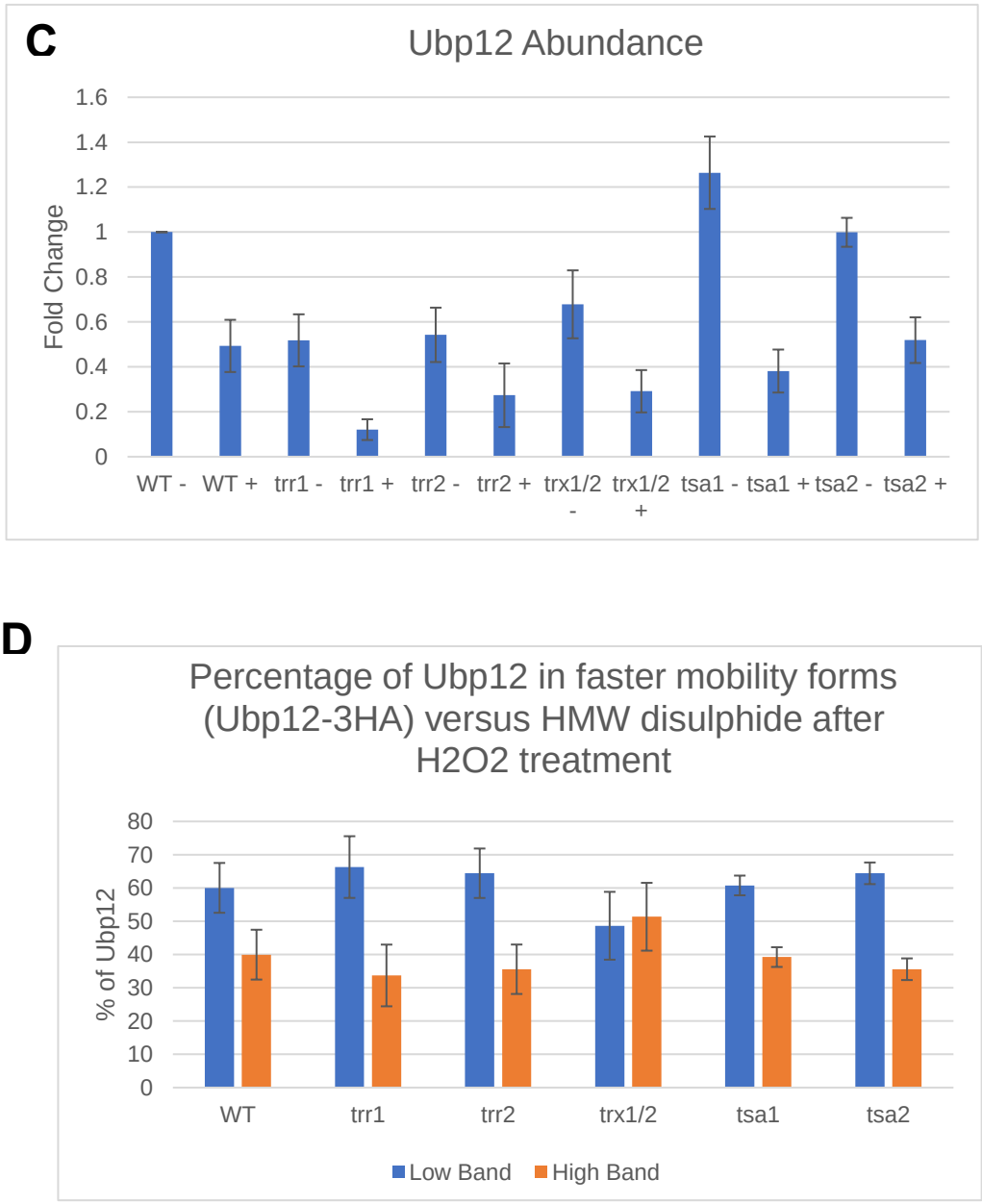

Figure 3.2. The thioredoxin system regulates Ubp12.

A) Western blot analysis of mid-log phase growing wild-type W303-1a cells (KA4) and wild-type W303-1a cells expressing Ubp12-3HA in YPD media and treated with 2 mM H_2O_2 for 0 (-) or 10 (+) minutes. Protein extracts were prepared in non-reducing conditions, separated by SDS-PAGE and proteins were visualised using anti-HA antibodies. A non-specific band is included as a loading control as this blot was developed using ECL and the Typhoon FLA 9500 (see section 2.2.8). B) Western blot analysis of mid-log phase growing wild type (W303-1a, KA10) *trr1*Δ (KA77), *trr2*Δ (KA50), *tsa1*Δ (KA65), *tsa2*Δ (KA64) and *trx1*Δ*trx2*Δ (KA81) cells expressing Ubp12-3HA in YPD media and treated with 2 mM H_2O_2 as indicated. Protein extracts were prepared in non-reducing conditions, separated by SDS-PAGE and visualised using anti-HA antibodies. C) The band intensities of all Ubp12 proteins were quantified using ImageStudio and the total protein loaded in each lane. Fold change represents the comparison between the samples and the wild type 0 minutes H_2O_2 which was set as

1. D) The band intensities of the Ubp12-3HA disulphide and the unstressed faster mobility form of Ubp12-3HA (after H_2O_2 treatment) were quantified using ImageStudio and the total protein loaded in each lane. (B and C) For all quantification n =3, except for wild-type data n=6. The error bars denote standard error of the mean. P values for these data were calculated by T test analysis (see Table 3.1). PageRuler Prestained Protein Ladder (ThermoScientific) was used.

Significantly, a specific band not present in the untagged control lane (untagged W303, Figure 3.2A) of the predicted mobility, 180 kDa, for 3HA epitope-tagged Ubp12 was detected in extracts from *trr1*ΔUbp12-3HA (KA77), *trr2*ΔUbp12-3HA (KA52), *tsa1*ΔUbp12-3HA (KA65), *tsa2*ΔUbp12-3HA (KA64) and *trx1*Δ/*trx2*ΔUbp12-3HA (KA81) cells indicating that the Ubp12-3HA cassette had integrated at the correct locus in the genome (Figure 3.2B). Previous experiments suggested that the abundance of Ubp12 was influenced by Trr1. In particular, the levels of Ubp12 (reduced and oxidised) were found to be significantly decreased in *trr1*ΔUbp12-3HA cells both in the absence or presence of 2 mM H_2O_2 (Curtis, 2019). Consistent with these observations the levels of Ubp12 were also found to be significantly lower in *trr1*ΔUbp12-3HA (KA77) cells compared to wild-type cells (Figure 3.2B and C and Table 3.1A and B). Specifically, prior to H_2O_2 exposure, Ubp12 levels in the *trr1*Δ strain are approximately 50% of the levels in the wild-type strain (Figure 3.2B and C). Moreover, after H_2O_2 exposure, Ubp12 levels decrease in the *trr1*Δ strain to approximately 15% of the levels of Ubp12 in unstressed wild-type cells whilst levels of Ubp12 decrease to approximately 50% in wild-type cells. Further analyses revealed that these differences in Ubp12 abundance between the wild-type and the *trr1*Δ strains are significant both before and after exposure to H_2O_2 (p = 0.0468 * before H_2O_2 addition and p = 0.0056 ** after H_2O_2 addition, Table 3.1 A and B). Interestingly, analyses of the western blot data also suggested that the abundance of Ubp12 decreased following H_2O_2 treatment in all of the strains tested (Figure 3.2B and C), although this decrease in abundance was only confirmed to be significant for wild-type Ubp12-3HA (p = 0.0016 **), *tsa1*ΔUbp12-3HA (p = 0.0151 *) and *tsa2*ΔUbp12-3HA (p = 0.0225 *) cells (Table 3.1C). This data is consistent with previous large-scale studies of several different yeast species which suggested that the levels of Ubp12 and homologues may decrease following H_2O_2 exposure (Gasch et al., 2000, Chen et al., 2003). Although the data obtained for the quantification of the *trr1*Δ, *trr2*Δ, and *trx1*Δ*trx2*Δ strains suggested that Ubp12 levels may also decrease following H_2O_2 treatment (Figure 3.2B

and C) the errors bars were quite large (Figure 3.2C) and calculated to be non-significant (Table 3.1C). Hence, further repeats would be necessary to confirm if Ubp12 levels also decrease following H_2O_2 treatment in these strains or whether in fact there is any evidence that the abundance of Ubp12 is different to unstressed cells in strains lacking *TRR1*, *TRR2*, *TRX1* and *TRX2* genes. As described above, the data revealed that the abundance of Ubp12 was significantly decreased in cells lacking *TRR1* in the absence of H_2O_2 (Figure 3.2B and C and Table 3.1A). However, despite indications that perhaps other proteins of the thioredoxin system such as Trr2, Trx1, Trx2 and Tsa1 may also influence the levels of Ubp12 in unstressed cells (Figure 3.2B and C), further statistical analysis did not demonstrate any significant links with these proteins (Table 3.1A). Further repeats of experiments with the relevant strains would be important to explore whether there are any significant links between Trr2, Trx1, Trx2 and Tsa1 with Ubp12 abundance. It is important to note the formation of an intermediate form of Ubp12 (red arrow with asterisk, Figure 3.2B) in the *trx1*Δ*trx2*Δ strain which was included in abundance calculations and will be discussed later in this chapter.

(A)

Sample	P value
***trr1*Δ -**	0.0468 (*)
***trr2*Δ -**	0.0634 (ns)
***trx1*Δ*trx2*Δ -**	0.1673 (ns)
***tsa1*Δ -**	0.2431 (ns)
***tsa2*Δ -**	0.9890 (ns)

(B)

Sample	P value
***trr1*Δ +**	0.0056 (**)
***trr2*Δ +**	0.2621 (ns)
***trx1*Δ*trx2*Δ +**	0.1671 (ns)
***tsa1*Δ +**	0.4160 (ns)
***tsa2*Δ +**	0.8525 (ns)

(C)

Sample	P value
Wild-type Ubp12-3HA	0.0016 (**)
***trr1*Δ**	0.0563 (ns)
***trr2*Δ**	0.2241 (ns)
***trx1*Δ*trx2*Δ**	0.1089 (ns)
***tsa1*Δ**	0.0151 (*)
***tsa2*Δ**	0.0225 (*)

Table 3.1. Unpaired T test P values for Figure 3.2.

A - C) P values for this data were calculated by T test analysis using Welch's correlation where appropriate. N = 3 for all data except for the wild-type data, where n = 6. Significance is indicated by the (*), (**), (***), and ns denotes non-significant data. The intermediate band (red arrow and asterisk, Figure 3.2B) was included in the abundance calculations for all strains examined. A) P values were calculated for Ubp12 abundance in each strain prior to H_2O_2 exposure relative to wild-type Ubp12-3HA 0 minutes H_2O_2 data. B) P values were calculated for Ubp12 abundance in each strain following H_2O_2 exposure relative to wild-type Ubp12-3HA + H_2O_2 for 10 minutes data. C) P values were calculated for Ubp12 abundance in each strain between the 0 minutes and 10 minutes exposure to H_2O_2 data.

Interestingly, despite the evidence that Trr1, and possibly several other thioredoxin system proteins, influence Ubp12 abundance, the percentages of the faster mobility unstressed Ubp12 band to HMW species of Ubp12 were very similar in most of the different strains following H_2O_2 treatment (Figure 3.2B and D). Furthermore, in most cases there appeared to be more of the protein detected in the faster mobility form of Ubp12 after H_2O_2 treatment (Figure 3.2B and D). Indeed, T test analyses revealed that in protein extracts from wild-type Ubp12-3HA, *trr1*ΔUbp12-3HA, *trr2*ΔUbp12-3HA and *tsa1*ΔUbp12-3HA *tsa2*ΔUbp12-3HA strains there was significantly more Ubp12 in the faster mobility unstressed species (p = 0.0304 *, p = 0.0126 *, p = 0.0089 **, p = 0.0008 ***, p = 0.0004 *** respectively). The exception to this result was observed using protein extracts from the *trx1*Δ*trx2*Δ strain (Figure 3.2B and D). In the case of the *trx1*Δ*trx2*Δ strain more of the Ubp12 protein was found in HMW species relative to the faster mobility form following H_2O_2 treatment compared with the other strains examined (Figure 3.2D). However, T test analysis revealed that there was no

significant difference between the amount of faster mobility Ubp12 and HMW disulphide in the *trx1*Δ*trx2*Δ strain. T test analyses also revealed there was no significant difference in the amount of Ubp12 disulphide between the *trx1*Δ*trx2*Δ strain and the other strains tested. In addition, a new HMW band (indicated with a red arrow and asterisk in Figure 3.2B), intermediate in mobility to the HMW species and the faster mobility unstressed Ubp12, was readily detectable in *trx1*Δ*trx2*Δ protein extracts either before or after H_2O_2 treatment, compared to protein extracts from the other strains (Figure 3.2B). Additional HMW band(s) were also detected in *trx1*Δ*trx2*Δ protein extracts (red asterisk, Figure 3.2B). These new, unidentified bands present in the *trx1*Δ*trx2*Δ strain will be discussed later in the chapter. Moreover, in the *trx1*Δ*trx2*Δ strain the amount of Ubp12 in the HMW species before H_2O_2 treatment is considerably higher than observed in any of the other strains tested suggesting that loss of cytoplasmic thioredoxin activity leads to oxidation of Ubp12 in the absence of any H_2O_2 treatment (Figure 3.2B).

In summary, the data in this section suggests that specific members of the thioredoxin system influence the abundance and oxidation of Ubp12 in response to H_2O_2. In addition to further supporting preliminary observations from the lab that Trr1 influences the abundance of Ubp12, the initial data reported here suggests that it is possible that other thioredoxin system proteins may also affect the abundance of Ubp12. However, more experiments would be required to confirm these conclusions. Finally, the results presented here suggest that the activity of the cytoplasmic thioredoxins Trx1 and Trx2 influence the oxidation of Ubp12. These results will be explored later in this chapter.

3.2.1.3 Analysis of Ubp12 abundance in the thioredoxin mutants in reducing conditions

The data presented above indicated that Trr1, and potentially other thioredoxin system proteins, influence the abundance of Ubp12 when examined under non-reducing conditions. In addition, there was also evidence of decreasing levels of Ubp12 following H_2O_2 treatment in several strains, including the wild-type (Table 3.1C). However, one possibility to explain these observations is that loss of specific thioredoxin system proteins such as Trr1 or the treatment of cells with H_2O_2 leads to

the oxidation of Ubp12 into species that do not resolve well on SDS PAGE in non-reducing conditions, which could hamper attempts to properly assess the levels of the Ubp12 protein. Hence, it was decided to next investigate whether Ubp12 abundance was altered following treatment with H_2O_2 and in the thioredoxin system mutant strains using SDS PAGE analysis under reducing conditions. Wild-type, *trr1*Δ, *trr2*Δ, *tsa1*Δ, *tsa2*Δ and *trx1*Δ *trx2*Δ cells all expressing Ubp12-3HA described in the previous section, were exposed to 2 mM H_2O_2 for 0 (-) or 10 (+) minutes and the protein extracts analysed by western blot in reducing conditions using β-mercaptoethanol (Figure 3.3).

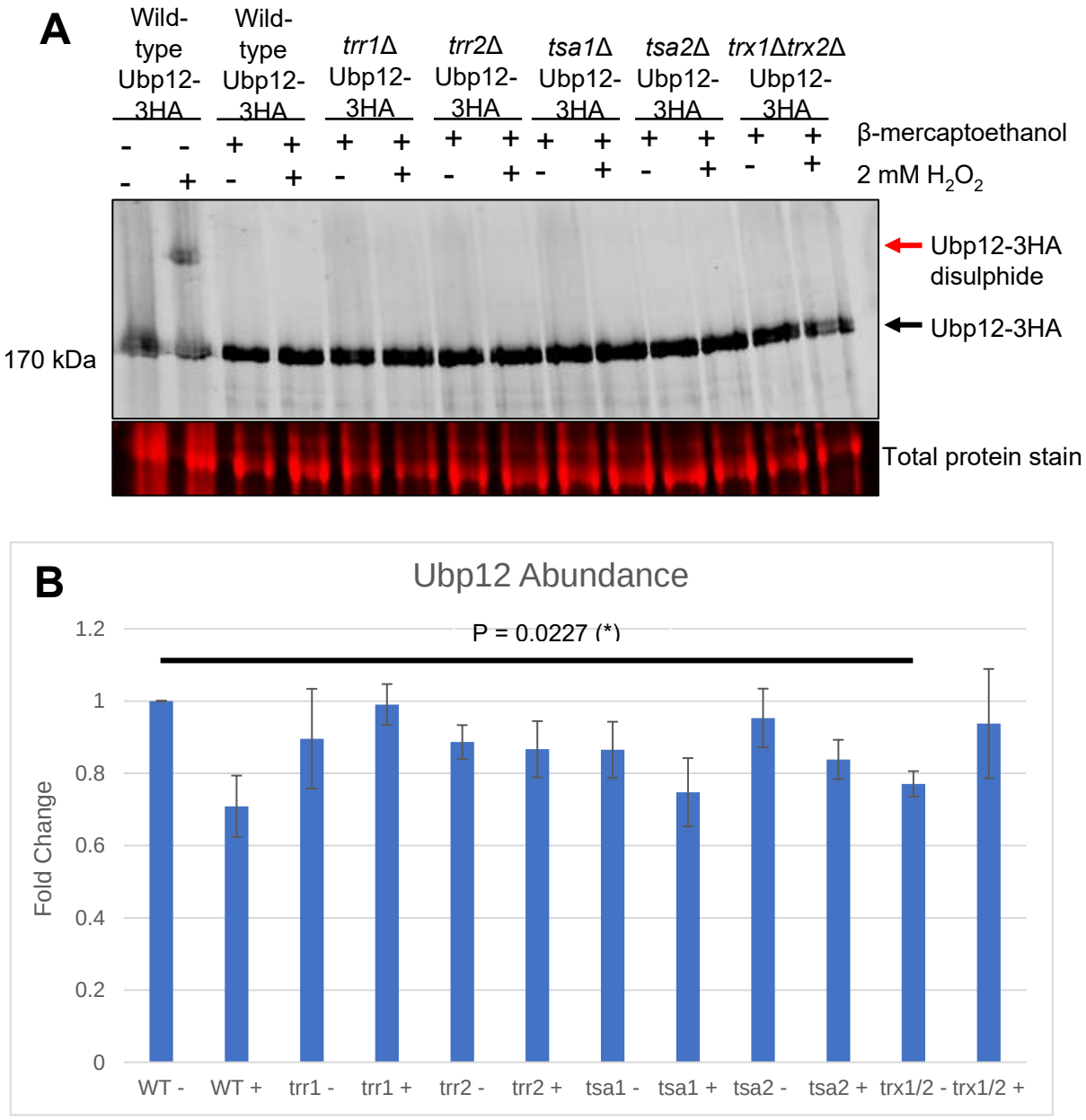

Figure 3.3. Analysis of Ubp12 abundance in reducing and non-reducing conditions.

A) Western blot analysis of mid-log phase growing wild type (W303-1a, KA10) *trr1*Δ (KA77), *trr2*Δ (KA50), *tsa1*Δ (KA65), *tsa2*Δ (KA64) and *trx1*Δ*trx2*Δ (KA81) cells expressing Ubp12-3HA in YPD media and treated with 2 mM H_2O_2 as indicated. Protein extracts were prepared in non-reducing conditions (lanes 1 and 2) and reducing conditions (all other lanes), separated by SDS-PAGE and visualised using anti-HA antibodies. B) Ubp12 specific band intensities were quantified against loaded total protein using ImageStudio, and fold change calculated by comparison to the wild type 0 minutes H_2O_2 sample (set as 1). N=3, error bars represent standard error of the mean. P values were calculated using T test analysis. Only significant P values are shown. PageRuler Prestained Protein Ladder (ThermoScientific) was used.

Interestingly, this data revealed that much of the decrease in levels of Ubp12 described above (Figure 3.2C and Table 3.1) was not detected when Ubp12 was analysed using reducing conditions. In particular, although there is some evidence of a drop in abundance in Ubp12 in wild-type cells treated with H_2O_2, in contrast to the analysis in non-reducing conditions described above, no significant difference in abundance in absence or presence of H_2O_2 was detected in wild-type cells. It is possible that more repeats of this experiment would show a significant decrease in abundance in Ubp12 following H_2O_2 treatment in wild-type cells but currently this is not the case. The analysis performed using reducing conditions also indicated that, with the exception of *trx1*Δ*trx2*ΔUbp12-3HA cells, there was no significant decrease in Ubp12 abundance in any of the thioredoxin mutants tested compared with the wild-type 0 minutes protein extract either before or following treatment with H_2O_2 (Figure 3.3 and T test analysis). Again, this contrasts with the analyses performed in non-reducing conditions which indicated that Ubp12 abundance significantly decreased in *tsa1*Δ and *tsa2*Δ cells following H_2O_2 treatment (Table 3.1C) and in *trr1*Δ cells before and after H_2O_2 treatment (Table 3.1A-C). Given that the differences in Ubp12 abundance in these different analyses (Figures 3.2C, 3.3, Table 3.1) are likely linked to using non-reducing versus reducing conditions these results suggest that much of the decreases in Ubp12 abundance presented above (Figure 3.2C, Table 3.1) are due to reduced detection of oxidised Ubp12 species on the western blots. It is possible for example that the oxidised species do not transfer as efficiently from the SDS-PAGE to the membrane or alternatively that other oxidised species are present that migrate in regions of the gel that were not quantified. However, an exception to this conclusion is perhaps the potential decrease of abundance of Ubp12 in wild-type cells following H_2O_2 treatment (Figures 3.2C, 3.3, Table 3.1C). In addition, a significant decrease (the only significant decrease that was detected by T test in Figure 3.3) in Ubp12 abundance was detected in *trx1*Δ*trx2*ΔUbp12-3HA cells before H_2O_2 treatment compared to the wild-type cells grown under the same conditions (Figure 3.3, $p = 0.0227$ *). A similar result appeared in *trx1*Δ*trx2*ΔUbp12-3HA cells using non-reducing conditions (Figure 3.2C), although in this case the difference in abundance was judged to be non-significant (Table 3.1A). More repeats of the analyses of Ubp12 abundance in the *trx1*Δ*trx2*ΔUbp12-3HA cells, and also in the wild-type cells, before and following H_2O_2 treatment using non-reducing

and reducing conditions would be useful in further clarifying these observations. However, if confirmation of a decrease in Ubp12 abundance in wild-type cells following H_2O_2 treatment and/or in *trx1*Δ*trx2*ΔUbp12-3HA cells before H_2O_2 treatment was obtained this would suggest that, in addition to oxidation, Ubp12 levels are regulated at the transcription/post transcriptional level in response to H_2O_2, and, moreover, that this regulation may involve the thioredoxin system. It is also interesting to note that preliminarily, Figure 3.3A suggests that the intermediate form(s) (red arrow and asterisk, Figure 3.2B) and unidentified HMW form(s) (red asterisk, Figure 3.2B) of Ubp12 formed in the *trx1*Δ*trx2*Δ strain are sensitive to β-mercaptoethanol, however this requires further analysis with appropriate controls. The data presented above also suggests that there are more oxidised forms of Ubp12 produced in response to H_2O_2 that are not completely detected by western blot analyses. This may be due to problems with protein transfer, or that some oxidised complexes may migrate with unpredicted mobilities due to alterations of their three-dimensional shape, hence may be missed from quantification.

3.2.2 Analyses of the Ubp12 intermediate band

The results presented above revealed that Ubp12 regulation by H_2O_2 involved Trx1 and Trx2. In particular, more of the Ubp12 protein was found in HMW species relative to the faster mobility form in *trx1*Δ*trx2*Δ cells following H_2O_2 treatment compared with the other strains examined (Figure 3.2C). In addition, a new intermediate mobility HMW species was identified in *trx1*Δ*trx2*Δ protein extracts compared to protein extracts from the other strains (Figure 3.2A). Although there was no similar intermediate band with a similar intensity obvious in the protein extracts from the other strains examined (Figure 3.2A) it was possible that this band was a non-specific band only detectable in cells lacking both Trx1 and Trx2. Hence to rule out this possibility *trx1*Δ*trx2*Δ cells expressing the normal Ubp12 (KD467) and *trx1*Δ*trx2*ΔUbp12-3HA cells expressing epitope-tagged Ubp12 were treated with 2 mM H_2O_2 for 0 or 10 minutes. Protein extracts were isolated and analysed by western blotting (Figure 3.4).

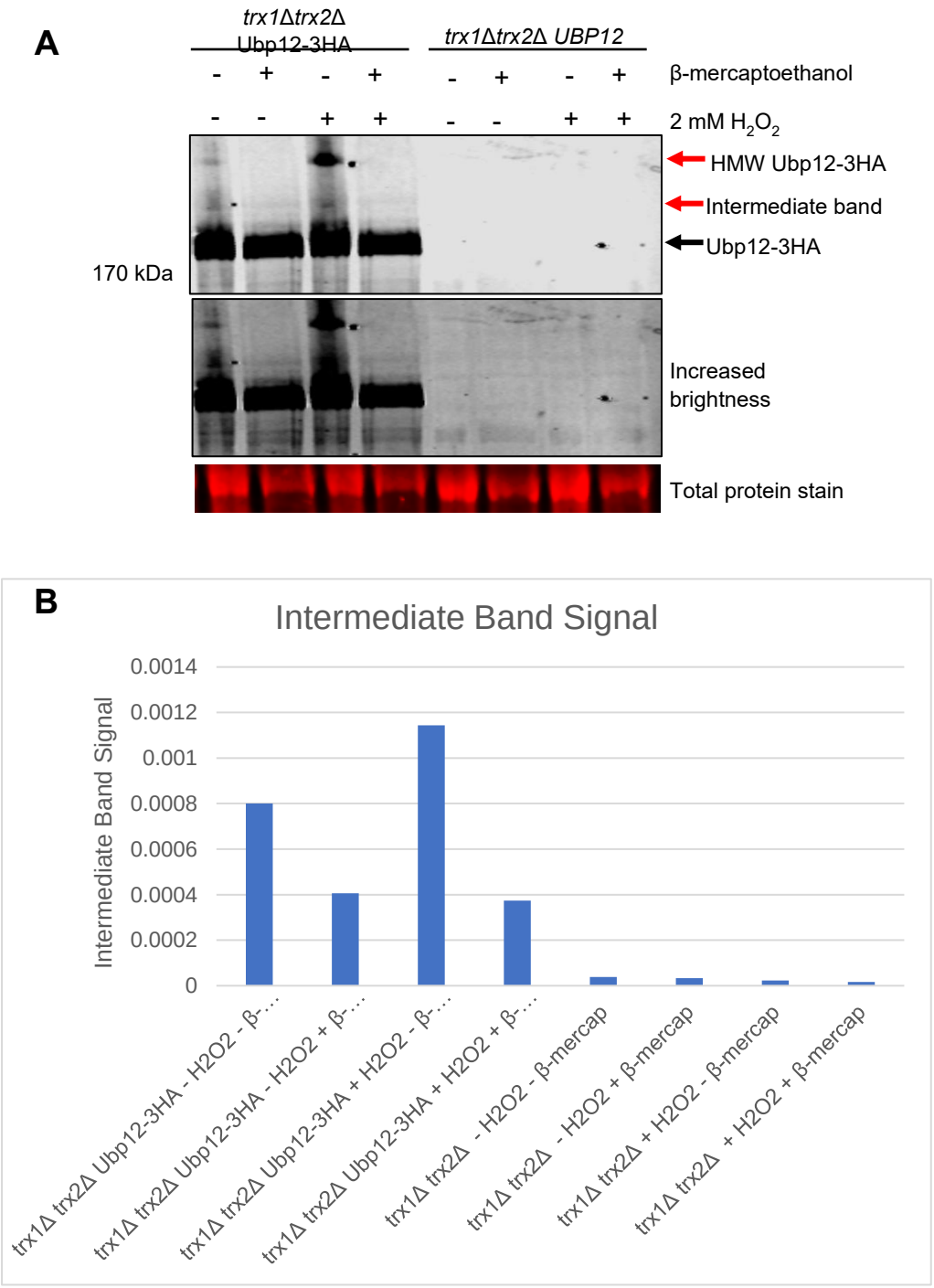

Figure 3.4. The intermediate band represents an oxidised form of Ubp12.

(A) Western blot analysis of mid-log phase growing wild-type and *trx1*Δ*trx2*Δ cells expressing Ubp12-3HA, and *trx1*Δ*trx2*Δ cells expressing untagged Ubp12 in YPD media and treated with 2 mM H_2O_2 for 0 (-) or 10 (+) minutes. Protein extracts were prepared in either reducing or non-reducing conditions separated by SDS-PAGE and proteins visualised using anti-HA antibodies. The brightness and contrast have been increased to attempt to detect weak signals of the intermediate band. (B) The band intensities of the intermediate HMW forms of Ubp12 were quantified using ImageStudio and the total protein loaded in each lane. N=1. PageRuler Prestained Protein Ladder (ThermoScientific) was used.

Although only performed once these results support the conclusion that the intermediate mobility HMW species identified in extracts from *trx1*Δ*trx2*Δ cells expressing Ubp12-3HA is not a non-specific band as no band of similar intensity was detected in extracts from *trx1*Δ*trx2*Δ cells expressing untagged Ubp12 (Figure 3.4). There was a faint non-specific band detected where the intermediate mobility HMW species migrates on the gel (seen more clearly in the blot with increased brightness) in the cells expressing untagged Ubp12 (Figure 3.4A). However, quantification of this signal in *trx1*Δ*trx2*Δ cells expressing either Ubp12 or Ubp12-3HA indicated that this signal contributes a minor component of the signal in *trx1*Δ*trx2*Δ cells expressing Ubp12-3HA (Figure 3.4B). It is also interesting to note that similar to the HMW disulphide Ubp12 complexes formed in response to H_2O_2, the intermediate mobility HMW species detected in *trx1*Δ*trx2*Δ cells expressing Ubp12-3HA appears to be sensitive to the presence of reducing agent suggesting that some (perhaps all) of this intermediate mobility HMW species is an oxidised form(s) of Ubp12 (Figure 3.4). However, this experiment has only been successfully performed once and would need repeating to allow detailed assessment of the effect of reducing agent on this intermediate mobility oxidised form of Ubp12. These data further support the hypothesis that Trx1 and/or Trx2 are responsible for regulating the formation of this intermediate mobility HMW Ubp12 species, further consolidating the connections between the thioredoxin system and the regulation of Ubp12.

The mechanism underlying the oxidation of Ubp12 is not clear. It is possible that H_2O_2 is involved directly in the oxidation of Ubp12 or alternatively another protein may be involved. The investigations of Ubp12 oxidation in *trx1*Δ*trx2*Δ cells suggest that the thioredoxin system is linked to this mechanism in some way. Previous studies in *S. cerevisiae* revealed that the Yap1 transcription factor becomes specifically oxidised and activated by H_2O_2 via a mechanism that involves an intermolecular disulphide complex between Yap1 and either Gpx3 in the BY4741 strain background or Tsa1 in the W303 strain background (see section 1.2.3.3) (Delaunay et al., 2002, Ross et al., 2000). This difference in mechanism in the two strain backgrounds is dependent on the presence (BY4741) or absence (W303) of functional Ybp1 protein (see section 1.2.3.3) (Veal et al., 2003, Ross et al., 2000). Given that the W303 strain background was studied above (Figures. 3.2 and 3.3) this raised the possibility that Tsa1 may be

directly involved in the oxidation of Ubp12. However, as shown above, the oxidation of Ubp12 was not inhibited in cells lacking either Tsa1 or Tsa2 (Figure 3.2). However, this result did not rule out the possibility that Gpx3 might act to regulate oxidation of Ubp12 in a Ybp1-independent manner, particularly as Gpx3 regulates Yap1 oxidation by H_2O_2. Hence to test whether Gpx3 influences the oxidation of Ubp12 into the different HMW complexes detected in wild-type and *trx1*Δ*trx2*Δ cells (Figure 3.2) the first step was to construct *TRX1TRX2* wild-type and *trx1*Δ*trx2*Δ strains expressing Ubp12-3HA but containing a deletion of the *GPX3* gene. The strategy to delete the *GPX3* gene in the *TRX1TRX2* wild-type Ubp12-3HA (KA10) and the *trx1*Δ*trx2*Δ Ubp12-3HA (KA81) strains is shown below in Figure 3.5. Briefly, the *GPX3* gene has been replaced with *HIS3* from the *yap1*Δ*gpx3*Δ strain (KA60) (Veal et al., 2003), and genomic DNA from this strain was used as a template to construct a 1550 bp *GPX3* gene replacement cassette. This cassette was successfully obtained using Phusion PCR (see Section 2.3.1.1 for PCR conditions) and Gpx3-Deletion Frag Fw and Gpx3-Deletion Frag Rev primers (Appendix C), which were designed to hybridise approximately 200 bp upstream and downstream from the *HIS3* replacement of the *GPX3* gene (Figure 3.6). Next, the *GPX3* gene replacement cassette was transformed into *TRX1TRX2* wild-type Ubp12-3HA (KA10) and the *trx1*Δ*trx2*Δ Ubp12-3HA (KA81) cells. His+ colonies were checked by DreamTaq PCR (see Section 2.3.1.2 for PCR conditions) using the primers Gpx3-Deletion Frag Fw and Gpx3-Deletion Frag Rev which checked the successful construction of the *TRX1TRX2gpx3*Δ Ubp12-3HA strain (KA116) and *trx1*Δ*trx2*Δ*gpx3*Δ Ubp12-3HA strain (KA114) strains (Figure 3.6B).

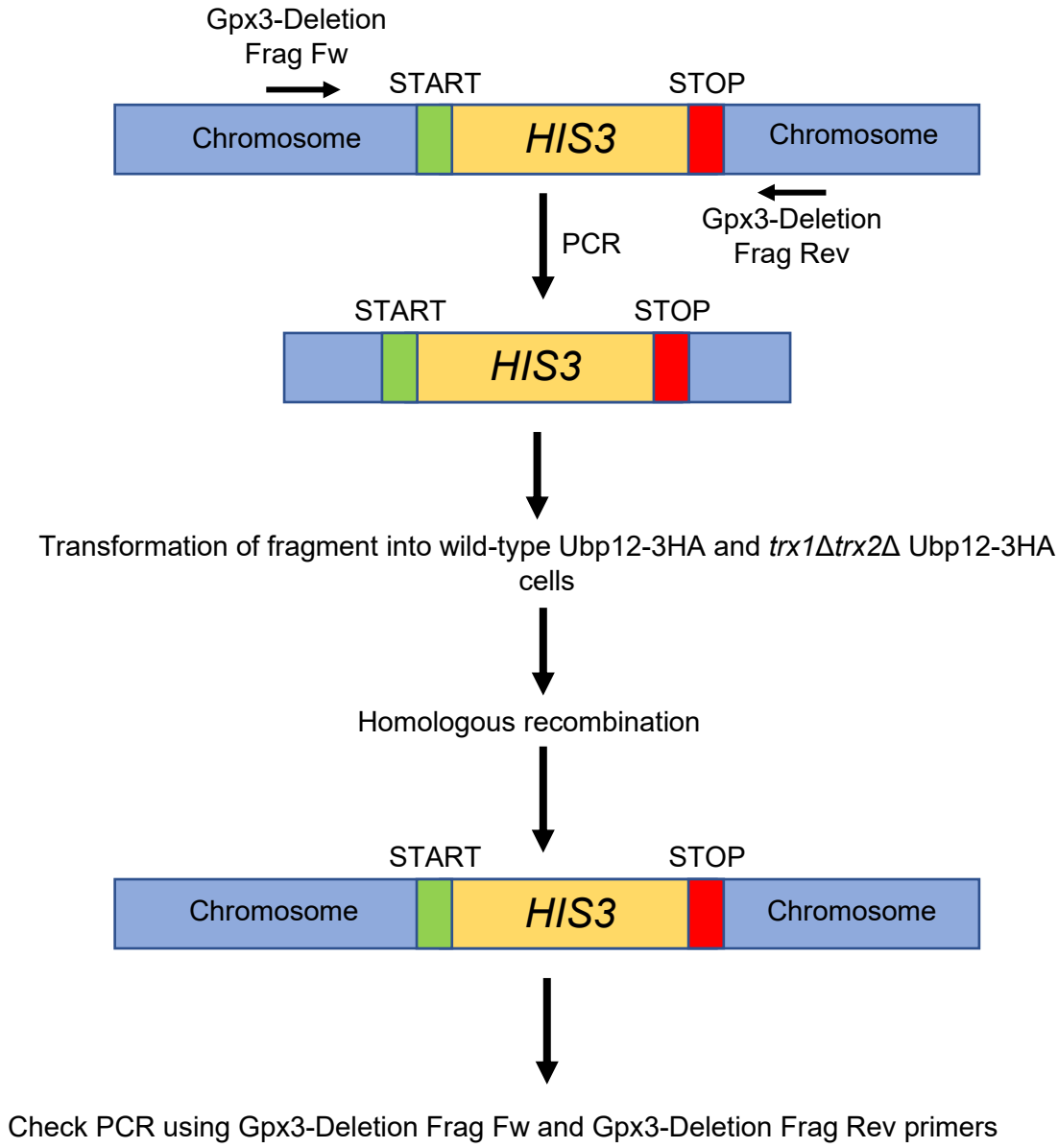

Figure 3.5. Strategy to delete *GPX3* in wild-type Ubp12-3HA and *trx1Δtrx2Δ* Ubp12-3HA cells.

Primers (Gpx3-Deletion Frag Fw and Gpx3-Deletion Frag Rev) were designed to create a fragment containing 20 bp homology to the DNA sequences 200 bp upstream of the start codon and 200 bp downstream of the stop codon of the *HIS3* gene at the genomic locus of *GPX3* using the *yap1Δgpx3Δ* strain (KA60) as a template. The PCR product was amplified and transformed into wild-type Ubp12-3HA (KA10) and *trx1Δtrx2Δ* Ubp12-3HA (KA81) cells. Check PCRs using the primers Gpx3-Deletion Frag Fw and Gpx3-Deletion Frag Rev checked the integration of *HIS3* at the correct genomic locus.

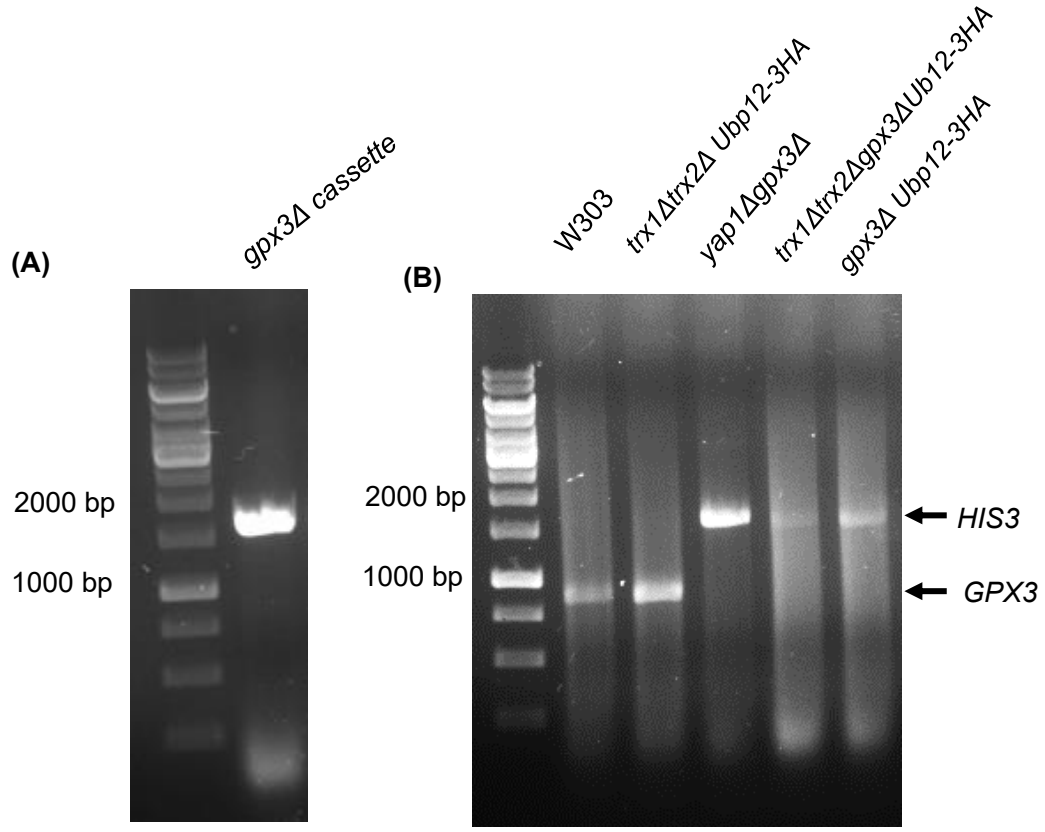

Figure 3.6. *GPX3* was successfully deleted in the *TRX1TRX2* Ubp12-3HA and the *trx1*Δ*trx2*Δ Ubp12-3HA strains.

(A) Agarose gel analysis of the Phusion PCR reaction (see section 2.3.1.1) to generate the 1550 bp *GPX3* gene replacement cassette using the Gpx3-Deletion Frag fw and Gpx3-Deletion Frag rev primers (Appendix C) and genomic DNA from the *yap1*Δ*gpx3*Δ strain (KA60) as template. PCR conditions are detailed in Table 2.4. (B) Agarose gel analysis of the DreamTaq PCR reactions (see section 2.3.1.2) using the Gpx3-Deletion Frag fw and Gpx3-Deletion Frag rev primers (Appendix C) of one His+ transformant from the *TRX1TRX2* Ubp12-3HA and the *trx1*Δ*trx2*Δ Ubp12-3HA strains to check the replacement of *GPX3* with *HIS3*. As controls identical PCR reactions were performed on genomic DNA from the W303 (*TRX1TRX2GPX3*), *trx1*Δ*trx2*Δ Ubp12-3HA (KA81) and *yap1*Δ*gpx3*Δ (KA60) strains. Expected products were 872 bp if the wild type *GPX3* gene is present and 1550 bp if the *GPX3* gene was replaced with *HIS3* (*gpx3*Δ). GeneRuler 1 kb DNA Ladder (ThermoScientific) was used.

To test whether Gpx3 influences the oxidation of Ubp12 into the different HMW complexes wild-type Ubp12-3HA (KA10), *trx1*Δ*trx2*Δ Ubp12-3HA (KA81), *TRX1TRX2gpx3*Δ Ubp12-3HA strain (KA116) and *trx1*Δ*trx2*Δ*gpx3*Δ Ubp12-3HA (KA114) strains were treated with 2 mM H_2O_2 for 0 (-) or 10 (+) minutes. Protein extracts were isolated and analysed by western blotting (Figure 3.7). To assess whether Gpx3 was essential for formation of any of the HMW species of Ubp12 the percentage of Ubp12 present in each band was quantified in the different strains in the absence or presence of H_2O_2 (Figure 3.7B). Although this analysis was only performed once there was no evidence that loss of Gpx3 prevented the formation of HMW Ubp12 complexes (High Band) in cells which contained Trx1 and Trx2 (Figure 3.7). Furthermore, although as expected, the intermediate HMW forms were detected in addition to the HMW species (High Band) in *trx1*Δ*trx2*Δ*GPX3* both before and after H_2O_2 treatment, there was no evidence from the analysis of *trx1*Δ*trx2*Δ*gpx3*Δ cells that Gpx3 was essential for the formation of any of the HMW Ubp12 species in cells lacking Trx1 and Trx2 (Figure 3.7). Hence, in conclusion there is no evidence that Gpx3 influences the oxidation of Ubp12 in the W303 strain background. However, this experiment has only been performed once and does not rule out the possibility that Gpx3 may have some role in the BY4741 strain where the protein has been shown to regulate oxidation of Yap1 (see section 1.2.3.3) (Delaunay et al., 2002).

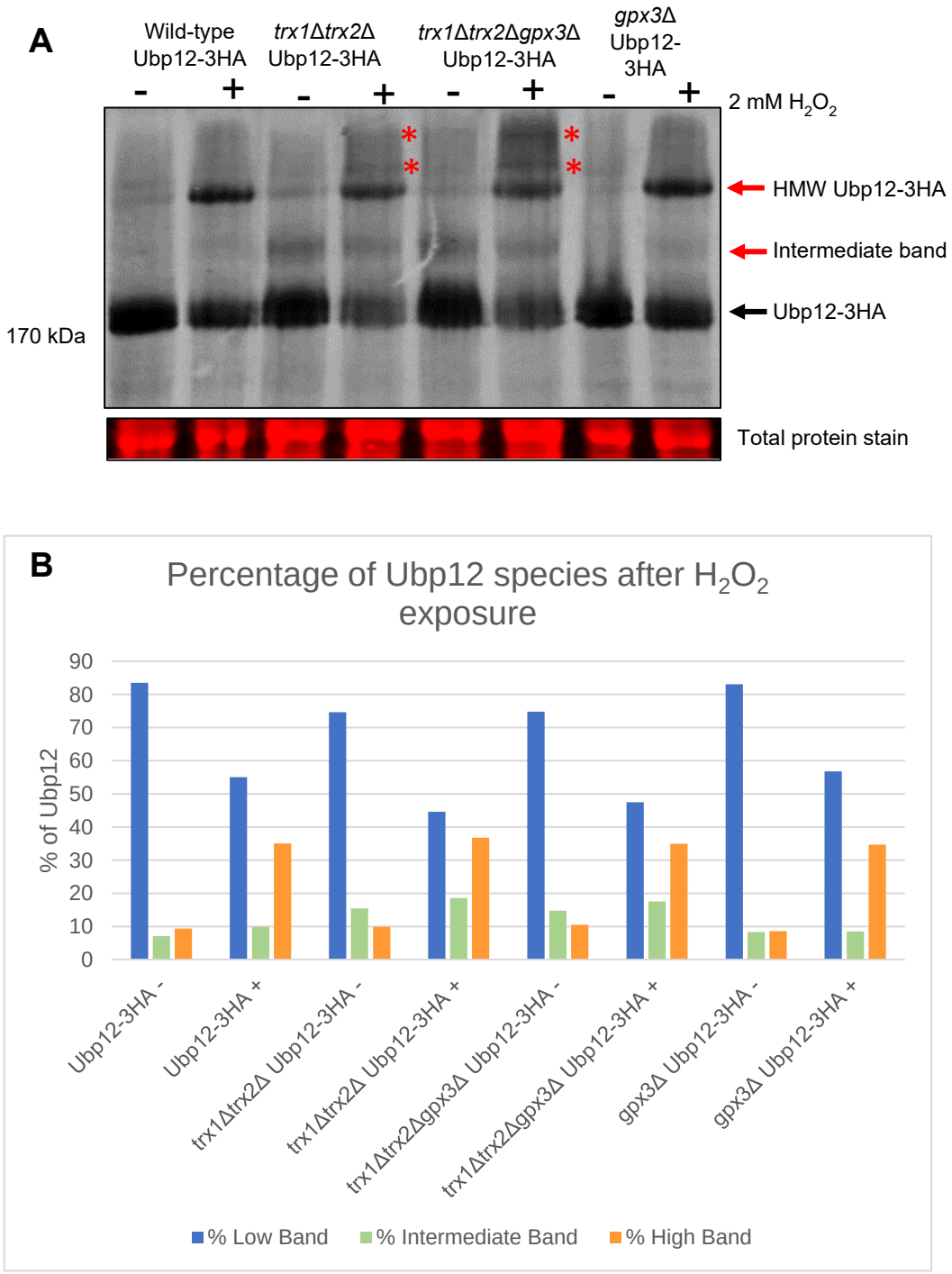

Figure 3.7. Gpx3 is not essential for the formation of the HMW Ubp12 complexes.

(A) Western blot analysis of mid-log phase growing *TRX1TRX2GPX3* Ubp12-3HA (KA10), *trx1Δtrx2ΔGPX3* Ubp12-3HA (KA81), *trx1Δtrx2Δgpx3Δ* Ubp12-3HA (KA114) and *TRX1TRX2gpx3Δ* Ubp12-3HA (KA116) cells in YPD media and treated with 2 mM H_2O_2 for 0 (-) or 10 (+) minutes. Protein extracts were prepared in non-reducing conditions, separated by SDS-PAGE and proteins visualised using anti-HA antibodies. Red asterisks indicate other possible oxidised forms of Ubp12. (B) The band intensities of Ubp12 species were quantified using ImageStudio and the total protein loaded in each lane. N=1. PageRuler Prestained Protein Ladder (ThermoScientific) was used.

Interestingly, the western blot analysis also revealed the presence of even higher molecular weight forms of Ubp12 which were readily detected in protein extracts from *trx1*Δ*trx2*Δ Ubp12-3HA and *trx1*Δ*trx2*Δ*gpx3*Δ Ubp12-3HA cells (Figure 3.7A, red asterisks). Indeed, there is evidence of similar new forms of Ubp12 on western blot analysis of *trx1*Δ*trx2*Δ Ubp12-3HA protein extracts presented earlier (see Figure 3.2A). Although these band(s) have not been characterised, they are not detectable in cells containing Trx1 and Trx2 (Figure 3.2B, 3.7A) suggesting a role for Trx1 and/or Trx2 in resolving these species. Moreover, the presence or absence of Gpx3 again had no effect on the detection of these species (Figure 3.7A). It is possible that these band(s) have a stronger signal when Gpx3 is missing in the *trx1*Δ*trx2*Δ*gpx3*Δ Ubp12-3HA strain, however quantification would be necessary to analyse this observation. Taken together, these data further consolidate the hypothesis that Trx1 and/or Trx2 regulate the oxidation of Ubp12 and, moreover, suggest that this regulation is independent of Gpx3 activity.

3.2.3 Exploring the kinetics of the HMW disulphide and intermediate band

Previous work from the lab revealed that the formation of the HMW Ubp12 disulphide complex is sensitive to H_2O_2 concentration. Lower levels of H_2O_2 (0.2 mM) resulted in the formation of a relatively small amount of the HMW disulphide complex, which was relatively transient in nature peaking at approximately 10 minutes after H_2O_2 addition (Curtis, 2019). In contrast, higher levels of H_2O_2 (2 mM) caused the formation of a relatively greater amount of the HMW disulphide complex which persisted over the time frame of the experiment (60 minutes) (Curtis, 2019). Hence, based on the results presented here that Trx1 and/or Trx2 influence the oxidation of Ubp12, the next step was to assess the potential effects of Trx1 and Trx2 on these HMW disulphide complex formation profiles. First, to assess the oxidation of Ubp12 by a range of H_2O_2 concentrations in cells lacking Trx1 and Trx2, wild-type Ubp12-3HA (KA10) and *trx1*Δ*trx2*Δ Ubp12-3HA (KA81) cells were exposed to 0, 0.5, 1, 2, 5, 10 mM H_2O_2 for 10 minutes and protein extracts were isolated and analysed by western blotting (Figure 3.8).

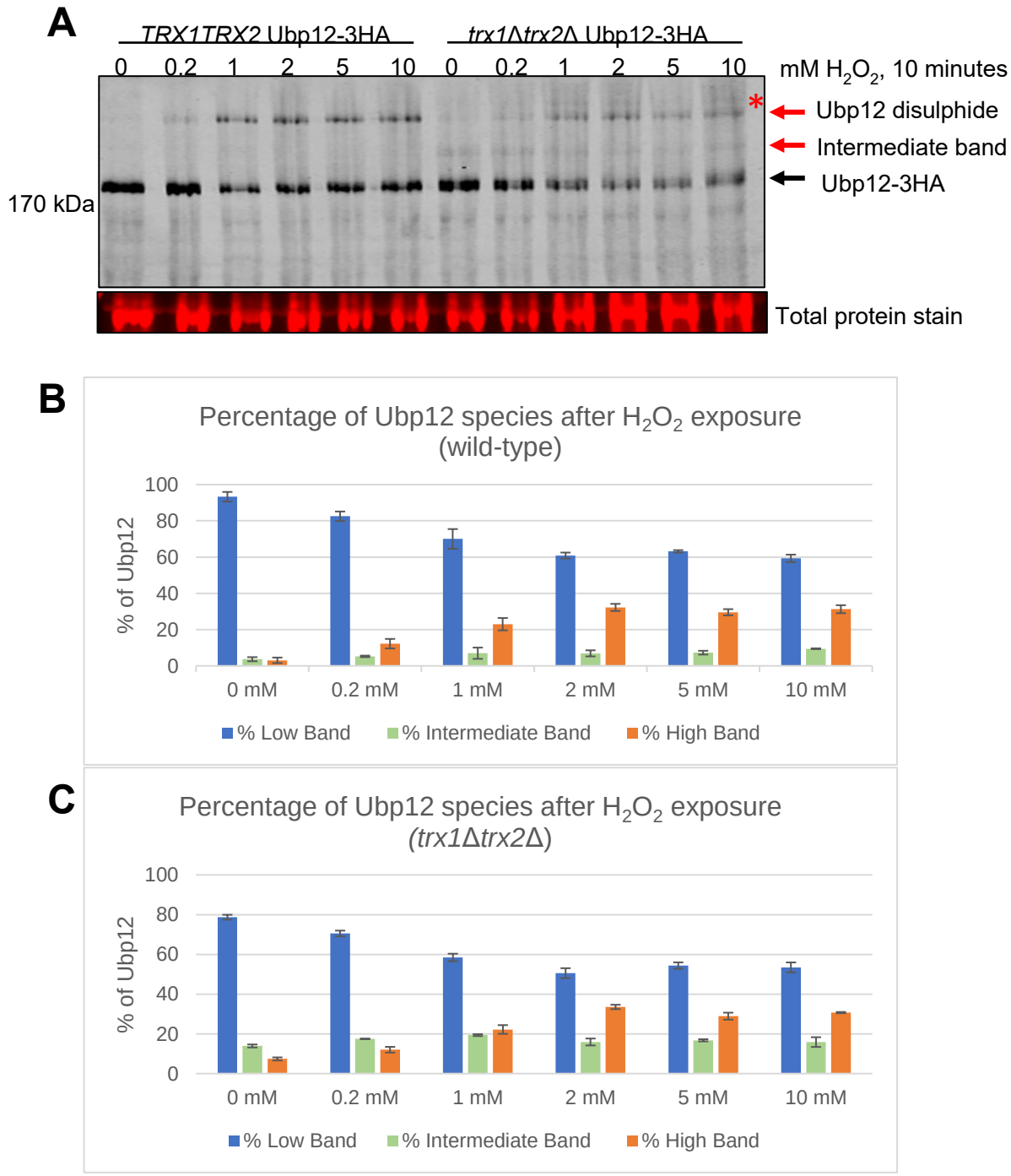

Figure 3.8. Trx1 and Trx2 influence the oxidation of Ubp12.

A) Western blot analysis of mid-log phase growing wild type Ubp12-3HA (KA10) and *trx1*Δ*trx2*Δ Ubp12-3HA (KA81) cells in YPD media and treated with 0, 0.5, 1, 2, 5, or 10 mM H_2O_2 for 10 minutes. Protein extracts were prepared in non-reducing conditions, separated by SDS-PAGE and proteins visualised using anti-HA antibodies. Red asterisks indicate other possible oxidised forms of Ubp12. (B and C) The band intensities of Ubp12 species were quantified using ImageStudio and the total protein loaded in each lane. Error bars denote standard error of the mean. N=3. PageRuler Prestained Protein Ladder (ThermoScientific) was used.

The analyses of the wild-type cells revealed that peak formation of the HMW Ubp12 complexes occurred at 10 minutes using approximately 2 mM H_2O_2 (Figure 3.8). Importantly this is very consistent with the previous studies from the lab using Ubp12-6HA in the BY4741 strain background which also revealed that peak formation of the HMW Ubp12 complex was detected at a similar concentration of H_2O_2 using the same 10-minute time frame (Curtis, 2019). Interestingly a similar result was also obtained with the *trx1*Δ*trx2*Δ cells which showed that peak oxidation was also detected at approximately 2 mM H_2O_2 (Figure 3.8). In previous data presented in this chapter there was an indication that more Ubp12 was in the HMW form, rather than the faster mobility, wild-type form, after treatment with 2 mM H_2O_2 for 10 minutes in the *trx1trx2*Δ strain (see Figure 3.2D). The difference in amount of Ubp12 in these forms was found to be non-significant in the previous experiment (Figure 3.2D) and indeed there was no significant difference detected in this new experiment (Figure 3.8). However, it is worth noting that unlike the present experiment (Figure 3.8) the data analyses presented in Figure 3.2D did not include the intermediate HMW forms of Ubp12-3HA. In the current experiment, in contrast to the wild-type cells, there appears to be an increased level of HMW disulphide complex in *trx1*Δ*trx2*Δ cells (~8%) compared to wild-type cells (~4%) before the addition of H_2O_2 (Figure 3.8). Although this was deemed to be non-significant ($P = 0.088$) by statistical analysis it is possible that further repeats would confirm the significance of this difference. Hence it is possible that Trx1 and/or Trx2 is important to reduce the HMW Ubp12 disulphide complexes or alternatively maintain the redox state of the cell to prevent oxidation of Ubp12. It is also interesting to note that both the timing of the peak levels of HMW complex formation and the absolute levels of the HMW complex are similar in wild-type and *trx1*Δ*trx2*Δ cells (Figure 3.8). One clear difference between wild-type and *trx1*Δ*trx2*Δ cells is the influence of loss of Trx1 and Trx2 on the increased formation of intermediate HMW forms of Ubp12-3HA (Figure 3.8). T test analyses of the levels of these intermediate forms of Ubp12-3HA indicated that there are significant differences detected between the wild-type and *trx1*Δ*trx2*Δ cells at the majority of H_2O_2 concentrations tested (Table 3.2). In a few cases where the data was not judged as significant more repeats of the experiment might be needed. Interestingly, approximately 15% - 20% of Ubp12 is oxidised in this intermediate form(s) in *trx1*Δ*trx2*Δ cells across the range of H_2O_2 concentrations tested (0-10 mM, Figure 3.8C). In the wild-type cells there was much less of these intermediate forms of Ubp12

detected at all concentrations of H_2O_2. T test analyses of the levels of Ubp12 intermediate forms in wild-type cells revealed there is no significant difference in levels across 0, 0.2, 1, 2 and 5 mM H_2O_2. However, the percentage of Ubp12 intermediate forms detected at 0 mM and 10 mM H_2O_2 was found to be significantly different ($p = 0.03369$). This particular oxidation event of Ubp12 may be triggered at a higher concentration of H_2O_2 than the HMW disulphide, and hence at 10 mM the proportion of this species in wild-type cells is significantly increased. This would also explain the non-significant difference in Ubp12 intermediate forms between wild-type and *trx1*Δ*trx2*Δ strains at 10 mM H_2O_2. The nature of these intermediate forms are not understood at present but are sensitive to the presence of Trx1 and/or Trx2 and β-mercaptoethanol suggesting that these intermediate forms represent oxidised Ubp12-3HA (Figure 3.4). Taken together these data suggest that Trx1 and/or Trx2 may be important for directly reducing the HMW Ubp12 complexes and/or intermediate forms of Ubp12 but do not appear to influence the sensitivity of Ubp12 to oxidation at different concentrations of H_2O_2.

H_2O_2 concentration (mM)	P value
0	0.0028 (**)
0.2	0.0012 (**)
1	0.0541 (ns)
2	0.0205 (*)
5	0.0051 (**)
10	0.1191 (ns)

Table 3.2. Unpaired T test P values for the percentage of the Ubp12 intermediate species between wild-type and *trx1*Δ*trx2*Δ over a range of H_2O_2 concentrations (Figure 3.8C).

P values were calculated for the percentage of the Ubp12 intermediate band in wild-type Ubp12-3HA and *trx1*Δ*trx2*ΔUbp12-3HA strains at all concentrations examined (indicated). P values for this data were calculated by T test analysis using Welch's correlation. N = 3. Significance is indicated by (*) and (**) and ns denotes non-significant data.

Having established the effects of loss of Trx1 and Trx2 on the Ubp12 protein at different concentrations of H_2O_2 at 10 minutes the next step was to investigate the potential influence of Trx1 and Trx2 on the kinetics of formation of the different forms of Ubp12 at low (0.2 mM) and high (2 mM) levels of H_2O_2. Hence, wild-type Ubp12-3HA (KA10) and *trx1*Δtrx2Δ Ubp12-3HA (KA81) cells were exposed to either 0.2 mM or 2 mM H_2O_2 for 0, 0.5, 2, 5, 10, 30 or 60 minutes and protein extracts were isolated and analysed by western blotting (Figures 3.9 and 3.10).

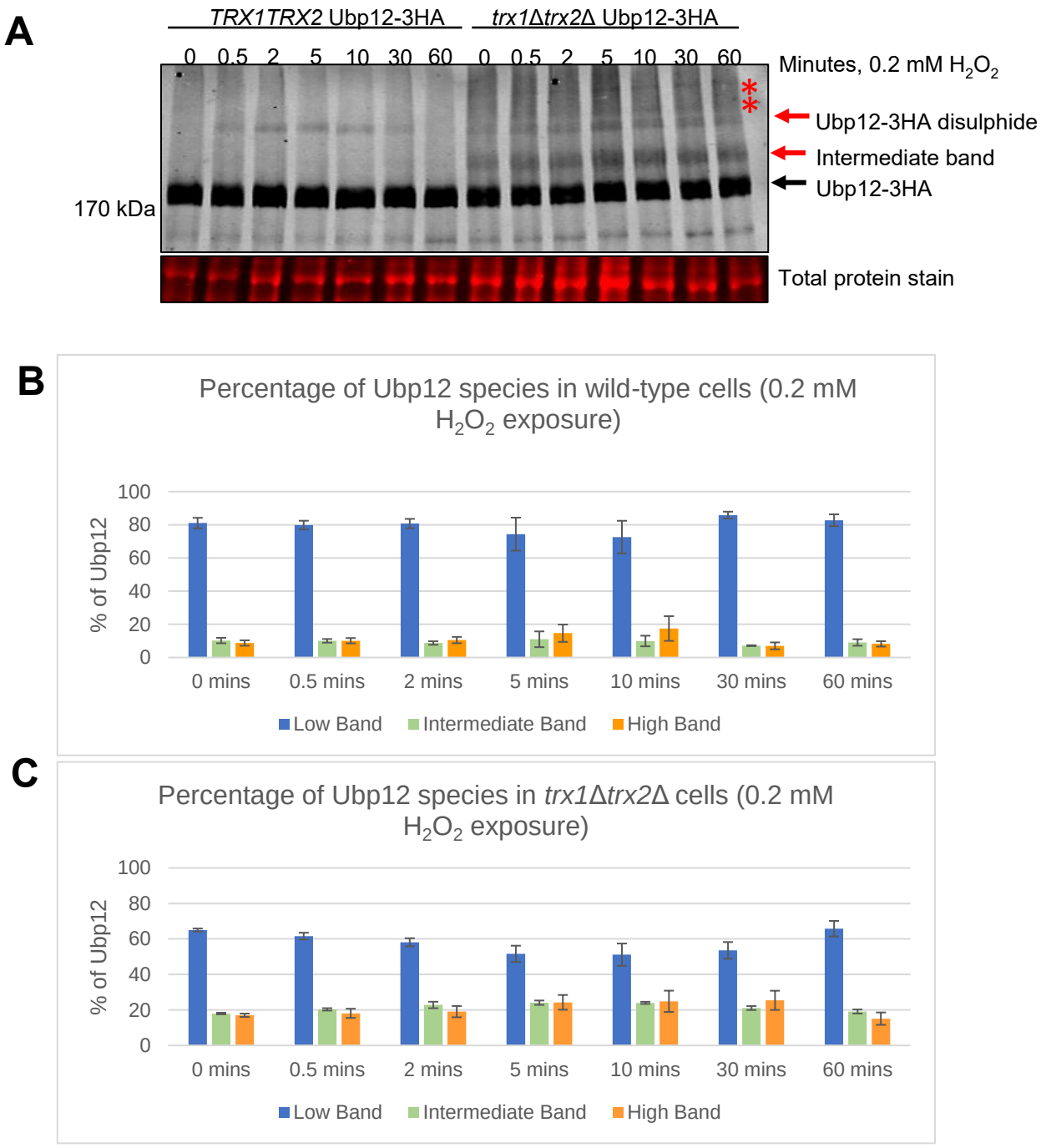

Figure 3.9. Deletion of Trx1 and Trx2 alters the kinetics of Ubp12 oxidation in response to low levels of H_2O_2.

A) Western blot analysis of mid-log phase growing wild-type cells Ubp12-3HA (KA10) and *trx1*Δ*trx2*Δ Ubp12-3HA (KA81) cells in YPD media and treated with 0.2 mM H_2O_2 for 0, 0.5, 2, 5, 10, 30 or 60 minutes. Protein extracts were prepared in non-reducing conditions, separated by SDS-PAGE and proteins visualised using anti-HA antibodies. Red asterisks indicate other possible oxidised forms of Ubp12. (B and C) The band intensities of Ubp12 species were quantified using ImageStudio and the total protein loaded in each lane. Error bars denote standard error of the mean. N=3 except for the 0-minute time points where n=6. PageRuler Prestained Protein Ladder (ThermoScientific) was used.

Previous work investigated the kinetics of formation of the HMW Ubp12 complexes in response to low (0.2 mM) and high (2 mM) levels of H_2O_2, although in this case the intermediate forms of Ubp12 were not examined (Curtis, 2019). Nevertheless, the general patterns of induction of the formation of the HMW Ubp12 complexes observed previously were observed in the experiments presented here using wild-type cells (Figures 3.9 and 3.10). These experiments were previously conducted in the BY4741 strain background, hence data here suggests that the pattern of disulphide induction is conserved between W303 and BY4741 strain backgrounds (Curtis, 2019). In particular, the accumulation of Ubp12 HMW complexes in wild-type cells occurred rapidly within the first 10 minutes following the addition of either low or high levels of H_2O_2 (Figures 3.9A and B and 3.10A and B). Moreover, at low levels of H_2O_2 the amount of HMW complexes falls after 10 minutes returning to levels seen in unstressed cells by 60 minutes (Figures 3.9A and B). In contrast, at high levels of H_2O_2 the amount of HMW complexes is maintained even after 60 minutes with very little, if any, increase compared to the levels detected by 10 minutes H_2O_2 (Figures 3.9A and B and 3.10A and B). It is also interesting that the maximum amount of HMW complexes is higher (~40%) at 2 mM H_2O_2 compared to the maximum amount detected (~18%) at 0.2 mM H_2O_2. Interestingly, the kinetics of Ubp12 oxidation match fairly well to the previous studies conducted in the BY4741 strain background, even though absolute levels are different (Curtis, 2019). Previous studies showed that approximately 40% of Ubp12 was oxidised into the disulphide in response to 0.2 mM H_2O_2 at 10 minutes in wild-type BY4741 cells (Curtis, 2019), compared to approximately 18% in wild-type W303 (Figure 3.9B). The same experiments also showed that at 2 mM H_2O_2, 65% of Ubp12 was oxidised into the disulphide by 60 minutes in wild-type BY4741 cells (Curtis, 2019), whereas data here shows only 40% of the protein is oxidised (Figure 3.10B). However, in both BY4741 and W303 strain backgrounds Ubp12 oxidation peaked at 10 minutes in response to 0.2 mM H_2O_2 however was maintained up to 60 minutes in response to 2 mM H_2O_2 (Curtis, 2019). These data support the hypothesis that the oxidation of Ubp12 is potentially utilised to sense and regulate cellular responses to increasing concentrations of H_2O_2. The analyses of the *trx1*Δ*trx2*Δ cells revealed differences in the formation of the HMW Ubp12 complexes at low and high levels of H_2O_2 compared to the wild-type cells. In particular, in the absence of H_2O_2 the proportion of Ubp12 in HMW complexes is approximately double the amount of these complexes detected in wild-type cells (~10% in wild-type cells compared to

~20% in *trx1*Δ*trx2*Δ cells) (Figures 3.9B and C and 3.10B and C). Indeed, T test analyses revealed that there was significantly more Ubp12 in the HMW disulphide at the 0-minute time point in the *trx1*Δ*trx2*Δ strain compared to wild-type cells at both low (0.2 mM) and high (2 mM) H_2O_2 concentrations (p = 0.0024 ** for both analyses). Then similar to the wild-type cells there is an increase in the amount of HMW complexes in the *trx1*Δ*trx2*Δ cells which, peaks at 10 minutes after addition of 0.2 mM H_2O_2 (Figure 3.9A and C). However, the increase at 10 minutes from the levels at 0 minutes in the *trx1*Δ*trx2*Δ cells is proportionally not as great as that observed in the wild-type cells (compare Figure 3.9B and C). Interestingly, similar to the wild-type cells at low levels of H_2O_2 the amount of HMW complexes in the *trx1*Δ*trx2*Δ cells returns to levels seen in unstressed cells by 60 minutes, although in the case of the *trx1*Δ*trx2*Δ cells this restoration in levels appears to take longer (compare Figures 3.9B and C). Finally at every time point examined at 0.2 mM H_2O_2 the relative proportion of Ubp12 in HMW complexes is consistently greater in *trx1*Δ*trx2*Δ cells compared with wild-type cells (compare Figures 3.9B and C). There are also differences in the formation of HMW complexes in *trx1*Δ*trx2*Δ cells compared to wild-type cells at higher levels (2 mM) of H_2O_2. Although the relative proportion of Ubp12 in HMW is higher at 0 minutes in *trx1*Δ*trx2*Δ cells compared to the wild-type cells, when treated with high levels of H_2O_2 the proportion of Ubp12 in HMW complexes in *trx1*Δ*trx2*Δ cells becomes much more similar to the amounts of HMW complexes observed in wild-type cells over the same time course (compare Figure 3.10B and C). Indeed, the amount of HMW complexes is maintained even after 60 minutes with very little, if any, increase compared to the levels detected by 10 minutes H_2O_2 (Figure 3.10A and B). It is also interesting that the maximum amount of HMW complexes is similar in the wild-type (~40%) and *trx1*Δ*trx2*Δ (~45%) cells 60 minutes after addition of 2 mM H_2O_2 (Figure 3.10B and C). Interestingly, even though there was a higher proportion of Ubp12 found in HMW complexes before stress in the *trx1*Δ*trx2*Δ cells, this did not result in significantly higher levels of the HMW complexes following addition of 2 mM H_2O_2 at least over the time course of the experiment. There was also no decrease in the amount of the HMW forms of Ubp12 in either wild type or *trx1*Δ*trx2*Δ cells over the time course at high levels of H_2O_2 and hence it would be important to investigate much later time frames to explore whether there is evidence that Trx1 and Trx2 are important for restoring reduced Ubp12. In summary, these results have revealed differences in the kinetics of formation of Ubp12 HMW complexes in cells lacking Trx1 and Trx2 compared to wild-

type cells in unstressed conditions and following treatment with both low and high levels of H_2O_2.

The kinetics of formation of the intermediate HMW forms of Ubp12 were also examined in these two experiments (Figures 3.9 and 3.10). In the experiments performed at 0.2 mM H_2O_2 the data for all time points, except 5 minutes, revealed that there was significantly more Ubp12 in the intermediate band in *trx1*Δ*trx2*Δ cells compared to wild-type cells (Table 3.3A). Experiments performed at 2 mM H_2O_2 obtained very similar results where, except the 60-minute time point, there was significantly more Ubp12 in the intermediate band in *trx1*Δ*trx2*Δ cells compared to wild-type cells (Table 3.3B). Although the 60-minute time point was not found to be statistically significant, the error bars for this data in both strains are quite big potentially explaining this result. All these data fit with data presented previously in this chapter, revealing a higher proportion of Ubp12 in the intermediate band in *trx1*Δ*trx2*Δ cells (Figures 3.2, 3.4, 3.8, Table 3.2).

Interestingly, in contrast to the HMW complexes of Ubp12, the proportion of the intermediate band in wild-type and *trx1*Δ*trx2*Δ cells does not significantly change across the time course of the experiment at either 0.2 mM H_2O_2 or 2 mM H_2O_2, with levels at ~10% in wild-type cells and ~20% in *trx1*Δ*trx2*Δ cells (compare Figures 3.9B and C, 3.10B and C). The nature of these intermediate HMW forms of Ubp12 are not clear at present. However, given the likelihood that this is an oxidised form(s) of Ubp12 it is very intriguing that they are influenced by the presence of Trx1 and Trx2 but do not appear to be affected by either low or high levels of H_2O_2 at least as assessed by western blot. This intermediate HMW form of Ubp12 will be discussed later in the chapter.

Finally, it also interesting to note very HMW forms of Ubp12 (Figures 3.9 and 3.10, red asterisks), not detected in wild-type cells, are induced in *trx1*Δ*trx2*Δ cells by low or high levels of H_2O_2. Although these bands were not quantified in the analyses it appears that the signal is comparable when exposed to both 0.2 and 2 mM H_2O_2. Further analysis of these forms of Ubp12 would be necessary to draw any conclusions regarding their oxidation status and nature. However, given that they are induced by H_2O_2 and influenced by the absence of Trx1 and Trx2 it is tempting to speculate that these forms of Ubp12 represent further oxidation products. Indeed, Ubp12 contains a

number of cysteine residues in addition to the catalytic cysteine residue (Figure 4.3). Further experimentation and characterisation would be required to gain further insight of these new forms of Ubp12.

In summary, the data presented here has revealed that the pattern of Ubp12 oxidation in wild-type cells is similar in BY4741 and W303 strain backgrounds, although the absolute amounts of Ubp12 species does differ. In addition, the data further supports the hypothesis that Trx1 and/or Trx2 regulate the oxidation of Ubp12. Different kinetics of oxidation in the presence of low and high levels of H_2O_2 were detected in cells lacking Trx1 and Trx2 compared to wild-type cells. In addition, new HMW forms of Ubp12 were detected in cells lacking Trx1 and Trx2 and some of these forms were dependent on the presence of H_2O_2. Taken together these data suggest that Trx1 and/or Trx2 are important for reducing oxidised Ubp12.

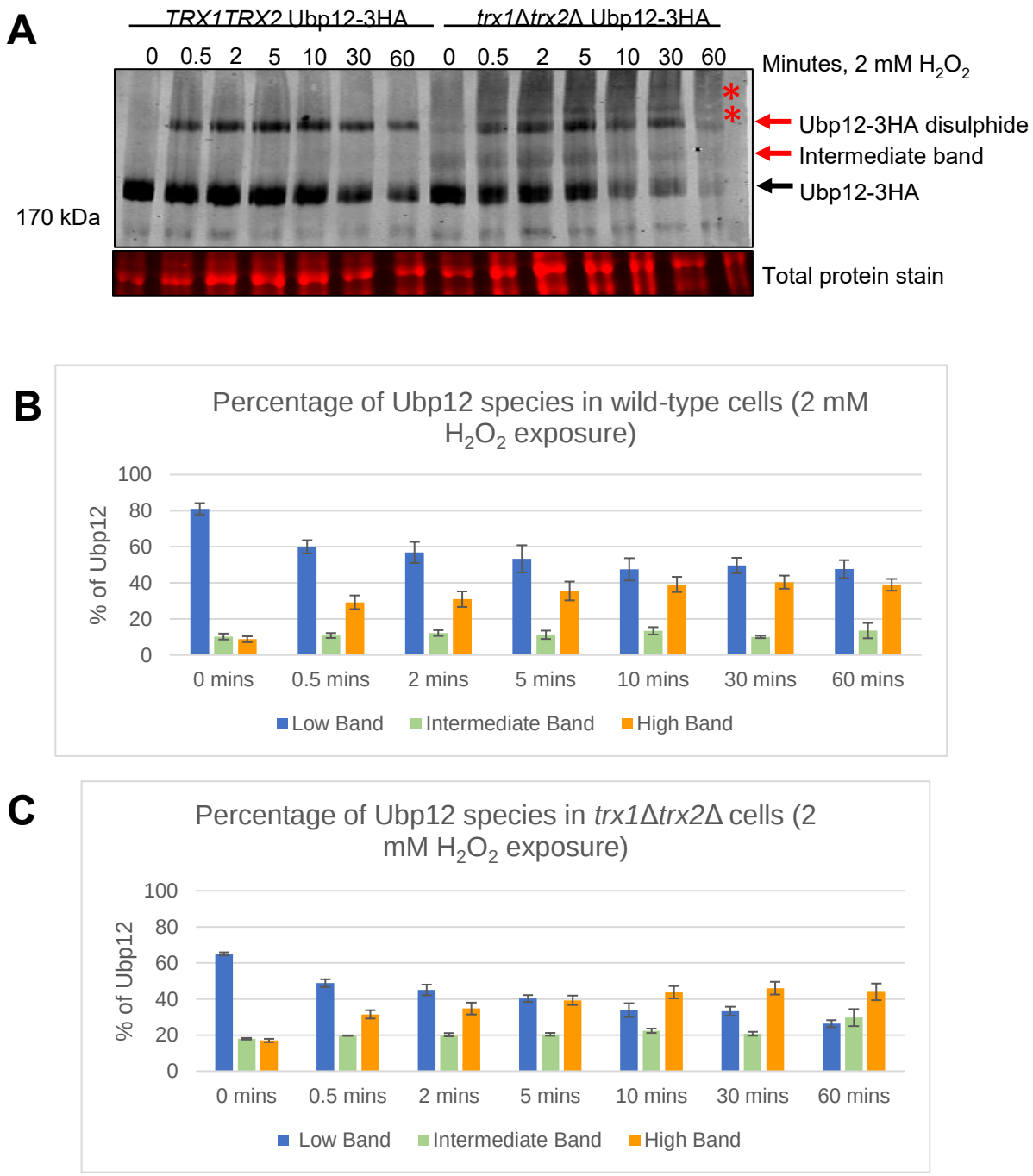

Figure 3.10. Deletion of Trx1 and Trx2 alters the kinetics of Ubp12 oxidation in response to high levels of H_2O_2.

A) Western blot analysis of mid-log phase growing wild type Ubp12-3HA (KA10) and *trx1*Δ*trx2*Δ Ubp12-3HA (KA81) cells in YPD media and treated with 2 mM H_2O_2 for 0, 0.5, 2, 5, 10, 30 or 60 minutes. Protein extracts were prepared in non-reducing conditions, separated by SDS-PAGE and proteins visualised using anti-HA antibodies. Red asterisks indicate other possible oxidised forms of Ubp12. B) and C) The band intensities of Ubp12 species were quantified using ImageStudio and the total protein loaded in each lane. Error bars denote standard error of the mean. N=3 except for the 0-minute time points where n=6. PageRuler Prestained Protein Ladder (ThermoScientific) was used.

(A)

Time point, 0.2 mM H_2O_2 (mins)	P value
0	0.0044 (**)
0.5	0.0029 (**)
2	0.0054 (*)
5	0.1022 (ns)
10	0.0439 (*)
30	0.0043 (**)
60	0.0185 (*)

(B)

Time point, 2 mM H_2O_2 (mins)	P value
0	0.0044 (**)
0.5	0.0214 (*)
2	0.0198 (*)
5	0.0455 (*)
10	0.0290 (*)
30	0.0024 (**)
60	0.0642 (ns)

Table 3.3. Unpaired T test P values of the kinetics of the Ubp12 intermediate species formation between wild-type and *trx1*Δ*trx2*Δ cells at low (A) and high (B) H_2O_2 concentrations (Figures 3.9 and 3.10).

P values for this data were calculated by T test analysis using Welch's correlation. N = 3 except for the 0-minute time point, where n = 6. Significance is indicated by (*) and (**) and ns denotes non-significant data. (A) P values were calculated for the percentage of the Ubp12 intermediate band in wild-type Ubp12-3HA and *trx1*Δ*trx2*ΔUbp12-3HA strains at 0.2 mM H_2O_2 over a time-course experiment (Figure 3.9). (B) P values were calculated for the percentage of the Ubp12 intermediate band in wild-type Ubp12-3HA and *trx1*Δ*trx2*ΔUbp12-3HA strains at 2 mM H_2O_2 over a time-course experiment (Figure 3.10).

3.2.4 Analysis of the potential role of the catalytic cysteine of Ubp12 on regulation by the Trr1 thioredoxin reductase

Previous work in the chapter revealed that Ubp12 abundance significantly decreased in *trr1*Δ cells before and after H_2O_2 treatment when analysed using non-reducing conditions but not when analysed reducing conditions (Figures 3.2B, 3.3, Table 3.1). This raised the possibility that the differences were due to reduced detection of oxidised Ubp12 species on the western blots, for example perhaps the oxidised species do not transfer as efficiently or alternatively perhaps that other oxidised species were not quantified due to their position on the gel. Previous work from the lab and data presented in Chapter 4 revealed that the catalytic cysteine of Ubp12 (C373) is essential for the formation of HMW disulphide complexes (Curtis, 2019). These experiments utilised expression of wild-type Ubp12-3HA or Ubp12-3HA-C373S (substitution of C373 with serine) from the multi-copy plasmids pRS426-Ubp12-3HA and pRS426-Ubp12-3HA-C373, respectively. Hence, the next step to investigate whether oxidation of Ubp12 affects the measurements of Ubp12 abundance using non-reducing and reducing conditions was to test whether C373 has any influence on the results. To explore this possibility wild-type W303-1a (KA4) and *trr1*Δ (KA11) cells were transformed with the pRS426-Ubp12-3HA and pRS426-Ubp12-3HA-C373S plasmids. Transformants from each strain were then grown in minimal media and exposed to 2 mM H_2O_2 for 0 or 10 minutes. Protein extracts were isolated and analysed by western blotting in both non-reducing and reducing conditions (Figures 3.11 and 3.12).

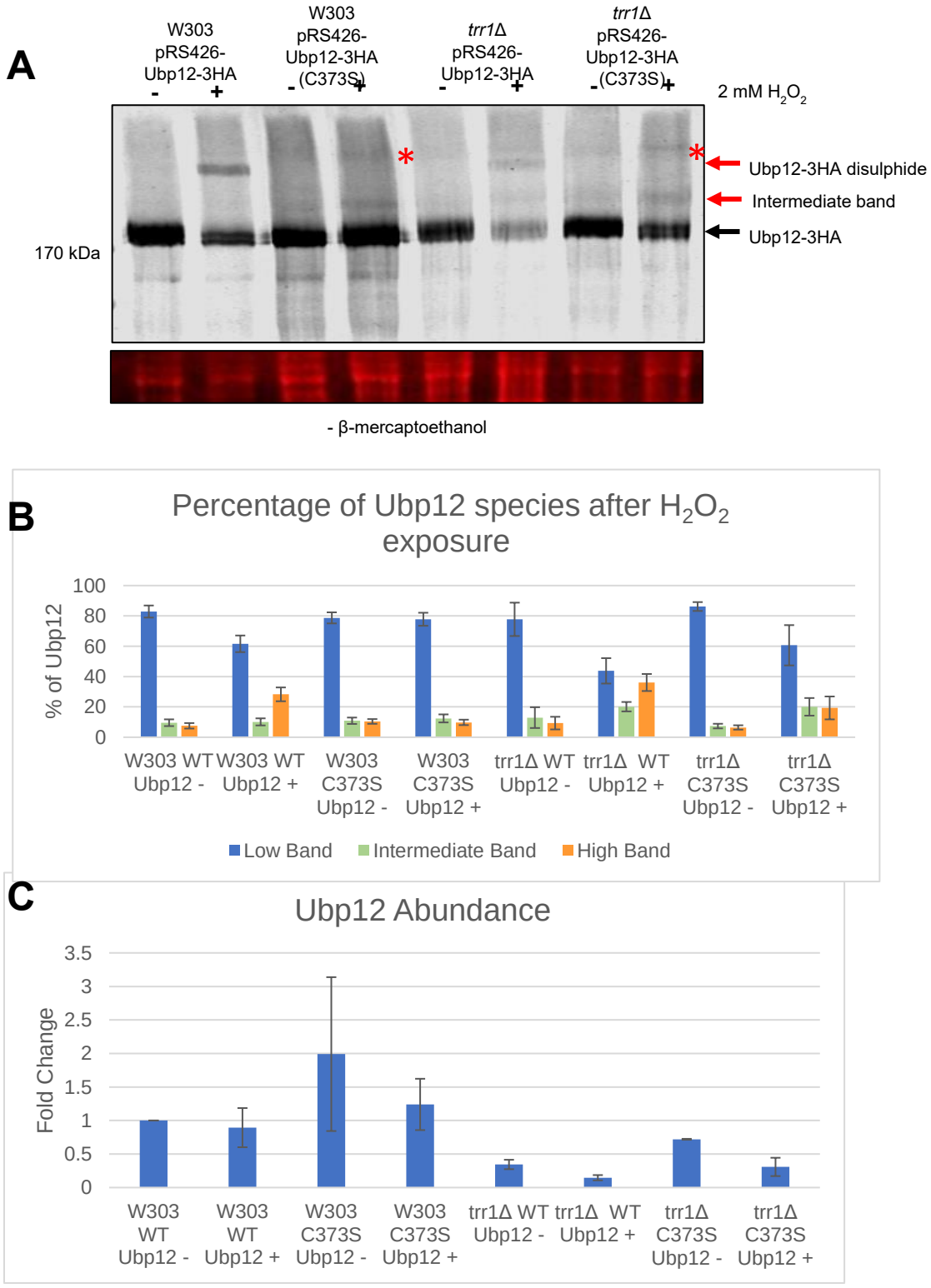

Figure 3.11 Analysis of the role of Ubp12 catalytic activity on Ubp12 abundance and oxidation in non-reducing conditions.

A) Western blot analysis of mid-log phase growing wild type (KA4) cells, containing pRS426-Ubp12-3HA and pRS426-Ubp12-3HA-C373S, and *trr1*Δ (KA11) cells, containing pRS416-Ubp12-3HA and pRS426-Ubp12-3HA-C373S, in minimal media

and treated with 2 mM H_2O_2 for 0 (-) or 10 (+) minutes. Protein extracts were prepared in non-reducing conditions, separated by SDS-PAGE and proteins visualised using anti-HA antibodies. B) The band intensities of Ubp12 species were quantified using ImageStudio and the total protein loaded in each lane. C) The band intensities of all Ubp12 proteins were quantified using ImageStudio and the total protein loaded in each lane. Fold change represents the comparison between the samples and the wild type pRS426-Ubp12-3HA sample at 0 minutes H_2O_2 which was set as 1. For all data error bars denote standard error of the mean and n=3. PageRuler Prestained Protein Ladder (ThermoScientific) was used.

Although the wild-type and *trr1*Δ cells express untagged Ubp12 from the normal genomic locus, importantly the H_2O_2-induced induction of the HMW form of Ubp12 was detected in cells containing pRS426-Ubp12-3HA (Figure 3.11A and C). Furthermore, as expected the HMW species was sensitive to the presence of β-mercaptoethanol or the C373S mutation of Ubp12 (Figures 3.11AC and 3.12A). Furthermore, the effect of the C373S mutation is consistent with previous studies in the lab which showed that formation of the HMW Ubp12 complexes is inhibited by this mutation (Curtis, 2019). Furthermore, the proportion of wild-type Ubp12 in the intermediate HMW forms was consistent with the data presented above (compare Figure 3.10A and B with Figure 3.11A and B). Interestingly, the formation of the intermediate HMW forms were not affected by the C373S mutation in wild-type cells suggesting that, in contrast to the HMW forms, the intermediate HMW forms are not dependent on C373 (Figure 3.11A and B). However, these forms are sensitive to the presence of β-mercaptoethanol indicating that they represent oxidised Ubp12 (Figure 3.12A). Interestingly, in contrast to the wild-type cells, the formation of the intermediate HMW forms appears to be induced by H_2O_2 in *trr1*Δ cells although T test analysis indicated that this induction was not currently significant. However, it is possible that further repeats of this experiment could reveal that this induction is significant. Another intriguing observation is the presence of the unidentified HMW forms of Ubp12 (indicated by asterisks), previously observed in *trx1*Δ*trx2*Δ cells (Figures 3.2, 3.9, 3.10). These bands are present in the *trr1*Δ strain, and possibly the wild-type strain expressing the C373S plasmid (Figure 3.11A), suggesting a possible role for the catalytic cysteine residue in resolving these HMW forms.

The next step was to analyse the abundance of Ubp12 in the wild-type and *trr1*Δ cells containing either the pRS426-Ubp12-3HA or the pRS426-Ubp12-3HA-C373S in non-reducing and reducing conditions. When examined in non-reducing conditions there

was a significant decrease in the abundance of Ubp12 in *trr1*Δ cells containing either the pRS426-Ubp12-3HA plasmid or the pRS426-Ubp12-3HA plasmid compared to wild-type unstressed cells containing the pRS426-Ubp12-3HA plasmid (Figure 3.11C). P values for this data are: 0.0112 (*) when the control is compared to *trr1*Δ cells containing the pRS426-Ubp12-3HA plasmid – H_2O_2; 0.0021 (**) when the control is compared to *trr1*Δ cells containing the pRS426-Ubp12-3HA plasmid + H_2O_2; 0.0006 (***) when the control is compared to *trr1*Δ cells containing the pRS426-Ubp12-3HA-C373S plasmid – H_2O_2; 0.0368 (*) when the control is compared to *trr1*Δ cells containing the pRS426-Ubp12-3HA-C373S plasmid + H_2O_2. Interestingly, the T test analyses also revealed that there were no significant differences between any of the samples from wild-type cells and no significant differences between any of the samples from *trr1*Δ cells. Hence this data was consistent with the data presented in Figure 3.2 and Table 3.1 which revealed that loss of Trr1 function resulted in significant reduction of abundance of Ubp12 in the presence or absence of H_2O_2 when analysed in non-reducing conditions. Interestingly, this new data suggests that this difference in abundance of Ubp12 in *trr1*Δ is unaffected by mutation of C373 (Figure 3.11). However, the work presented above also showed that the analyses of Ubp12 abundance in reducing conditions removed the significance of any differences in Ubp12 abundance between wild type and *trr1*Δ cells (Figure 3.3). Hence, it was predicted that the same results would be obtained here when Ubp12 was examined in reducing conditions from the wild type and *trr1*Δ cells containing either the pRS426-Ubp12-3HA or the pRS426-Ubp12-3HA-C373S plasmid. Intriguingly, in contrast to the results in Figure 3.3, the data presented in Figure 3.12 revealed that Ubp12 abundance remains decreased under reducing conditions in *trr1*Δ cells containing either the pRS426-Ubp12-3HA or the pRS426-Ubp12-3HA-C373S plasmid compared to wild-type cells. Ubp12 levels in *trr1*Δ cells are approximately 0.4 – 0.6-fold of the levels detected in wild-type unstressed cells containing the pRS426-Ubp12-3HA plasmid. T test analyses revealed that there were no significant differences between any of the samples from wild-type cells when analysed under reducing conditions. However, when compared to wild-type unstressed cells containing the pRS426-Ubp12-3HA plasmid, all but one of the *trr1*Δ samples yielded significant P values (*trr1*Δ pRS426-Ubp12-3HA plasmid - H_2O_2 = 0.0119 (*), *trr1*Δ pRS426-Ubp12-3HA plasmid + H_2O_2 0.0219 (*), *trr1*Δ pRS426-Ubp12-3HA-C373S plasmid - H_2O_2 = 0.0727 (ns), *trr1*Δ pRS426-Ubp12-3HA-C373S plasmid + H_2O_2 = 0.0162 (*)). Hence, in most of the

*trr1*Δ samples analysed, including cells expressing the catalytic cysteine mutant version of Ubp12, there was significantly less Ubp12 detected compared to wild-type cells under both non-reducing and reducing conditions.

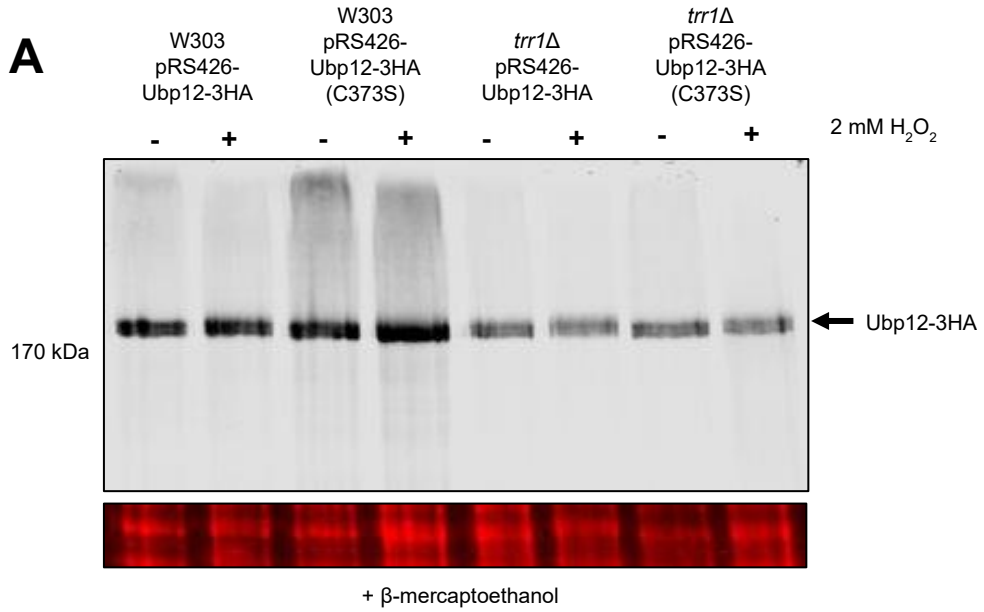

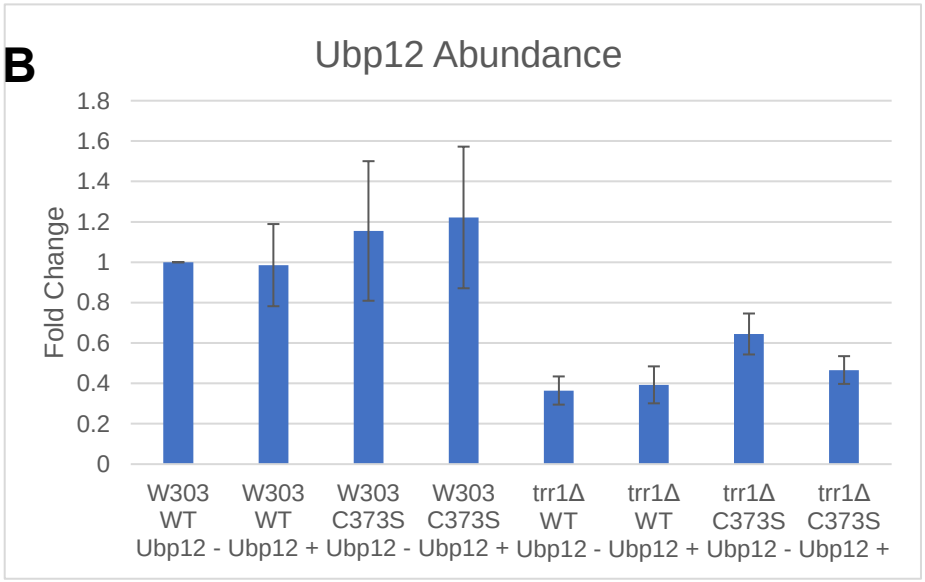

Figure 3.12. Analysis of the role of Ubp12 catalytic activity on Ubp12 abundance in reducing conditions.

(A) Western blot analysis of mid-log phase growing wild type (KA4) cells, containing pRS426-Ubp12-3HA and pRS426-Ubp12-3HA-C373S, and *trr1*Δ (KA11) cells, containing pRS416-Ubp12-3HA and pRS426-Ubp12-3HA-C373S, in minimal media and treated with 2 mM H_2O_2 for 0 (-) or 10 (+) minutes. Protein extracts were prepared in reducing conditions, separated by SDS-PAGE and proteins visualised using anti-HA antibodies. (B) The band intensities of all Ubp12 proteins were quantified using ImageStudio and the total protein loaded in each lane. Fold change represents the comparison between the samples and the wild type pRS426-Ubp12-3HA sample at 0 minutes H_2O_2 which was set as 1. Error bars denote standard error of the mean and n=3. PageRuler Prestained Protein Ladder (ThermoScientific) was used.

Hence, these results appear to contradict the earlier conclusions in Figure 3.3 and suggest that Trr1 does influence the abundance of Ubp12. However, it is important to point out that there are significant differences in the experiments described in Figures 3.2 and 3.3 versus Figures 3.11 and 3.12, such as the media used and the use of over-expression plasmids in Figures 3.11 and 3.12.

In summary the results presented here suggest that, in contrast to the earlier analysis (Figures 3.2 and 3.3), Trr1 may influence the abundance of Ubp12 and, furthermore that this is independent of the catalytic cysteine residue C373 of Ubp12. Further experiments would be necessary to explore the differences with the analysis in Figures 3.2 and 3.3. It is also clear that in contrast to the HMW forms of Ubp12, the intermediate HMW forms of Ubp12 are not influenced by C373. However, the data suggest that these are the result of oxidation and therefore suggest that other cysteine(s) in Ubp12 are involved in these oxidation complexes.

3.2.5 The glutathione system does not have a major role in the regulation of Ubp12

Results presented in this chapter revealed that proteins in the thioredoxin system influences the oxidation of Ubp12 in response to H_2O_2. Furthermore, previous work from the lab revealed that Ubp12 forms a HMW oxidised complex in response to H_2O_2 but not diamide (Curtis, 2019). As discussed earlier (see section 1.2.3.2.1) the thioredoxin system responds to H_2O_2 but not diamide in *S. cerevisiae* (Wheeler et al., 2003, Garrido and Grant, 2002). In contrast, the glutathione system, another major antioxidant system in *S. cerevisiae* responds to both H_2O_2 and diamide (Wheeler et al., 2003, Kosower and Kosower, 1995). Interestingly, consistent with these different functions of these antioxidant systems previous work demonstrated that the glutathione system but not the thioredoxin system regulates the oxidation of the ubiquitin pathway Uba1 and Cdc34 disulphide complex in response to both H_2O_2 and diamide (see section 1.3.2) (Doris et al., 2012). Hence, based on the specificity of HMW Ubp12 disulphide complex formation to the presence of H_2O_2 but not diamide we would predict that the glutathione system would play only a minor role, if any, in the regulation of Ubp12 oxidation. Previous experiments with Uba1 and Cdc34

demonstrated that treatment of cells with buthionine sulphoximine (BSO), a drug that inhibits gamma-glutamylcysteine synthetase, the first enzyme in the glutathione synthesis pathway, stimulated formation of the Uba1-Cdc34 disulphide complex (Doris et al., 2012). Hence, to test whether the glutathione pathway influences oxidation of Ubp12, BY4741 cells expressing Ubp12-TAP (KA24) were grown at 30°C and treated with 5 mM BSO for 0 (-) or 4 (+) hours. Protein extracts were isolated and analysed by western blotting (Figure 3.13).

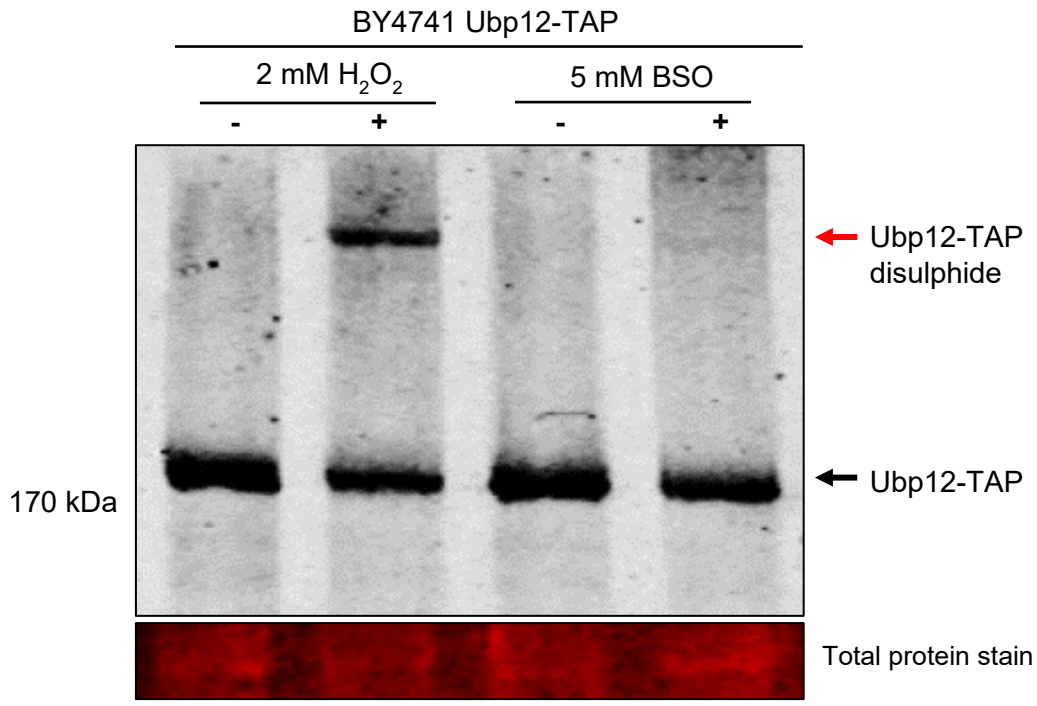

Figure 3.13. Inhibition of the glutathione system does not mimic the oxidation of Ubp12 by H_2O_2.

Western blot analysis of mid-log phase growing BY4741 cells expressing Ubp12-TAP in minimal media and treated with either 2 mM H_2O_2 for 0 (-) or 10 (+) minutes, or 5 mM BSO for 0 (-) or 4 (+) hours. Protein extracts were prepared in non-reducing conditions, separated by SDS-PAGE and proteins visualised using anti-PαP antibodies. Brightness and contrast have been increased to detect weak signal in the -/+ BSO lanes. N=2. PageRuler Prestained Protein Ladder (ThermoScientific) was used.

In contrast to H_2O_2 addition very little signal was detected for the band representing the HMW Ubp12 oxidised complex when cells were treated with BSO (Figure 3.13). This analysis was n=2 and is therefore preliminary. However, although this data does not completely exclude the possibility that the glutathione pathway is involved in the regulation of oxidation of Ubp12, this preliminary analysis suggests that, in contrast to the Uba1-Cdc34 disulphide complex, the glutathione pathway does not play a major role in the regulation of oxidation of Ubp12. Furthermore, these preliminary results are consistent with the hypothesis that the thioredoxin system but not the glutathione system plays a more significant role in the regulation of Ubp12.

3.2.6 Analysis of other potential modification(s) of Ubp12

The experiments described in this Chapter have focused on several HMW Ubp12 species that are influenced H_2O_2 and by components of the thioredoxin system. However, the analysis of some lighter exposures of several western blots revealed that the unstressed form of Ubp12 with the mobility predicted for the full-length epitope-tagged Ubp12 actually appears to consist of two bands with very similar mobilities (Figure 3.14). These bands are very difficult to distinguish on many of the western blots due to their similar mobility. Interestingly, however, these two bands can be detected from Ubp12 expressed in both the BY4741 and W303 strain backgrounds, indicating that this is unlikely to be a strain background effect in *S. cerevisiae* (Figure 3.14). These two bands and their potential conservation have not been explored in the studies to date, but, given the role(s) of the thioredoxin system in the regulation of Ubp12 presented in this chapter, it was possible that the thioredoxin system also influences the relationship between these two bands. Hence, to examine these two bands more closely several protein analyses were conducted. Firstly, to assess if the double band represented a form of Ubp12 oxidation, wild-type cells expressing Ubp12-3HA in the W303 strain background (KA10) were grown to mid-log phase and exposed to 2 mM H_2O_2 for 0 and 10 minutes. Proteins were extracted and analysed by western blot under non-reducing and reducing conditions (Figure 3.14A-C). This analysis is consistent with the conclusion that the normal Ubp12-3HA band actually consists of two separate bands (Figure 3.14A). Furthermore, both bands appeared to be unaffected by the presence of β-mercaptoethanol (Figure 3.14C). Interestingly, treatment of wild-type Ubp12-3HA cells with 2 mM H_2O_2 altered the proportion of Ubp12 that was present in each of the two bands (Figure 3.14A and B). Prior to exposure to H_2O_2, the ratio of Ubp12 that was present in the faster and slower mobility bands was ~ 55%:45%, respectively (Figure 3.14B). In contrast, after exposure of the cells to 2 mM H_2O_2 for 10 minutes this ratio changed to ~ 68%:32% (Figure 3.14B). Statistical analysis using unpaired T tests revealed no significant difference between the proportion of Ubp12 present in each band prior to H_2O_2 exposure (P = 0.1136 (ns)). However, following exposure to H_2O_2, the difference in the proportion of Ubp12 present in each band was deemed significant (P = 0.0003 (***)). Although the underlying explanation for the different mobility of these two bands is still unknown, it is tempting

to suggest that perhaps the slower mobility band represents a modified form of Ubp12 that is involved in the formation of the H_2O_2-induced HMW disulphide complex.

Having established that these two Ubp12 bands are present in the W303 strain background next wild-type cells expressing Ubp12-TAP in the BY4741 strain background (KA24) were grown to mid-log phase and exposed to 2 mM H_2O_2 for 0 and 10 minutes. Proteins were extracted and analysed by western blot under non-reducing conditions (Figure 3.14D). Similar to the analysis in the W303 strain background, the normal Ubp12-TAP band in cells from the BY4741 strain background also consists of two separate bands (Figure 3.14D). There is an indication that there is less of the slower-mobility band in the BY4741 strain compared to W303 (compare Figure 3.14 A and D) but no quantification was performed to check this. It is also important to note that Figure 3.14D is only representative of N=2 repeats and is therefore preliminary. Nevertheless, these results suggest that both bands are formed regardless of the use of different epitope tags or different strain backgrounds and that further experimentation is necessary to explore the ratios of the double band (Figure 3.14A-D).

Finally, to assess if any proteins in the thioredoxin system in the W303 strain background influence these two Ubp12 bands, *trr1*ΔUbp12-3HA (KA77), *trr2*ΔUbp12-3HA (KA50), *tsa1*ΔUbp12-3HA (KA65), *tsa2*ΔUbp12-3HA (KA64) and *trx1*Δ*trx2*ΔUbp12-3HA (KA81) cells were grown to mid-log phase and exposed to 2 mM H_2O_2 for 0 and 10 minutes. Protein extracts were analysed by western blot under non-reducing conditions (Figure 3.14E). Consistent with the results above, the normal Ubp12-3HA band also consists of two separate bands in different thioredoxin system mutant cells (*trr1*Δ, *trr2*Δ, *trx1*Δ*trx2*Δ, *tsa1*Δ and *tsa2*Δ) (Figure 3.14E). Note that the protein extract obtained from *trr1*Δ cells after 2 mM H_2O_2 treatment was not included due to the characteristic low signal detected and the difficulty observing the normal Ubp12-3HA band(s). Furthermore, although not quantified, there is some evidence from the western analysis that the ratio of Ubp12 present in the faster and slower mobility bands changed in a similar manner to the W303 wild-type control cells after exposure of the cells to 2 mM H_2O_2 (compare Figure 3.14A and B with Figure 3.14E). However, there is also an indication that the proportion of Ubp12 present in the two band differs in thioredoxin system mutant cells compared to wild-type cells. For example, there is a suggestion that there is more of the slower mobility band in the

*trr1*Δ cells compared to W303 wild-type control cells prior to H_2O_2 exposure (compare Figures 3.14 A and E). However, Figure 3.14E is only representative of N=2 repeats and no quantification has been performed so this is only a preliminary result. Nevertheless, there is preliminary evidence that the thioredoxin system may influence the proportions of Ubp12 present in these two bands.

In summary, the data presented in this section revealed that the unstressed normal Ubp12 protein actually consists of two bands of very similar mobility on western blots. These bands are present in different strain backgrounds (W303 and BY4741), using different epitope tags and in different thioredoxin system mutant strains. Furthermore, these bands were not altered by the use of non-reducing or reducing conditions in the analyses, suggesting that protein oxidation is not involved. However, there is evidence that the slower mobility form may be linked to the H_2O_2-induced formation of HMW oxidised forms of Ubp12 in wild type cells (W303 and BY4741). Moreover, the proportion of Ubp12 in each band appeared to be influenced by the genetics of the strain background and by different thioredoxin system mutations. The underlying explanation for the difference in mobility of these two bands is currently unknown but it is tempting to suggest that the two bands provide evidence of post translational modification(s) of Ubp12 different to protein oxidation.

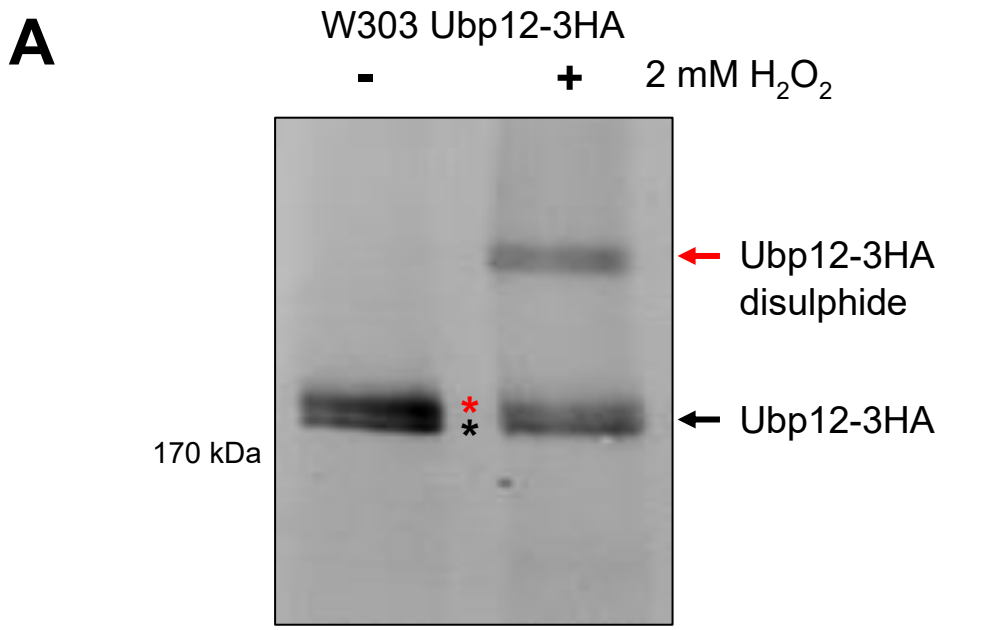
A
W303 Ubp12-3HA
-
+
2 mM H_2O_2
Ubp12-3HA
disulphide
Ubp12-3HA
170 kDa

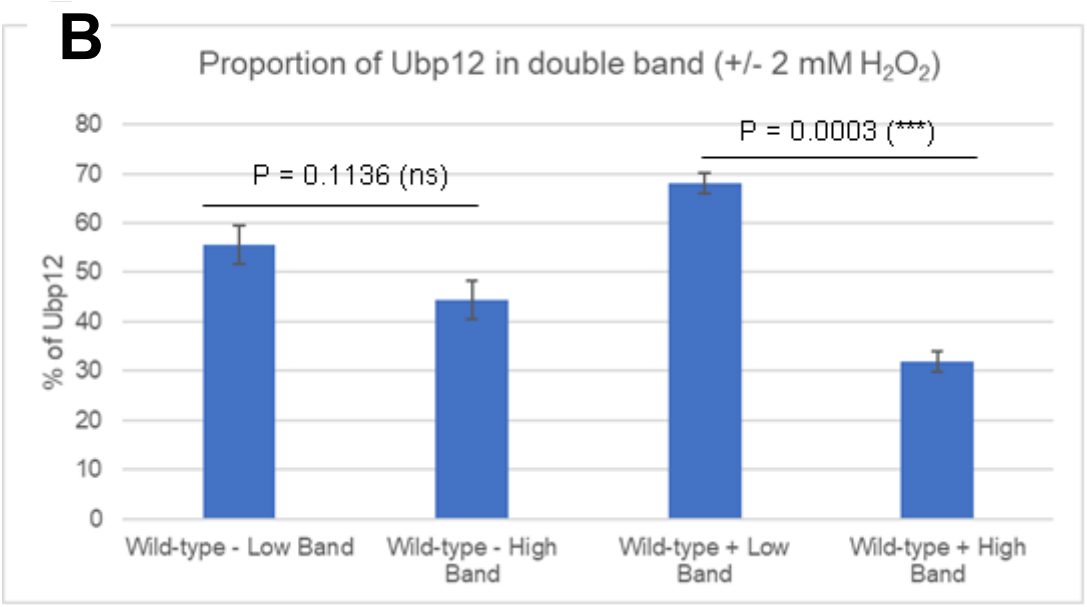
B
Proportion of Ubp12 in double band (+/- 2 mM H_2O_2)
P = 0.1136 (ns)
P = 0.0003 (***)
% of Ubp12
80
70
60
50
40
30
20
10
0
Wild-type - Low Band
Wild-type - High Band
Wild-type + Low Band
Wild-type + High Band

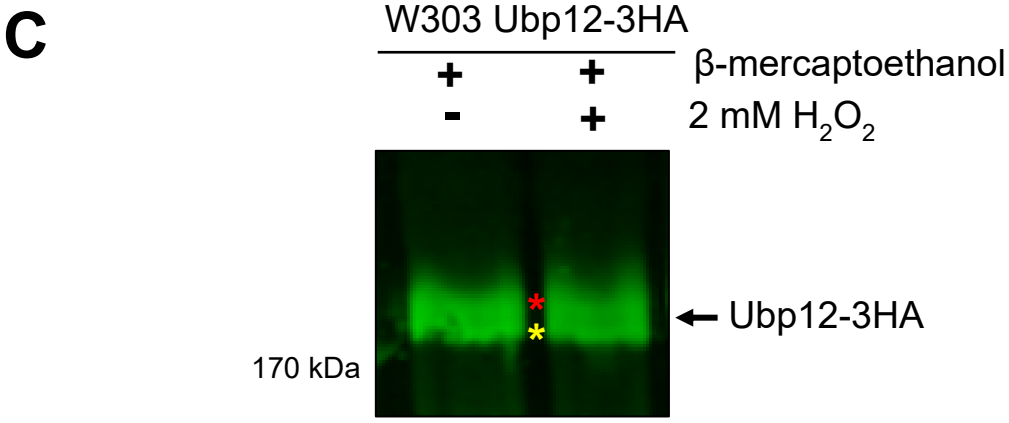
C
W303 Ubp12-3HA
+
+
β-mercaptoethanol
-
+
2 mM H_2O_2
Ubp12-3HA
170 kDa

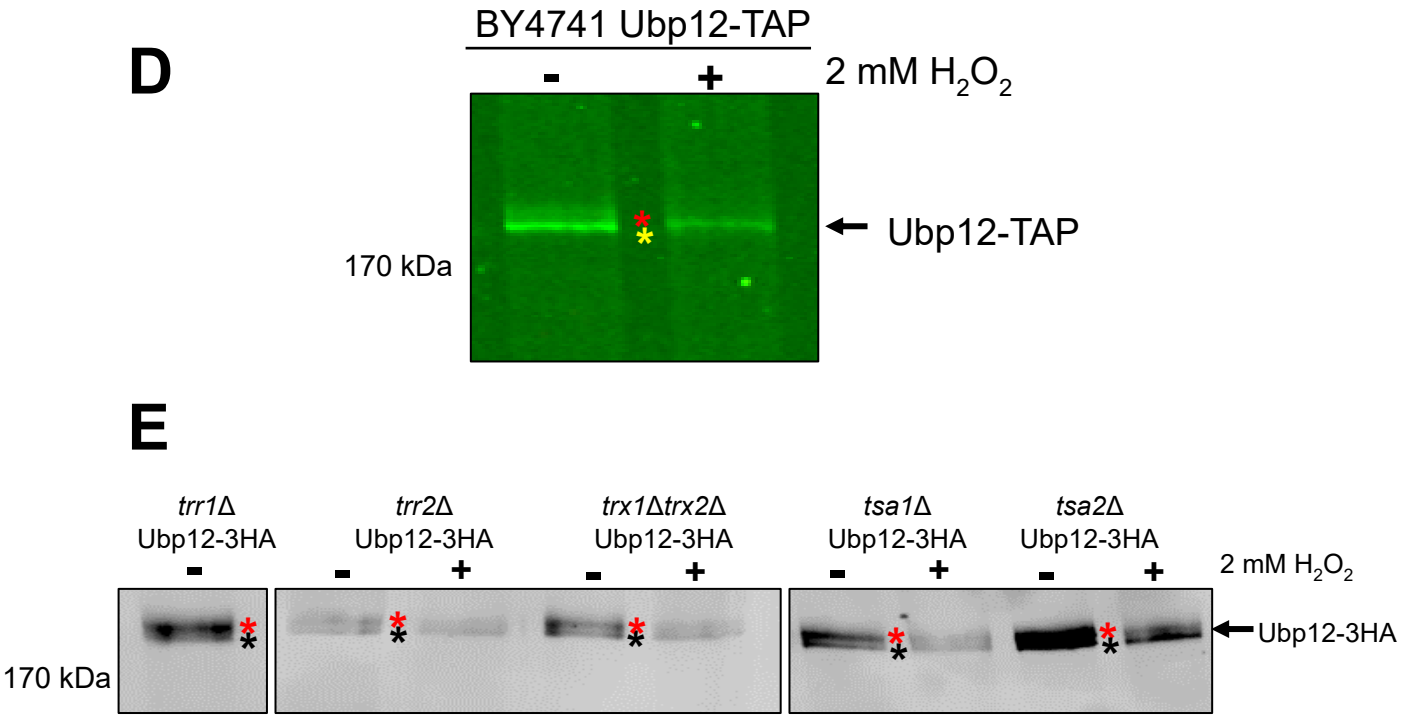

Figure 3.14. Analyses of the Ubp12 double band.

(A) Western blot analysis of mid-log phase growing W303 wild-type Ubp12-3HA (KA10) cells in YPD and treated with the indicated concentration of H_2O_2 for 0 (-) and 10 (+) minutes. Protein extracts were prepared in non-reducing conditions, separated by SDS-PAGE and the two Ubp12-3HA "unstressed" mobility bands were visualised using anti-HA antibodies. N = 3. B) Quantification of the proportions of the two bands (asterisks) shown in Figure 3.14A. Bars represent standard error of the mean. P values were calculated using unpaired T tests. N = 3. C) Western blot analysis of mid-log phase growing W303 wild-type Ubp12-3HA (KA10) cells in YPD and treated with the indicated concentration of H_2O_2 for 0 (-) and 10 (+) minutes. Protein extracts were prepared in reducing conditions, separated by SDS-PAGE and the two Ubp12-3HA "unstressed" mobility bands (asterisks) were visualised using anti-HA antibodies. N=3. D) Western blot analysis of mid-log phase growing BY4741 wild-type Ubp12-TAP (KA24) cells in YPD and treated with the indicated concentration of H_2O_2 for 0 (-) and 10 (+) minutes. Protein extracts were prepared in non-reducing conditions, separated by SDS-PAGE and the two Ubp12-3HA "unstressed" mobility bands (asterisks) were visualised using PαP antibodies. N=2. E) Western blot analysis of mid-log phase growing *trr1*Δ (KA77), *trr2*Δ (KA50), *tsa1*Δ (KA65), *tsa2*Δ (KA64) and *trx1*Δ*trx2*Δ (KA81) cells expressing Ubp12-3HA in YPD media and treated with the indicated concentration of H_2O_2 for 0 (-) and 10 (+) minutes. Protein extracts were prepared in non-reducing conditions, separated by SDS-PAGE and the two Ubp12-3HA "unstressed" mobility bands (asterisks) were visualised using anti-HA antibodies. N=2. (A, C-E) PageRuler Prestained Protein Ladder (ThermoScientific) was used. The faster migrating form of the "unstressed" Ubp12-3HA double band is indicated with a black or yellow asterisk and the slower migrating form is indicated with a red asterisk.

3.3 Discussion

Previous studies had revealed that the cytoplasmic thioredoxin reductase Trr1 influences the abundance of the Ubp12 DUB in *S. cerevisiae (Curtis, 2019)*. However, the potential roles of other members of the thioredoxin system were not examined. In addition, the potential influence of the mitochondrial thioredoxin system was not explored previously. Here the oxidation and abundance of Ubp12 was investigated in strains lacking many of the individual components of the cytoplasmic thioredoxin system and in a strain lacking Trr2, the mitochondrial thioredoxin reductase. The results presented here confirmed and extended the previous analysis linking Trr1 with regulation of Ubp12. Excitingly, the data also revealed that several other proteins in the cytoplasmic thioredoxin system, including the cytoplasmic thioredoxin proteins Trx1 and Trx2, regulate the Ubp12 protein. Furthermore, deletion of the genes encoding Trr1 and Trx1/Trx2 were found to have different effects on Ubp12 oxidation and abundance. Interestingly, in contrast to the thioredoxin system, the glutathione system appears to not play a major role in the regulation of Ubp12, consistent with previous observations that diamide, unlike H_2O_2, does not induce the formation of HMW Ubp12 complexes. Finally, several previously unobserved HMW species of Ubp12 were identified in specific mutations of the cytoplasmic thioredoxin system. These species were identified as oxidation products, and excitingly, there is a suggestion the catalytic cysteine residue may be important for resolving some of these unidentified species.

Previous analyses of Ubp12 were performed in non-reducing conditions and involved investigation of the role of Trr1 in potential regulation of Ubp12. These initial studies indicated that the abundance of Ubp12 was significantly decreased in *trr1*Δ cells compared to wild-type cells both before and after treatment with H_2O_2 (Curtis, 2019). The studies presented in this chapter significantly extended these studies to investigate the potential role of many of the cytoplasmic thioredoxin system proteins in the regulation of abundance of Ubp12 using reducing and non-reducing conditions. In addition, the potential role of the mitochondrial thioredoxin system was examined by studying Ubp12 abundance in cells lacking the mitochondrial thioredoxin reductase Trr2. Interestingly, three thioredoxin system mutants (*trr1*Δ, *trr2*Δ and *trx1*Δ*trx2*Δ) suggested a decrease in Ubp12 abundance in non-reducing conditions (Figure 3.2),

however this was found only to be significant for the *trr1*Δ mutant, consistent with previous data (Curtis, 2019). Under reducing conditions however, the drop in Ubp12 abundance is rectified in all but one strain, where significantly less Ubp12 is detected in the *trx1*Δ*trx2*Δ mutant compared to wild-type cells prior to H_2O_2 exposure (Figure 3.3). These data imply that in these strains (*trr1*Δ, *trr2*Δ and *trx1*Δ*trx2*Δ), there are unidentified forms of oxidised Ubp12 that migrate elsewhere on the gel and are therefore not accounted for in the quantification. Excitingly, this result does therefore suggest that the thioredoxin system is responsible for reducing these oxidised forms of Ubp12 however it is important to note that technical factors, such as issues with the protein transfer, could be responsible. For example, different buffer compositions and types of membrane can aid the transfer of differently sized proteins, hence it is possible some forms of Ubp12 may not transfer as well as others under the conditions used. Interestingly however, data presented in Figure 3.12 suggests that there is a genuine drop in the abundance of Ubp12 in the *trr1*Δ mutant even when samples were prepared in reducing conditions. This data also suggests that the catalytic cysteine residue of Ubp12 is not involved in the decreased Ubp12 abundance in this strain. However, there are some experimental differences between Figure 3.3 and 3.12 that are important to note. For example, rich YPD media was used for the experiments described in Figures 3.2 and 3.3 whilst minimal media was used for the experiments in Figures 3.11 and 3.12. Minimal media lacks many components that are present in YPD, such as glutathione, which could affect results. The possible reduction in Ubp12 abundance seen in the *trr2*Δ and *trx1*Δ*trx2*Δ mutants in Figure 3.2 and 3.3 was not confirmed using minimal media, and hence Ubp12 may be regulated in these strains this way too. In addition, the experiments in Figures 3.11 and 3.12 utilised multi copy vectors to express Ubp12, so the copy number of *UBP12* in these two experiments is also not comparable. Although there is no evidence to suggest that Trr1 directly regulates plasmid copy number, it is possible that loss of Trr1 could alter plasmid copy number due to the effect(s) on down-stream processes that Trr1 is involved in. Finally, the wild-type untagged Ubp12 was still expressed from the genome in the cells used in the experiments described in Figures 3.11 and 3.12 and perhaps this had an effect on the results. Hence, in the future it would be important to attempt to repeat these experiments with cells lacking genomic expression of wild type untagged Ubp12. In addition, a CEN single copy expression plasmid could be utilised to assess whether plasmid copy number influenced the results. It might also be possible to modify the

minimal media to assess effects of the media. It is tempting to speculate that, despite the suggestion that the glutathione system only has a minor role in the regulation of Ubp12 (Figure 3.13), that in *trr1*Δ cells the glutathione system can compensate for the lack of a functional cytosolic thioredoxin system. Therefore, the absence of glutathione in the media in experiments presented in Figure 3.12 may account for the reduction in Ubp12 abundance, repetition of the experiment using media supplemented with glutathione would address this. Interestingly however, in *trr1*Δ cells, a large proportion of Trx1 and Trx2 proteins are constitutively oxidised, implying that there is no compensation by the glutathione system for the role of Trr1 (Trotter and Grant, 2005). Additionally, preliminary qPCR analysis did reveal a drop in *UBP12* expression in the *trr1*Δ mutant compared to wild-type cells grown in YPD media (data not shown). *UBP12* expression decreased 0.75-fold in *trr1*Δ cells prior to H_2O_2 treatment when compared to wild-type cells, and decreased 0.45-fold after H_2O_2 treatment. This data is only representative of one repeat and so further repeats would be necessary to validate this finding. Together, this data does suggest a possible role for Trr1 in regulating Ubp12 abundance/stability.

This chapter also reveals a role for the cytosolic thioredoxins (Trx1 and Trx2) in the regulation of Ubp12 oxidation. Upon first analysis, levels of the Ubp12 HMW disulphide were increased in the *trx1*Δ*trx2*Δ mutant (Figure 3.2), however it is important to note that this quantification did not include the unidentified intermediate band (red arrows with asterisks) or unidentified HMW Ubp12 species (res asterisks). Quantification including the intermediate species (Figure 3.8) across a range of H_2O_2 concentrations revealed that there were comparable levels of HMW disulphide in wild-type cells and the *trx1*Δ*trx2*Δ mutant at all concentrations examined, suggesting the primary point of regulation of Ubp12 by Trx1 and/or Trx2 may be the intermediate Ubp12 species. In agreement with this, *trx1*Δ*trx2*Δ cells expressed a comparable level of HMW disulphide to wild-type cells across time-course experiments when exposed to high (2 mM) H_2O_2 (Figure 3.10). Interestingly however, when exposed to 0 mM H_2O_2, *trx1*Δ*trx2*Δ mutants have significantly higher levels of the Ubp12 HMW disulphide compared to wild-type cells (Figures 3.9 and 3.10), suggesting Trx1 and/or Trx2 are important for its reduction. In future experiments, creation of single *trx1*Δ and *trx2*Δ mutants expressing Ubp12-3HA would be useful to address if it is one or both of the cytosolic thioredoxin proteins responsible for regulating Ubp12. Indeed, Trx1 and Trx2 are expressed under

different conditions, for example, it has been found that Trx2 is more important for cell responses to exogenous H_2O_2 than Trx1 (Garrido and Grant, 2002). Hence it is possible they interact differently with Ubp12, or that simply only one is responsible for Ubp12 regulation. Given the link between Trx2 and cellular responses to H_2O_2 (Garrido and Grant, 2002), it is tempting to speculate that Trx2 may be key for Ubp12 regulation however it is necessary to explore the specific roles of each thioredoxin in regulating Ubp12.

As mentioned, Trx1 and/or Trx2 were found across multiple experiments (Figures 3.8, 3.9 and 3.10) to regulate the Ubp12 intermediate band, with *trx1*Δ*trx2*Δ cells expressing consistently higher levels compared to wild-type cells. Indeed, the majority of this data was found to be significant. One data point that was found to be not significant was comparison of the *trx1*Δ*trx2*Δ mutant and wild-type cells exposed to 10 mM H_2O_2, where levels of the intermediate band in wild-type cells was increased (Figure 3.8). This could suggest that the intermediate band is a concentration-sensitive modification in wild-type cells, induced only to very high concentrations of H_2O_2. Analysis of this intermediate band revealed it was a specific form of Ubp12 oxidation (Figure 3.4), that did not contain Gpx3 as originally hypothesized (Figure 3.7). Gpx3 is approximately 18 kDa, which could fit the mobility of the intermediate band, and has a role in H_2O_2 responses; *gpx3*Δ mutants are sensitive to H_2O_2 stress (Delaunay et al., 2002). Gpx3 is also important in the oxidation and activation of Yap1 in BY4741 cells (Delaunay et al., 2002), hence it was possible in absence of Trx1 and Trx2, Gpx3 could regulate Ubp12, however data presented in this chapter found no evidence of this. It is possible another oxidase fulfils this role; however further experimentation is necessary to assess this. No further conclusions were drawn regarding the intermediate band, however clarification of this intermediate band as a heterodimer, homodimer or another intramolecular disulphide is important before further experimentation. It is unlikely that this band is a homodimer of Ubp12 based on the predicted size of the intermediate band, however the molecular weight ladder used in this thesis did not exceed 170 kDa and so any predictions of size are not reliable. It is possible that it is a heterodimer with another protein that Ubp12 for example interacts with/deubiquitinates, where the thioredoxin system is essential in the resolving of this complex. It is also possible that it is another intramolecular disulphide forming within Ubp12, given that Ubp12 contains 19 cysteine residues including the catalytic

cysteine. The intermediate band was also observed in *trr1*Δ cells (Figure 3.11), further suggesting a role for thioredoxin system proteins in its regulation. Importantly, the catalytic cysteine is not required for the formation of the intermediate band (Figure 3.11) however as mentioned above, there are experimental differences between Figures 3.8, 3.9, 3.10 and Figure 3.11 that are important to consider. Interestingly, data suggested that the intermediate band was induced by H_2O_2 in the *trr1*Δ mutant, however currently the differences were found to be non-significant. In *trr1*Δ cells, the cytosolic thioredoxins Trx1 and Trx2 are constitutively oxidised as there is no reductase present to reduce them (Trotter and Grant, 2005). If induction of the intermediate band in response to H_2O_2 is proven in the *trr1*Δ mutant, then any induction might be connected to the effect of loss of Trr1 on the oxidation of Trx1 and/or Trx2, which have been shown to influence the formation of these intermediate forms (Figures 3.9 and 3.10). It is interesting that the regulation of Ubp12 by Trx1 and/or Trx2 is different to its regulation by Trr1, given that deletion of Trr1 causes the oxidation of Trx1 and Trx2 presumably meaning these proteins can no longer function as reductants (Ragu et al., 2014). Interestingly, research has found that the two mutant strains do confer different phenotypes and sensitivities with the *trr1*Δ strain displaying a slower growing phenotype compared to the double thioredoxin mutant and a heightened sensitivity to H_2O_2 stress (Trotter and Grant, 2005, Toledano et al., 2013). Additionally, the double thioredoxin mutant displays defects in the cell cycle and in sulphur metabolism which are not observed in the *trr1*Δ strain (Muller, 1991). It is possible that Trr1 may exhibit functions outside of the regulation of Trx1/Trx2, as seen with the mammalian Trr (Arnér and Holmgren, 2000). Thus, Trr1 and the cytosolic thioredoxins Trx1 and Trx2 do fulfil specific roles which may account for the differences in Ubp12 regulation in these two strains.

Unidentified HMW forms of Ubp12 were also observed across various experiments in the double thioredoxin mutant (asterisks in Figures 3.2, 3.8, 3.9 and 3.10). Treatment of samples with β-mercaptoethanol suggested that these HMW forms were a form of oxidation (Figure 3.3), and were found to be formed in a H_2O_2-concentration dependent manner (Figure 3.8). No quantification was performed on these bands, and hence all conclusions are qualitative, however data suggests that these bands represent further oxidised forms of Ubp12 that are regulated by the cytosolic thioredoxin system. This data is consistent with the conclusions from Figures 3.2 and

3.3, where unidentified forms of oxidised Ubp12 are formed in various thioredoxin system mutant strains. As with the intermediate band, the unidentified HMW forms of Ubp12 are also observable in the *trr1*Δ mutant, and possibly in wild-type cells expressing the C373S plasmid (Figure 3.11). The signal for these HMW forms increases after H_2O_2 treatment, consistent with the observation that they are a concentration-dependent modification. The signal also seems to increase in *trr1*Δ cells expressing the C373S plasmid (although no quantification was performed), suggesting that the catalytic cysteine is not essential for their formation but could be involved in resolving these HMW oxidised forms of Ubp12. Further analysis of these bands, including mass spectrometry and further cysteine mutation analysis, could address the composition of these species' but fell outside of the timescale of this project. Data presented here however does heavily suggest they are another oxidised form of Ubp12.

Data presented in this chapter has heavily suggested that certain thioredoxin system mutants are involved in the regulation of various oxidised forms of Ubp12. Thioredoxin proteins utilise their conserved CXXC motif to modulate redox events within the cell, however this CXXC motif can have other functions (Chivers et al., 1997). Indeed, thioredoxin and thioredoxin-related proteins have also been noted to possess protein chaperone activity, for example, the peroxiredoxin Tsa1 has been well-characterised as a chaperone protein (see 1.2.3.1) (MacDiarmid et al., 2013). In addition to this, various thioredoxin proteins have been found to have protein chaperone functions (Lee et al., 2009, Sanz-Barrio et al., 2012, Du et al., 2015). In addition to aiding protein folding, thioredoxin and thioredoxin-related proteins can utilise their CXXC motifs to function as disulphide isomerases, rearranging disulphides within a protein (Quan et al., 2007). Mutation of the CXXC motif in the oxidoreductase, DsbA, inhibited its role as an oxidoreductase, a disulphide isomerase and as a chaperone protein (Quan et al., 2007). Given the various forms of oxidised Ubp12 formed in thioredoxin system mutants, it is tempting to speculate that thioredoxin proteins may function to rearrange disulphides within Ubp12 rather than directly reducing or oxidising Ubp12. Future work assessing the possible role of thioredoxin system proteins in *S. cerevisiae* as chaperones/disulphide isomerases would begin to address this hypothesis.

Data presented in this chapter strongly suggests a role for the thioredoxin system in the regulation of Ubp12, however it was necessary to explore if the glutathione system

had any role. Previous data from our lab found that the Uba1/Cdc34 disulphide (see 1.3.2) was regulated entirely by the glutathione system, with no observable effects in thioredoxin pathway mutants and significant induction of the disulphide with BSO treatment (Doris et al., 2012). Additionally, the Uba1/Cdc34 disulphide is induced in response to H_2O_2 and diamide, consistent with regulation by the glutathione system and not the thioredoxin system. Data presented in this chapter suggests a minor role for the glutathione system in regulating Ubp12 (Figure 3.13). Although no further analysis was performed, BSO did not induce the Ubp12 HMW disulphide to comparable levels of the H_2O_2 induction, which was observed in the BSO and H_2O_2-induced formation of the Uba1/Cdc34 disulphide (Doris et al., 2012). This data is consistent with the findings that the Ubp12 disulphide is only formed in response to H_2O_2 and not diamide (Curtis, 2019). It is also possible that BSO induced the Ubp12 HMW disulphide because the thioredoxin system becomes overwhelmed due to the loss of glutathione in the cell. However, it is important to note that there are overlapping functions between the thioredoxin and glutathione systems. For example, in *trr2*Δ cells Glr1 is able to maintain the oxidation state of Trx3 (Trotter and Grant, 2005). Thus, due to the suggestion of a minor role for the glutathione system in Ubp12 regulation, it is important to consider the redundancy between the two systems when analysing thioredoxin pathway mutants. For example, in *S. cerevisiae*, Ubp12 is known to regulate mitochondrial morphology through deubiquitination of the mitofusin Fzo1 (see 1.3.4.1) (Anton et al., 2013). The mitochondria produces a large amount of ROS through electron leakage during oxidative phosphorylation (see Section 1.2.1.1) (Jensen, 1966), hence it is interesting that there was no significant evidence found of a role for the mitochondrial thioredoxin system in Ubp12 regulation (Figure 3.2). However, the role of the mitochondrial thioredoxin Trx3 was not analysed and hence analysis of the *trx3*Δ mutant could shed insight into Ubp12 regulation within the mitochondria. Given that Trx3 can be reduced by Glr1 in the absence of Trr2, it is possible that deletion of Trr2 did not confer any significant phenotypes due to redundancy between Trr2 and Glr1 (Trotter and Grant, 2005). Further analysis of specific glutathione pathway mutants would help to clarify the role of the glutathione system in the regulation of Ubp12 but fell outside of the time-frame of this work.

This chapter has also revealed interesting information regarding the reduced form of Ubp12. Ubp12 was found to migrate as a doublet on western blots, in both BY4741

and W303 strains of *S. cerevisiae* and in *C. albicans* (Figure 5.7). This doublet was proven to not be a form of oxidation (Figure 3.14). Interestingly, preliminary data presented in Figure 3.14 suggested that the ratio of the doublet band was different in W303 and BY4741 cells, and in some thioredoxin system mutants (Figure 3.14). Thus, it is possible that in different strain backgrounds of *S. cerevisiae* Ubp12 is modified differently into these two different forms, and that the thioredoxin system may regulate their formation, although repeats and quantification are necessary to further this hypothesis. It is possible that Ubp12 forms a heterodimer with a very small protein to cause this doublet band however this seems unlikely as the change in mobility of the higher doublet band is so small. Doublet bands often form due to the presence of an unmodified and a modified form of a protein via the addition of post translational modifications such as ubiquitination, sumoylation or phosphorylation. The difference in molecular weight between the two species is relatively small, which could be attributed to a single site of ubiquitination or sumoylation, or multiple sites of phosphorylation. Data does show that Ubp12 itself can be ubiquitinated, with one paper attributing this ubiquitination to the eventual degradation of Ubp12 (Simões et al., 2018). In addition, various serine, threonine and tyrosine residues of Ubp12 are able to become phosphorylated, hence it is possible these phosphorylation events explain the double band (Albuquerque et al., 2008, Zhou et al., 2021, Lanz et al., 2021). Interestingly, USP15 is found to be differentially phosphorylated at residues T149 and T219, a process noted to affect the localisation of the protein between the cytoplasm and the nucleus and its function in the spliceosome (Das et al., 2019a). In *S. cerevisiae*, the T219 residue is conserved however the T149 residue is a tyrosine residue. It is therefore possible both of the phosphorylation events observed in USP15 are conserved in Ubp12. Treatment of samples with phosphatase inhibitors could address this. Thus, the different forms of Ubp12 observed in the doublet could be localized to different parts of the cell, as observed with USP15. Following this, it is interesting to note that quantification from Figure 3.14 suggests that this it is the slower mobility band of the doublet that is decreased in abundance following addition of H_2O_2 in wild-type cells and perhaps tempting to link this modified form of the protein to the formation of the HMW disulphide complex.

Conclusively, Chapter 3 of this thesis has revealed some important information regarding the regulation of Ubp12. Excitingly, data here presents the first known

evidence for the regulation of Ubp12 by the thioredoxin system. Elucidating the regulation of Ubp12 is vital for research into the conserved human homologue USP15, a protein implicated in various pathologies. Hence, research presented here is important for understanding the regulation of DUBs in *S. cerevisiae*, but also for aiding therapeutic efforts into USP15 research. To further understand the oxidation of Ubp12 in *S. cerevisiae*, it was next important to employ a mutagenic approach to analyse which cysteine residues of Ubp12 are involved in its oxidation.

Chapter Four: Mutational analysis of Ubp12 in *S. cerevisiae*

4.1 Introduction

Ubp12 is a large, 143 kDa DUB that is a member of the USP group of DUBs (see section 1.1.6.1.1). The DUB activity of Ubp12 utilises a catalytic triad that consists of three amino acids, the catalytic cysteine residue (C373), a histidine residue and an aspartate residue. In the previous chapter several proteins in the thioredoxin system were found to have a role in the regulation of the oxidation and abundance of Ubp12 in response to H_2O_2. Furthermore, several new HMW species of Ubp12 were observed suggesting that the formation of the previously identified H_2O_2-induced HMW oxidised disulphide complex (Curtis, 2019) (Figures 3.2, 3.8, 3.9, 3.10) might be more complex than first suspected. Previous studies and work presented in chapter 3 revealed that C373 is essential for the formation of the HMW disulphide complex in response to H_2O_2 (Curtis, 2019) (Figures 3.11). Interestingly, however, several of the newly identified HMW forms of Ubp12, at least one of which represents an oxidised form of the DUB, were formed regardless of the presence or absence of C373 (Figure 3.11). Hence, these data suggest that other cysteine(s) in Ubp12 are involved in the oxidation of Ubp12. Indeed, the identity of other cysteine(s) residues that determine the formation of the original H_2O_2-induced HMW disulphide complex has not been elucidated.

Ubp12 activity has been linked with several fundamental processes in *S. cerevisiae*, including the regulation of mitochondrial dynamics, DNA replication, genome stability, cell cycle regulation and proteasomal degradation (see section 1.3.4.1) (Anton et al., 2013, Álvarez et al., 2019, Ang et al., 2016, Gödderz et al., 2017). Despite these links, relatively little is known about the regulation of Ubp12 activity in these processes and connections with ROS. However, it is important to note the relevance of ROS in Ubp12-regulated processes, such as mitochondrial dynamics, and genome stability (Anton et al., 2013, Ang et al., 2016). It is also interesting that dysregulation of USP15, the human homologue of Ubp12, has been implicated in numerous cancers, displaying seemingly contradictory roles in tumorigenesis where in some cases it functions as a tumour-suppressor whilst in others it functions as an oncogene (see section 1.3.4.2) (Zou et al., 2014, Huang et al., 2009). These roles highlight the importance of

understanding USP15 and make it a potential biomarker for cancer progression. However, at present there are gaps in our knowledge of USP15 and related pathologies, and it is possible that ROS play some role in the links between USP15 and human disease processes. Hence it is important to elucidate the roles and regulation of Ubp12 in responses to ROS as these studies could potentially provide insight of the roles and regulation of USP15 in human cells. Thus, the specific objectives of this chapter were to investigate the potential roles of conserved cysteine residues in Ubp12 in the roles and regulation of this DUB in *S. cerevisiae*.

4.2 Results

4.2.1 Analyses of the role of Ubp12 in response to oxidising agents

As described in this thesis Ubp12 forms HMW complexes in response to H_2O_2 and in the absence of specific proteins in the thioredoxin system (Figures 3.2, 3.8, 3.9, 3.10) (Curtis, 2019). Previous work proposed that the formation of the HMW disulphide complexes acted to inhibit Ubp12 activity in response to H_2O_2 (Curtis, 2019). However, the BY4741 and W303 strain backgrounds of *S. cerevisiae* respond differently to oxidative stress and hence it was important to assess the potential roles of Ubp12 in response to different oxidising agents in these two strain backgrounds (Veal et al., 2003). Hence, the sensitivity of *ubp12*Δ cells in both strain backgrounds was examined. In particular, serial dilutions of BY4741 wild-type (KA1), W303-1a wild-type (KA4), *ubp12*Δ (BY4741 background – KA107) and *ubp12Δ* (W303 background – KA7) cells were spotted onto YPD plates at 30^{o}C containing various oxidising agents (Figure 4.1).

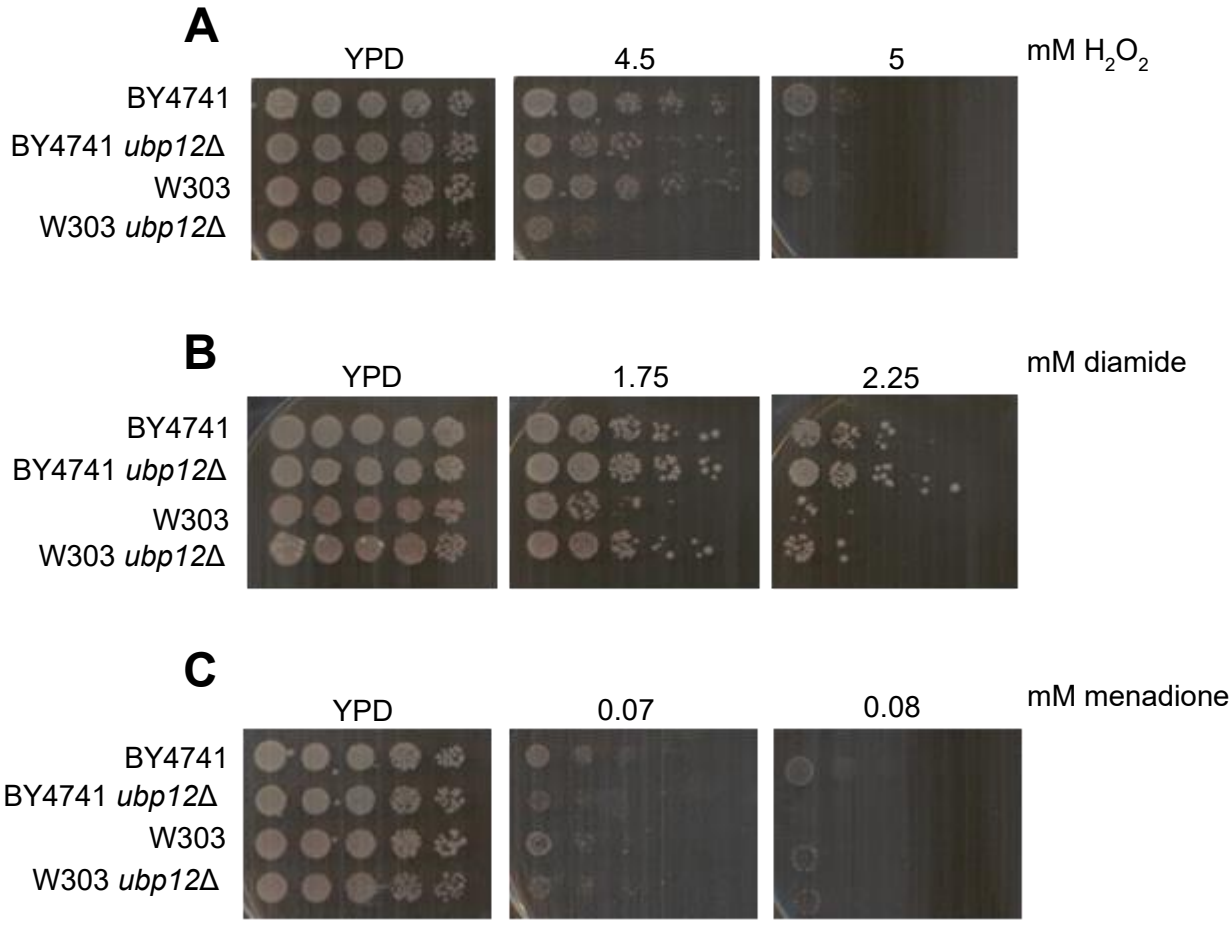

Figure 4.1. Ubp12 is involved in responses to oxidative stress in both the BY4741 and W303 strain backgrounds.

(A – C) 5-fold serial dilutions of mid-log phase growing wild-type BY4741 (KA1), BY4741 *ubp12*Δ (KA107), wild-type W303 (KA4) and W303 *ubp12*Δ (KA7) cells were spotted onto YPD plates containing the indicated stress condition. Plates were incubated at 30°C for 2 days before imaging. N = 3.

As predicted the results presented in Figure 4.1 revealed that wild-type cells in the W303 and BY4741 strain backgrounds display different sensitivities to the three oxidising agents tested. The BY4741 wild type cells were found to be more resistant to H_2O_2, diamide and menadione (a superoxide generator) than W303 wild type cells (Figure 4.1). Interestingly, the data also suggested that Ubp12 is involved in the

responses to these three oxidising agents in both the BY4741 and W303 strain backgrounds (Figure 4.1). Cells lacking Ubp12 in both strain backgrounds were more sensitive than the corresponding control wild type cells to H_2O_2 and menadione and more resistant than the corresponding control wild type cells to diamide (Figure 4.1). It is also noteworthy that the differences in the sensitivity/resistance of *ubp12*Δ cells compared with their respective wild type control cells were similar in the two strain backgrounds (Figure 4.1). Hence, taken together these results imply that Ubp12 has different roles in response to different oxidising agents. Furthermore, the relative differences in sensitivity/resistance in the strain backgrounds tested raise the possibility that these roles of Ubp12 are conserved in strains that respond in different ways to different oxidising agents.

To gain further insight into the roles of Ubp12 in the oxidative stress responses observed in the BY4741 and W303 strain backgrounds, the next step was to assess if Ubp12 plays any role in the adaptive response to oxidative stress. Previous studies have shown that pre-exposure of *S. cerevisiae* cells to low levels of H_2O_2 can increase cell viability when subsequently exposed to high levels of H_2O_2 (Collinson and Dawes, 1992). Hence to assess whether Ubp12 plays any role in this adaptive response to oxidative stress, BY4741 wild-type (KA1), W303-1a wild-type (KA4), *ubp12*Δ (BY4741 background – KA107) and *ubp12Δ* (W303 background – KA7) were exposed to either 0 mM or 0.05 mM (low levels) H_2O_2 for 30 minutes before serial dilutions were spotted onto YPD plates containing high levels of H_2O_2 and grown at 30^{o}C (Figure 4.2).

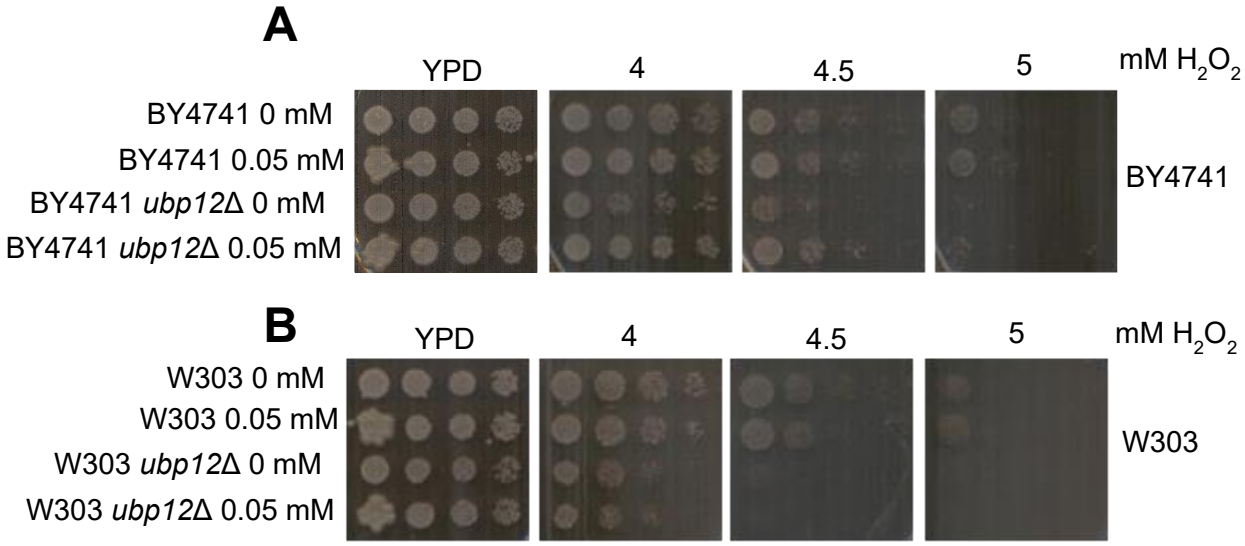

Figure 4.2. Pre-exposure to low levels of H_2O_2 reverses the sensitivity of *ubp12*Δ cells to H_2O_2 in the BY4741 but not the W303 strain background.

5-fold serial dilutions of mid-log phase growing (A) wild-type BY4741 (KA1) and BY4741 *ubp12*Δ (KA107) cells, and (B) wild-type W303 (KA4) and W303 *ubp12*Δ (KA7) cells, exposed to either 0 mM or 0.05 mM (indicated in brackets) H_2O_2 for 30 minutes, were spotted onto YPD plates containing the indicated concentration of H_2O_2. Plates were incubated at 30°C for 2 days before imaging. N = 3.

As expected, *ubp12*Δ cells in both strain backgrounds which had not been pre-treated with low levels of H_2O_2 for 30 minutes were found to be more sensitive to H_2O_2 stress when compared to the respective wild-type control cells in the same strain background (Figure 4.2). Interestingly, the pre-exposure of *ubp12*Δ cells to low levels of H_2O_2 only appeared to have a beneficial effect on growth in the BY4741 strain background and not in the W303 strain background (Figure 4.2). It is also interesting to note that the low level of H_2O_2 used in this experiment had no detectable effect on the sensitivity of wild-type BY4741 cells or wild-type W303-1a cells to high levels of H_2O_2 (Figure 4.2). Furthermore, these results were confirmed over several repeats (n=3). It is possible that the concentration of H_2O_2 used for the low-level pre-exposure to induce the adaptive response to higher levels of H_2O_2 was not sufficient in the experiments presented here and it would be useful to repeat these experiments using different concentrations of H_2O_2 to attempt to induce the adaptive response. Nevertheless, the experiments presented here suggest that perhaps Ubp12 has different roles in the

BY4741 and W303 strain backgrounds in responses to H_2O_2. For example, it is possible that the increased sensitivity of *ubp12*Δ cells to H_2O_2 in the W303 strain background is linked to the adaptive response to H_2O_2 whilst the increased sensitivity of *ubp12*Δ cells to H_2O_2 in the BY4741 strain background could be because Ubp12 functions in H_2O_2 responses independently of the adaptive response. However, these conclusions would require further experimentation to fully understand the differences in function of Ubp12 in the two strain backgrounds.

In summary the data presented above highlight that Ubp12 is important for oxidative stress responses and, moreover, suggest that there may be some potential differences in the roles of Ubp12 in different strain backgrounds.

4.2.2 Characterisation of the roles of conserved cysteine residues of Ubp12

4.2.2.1 Construction of triple cysteine mutants

Ubp12 functions in oxidative stress responses in *S. cerevisiae* and previous work from our lab (Curtis, 2019) and work presented here (Chapter 3) revealed that the protein is oxidised in response to H_2O_2 but not to other oxidative stress conditions. Furthermore, the kinetics of oxidation of Ubp12 in the presence of H_2O_2 occurs in a concentration-dependent manner (Figures 3.8, 3.9, 3.10) (Curtis, 2019). Further analysis also revealed that the catalytic cysteine residue (C373) is essential for the formation of the HMW disulphide complexes but not other HMW forms of Ubp12 (see Figure 3.11) (Curtis, 2019). However, in the case of all of the HMW forms of Ubp12 the contribution (if any) of other cysteine(s) in the Ubp12 protein in their formation was unknown. To attempt to identify cysteine residues in Ubp12 that may contribute to oxidation of the protein, the protein sequences of Ubp12 from *S. cerevisiae*, *Candida albicans*, *Schizosaccharomyces pombe* and humans were compared to highlight conserved cysteine residues (Figure 4.3). This approach was chosen as experiments described in Chapter 5 revealed that Ubp12 in *C. albicans* also forms HMW complexes in response to oxidative stress that are sensitive to β-mercaptoethanol (for example see Figure 5.7), suggesting that perhaps equivalent cysteine residue(s) may be involved in the oxidation of this DUB in these two yeast species. The 19 cysteine

residues of Ubp12 in *S. cerevisiae* and their conservation in other organisms are shown below (Figure 4.3).

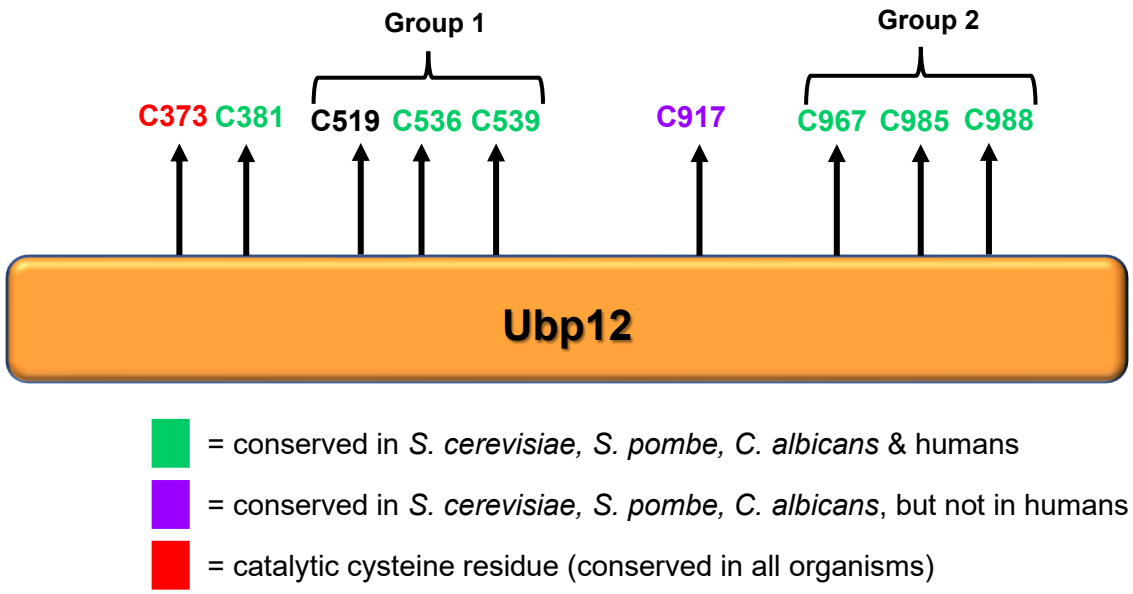

Cysteine residues 11, 28, 124, 154, 168, 519, 609, 817, 1166, 1190, 1234 are not widely conserved

Figure 4.3. Schematic diagram of cysteine residues in Ubp12 in *S. cerevisiae*.

The 19 cysteine residues of Ubp12 in *S. cerevisiae* were compared with the cysteine residues in Ubp12 homologues from *S. pombe*, *C. albicans* and humans (USP15). The catalytic cysteine residue (C373 in *S. cerevisiae* Ubp12) is highlighted in red; cysteine residues conserved in *S. cerevisiae*, *S. pombe*, *C. albicans* and human cells are highlighted in green; and cysteine residues conserved in *S. cerevisiae*, *S. pombe* and *C. albicans*, but not in human cells, are highlighted in purple. Non-conserved residues (except C519) are not highlighted on the diagram. Group 1 and Group 2 correspond to the two sets of cysteine residues chosen for mutagenesis (discussed later).

Of the 19 cysteine residues present in Ubp12 in *S. cerevisiae*, 8 are conserved in the homologues of Ubp12 in other yeast species, and of those 7 are also conserved in humans (Figure 4.3). Given the results presented here that revealed that Ubp12 in *C. albicans* also becomes oxidised in response to oxidative stress (see Chapter 5) it was decided to focus on mutational analyses of highly conserved cysteine residues in Ubp12 in *S. cerevisiae*. Hence, to attempt to identify other cysteine residues, in addition to the catalytic cysteine residue, C373, involved in the formation of the Ubp12 HMW disulphide complex a strategy was developed to mutate two groups of three

cysteine residues to serine residues (Figure 4.3; Group 1 and Group 2). These cysteine residues were chosen based on their conservation, their proximity to each other which is useful in the mutagenesis protocol (C519 is not a highly conserved cysteine residue but was included due to proximity to C536 and C539), and the identification of CXXC motifs in Ubp12. The Group 1 and Group 2 cysteine residues both contain a conserved CXXC motif (C536 and C539, and C985 and C988, respectively), which raises the possibility that these may be redox-active motifs involved in the formation of oxidation products of Ubp12 (Chivers et al., 1997).

The strategy applied to mutate specific cysteine residues of Ubp12 to serine residues is based on a previously described technique (Oldenburg et al., 1997), and is shown in Figure 4.4. Serine codon usage within Ubp12 was assessed and the most commonly used serine codon (TCA) was selected for this mutagenesis. For each triple mutant two overlapping fragments were generated by PCR (Figure 4.5A-D) using the pRS426-Ubp12-3HA plasmid (Table 2.1) as template DNA and the oligonucleotide primers described in Figure 4.5. These fragments contained overlapping regions of 70 bp homology to each other, which included the codons for the cysteine residues to be mutagenised. By using the M13 forward and reverse primers (M13F, M13R) the PCR products also contained homology to the pRS426-Ubp12-3HA plasmid upstream and downstream of the EcoRI and SalI restriction enzyme cut sites, respectively (Figure 4.4). The pRS426-Ubp12-3HA plasmid was then digested using the restriction enzymes SalI and EcoRI (Figure 4.5E). The appropriate PCR products were purified and co-transformed with EcoRI and SalI digested pRS426-12-3HA into *ubp12*Δ (KA7) cells to allow homologous recombination of the fragments with the linearised plasmid, using a vector to insert ratio of 3:1. Transformants were grown on SD – uracil plates, to select for the presence of the recombined plasmid. Ura+ transformants were checked by PCR to assess if *UBP12-3HA* was inserted into linearised pRS426 using the M13F and M13R primers (data not shown, DreamTaq PCR conditions are detailed in section 2.3.1.2). Plasmids were then extracted, expressed in *E. coli* and extracted for DNA sequencing. DNA sequence analyses confirmed the presence of the mutations of the respective cysteine codons to serine codons (primers detailed in Figure 4.4). This technique produced two plasmids; pRS426-Ubp12-3HA-Group1C-S (C519S, C536S, C539S) and pRS426-Ubp12-3HA-Group2C-S (C967S, C985S, C988S), expressing mutated Ubp12-3HA from its own promoter. It is important to note

that there are synonymous mutations within the pRS426-Ubp12-3HA-Group1C-S plasmid, at the serine residue 2 codons upstream of the start codon and S987. Additionally, in the pRS426-Ubp12-3HA-Group1C-S plasmid there is one non-synonymous mutation, V52L, and in the pRS426-Ubp12-3HA-Group2C-S one non-synonymous mutation, L814V.

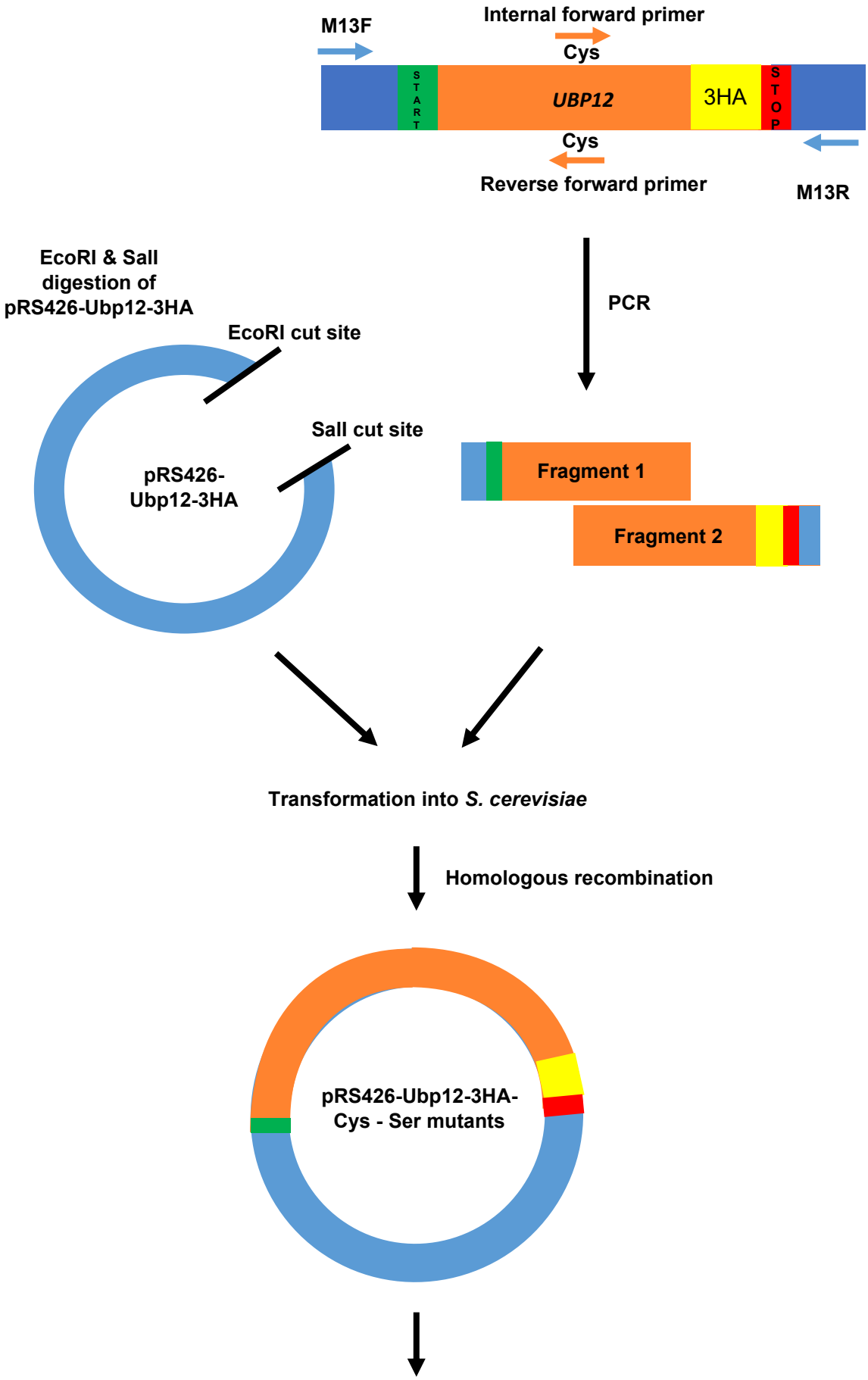
M13F
Internal forward primer
Cys
START
UBP12
3HA
STOP
Cys
Reverse forward primer
M13R
EcoRI & SalI digestion of pRS426-Ubp12-3HA
EcoRI cut site
SalI cut site
pRS426-Ubp12-3HA
PCR
Fragment 1
Fragment 2
Transformation into S. cerevisiae
Homologous recombination
pRS426-Ubp12-3HA-Cys - Ser mutants
Check PCRs, plasmid extraction, transformation into E. coli, sequencing and re-transformation into W303 ubp12Δ cells

Figure 4.4. Strategy to create the cysteine to serine substitutions of Ubp12.

The plasmid pRS426-Ubp12-3HA was linearised and the wild-type Ubp12-3HA excised by digestion with the EcoRI and SalI restriction enzymes in the multiple cloning region. Two PCR products (Fragment 1 and Fragment 2) containing an overlapping region spanning the codons for the cysteine to serine substitutions were produced using wild-type pRS426-Ubp12-3HA DNA as a template, and the appropriate forward and reverse primers for each fragment. The PCR products (Fragment 1 and Fragment 2) contained approximately 70 bp of overlap with each other which allowed *in vivo* homologous recombination to create pRS426-Ubp12$^{C\text{-}S}$3HA plasmids. The linearised pRS426-Ubp12-3HA plasmid and the two PCR products were transformed into W303-1a *ubp12*Δ cells (KA7) and Ura+ colonies screened for successful recombination by PCR. Plasmids were also extracted and transformed into *E. coli* to allow DNA sequencing and analysis by Western blotting. DNA sequencing reactions used the following primers; bp12ChkDelF, Ubp12 KA Fw 1, Ubp12 Frag 2 Fw, Ubp12 KA Fw 2, Ubp12 Frag 3 Fw, Ubp12 KA Fw 3, Ubp12 Rev 1, Ubp12 Rev 2, Ubp12 Rev 3, Ubp12 Rev 4, Ubp12 Rev 5, Ubp12 Rev 6 and ubp12ChkTagR (Appendix C).

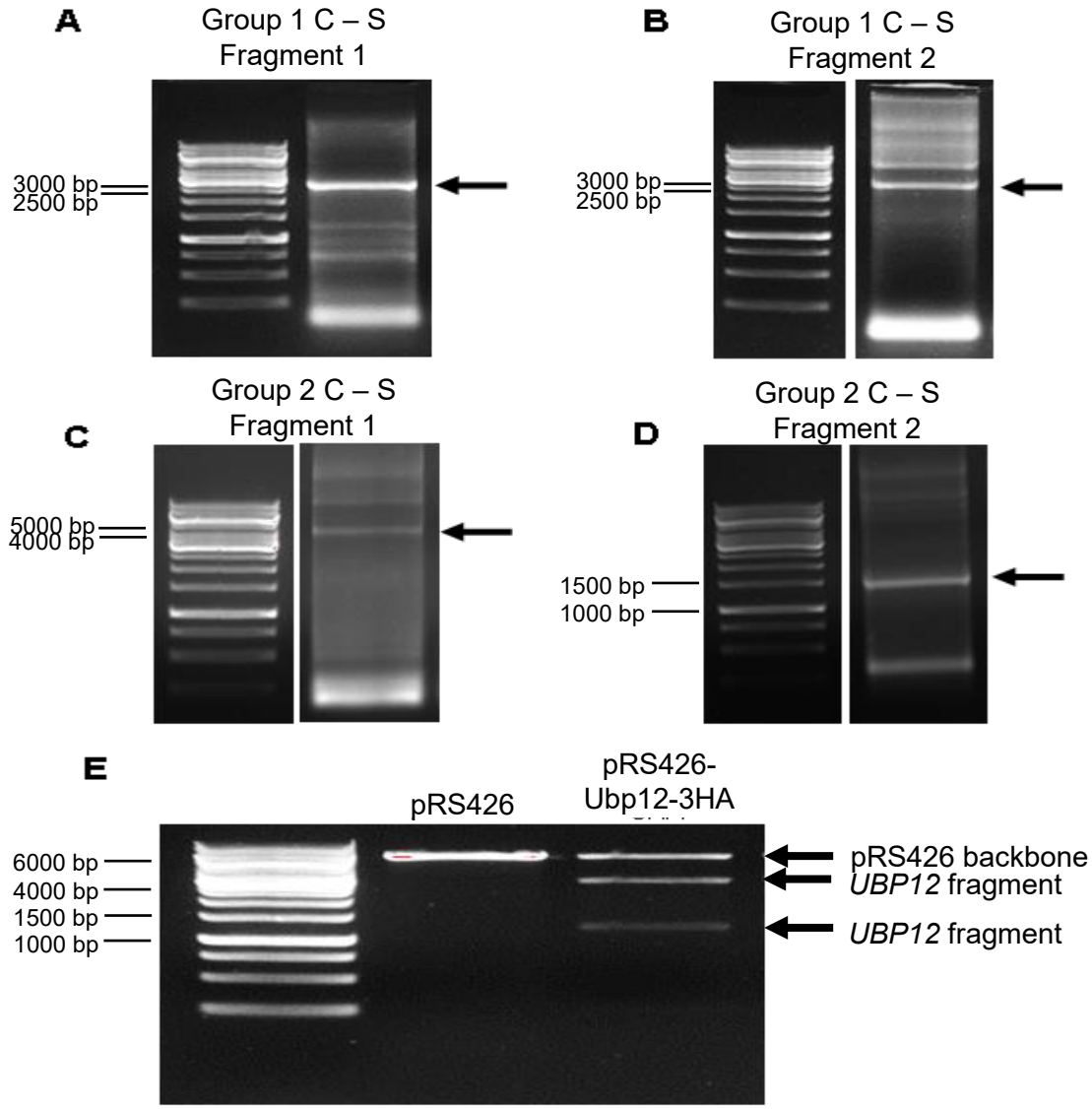

Figure 4.5. PCR products and linearised plasmid required to generate pRS426-Ubp12-3HA-Group1C-S and pRS426-Ubp12-3HA-Group2C-S.

(A-D) Agarose gel analysis of the Phusion PCR reactions (see section 2.3.1.1 for all PCR conditions) to generate (A) fragment 1 (~2800bp) and (B) fragment 2 (~3000bp) for the Group 1 C-S plasmid using plasmid pRS426-Ubp12-3HA as template DNA and M13F and 426-12-3HA-1-rev primers and 426-12-3HA-2-fw and M13R primers respectively. To generate (C) fragment 1 (~4400bp) and (D) fragment 2 (~1400bp) for the Group 2 C-S plasmid Phusion PCR reactions were performed using pRS426-Ubp12-3HA as template DNA and M13F and 426-12-3HA-2-rev primers and 426-12-3HA-3-fw and M13R primers respectively. (E) The pRS426-Ubp12-3HA-*URA3* plasmid backbone (black arrow) was obtained using the EcoRI and SalI restriction enzymes according to manufacturer's instructions. The digestion was analysed by agarose gel. Linearised plasmid pRS426 (digested with SalI and EcoRI according to the manufacturer's instructions) was analysed as a control to confirm the correct band. GeneRuler 1 kb DNA Ladder (ThermoScientific) was used.

4.2.2.2 Analyses of Group 1 and Group 2 mutations

Given the nature of the extra mutations in these plasmids and the difficulty associated with obtaining these plasmids it was decided to test whether mutant Ubp12 protein expressed from pRS426-Ubp12-3HA-Group1C-S and pRS426-Ubp12-3HA-Group2C-S can form the Ubp12 HMW disulphide complex in response to H_2O_2. Hence, W303 *ubp12*Δ (KA7) cells were transformed with pRS426-Ubp12-3HA (expressing wild-type Ubp12-3HA), pRS426-Ubp12-3HA-C373S (expressing the catalytic cysteine mutant version of Ubp12-3HA), pRS426-Ubp12-3HA- Group1C-S and pRS426-Ubp12-3HA-Group2C-S. Transformants were then grown to mid-log phase in minimal media and exposed to 2 mM H_2O_2 for 0 or 10 minutes. Proteins were extracted and analysed by western blot under non-reducing conditions (Figure 4.6).

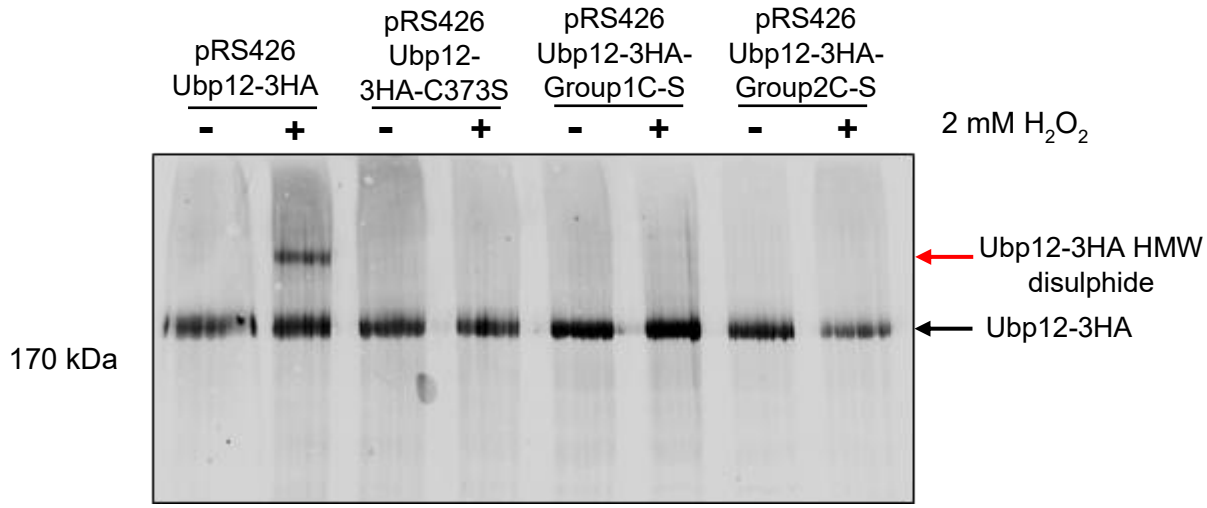

Figure 4.6. Both Group 1 and Group 2 mutations prevent the formation of the Ubp12 HMW disulphide complex.

Western blot analysis of protein extracts isolated from mid-log phase growing W303 *ubp12*Δ (KA7) cells, containing the indicated plasmids, in minimal media and treated with 2 mM H_2O_2 for 0 (-) or 10 (+) minutes. Protein extracts were prepared in non-reducing conditions, separated by SDS-PAGE and proteins were visualised using anti-HA antibodies. N=3. PageRuler Prestained Protein Ladder (ThermoScientific) was used for molecular weight reference.

As expected, treatment of cells containing the wild type pRS426-Ubp12-3HA plasmid resulted in the formation of the H_2O_2-induced HMW disulphide complex (Figure 4.6). Furthermore, in agreement with previous studies (for example see Figure 3.11) the formation of the H_2O_2-induced HMW disulphide complex was not detected in cells containing the pRS426-Ubp12-3HA-C373S plasmid (Figure 4.6). Excitingly, although the expression of Ubp12-3HA could be readily detected suggesting that the mutations do not affect the stability of the protein, the H_2O_2-induced HMW disulphide complex was also not detected in cells containing either the pRS426-Ubp12-3HA-Group1C-S plasmid or the pRS426-Ubp12-3HA-Group2C-S plasmid (Figure 4.6). The basis for this effect of the Group 1 and Group 2 mutations is not clear. For example, it could indicate that one or more of the Group 1 and Group 2 cysteine residues is involved directly in the formation of the HMW disulphide complex in response to H_2O_2, perhaps by forming transient intermediary disulphide bonds such as those detected in the studies in Chapter 3 in steps required to form the HMW disulphide complex. If true

perhaps this is also the role of C373 in the formation of the HMW disulphide complex. It is also possible that, like the C373S mutation, the Group 1 and Group 2 mutations interfere with the catalytic activity of Ubp12, and hence would block the formation of the HMW disulphide complex if the catalytic activity of Ubp12 is required for formation of this complex. As described above, there are some random mutations in the coding sequence for Ubp12 in the Group 1 and Group 2 C - S plasmids and so it cannot be ruled out that these also somehow affect the ability to form the HMW disulphide complex. However, it is noteworthy that the synonymous mutations only change the codon for an amino acid and even the predicted amino acid substitutions (a valine to leucine, and a leucine to valine) are likely to be relatively neutral in their affects. Hence taken together these data suggest that several conserved cysteine residues in Ubp12 may be required for the formation of the HMW disulphide complex.

4.2.2.3 Analysis of the C536S mutation

In an attempt to gain further insight into the potential roles of the cysteine residues in the Group 1 mutations it was decided to develop a strategy to substitute C536 individually with a serine residue. C536 was chosen for two main reasons: 1) it is one of the two highly conserved cysteine residues within the Group 1 cysteine residues and 2) C536 is the first cysteine residue in the CXXC motif in this section of the protein and this substitution would be predicted to inhibit any potential role of this motif in redox signalling (Chivers et al., 1997). Using a strategy identical to that described earlier (Figure 4.4) a plasmid expressing Ubp12-3HA with the C536S mutation (pRS426-Ubp12-3HA-C536S) was generated (data not shown). The primers used in the Phusion PCR reaction for fragment 1 were M13F and Ubp12-C536S-frag-1-rev and for fragment 2 were Ubp12-C536S-frag-2-fw and M13R (Appendix C). Phusion PCR reaction conditions can be found in section 2.3.1.1. DNA sequence analyses confirmed the presence of the C536S codon mutation (data not shown). It is important to note there is a synonymous mutation in this plasmid (F178). To test whether mutant Ubp12 protein expressed from pRS426-Ubp12-3HA-C536S can form the Ubp12 HMW disulphide complex in response to H_2O_2, W303 *ubp12*Δ (KA7) cells were transformed with pRS426-Ubp12-3HA (expressing wild-type Ubp12-3HA) and pRS426-Ubp12-3HA-C536S. Transformants were then grown to mid-log phase in minimal media and

exposed to 2 mM H_2O_2 for 0 or 10 minutes. Proteins were extracted and analysed by western blot under non-reducing conditions (Figure 4.7).

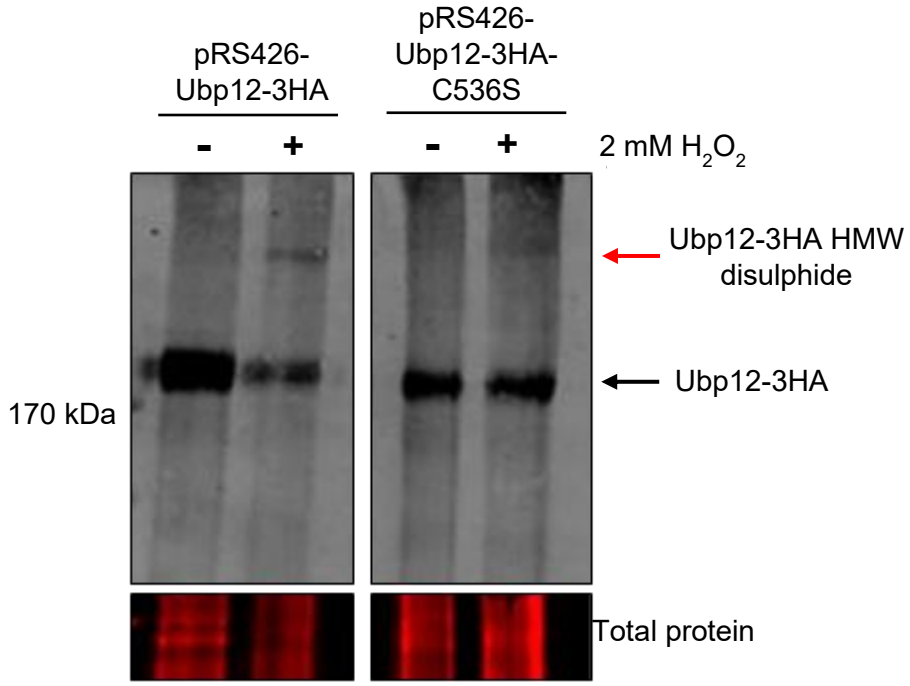

Figure 4.7. The C536S mutation does not prevent the formation of the Ubp12 HMW disulphide complex.

Western blot analysis of protein extracts isolated from mid-log phase growing W303 *ubp12*Δ (KA7) cells, containing the indicated plasmids, in minimal media and treated with 2 mM H_2O_2 for 0 (-) or 10 (+) minutes. Protein extracts were prepared in non-reducing conditions, separated by SDS-PAGE and proteins were visualised using anti-HA antibodies. Protein loading is shown (total protein stain). N=1. PageRuler Prestained Protein Ladder (ThermoScientific) was used.

Again, as expected, treatment of cells containing the wild type pRS426-Ubp12-3HA plasmid resulted in the formation of the H_2O_2-induced HMW disulphide complex (Figure 4.7). Similar to the analyses of the Group 1 and Group 2 mutations of Ubp12 the expression of Ubp12-3HA-C536S could be readily detected in cells suggesting that the mutation does not affect the stability of the protein (Figure 4.7). However, in contrast to the Group 1 and Group 2 mutations, the formation of a H_2O_2-induced HMW complex was detected in cells containing the pRS426-Ubp12-3HA-C536S plasmid (Figure 4.7). However, it is interesting to note that the relative amount of Ubp12-3HA-

C536S in the HMW complex versus the unstressed faster mobility form of Ubp12-3HA-C536S appears to be qualitatively lower compared to the same bands in cells containing the wild-type pRS426-Ubp12-3HA plasmid (Figure 4.7). Although not quantified and only performed once the data suggests a potential role for C536 in the formation of the HMW disulphide complex. There is also the intriguing possibility that the HMW band from cells expressing the Ubp12-3HA-C536S mutant protein actually has a slightly slower mobility than the HMW disulphide complex formed in cells containing the wild-type plasmid (see Figure 4.7). Indeed, work presented in Chapter 3 revealed new slower mobility HMW species of Ubp12 in certain thioredoxin system mutants (Figures 3.2, 3.7, 3.8, 3.9, 3.10 and 3.11). Furthermore, one of these bands appears to have a mobility slightly slower than the HMW disulphide complex (for example see Figure 3.2), and it is possible that this is the band observed in cells expressing Ubp12-3HA-C536S protein (compare Figures 3.2 and 4.7). However, this is difficult to validate based on the current data due to the proximity of the different HMW species on the various gels, together with the fact that the equivalent lanes expressing the HMW forms of Ubp12 were not placed next to each other when the gel in Figure 4.7 was ran.

Taken together, this data suggests that the C536S mutation of Ubp12-3HA does not have the same effect on the formation of HMW Ubp12 complexes as the Group 1 mutations. If the data is repeated in future experiments, it could possibly indicate a role for C536, perhaps in the context of a redox-active CXXC motif, in influencing the oxidation status of Ubp12 in response to H_2O_2 perhaps through intermediate oxidation steps and/or influencing the kinetics of formation of the HMW disulphide complex.

4.2.2.4 Analyses of the relationship of Group 1 and Group 2 cysteine residues to HMW forms of Ubp12 in trx1Δtrx2Δ cells

Previous work presented in this thesis revealed that several new HMW species of Ubp12, in addition to the HMW disulphide complex, can be detected in cells lacking the cytoplasmic thioredoxins, Trx1 and Trx2 (see Figure 3.2). For example, intermediate HMW oxidised forms of Ubp12-3HA were observed in *trx1*Δ*trx2*Δ cells (see Figures 3.2, 3.8, 3.9, 3.10). Hence, it was possible that the Group 1 and Group 2 mutations might affect the formation of these HMW forms of Ubp12-3HA in *trx1*Δ*trx2*Δ

cells. To explore this possibility the first step was to construct a *trx1*Δ*trx2*Δ strain that also lacked the *UBP12* gene following the same strategy detailed in Figure 3.5 but using Ubp12 specific primers. To construct a *trx1*Δ*trx2*Δ*ubp12*Δ strain, where the wild type *UBP12* gene was replaced with the *HIS3* selectable marker, a PCR product was generated using W303 *ubp12*Δ (KA7) genomic DNA as template and the ubp12ChkDelF and ubp12ChkTagR primers (Appendix C, conditions are detailed in section 2.3.1.1). The resulting 1600bp PCR product contained sequences located in the 5' and 3' regions of the *UBP12* gene flanking the *HIS3* selectable marker (Figure 4.8A). The PCR product was then purified from the gel and transformed into W303 *trx1*Δ*trx2*Δ (KD467) cells. His+ transformants were selected using minimal media plates and transformants analysed by PCR (using the same primers, ubp12ChkDelF and ubp12ChkTagR) to confirm the integration of the *HIS3* disruption cassette at the correct genomic locus and the construction of the *trx1*Δ*trx2*Δ*ubp12*Δ strain (KA119, Figure 4.8B).

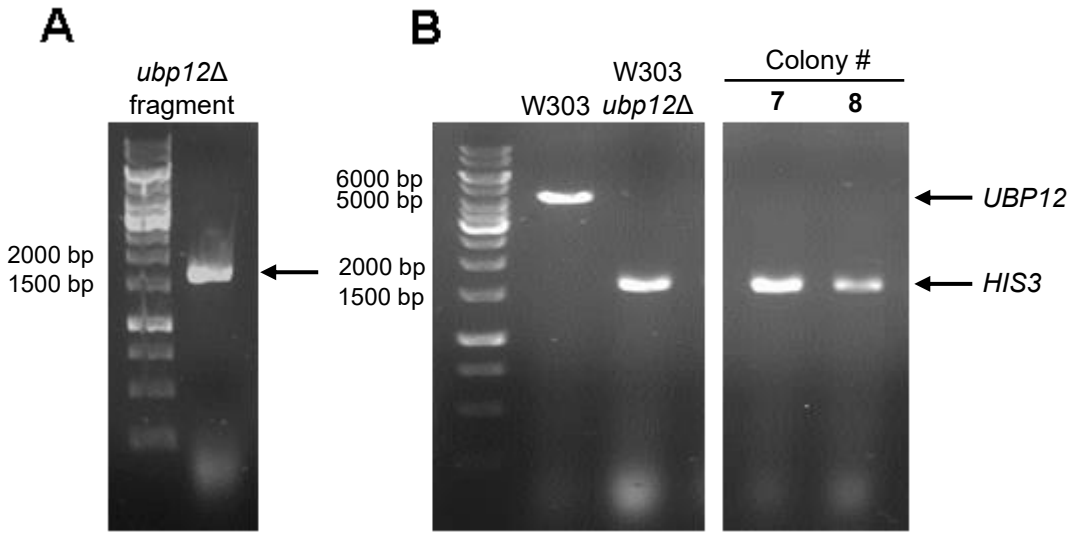

Figure 4.8. Successful construction of the *trx1*Δ*trx2*Δ*ubp12*Δ strain.

(A) Agarose gel analysis of the Phusion PCR reaction (see section 2.3.1.1) to generate the ~1600bp *UBP12* gene replacement cassette (arrow) using the ubp12ChkDelF and ubp12ChkTagR primers (Appendix C) and genomic DNA from the *ubp12*Δ strain (KA7) as template. (B) Agarose gel analysis of the DreamTaq PCR reactions (see section 2.3.1.2), using the ubp12ChkDelF and ubp12ChkTagR primers (Appendix C), of two His+ transformants (Colonies #7 and #8) of the *trx1*Δ*trx2*Δ strain (KD467) to check the replacement of *UBP12* with *HIS3*. As controls identical PCR reactions were performed on genomic DNA from the W303-1a (KA4) and *ubp12*Δ (KA7) strains. Expected products were 4500bp if the wild type *UBP12* gene is present and 1600bp if the *UBP12* gene was replaced with *HIS3* (*ubp12*Δ). GeneRuler 1 kb DNA Ladder (ThermoScientific) was used.

To investigate whether Group 1 and/or Group 2 mutations of Ubp12 influence the formation of HMW forms of Ubp12 in cells lacking Trx1 and Trx2 *trx1*Δ*trx2*Δ*ubp12*Δ (KA119) cells were transformed with the pRS426-Ubp12-3HA, pRS426-Ubp12-3HA-C373S, pRS426-Ubp12-3HA-Group1-C-S and pRS426-Ubp12-3HA-Group2-C-S plasmids. Transformants were then grown to mid-log phase in minimal media and exposed to 2 mM H_2O_2 for 0 or 10 minutes. Proteins were extracted and analysed by western blot under non-reducing conditions (Figure 4.9).

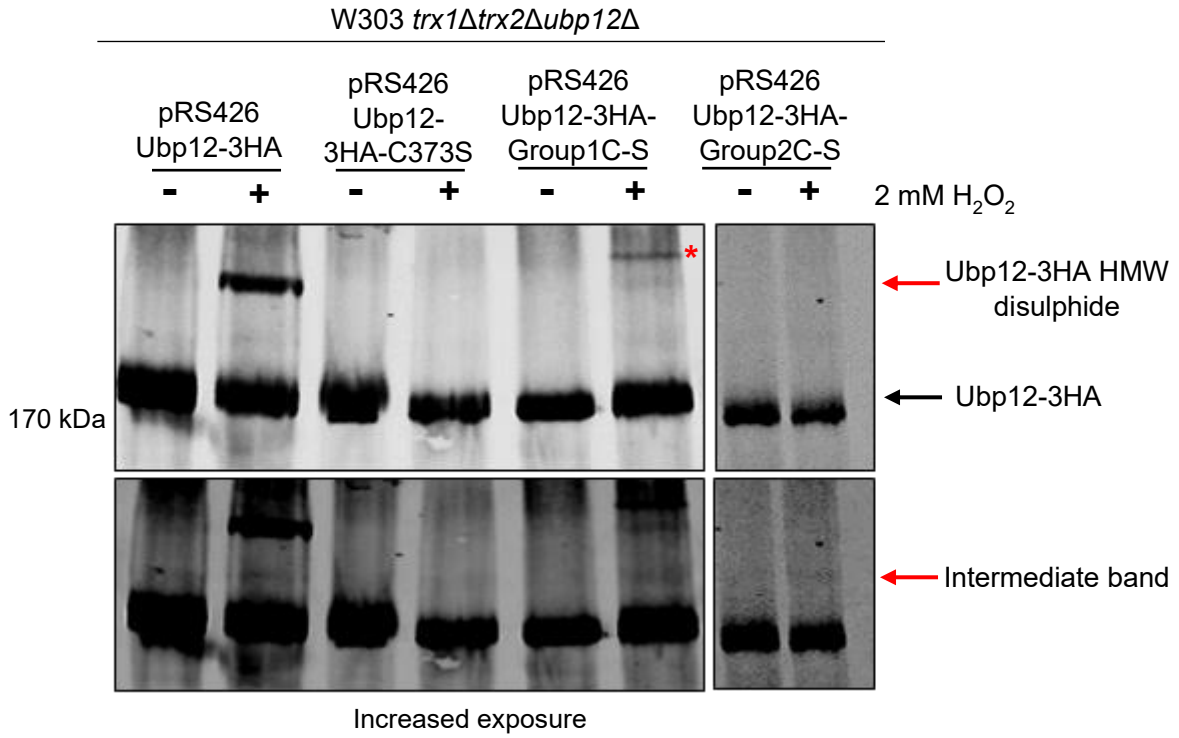

Figure 4.9. Cysteine mutations of Ubp12 influence the formation of HMW species in cells lacking Trx1 and Trx2.

Western blot analysis of protein extracts isolated from mid-log phase growing W303 *trx1*Δ*trx2*Δ*ubp12*Δ (KA119) cells, containing the indicated plasmids, in minimal media and treated with 2 mM H_2O_2 for 0 (-) or 10 (+) minutes. Protein extracts were prepared in non-reducing conditions, separated by SDS-PAGE and proteins were visualised using anti-HA antibodies. The red asterisk indicates another possible oxidised form of Ubp12. Increased exposures of the blots are displayed below. N=3. PageRuler Prestained Protein Ladder (ThermoScientific) was used.

As can be seen, treatment of *trx1*Δ*trx2*Δ*ubp12*Δ cells containing the wild-type pRS426-Ubp12-3HA plasmid resulted in the formation of the H_2O_2-induced HMW disulphide complex (Figure 4.9). In addition, although the intermediate HMW form of Ubp12 is detectable, and possibly other HMW species that have a mobility slower than the HMW disulphide complex present in wild type cells (for example see Figure 3.2), the signal strength of these forms of Ubp12 appears decreased compared to western blot analyses presented in Chapter 3 (for example see Figures 3.2, 3.8. 3.9, 3.10). As noted in section 3.3, there are significant differences in the experiment present here using *trx1*Δ*trx2*Δ*ubp12*Δ cells compared with those presented in Chapter 3. For example, rich YPD media was used for the experiments described in Chapter 3 whilst

minimal media was used for Figure 4.9. Minimal media lacks many components that are present in YPD which could affect results. In addition, the experiments in Figure 4.9 utilised multicopy vectors to express Ubp12 and it is possible that loss of Trx1 and Trx2 influences plasmid copy number and/or potentially Ubp12 oxidation status when Ubp12 expression is increased. Despite these differences in experimental protocol, it is interesting to note that a band with the mobility of the intermediate HMW species is observable, irrespective of the mutation status of any of the cysteine resides examined, suggesting that the cysteine mutations tested are not essential for the formation of this oxidation product (Figure 4.9). It is also interesting that a band corresponding to the mobility of the HMW disulphide species can be faintly detected in cells containing the pRS426-Ubp12-3HA-Group1-C-S plasmid but not the pRS426-Ubp12-3HA-Group2-C-S plasmid. This appears to contrast with the results observed in cells that contain Trx1 and Trx2 and pRS426-Ubp12-3HA-Group1-C-S, although it is possible that there may be a very faint band present in this experiment (Figure 4.6). With the caveat that these results may suggest that the Trx1 and Trx2 thioredoxin proteins inhibit formation of this HMW species in cells containing pRS426-Ubp12-3HA-Group1-C-S, the results suggest that the Group 1 cysteine residues are not essential for the formation of the HMW disulphide complex, at least in the absence of Trx1 and Trx2. However, at present it is unclear whether the faint band represents slower kinetics of formation of the HMW disulphide species and/or a reduced amount of Ubp12 that forms this complex.

Finally, the western blot analysis also revealed the presence of an even higher molecular weight form of Ubp12 in protein extracts from *trx1*Δ*trx2*Δ*ubp12*Δ cells containing the pRS426-Ubp12-3HA-Group1-C-S plasmid (Figure 4.9, red asterisk). This may be the same species potentially previously identified in cells containing pRS426-Ubp12-3HA-C536S (Figure 4.7) and/or observed in data presented in Chapter 3 (for example see Figures 3.2, 3.8. 3.9, 3.10). In Chapter 3 these HMW forms (red asterisks) were not detectable when the equivalent experiments were performed in cells containing Trx1 and Trx2 (Figure 3.2) suggesting a role for Trx1 and/or Trx2 in resolving these species. This is also consistent with the work presented in this Chapter where the HMW species formation (red asterisk) displayed by *trx1*Δ*trx2*Δ*ubp12*Δ cells containing the pRS426-Ubp12-3HA-Group1-C-S plasmid was inhibited in cells containing Trx1 and Trx2 (compare Figures 4.6 and 4.9). Together, these data suggest

a role for the thioredoxin system in reducing this HMW form of Ubp12, supporting the hypothesis that this is an oxidised form of Ubp12. In addition, this suggests that one or more of the Group 1 cysteines (perhaps just C536 based on the data in Figure 4.7), inhibit and/or resolve this HMW species in the absence of thioredoxin. Given the potential relationship identified previously about the formation of HMW species in the studies of the Group 1 and C536S mutation (Figures 4.6 and 4.7) it would be interesting in the future to gain further insight of this process of Ubp12 modification to test the effect of the individual C536S mutation on the formation of this HMW species in *trx1*Δ*trx2*Δ*ubp12*Δ cells.

In summary, data presented in this section has revealed that the formation of the HMW disulphide complex first identified in studies of wild type Ubp12 in response to H_2O_2 is dependent upon multiple conserved cysteine residues, including the catalytic cysteine residue, in Ubp12. Data also corroborates evidence presented in Chapter 3, suggesting that there are multiple forms of Ubp12 induced in response to H_2O_2, indicating that the oxidation of wild-type Ubp12 into a HMW disulphide complex may involve other intermediate forms of the protein. The results in this section also suggest that the formation of the intermediate HMW form described in Chapter 3 does not appear to be affected by any of the cysteine mutations analysed. Finally, the data further supports the hypothesis that Trx1 and/or Trx2 influence the formation of HMW species of Ubp12 in response to H_2O_2.

4.2.3 Analyses of the effects of the cysteine mutations on responses to oxidising agents

Work presented above revealed that Ubp12 is involved in the responses to the oxidising agents H_2O_2, diamide and menadione in both the BY4741 and W303 strain backgrounds (Figure 4.1). Given the effects of cysteine mutations of Ubp12 on the formation of HMW species of Ubp12 described above it was important to investigate whether these mutations also affect the response of cells to oxidative stress. Hence, BY4741 *ubp12*Δ (KA107) and W303 *ubp12*Δ (KA7) cells were transformed with either the pRS426 plasmid, the wild-type pRS426-Ubp12-3HA plasmid, the catalytic cysteine mutant pRS416-Ubp12-3HA-C373S plasmid, the Group 1 triple mutant pRS426-Ubp12-3HA-Group1-C-S plasmid or the Group 2 triple mutant pRS426-Ubp12-3HA-

Group2-C-S plasmid. Next serial dilutions of the transformants were spotted onto minimal media plates at 30°C containing the indicated concentrations of H_2O_2 (Figure 4.10, BY4741 strain background; Figure 4.11, W303 strain background).

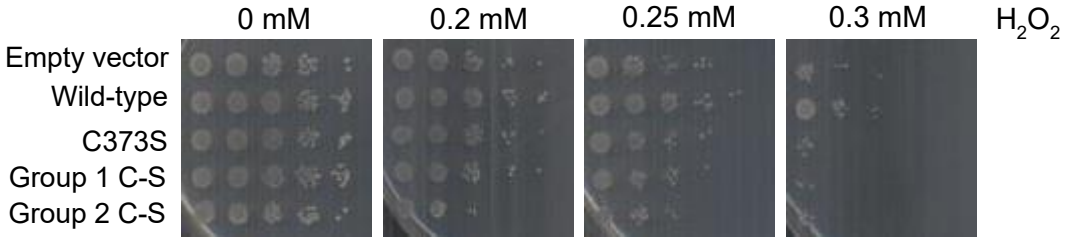

Figure 4.10. Cysteine mutations of Ubp12 affect responses of *ubp12*Δ BY4741 cells to H_2O_2.

5-fold serial dilutions of mid-log phase growing *ubp12*Δ BY4741 (KA107) cells containing either the pRS426 (empty vector), pRS426-Ubp12-3HA (wild-type), pRS426-Ubp12-3HA-C373S (C373S), pRS426-Ubp12-3HA-Group1-C-S (Group 1 C-S) or pRS426-Ubp12-3HA-Group2-C-S (Group 2 C-S) plasmid were spotted onto minimal media plates lacking uracil and containing H_2O_2 at the indicated concentrations. Plates were grown at 30°C for 2 days before imaging. Representative image of n=3.

Previous results presented above revealed that cells lacking Ubp12 in either the BY4741 or the W303 strain backgrounds are more sensitive to H_2O_2 than cells expressing Ubp12 from the genomic locus (Figure 4.1). Consistent with these observations when pRS426-Ubp12-3HA expressing the epitope-tagged wild type Ubp12 protein is introduced into *ubp12*Δ cells in the BY4741 strain background then this H_2O_2 sensitivity is reversed (Figure 4.10). Consistent with this result *ubp12*Δ cells in the BY4741 strain background containing pRS426-Ubp12-3HA-C373S, which expresses the catalytic cysteine mutant version of Ubp12, displays similar H_2O_2 sensitivity to the cells containing the empty vector (Figure 4.10). This suggests that the catalytic activity of Ubp12 is required for H_2O_2 resistance. Interestingly, *ubp12*Δ (BY4741) cells containing either pRS426-Ubp12-3HA-Group1-C-S or pRS426-Ubp12-3HA-Group2-C-S, similar to cells containing pRS426-Ubp12-3HA-C373S, also displayed increased sensitivity to H_2O_2 compared to the cells containing pRS426-Ubp12-3HA (Figure 4.10). There is also a small increase in sensitivity to H_2O_2 in cells containing pRS426-Ubp12-3HA-Group2-C-S versus the cells containing the empty

vector (Figure 4.10). Although this result has been reproduced in n=3 number of experiments it is possible that there is some variation, for example due to plasmid copy number. It is interesting that the Group 1 and Group 2 mutations do not reverse the sensitivity of *ubp12*Δ (BY4741) cells to H_2O_2. Although further experimentation is required to gain more insight into these results it is tempting to propose that this inability to restore H_2O_2 resistance is due to defects in catalytic activity of Ubp12 and/or the ability to form HMW disulphide complexes in response to H_2O_2.

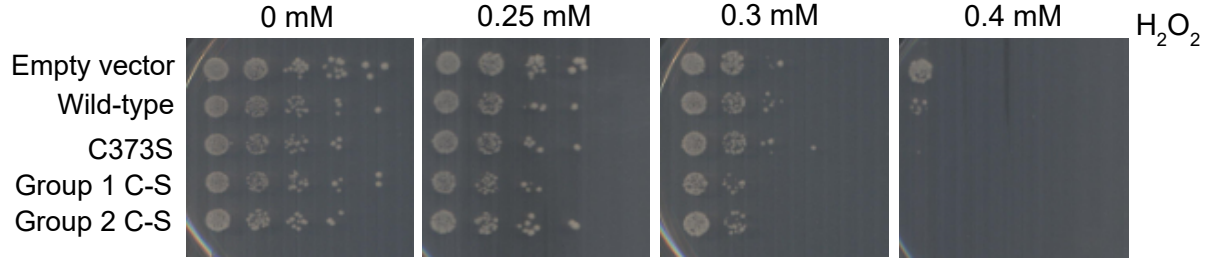

Figure 4.11. Cysteine mutations of Ubp12 affect responses of *ubp12*Δ W303 cells to H_2O_2.

5-fold serial dilutions of mid log phase growing *ubp12*Δ W303 (KA7) cells containing either the pRS426 (empty vector), pRS426-Ubp12-3HA (wild-type), pRS426-Ubp12-3HA-C373S (C373S), pRS426-Ubp12-3HA-Group1-C-S (Group 1 C-S) or pRS426-Ubp12-3HA-Group2-C-S (Group 2 C-S) plasmid were spotted onto minimal media plates lacking uracil and containing H_2O_2 at the indicated concentrations. Plates were grown at 30°C for 2 days before imaging. Representative image of n=3.

In striking contrast to the results obtained using *ubp12*Δ (BY4741) cells, pRS426-Ubp12-3HA did not reverse the sensitivity of *ubp12*Δ W303 cells to H_2O_2 (compare Figures 4.10 and 4.11). In fact, it had the opposite affect and made the cells even more sensitive to H_2O_2 (Figure 4.11). The explanation for these different affects in different strain backgrounds is unclear but suggests that Ubp12 has different roles in these strains. Another apparent difference between results in the *ubp12*Δ BY4741 cells and those in *ubp12*Δ W303 cells is that *ubp12*Δ W303 cells containing either pRS426-Ubp12-3HA-C373S, pRS426-Ubp12-3HA-Group1-C-S or pRS426-Ubp12-3HA-Group2-C-S appear to also be more sensitive to H_2O_2 than cells containing the empty vector (Figure 4.11). Given the results obtained in the BY4741 strain background (Figure 4.10) the results obtained in the W303 strain background were unexpected.

However, these differences suggest that perhaps Ubp12 has different functions and potentially different regulation in different strain backgrounds. Indeed, based on these observations it would be interesting to investigate the oxidation of Ubp12 in *trx1*Δ*trx2*Δ cells in BY4741 strain background.

4.2.4 Growth analyses of cells expressing mutant versions of Ubp12

Although there were no obvious differences in the growth of *ubp12*Δ cells containing the various plasmids on the 0 mM plate in Figure 4.10 it was possible that altered growth rates associated with the different plasmids was influencing the results of the H_2O_2 sensitivity spot tests. Hence, growth curves were obtained for *ubp12*Δ BY4741 (KA7) cells containing either pRS426, pRS426-Ubp12-3HA, pRS416-Ubp12-3HA-C373S, pRS426-Ubp12-3HA-Group1-C-S or pRS426-Ubp12-3HA-Group2-C-S. Overnight cultures of BY4741 *ubp12*Δ cells containing these plasmids were diluted to an OD_{660} of 0.2 and then growth monitored over an 8-hour period (Figure 4.12).

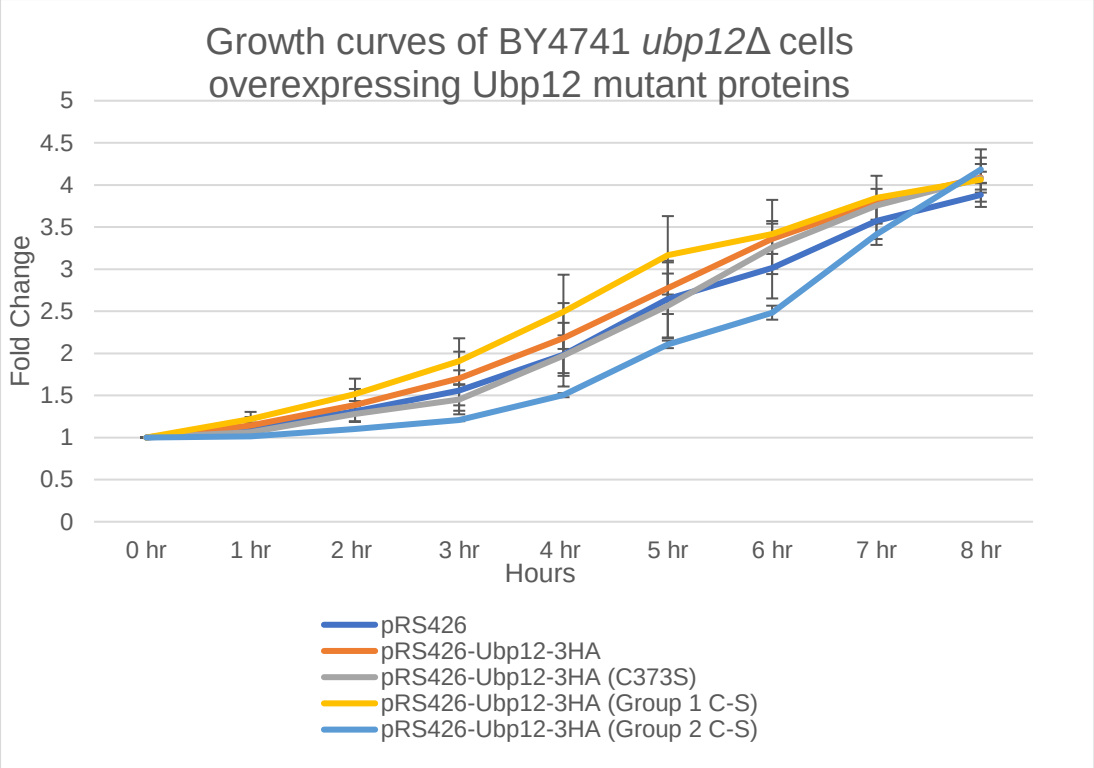

Figure 4.12. Growth curves of BY4741 *ubp12*Δ cells overexpressing different Ubp12 mutant proteins.

Overnight cultures of BY4741 *ubp12*Δ (KA7) cells containing the indicated plasmids in minimal media lacking uracil were diluted to an OD_{660} of 0.2 in the same media and then growth monitored over an 8-hour period. The OD_{660} of each culture was measured hourly and converted into fold growth relative to the 0 hours value which was set at 1. Error bars denote standard error of the mean. N = 3.

Based on the growth curves displayed in Figure 4.12, the doubling times of BY4741 *ubp12*Δ cells containing each plasmid were calculated (Figure 4.13, Table 4.1). Although there is some variation in doubling time and growth rates, there was no significant difference in the doubling times of each strain. Hence, differences in growth rate are unlikely to explain the spot test phenotypes observed in Figure 4.10. Conclusively, this section has clarified that the growth rates of BY4741 *ubp12*Δ cells over-expressing wild-type Ubp12-3HA and the various cysteine mutants are not significantly different during mid-log growth.

Plasmid expressed	Average doubling time (mins)
pRS426	**192 (+/- 22)**
pRS426-Ubp12-3HA	**184 (+/- 35)**
pRS426-Ubp12-3HA-C373S	**172 (+/- 10)**
pRS426-Ubp12-3HA-Group1C-S	**196 (+/- 21)**
pRS426-Ubp12-3HA-Group2C-S	**192 (+/-15)**

Table 4.1. Average doubling times calculated for BY4741 *ubp12Δ* cells (KA7) expressing pRS426, pRS426-Ubp12-3HA, pRS426-Ubp12-3HA-C373S, pRS426-Ubp12-3HA-Group1C-S or pRS426-Ubp12-3HA-Group2C-S plasmids (Figure 4.12). N=3.

4.3 Discussion

Previous work in the lab and work described in Chapter 3 revealed that Ubp12 forms several HMW species in response to H_2O_2 and when specific proteins in the thioredoxin system are deleted from cells. Furthermore, at least some of these HMW species have been shown to involve oxidation of Ubp12 and that the catalytic cysteine residue is essential for the H_2O_2 induced formation of the predominant HMW disulphide complex observed in wild-type cells (see Figure 3.11) (Curtis, 2019). However, the potential roles of other cysteine residues in the formation of this complex and other detected HMW species described in this thesis had not been investigated. To gain more insight into the potential roles of other cysteines in Ubp12 in the formation of HMW species the work described in this chapter focused on studies of mutations of Ubp12 with a specific focus on several cysteine residues that are conserved in the homologues of Ubp12 in closely and distantly related yeast and in humans. Significantly, the results revealed that Ubp12 is linked with oxidative stress responses in different strain backgrounds of *S. cerevisiae*, cells lacking Ubp12 display increased sensitivity to H_2O_2 and menadione (superoxide generator) and increased resistance to diamide. Furthermore, the data revealed that conserved cysteine residues in Ubp12, including the catalytic cysteine C373, influence the H_2O_2-induced formation of the HMW disulphide species originally identified in wild-type Ubp12 and other newly identified HMW forms of the DUB. The data further supports the idea that the thioredoxin system regulates Ubp12. Phenotype analyses suggests that the mutation

of Group 1 and Group 2 potentially affect the catalytic activity/disulphide and this affects sensitivity to H_2O_2 and also reveal again strain specific roles of these cysteines. Finally, overexpression of the triple mutants and the catalytic cysteine mutant do not significantly affect the doubling time of BY4741 *ubp12*Δ cells, hence it is unlikely that growth rates explain the phenotypic differences of overexpressing these cysteine mutant plasmids.

This chapter has revealed some interesting points regarding the role of Ubp12 in ROS responses. Firstly, in both strain backgrounds analysed (BY4741 and W303), responses to the three oxidising agents examined are conserved (Figure 4.1). These two strain backgrounds have different ROS-response mechanisms with the activation of Yap1 (either via Ybp1 and Gpx3 in BY4741 or Tsa1 in W303, discussed in detail in section 1.2.3.3) and hence it was possible that ROS responses in cells lacking Ubp12 might be different. Deletion of *UBP12* resulted in increased sensitivity when cells are exposed to H_2O_2 or the superoxide generator menadione, and increased resistance when exposed to diamide. This implies that Ubp12 fulfils different roles in response to H_2O-$_2$, menadione- and diamide-induced stress. The basis of these differences in functions to different oxidising agents is unknown but is presumably linked to the substrates of Ubp12 which are likely to be conserved in the BY4741 and W303 strain backgrounds. However, differences in the potential relationships between Ubp12 and the adaptive response to low levels of H_2O_2 were apparent in the BY4741 and W303 strain backgrounds. Interestingly, pre-exposure of *ubp12*Δ cells to low levels of H_2O_2 conferred resistance to high levels of H_2O_2 in the BY4741 strain background, but not in the W303 strain background (Figure 4.2). The reason for this is not currently clear, but it could be linked to the differences in H_2O_2 signalling between these two strains. In the activation of Yap1 in response to H_2O_2, BY4741 cells use Gpx3 and Ybp1 to transduce oxidation to Yap, however W303 cells which do not have a functional copy of Ybp1 use Tsa1 (Ross et al., 2000, Delaunay et al., 2002, Veal et al., 2003). Given that Ubp12 is regulated by the thioredoxin system (Chapter 3), it is possible the involvement of Gpx3 and Ybp1 in BY4741, or only Tsa1 in W303, in Yap1 activation causes this difference in their adaptive response to H_2O_2. Chapter 3 only explored the role of the thioredoxin system in Ubp12 regulation in the W303 strain background, thus it is possible that the thioredoxin system may regulate Ubp12 differently in BY4741 cells. Therefore, to fully explore this speculation analysis of thioredoxin system

pathway mutants in BY4741 cells, as performed for W303 cells in Chapter 3, would be useful.

This chapter has also shed light on the formation of Ubp12 HMW complexes. *S. cerevisiae* Ubp12 contains 19 cysteine residues, 7 of which are conserved in *S. pombe, C. albicans* and *H. sapiens* (Figure 4.3). Previous work from our lab identified that the catalytic cysteine, C373, was necessary for the formation of the Ubp12 HMW disulphide, and found that the HMW disulphide was likely an intramolecular disulphide (Curtis, 2019). As the catalytic cysteine residue is involved in this disulphide, it was proposed that the HMW disulphide is formed to inactivate Ubp12 function in response to oxidative stress. Given that Ubp12 in *C. albicans* also forms an oxidised HMW complex(es) in response to H_2O_2 (Figure 5.7), it was hypothesized that conserved cysteine residues may be important in the generation of Ubp12 HMW species. The successful generation of the triple cysteine mutants allowed for assessment of their role in the formation of the HMW disulphide. Western blot analysis (Figure 4.6) suggested at least one cysteine residue from Group 1 (C519S, C536S and C539S) and one cysteine residue from Group 2 (C967S, C985S and C988S) were necessary to form the HMW disulphide. However, later analysis did reveal a small proportion of a band with comparable mobility to that of the Ubp12 disulphide in *trx1*Δ*trx2*Δ*ubp12*Δ cells expressing the Group 1 mutant (Figure 4.9), which is possibly observable in Figure 4.6. Therefore, it is likely that the Group 1 cysteine residues are not essential for the formation of the Ubp12 HMW disulphide. It is interesting to note the relative amount of Ubp12 that is oxidised in *trx1*Δ*trx2*Δ*ubp12*Δ cells expressing the Group 1 mutant is much less compared to cells expressing the wild-type plasmid, suggesting that perhaps the mutation of the Group 1 cysteines decreases the ability and/or kinetics of the formation of the Ubp12 disulphide complex (Figure 4.9). In addition, a HMW species was observed in the single C536S mutant of a similar mobility to the Ubp12 HMW disulphide (Figure 5.7). If validated as the Ubp12 disulphide complex, this suggests that C536 is not involved in its formation. Cysteine mutant plasmids were also used to assess the intermediate mobility band observed in *trx1*Δ*trx2*Δ cells in Chapter 3 of this thesis (Figure 3.2, 3.8, 3.9, 3.10). Interestingly, the intermediate band is observable in cell extracts using all of the cysteine mutant plasmids, indicating they are not essential for its formation (Figure 4.9). It is important to note that mutation of these cysteine residues may actually affect the formation of structural disulphides, and

hence disrupting these disulphides may affect the proximity of residues to the active site cysteine, thus affecting pKa. It is also possible that cysteines not examined in this thesis are important for this oxidation event, hence further experimentation is necessary. A final technical point to consider is expressing Ubp12 and mutant versions of Ubp12 from a high-copy plasmid instead of its native locus. Mutational analysis of Ubp12 presented in this chapter has utilised the high-copy plasmid pRS426, hence the levels of Ubp12 and mutant versions will be significantly increased compared to expression from its native locus. This makes interpretation of data challenging, particularly with protein oxidation, where the ratio of thioredoxins and thioredoxin substrates (such as Ubp12) is important. Expression of tagged Ubp12 and tagged mutant versions of Ubp12 on the chromosome from their native loci would address whether use of high-copy plasmids in this work has affected the results presented here.

Interestingly, the data presented in this chapter also revealed that there is another form of Ubp12 formed in response to H_2O_2 in cells expressing the Group 1 mutant plasmid and possibly the C536S plasmid (Figures 4.7 and 4.9). This has also potentially been observed in experiments presented in Chapter 3 in the *trx1*Δ*trx2*Δ strain (Figures 3.2, 3.8, 3.9, 3.10) and *trr1*Δ strain (Figure 3.11). The presence of potentially another form of Ubp12 in the Group 1 mutant indicates that one of these cysteines, possibly C536, is essential for resolving this species. If this unidentified form of Ubp12 is confirmed as a disulphide, it is possible that the decreased abundance of the HMW Ubp12 disulphide in the Group 1 mutant (Figure 4.9) is because this slower mobility disulphide cannot be reduced, hence much less Ubp12 is oxidised into the HMW disulphide in this mutant. This could therefore suggest that Ubp12 does not form a single disulphide utilising two cysteine residues as previously hypothesized. It is possible that Ubp12 forms various disulphides that are resolved before the final HMW disulphide is formed. In current literature, disulphide bond shuffling has been observed in response to various stresses, one of which is oxidative stress (Coghlan et al., 2022). This therefore suggests that cells exposed to high levels of ROS, such as H_2O_2, could trigger disulphide shuffling within the protein and hence there are various cysteines involved in the formation of the final HMW disulphide. It is important to assess the structure of Ubp12 and the positions of the mutated cysteine residues within the protein, and thus PyMOL was used to generate Figure 4.13 below.

The average length of a disulphide bond is 2.05 Å, however the distance between the CXXC motifs and the catalytic triad is approximately 40 Å. Additionally, C519 and C967 are too far away to allow disulphide formation. This suggests that the catalytic cysteine could not directly interact with the triple mutant cysteines to form a disulphide bond whilst the protein exists in this structure. However, it is important to note that the structure presented in Figure 4.13 is only a predicted structure, and that the protein likely undergoes considerable conformational change upon oxidation, indicated by the large change in migration of the protein upon HMW disulphide formation. Nevertheless, Figure 4.13 does suggest that the initial disulphide formed is not between the catalytic cysteine residue and any residue in the triple mutants. It is however possible that conformational changes within the protein upon oxidation could allow disulphide bond formation between cysteine residues that cannot interact in the reduced state. It is also possible that any of the other cysteine residues that have not been investigated as part of this thesis are involved in the disulphide shuffling, allowing movement of the disulphide throughout the protein. For example, Figure 4.13 suggests that C381, a conserved cysteine residue not investigated in this work, is situated closely to the catalytic cysteine residue and therefore may be involved in forming a disulphide with the catalytic cysteine. In contrast, Figure 4.13 indicates that C917, the other conserved cysteine not examined here, is not proximal enough to any other conserved cysteine residue to allow disulphide formation. However, as previously mentioned, structural changes within the protein upon oxidation may result in disulphide formation that could not occur whilst Ubp12 is in its reduced state. Thus, further mutational analysis examining C381 and C917 in Ubp12 oxidation would be necessary to clarify their roles in disulphide shuffling.

A

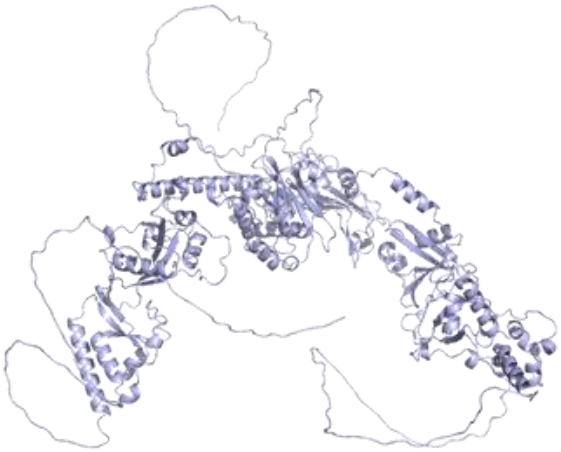

B

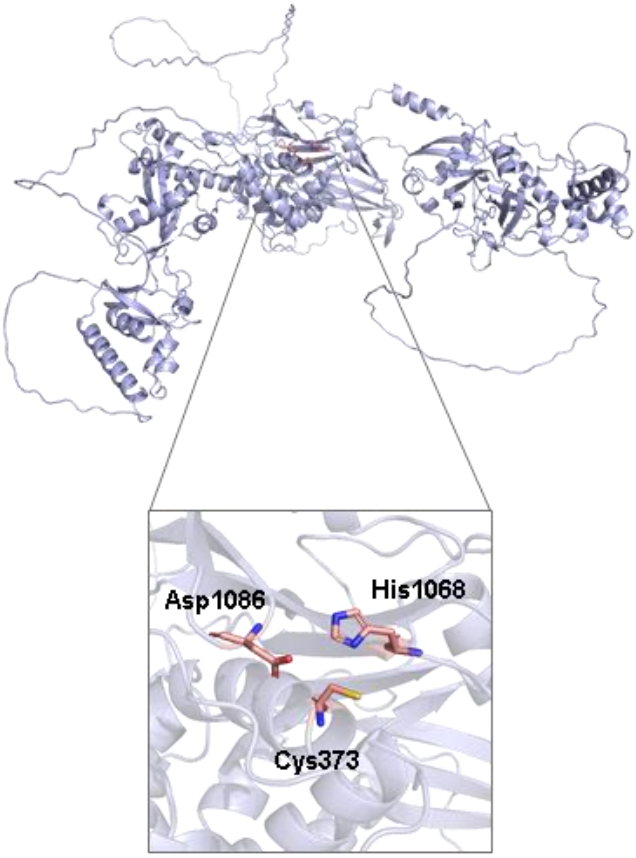

C

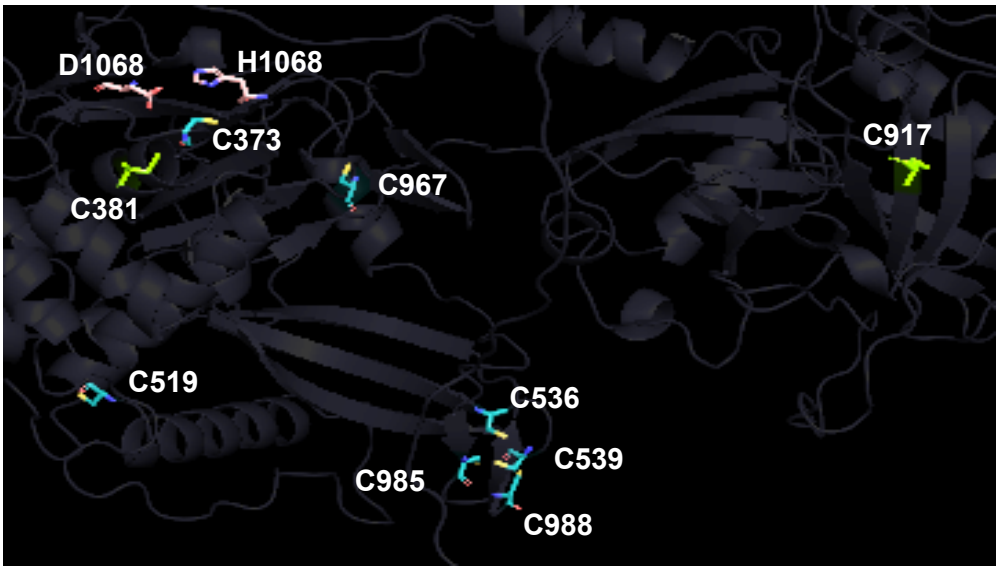

D

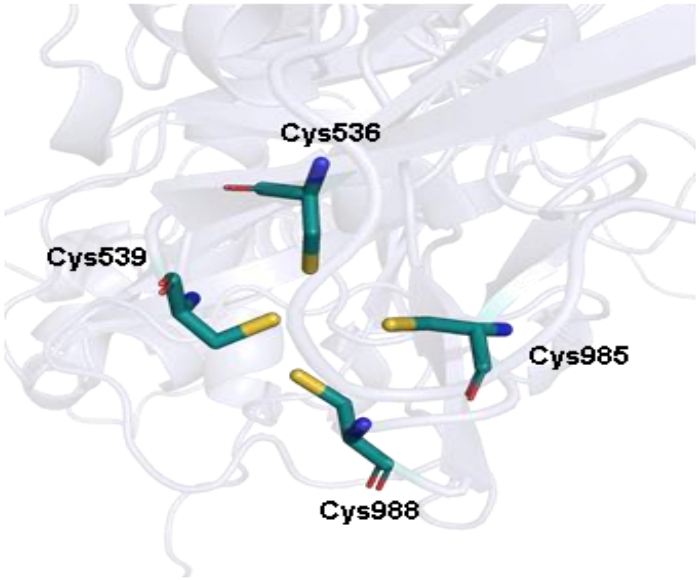

Figure 4.13. The tertiary structure, catalytic triad and conserved cysteine residues of Ubp12.

Cartoon ribbon representations of Ubp12 created using The PyMOL Molecular Graphics System (Schrödinger, 2015). Key catalytic residues (C373, H1068, D1086) and mutated cysteine residues (C519, 536, 539, 967, 985, 988) are presented as stick representations. (A) The general tertiary structure of Ubp12. (B) The position of the catalytic triad within Ubp12. (C) The positions of the eight conserved cysteine residues and one non-conserved (C519) relative to the position of the catalytic triad. Cysteines mutated in the triple mutants (C519, C536, C539, C967, C985, C988) are shown in teal and the two residues not selected for mutation (C381 and C917) are shown in green. (D) The two CXXC motifs included in the triple mutants.

Following this data, the original model hypothesising that the HMW disulphide inactivates Ubp12 by oxidising the catalytic cysteine, cannot be verified, as the catalytic cysteine could be involved in formation of an intermediate disulphide. However, inactivating protein function via oxidation of the catalytic cysteine residue is a commonly used mechanism. Indeed, some mammalian DUBs are inactivated at their catalytic cysteine residue via oxidation, such as USP1 and USP7 (Cotto-Rios et al., 2012). Additionally, in *S. cerevisiae*, various members of the ubiquitin and SUMO pathways are inhibited by oxidation at their catalytic cysteine residue, such as the E1-activating enzyme Uba1 and the E2-conjugating enzyme Cdc34 (discussed in detail in section 1.3.2) (Doris et al., 2012). SENPs, the desumoylase machinery in *S. cerevisiae* can also be inhibited at their catalytic cysteine residue by oxidation (Xu et al., 2008). Thus, it is reasonable to suggest that the catalytic cysteine residue is involved in the formation of the final HMW disulphide with another cysteine residue, and that potentially Group 1 and Group 2 cysteine residues are involved in the formation of intermediate disulphides. Given the increased sensitivity phenotype of *ubp12*Δ cells when exposed to H_2O_2, it is possible that inactivation of Ubp12 would prevent any irreversible oxidation of Ubp12, thus allowing for Ubp12 availability to aid cell recovery when ROS has been removed. Therefore, an alternative model is that the temporary inactivation of Ubp12 at the catalytic cysteine residue functions as a protective mechanism rather than an inhibitory one.

It is possible that the CXXC motifs mutated in the Group 1 and Group 2 mutations fulfil other roles, thus affecting the ability of Ubp12 to form the HMW disulphide in these mutant strains. The conserved C536 and C539, and C985 and C988 form CXXC motifs, a motif linked to redox action within thioredoxin and related proteins (Figure 4.3) (Chivers et al., 1997). The non-cysteine residues in the CXXC motif vary between proteins and alter the redox potential of the protein. For example, mutation of the XX residues in DsbA, a strong oxidant found in *E. coli,* to either the Pro-Tyr or Gly-Pro XX residues of *E. coli* glutaredoxin and thioredoxin respectively, significantly reduced its oxidising ability (Huber-Wunderlich and Glockshuber, 1998). Interestingly, the CXXC motifs of Ubp12 in *S. cerevisiae, C. albicans, S. pombe* and human cells contain a proline at the first X position (CPXC). DsbA also contains a proline at this position, hence the CPXC motif of Ubp12 could suggest a redox role for this motif (Huber-

Wunderlich and Glockshuber, 1998). Given that the triple mutants affect the formation of the HMW disulphide, perhaps the redox potential of the CPXC motifs is involved in the formation of various oxidised forms of Ubp12, such as the species' identified in the single C536S mutant and the Group 1 triple mutant (Figures 4.7 and 4.9). Indeed, research has found that CXXC motifs can function as disulphide isomerases (Quan et al., 2007). However, CXXC motifs are also known to function as a zinc finger motif (Frauer et al., 2011). Although to date no DUBs in *S. cerevisiae* have been shown to bind zinc ions, the human homologue of Ubp12 (USP15) has a known zinc finger domain, that when mutated, can no longer deubiquitinate substrates (Hetfeld et al., 2005). Interestingly, the four conserved cysteine residues of the two CPXC motifs of USP15 are predicted to be essential for zinc binding (Hetfeld et al., 2005). It is therefore possible that mutation of these cysteine residues could prevent zinc binding which alters the oxidation state of Ubp12. Metal content analysis such as ICP-MS could clarify if there is any zinc binding in Ubp12. If so, it would be interesting to analyse if zinc binding is disrupted in the various cysteine mutants and the thioredoxin system mutants, *trx1*Δ*trx2*Δ and *trr1*Δ.

Interestingly, the cysteine mutants did affect cell growth in response to H_2O_2 differently between the BY4741 and W303 strain backgrounds (Figures 4.10 and 4.11). Firstly, over-expressing wild-type Ubp12 caused a resistance to H_2O_2 in the BY4741 background, however this was not conserved in W303. This fits with the data presented in Figure 4.1, which shows loss of Ubp12 causes a sensitivity of cells in response to H_2O_2. Together, this data suggests that Ubp12 is an important protein in cellular responses to H_2O_2 in BY4741 cells. It is interesting that overexpression of Ubp12 in W303 cells did not cause resistance to H_2O_2, given that in both BY4741 and W303 strain backgrounds *ubp12*Δ cells were sensitive to H_2O_2 (Figures 4.1 and 4.11). This could suggest that Ubp12 has different roles in these strain backgrounds in response to H_2O_2. In BY4741 cells, Ubp12 may generally aid cell responses to H_2O_2, with deletion of Ubp12 conferring sensitivity and overexpression causing resistance (Figures 4.1 and 4.10). However, in W303 cells, the level of Ubp12 in cells may be important in cellular responses to H_2O_2, whereby it has important roles in the oxidative stress response (hence sensitivity of *ubp12*Δ cells, Figure 4.1), but an increased amount of Ubp12 may have detrimental effects (Figure 4.11). This could suggest differences in substrates of Ubp12 between these two strains, or that Ubp12 is

regulated differently in these two strains, as seen with Yap1 (Ross et al., 2000, Delaunay et al., 2002). BY4741 cells expressing the various cysteine mutants (C373S, Group1C-S, Group2C-2) were more sensitive to H_2O_2 than cells overexpressing wild-type Ubp12, growing comparably to the empty vector control (Figure 4.10). It is therefore tempting to speculate that these cysteine residues are important for cellular responses to H_2O_2, either through catalysis, the formation of the HMW disulphide complex, or both. Interestingly, BY4741 cells expressing the Group 2 cysteine mutant plasmid were more sensitive to H_2O_2 than the Group 1 mutant and the C373S mutant, suggesting a possible additional role for these cysteine residues in the protein. Importantly, the doubling times of BY4741 cells expressing the various cysteine mutant plasmids were not significantly different to wild-type or empty vector (Figure 4.12), suggesting that growth rates of these cells are not responsible for the phenotypes observed in response to H_2O_2. W303 cells overexpressing the cysteine mutant plasmids were slightly more sensitive to H_2O_2 than cells expressing the empty vector, growing comparably to cells overexpressing wild-type Ubp12 (Figure 4.11). Thus, the role of these cysteine residues in catalysis and/or the formation of the HMW disulphide complex does not seem to affect cell responses to H_2O_2. This result was unexpected; however, it does further suggest different roles and/or regulation of Ubp12 in W303 compared to BY4741. However, no growth curve analysis for W303 cells expressing these plasmids was performed, hence growth rates may explain these phenotypes. In addition to this, DUBs display a lot of redundancy and so it is possible that any role normally performed by Ubp12 is being at least partially fulfilled by another DUB in cells expressing these mutants (Rossio et al., 2021). This makes elucidating the specific roles of DUBs particularly challenging. It is also important to note that the copy number of *UBP12* may vary in these two experiments (Karim et al., 2013), and hence could affect results. Repetition of these experiments using a CEN, single copy plasmid could address these issues. Additionally, growth curve analysis and survival assays of both BY4741 and W303 cells expressing these plasmids may provide a more accurate way to assess the roles of specific cysteines and Ubp12 in cell responses to H_2O_2. These assays would also allow quantification and significance testing which is challenging with spot test assays.

The apparent difference in Ubp12 function in BY4741 and W303 cells highlights the importance for identification of Ubp12 substrates, which may differ between the two.

Of the known Ubp12 substrates in *S. cerevisiae*, some have been identified in both BY4741 and W303 strain backgrounds (PCNA, Fzo1) (Álvarez et al., 2019, Anton et al., 2013), however some have only been validated in BY4741 cells (Rad23, Gpa1) (Gödderz et al., 2017, Wang et al., 2005). Thus, it would be interesting analyse the ubiquitination of Rad23 and Gpa1 in *ubp12*Δ W303 cells. Considering the substrates of Ubp12 (and validating new ones) is interesting when considering the data presented in this chapter. The current hypothesis about how Ubp12 is regulated via H_2O_2 is that the formation of the HMW disulphide is a concentration-dependent mechanism, cycling through multiple disulphides utilising various cysteine residues before settling in the final HMW complex. This allows for inactivation of the protein (due to involvement of the catalytic cysteine residue) to either protect it from irreversible oxidation, inhibit its activity, or both. Ubp12 is then presumably able to fulfil its regular functions when the H_2O_2 concentration has returned to homeostatic levels. Ubp12 regulation of known substrates regulates diverse cellular processes; Fzo1 regulates mitochondrial morphology (Anton et al., 2013), PCNA regulates DNA repair and maintenance (Álvarez et al., 2019), Gpa1 regulates pheromone responses, endosomal regulation and DNA replication stress (Wang et al., 2005) and Rad23 regulates DNA damage responses and glycosylation events (Gödderz et al., 2017). The specific role of Ubp12 in regulating these substrates is discussed in detail in section 1.3.4.1. In addition, one paper found that overexpression of *UBP12* significantly increased the mutation rate of DNA and hence Ubp12 has a role in maintaining genome stability (Ang et al., 2016). It is interesting to note the relevance of oxidative stress in many of these processes, specifically, mitochondrial dynamics, DNA damage, and genome stability (Ježek et al., 2018, Auten and Davis, 2009). Further work analysing the ubiquitination of Ubp12 substrates in a mutant strain that cannot form the Ubp12 HMW disulphide could reveal the relevance of Ubp12 oxidation in these processes. Despite the identification of some Ubp12 substrates in *S. cerevisiae*, the identification and validation of further Ubp12 substrates is important for fully understanding the role of this DUB in ROS responses.

Conclusively, this chapter has revealed interesting information regarding the role and regulation of Ubp12 in *S. cerevisiae*. Firstly, Ubp12 is an important protein in both BY4741 and W303 strain backgrounds for ROS responses, however evidence suggests that the specific role(s) of the DUB may differ between strains. Secondly, it

is suggested that Ubp12 forms multiple disulphides that involve various cysteine residues in response to H_2O_2. The catalytic cysteine and at least one residue from each of the triple mutants are important for formation of the HMW disulphide, either through forming it directly (likely with the catalytic cysteine) or via disulphide shuffling throughout the protein (triple mutant residues). This data could have important implications for various cellular processes Ubp12 is known to regulate or be involved with, and opens up various lines of potential investigation into the high-interest human homologue, USP15. Hence, the next step was to explore the conservation of Ubp12 in a closely related yeast species, *C. albicans,* which is medically relevant for human health.

Chapter Five: Ubp12 is involved in responses to oxidative stress in the pathogenic yeast *Candida albicans*

5.1 Introduction

The work described in Chapters 3 and 4 revealed that Ubp12 in *S. cerevisiae* is involved with responses to oxidative stress. However, although homologues of Ubp12 are present in other organisms, including *S. pombe, C. albicans* and in human cells, the relationships between these homologues and responses to oxidative stress and ROS have not been previously explored. Hence, to begin studies to explore the conservation of the functions and regulation of homologues of Ubp12 in eukaryotes we decided to focus initial research on the Ubp12 homologue, also named Ubp12 (with 34% sequence identity), in the closely related yeast *C. albicans* (Figure 5.1). This yeast was chosen because we reasoned that if the functions and/or regulation of Ubp12 are not conserved in this closely related organism then it might be more likely that Ubp12 actually plays different roles in different eukaryotes. Furthermore, many of the key cysteine residues identified in Ubp12 in *S. cerevisiae* (see Figure 4.3), including the catalytic cysteine residue and the two CXXC motifs, are conserved in Ubp12 in *C. albicans* (Figure 5.1), suggesting that Ubp12 in *C. albicans* may also be regulated by ROS. *C. albicans* is an opportunistic pathogen that exists commensally in humans but it can transition into a pathogenic fungus under certain conditions, such as high pH, the presence of serum and physiological temperature (37°C) (Mayer et al., 2013). Significantly, the cellular responses of *C. albicans* to oxidative stress is important for this pathogen to evade immune responses. Indeed, upon detection of *C. albicans*, innate immune cells produce ROS (specifically H_2O_2 and superoxide) as a fungicidal mechanism (Murphy, 1991), which triggers a variety of responses from *C. albicans* cells, including induction of antioxidant gene expression and also morphological changes to evade phagocytosis (Dantas et al., 2015, Nasution et al., 2008). Furthermore, H_2O_2 has specifically been shown to induce the formation of hyper-polarised buds, a distinct form of *C. albicans*, to evade host immune responses (da Silva Dantas et al., 2010). Hence, given the importance of studies of this fungal pathogen and role of ROS, particularly H_2O_2, in virulence, new insight into ROS responses potentially involving the Ubp12 DUB has the potential to open up new avenues of research to understand the pathogenesis of *C. albicans*. Indeed, *UBP12*

was identified as one gene of 23 genes where polymorphisms arise in particularly virulent strains collected from patient samples (Zhang et al., 2009). Although not studied further, this suggests that Ubp12 activity is linked to the pathogenicity of *C. albicans*. Therefore, the main aim of this chapter was to investigate the potential function and/or regulation of Ubp12 in *C. albicans* in response to ROS.

A

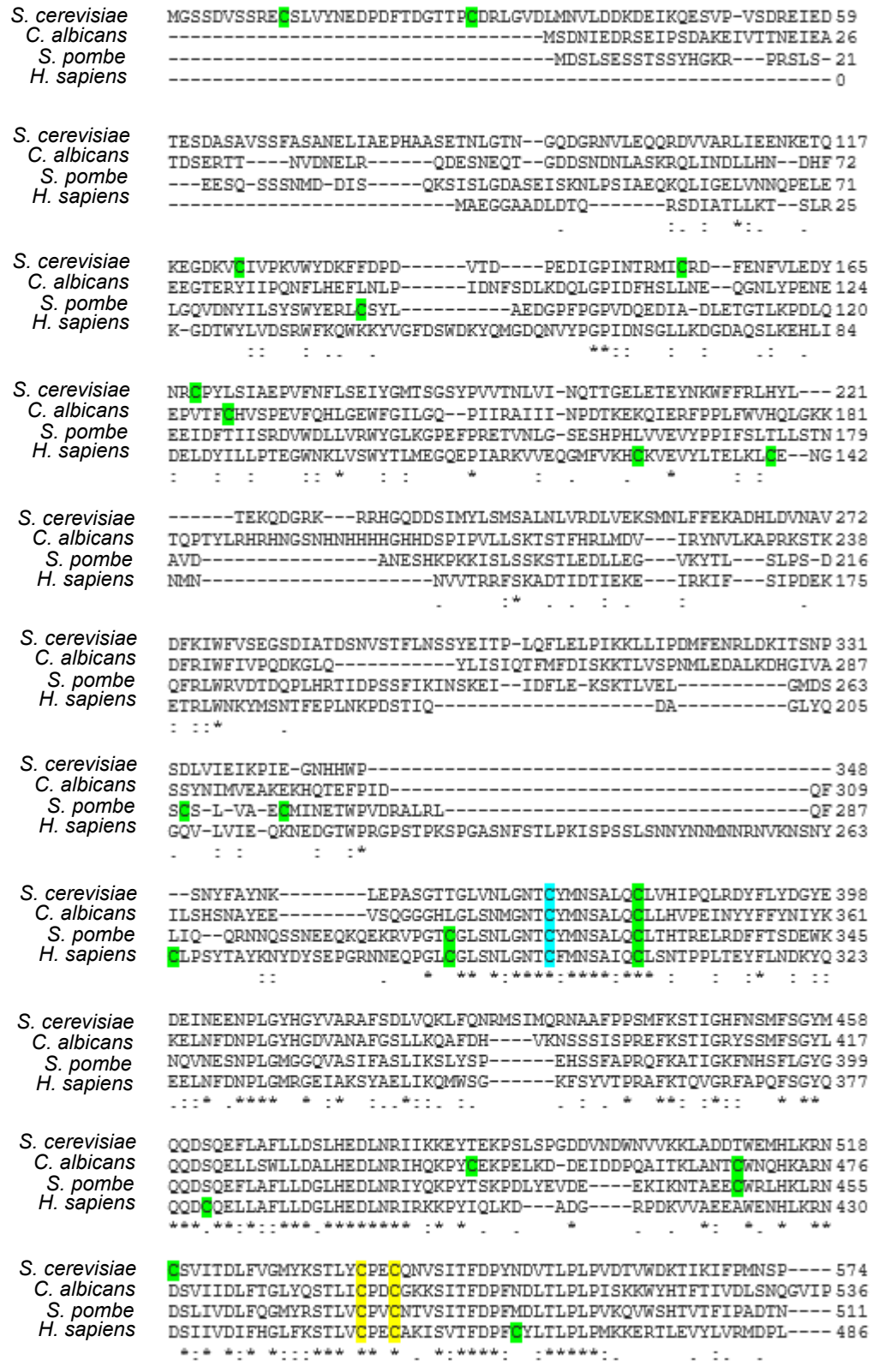

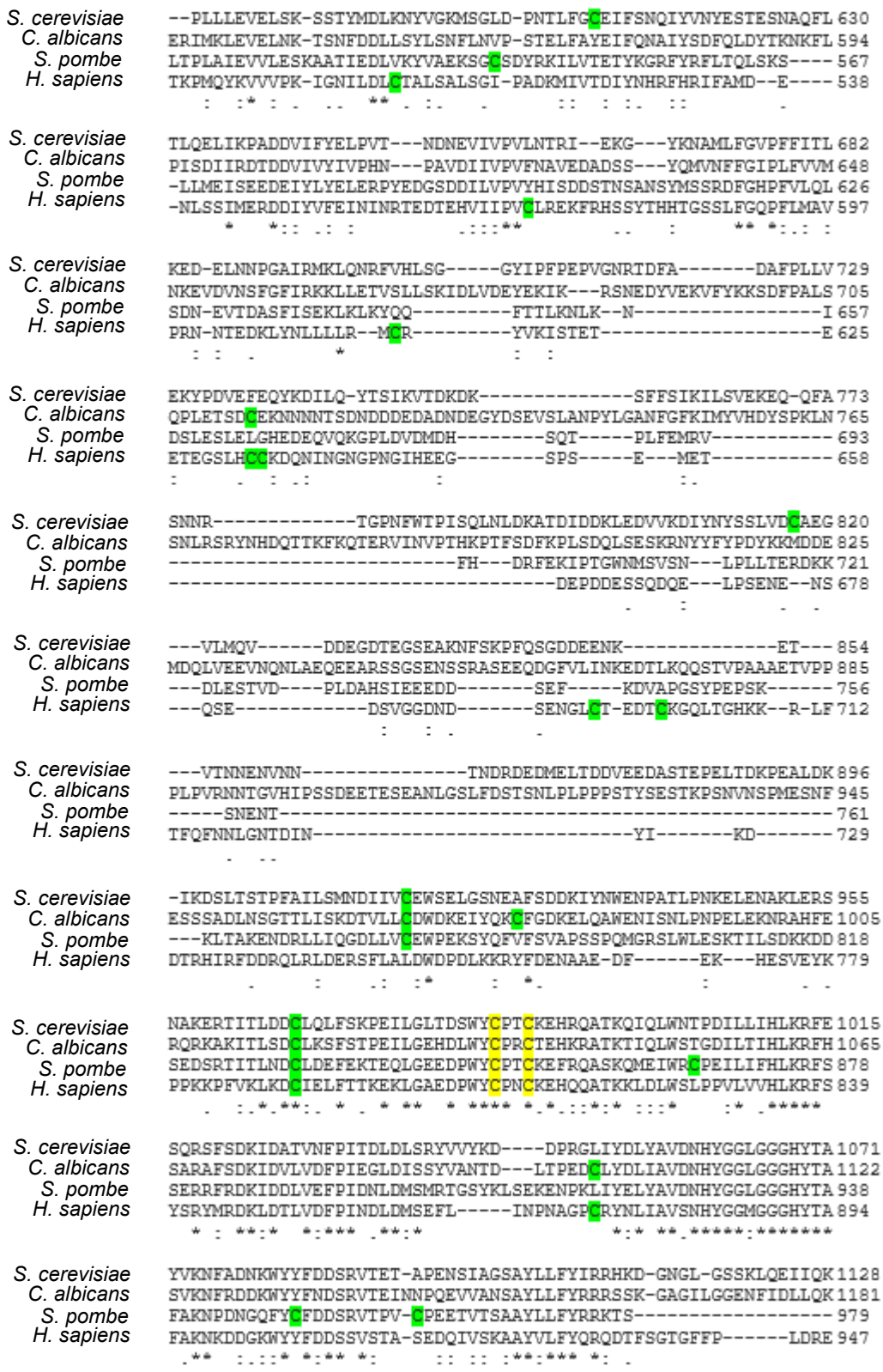
S. cerevisiae
C. albicans
S. pombe
H. sapiens

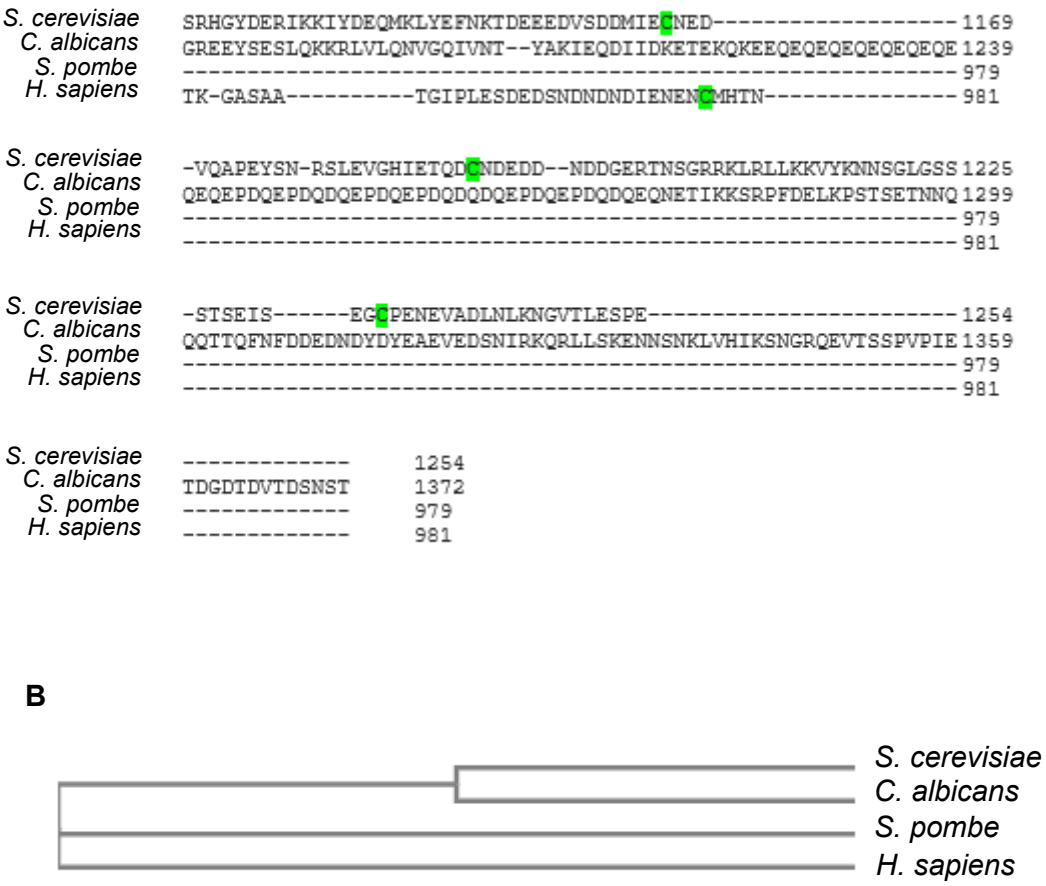

Figure 5.1. Analyses of conservation of Ubp12 in *S. cerevisiae*, *C. albicans*, *S. pombe*, and *H. sapiens*.

A) Protein sequence alignments of Ubp12 in *S. cerevisiae, C. albicans, S pombe* and *H. sapiens* produced in Clustal Omega (Sievers et al., 2011). 7 cysteine residues are conserved between Ubp12 homologues in *S. cerevisiae*, *C. albicans*, *S. pombe* and *H. sapiens*, including the catalytic cysteine residue and both CXXC motifs. The catalytic cysteine is highlighted in turquoise, the two CXXC motifs in yellow, and all other cysteine residues in green. Identical amino acids found in all the proteins are annotated with *. Gaps were introduced to maximise alignment, indicated by dashes. Colons indicate conservation between groups of strongly similar properties, periods indicate conservation between groups of weakly similar properties. B) Cladogram indicating the phylogenetic relationship between homologues of Ubp12 in *S. cerevisiae*, *C. albicans*, and *S. pombe* and USP15 in *H. sapiens*.

5.2 Results

5.2.1 Strain constructions for analyses of Ubp12 in C. albicans

5.2.1.1 Gene deletion

To begin investigations of the potential links between Ubp12 and responses to oxidative stress in *C. albicans* it was important to construct a strain containing a deletion of the *UBP12* gene. *C. albicans* is a diploid yeast and hence it was necessary to delete both copies of the *UBP12* gene by replacing them with two different selectable markers. This strategy is shown below in Figure 5.2. Deletion of both copies of *UBP12* in *C. albicans* was achieved using two disruption cassettes which were amplified by PCR (Shahana et al., 2014). Ubp12-Del-Fw-CA and Ubp12-Del-Rev-CA primers (Appendix C) were designed with 100 bp homology immediately before (forward primer) and immediately after (reverse primer) the start and stop codons of the *UBP12* gene, respectively. The primers also contained 20 bp homology to the loxP-*HIS1*-loxP (pLHL) and loxP-*ARG4*-loxP (pLAL) plasmids (Table 2.1), approximately 500 bp before the start codon, and approximately 500 bp after the stop codon, of the relevant selectable marker gene. Phusion PCR was performed, using either the loxP-*HIS1*-loxP or the loxP-*ARG4*-loxP plasmids as template DNA and the Ubp12-Del-Fw-CA and Ubp12-Del-Rev-CA primers (PCR conditions are detailed in 2.3.1.1). This generated two disruption cassettes, one with *HIS1* as a marker and one with *ARG4* as a marker. The *ARG4* disruption cassette was then transformed into SN148 *C. albicans* cells (KA57) and colonies that grew on selective plates lacking *ARG4* were assessed by Dream-Taq PCR for integration using Ubp12-DelChk-Fw-CA and Arg4-Chk-EarlyRev-CA primers. The *HIS1* disruption cassette was then transformed into successful integrants of the *ARG4* disruption cassette, successful integration was confirmed using selective plates and DreamTaq PCR (see 2.3.1.2) using the Ubp12-DelChk-Fw-CA and His1-Chk-EarlyRev-CA primers. An additional DreamTaq check PCR was conducted using Ubp12-DelChk-Fw-CA and Ubp12-DelChk-Rev-CA primers to confirm the integration of the disruption cassettes. To check that *UBP12* had not duplicated in the chromosome, a check DreamTaq PCR using internal *UBP12* primers (Ubp12-check-fw-CA-internal and Ubp12-check-rev-CA-internal) was conducted. For DreamTaq PCR conditions see 2.3.1.2. Finally, the CIp10 plasmid (Table 2.1) was

linearised using StuI (section 2.3.3) and transformed into the successful integrants for re-introduction of the *URA3* marker. Successful integration of StuI was confirmed using appropriate selective plates. The gene deletion strategy is described in Figure 5.2. The PCR confirmation of gene replacement of both copies of the *UBP12* gene in the SN148 strain background of *C. albicans* is shown in Figure 5.3.

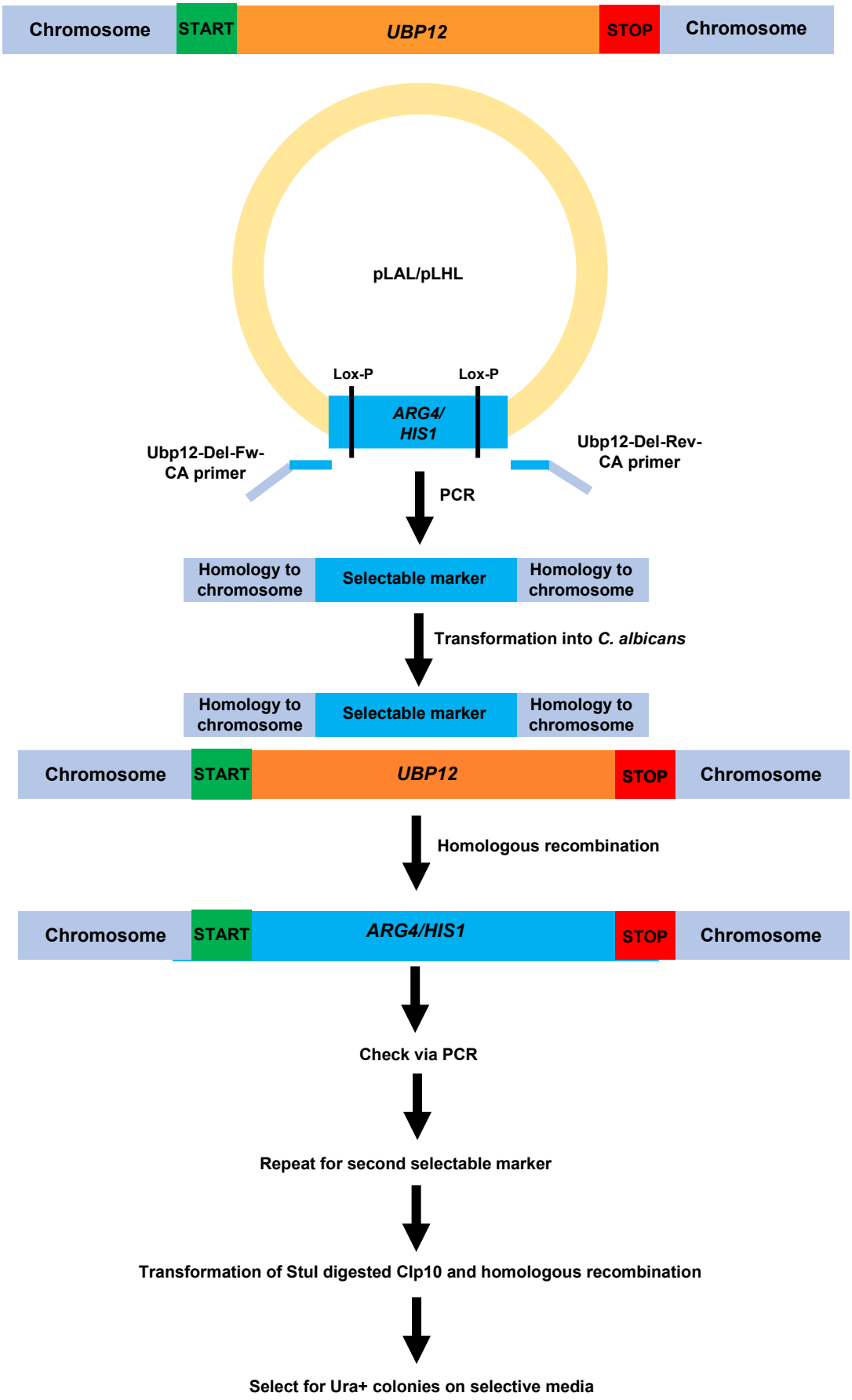
Chromosome
START
UBP12
STOP
Chromosome
pLAL/pLHL
Lox-P
Lox-P
ARG4/
HIS1
Ubp12-Del-Fw-
CA primer
Ubp12-Del-Rev-
CA primer
PCR
Homology to
chromosome
Selectable marker
Homology to
chromosome
Transformation into C. albicans
Homology to
chromosome
Selectable marker
Homology to
chromosome
Chromosome
START
UBP12
STOP
Chromosome
Homologous recombination
Chromosome
START
ARG4/HIS1
STOP
Chromosome
Check via PCR
Repeat for second selectable marker
Transformation of StuI digested Clp10 and homologous recombination
Select for Ura+ colonies on selective media

Figure 5.2. Strategy to delete the UBP12 gene in *C. albicans*.

Both alleles of *UBP12* in *C. albicans* were deleted using the Clox system plasmids, pLAL and pLHL (Shahana et al., 2014). Primers (Ubp12-Del-Fw-CA and Ubp12-Del-Rev-CA) were designed to create a disruption cassette containing 100 bp homology to the DNA sequences located immediately upstream and downstream of the start and stop codons of the UBP12 gene, respectively. These primers also contained 20 bp homology to DNA sequences located approximately 500 bp before/after the *HIS1* or *ARG4* marker of the pLAL/pLHL plasmids, respectively. The PCR products were amplified and transformed into *C. albicans* SN148 cells (KA57) in two separate transformations. Check PCRs using the primers Ubp12-DelChk-Fw-CA and Arg4-Chk-EarlyRev-CA confirmed the integration of the *ARG4* disruption cassette at the correct genomic locus. Check PCRs using the primers Ubp12-DelChk-Fw-CA and His1-Chk-EarlyRev-CA confirmed the integration of the *HIS1* disruption cassette at the correct genomic locus. All PCR reaction conditions are detailed in section 2.3.1. Finally, CIp10 was linearised with StuI and transformed into the *ubp12*Δ mutant and integrated into the genome.

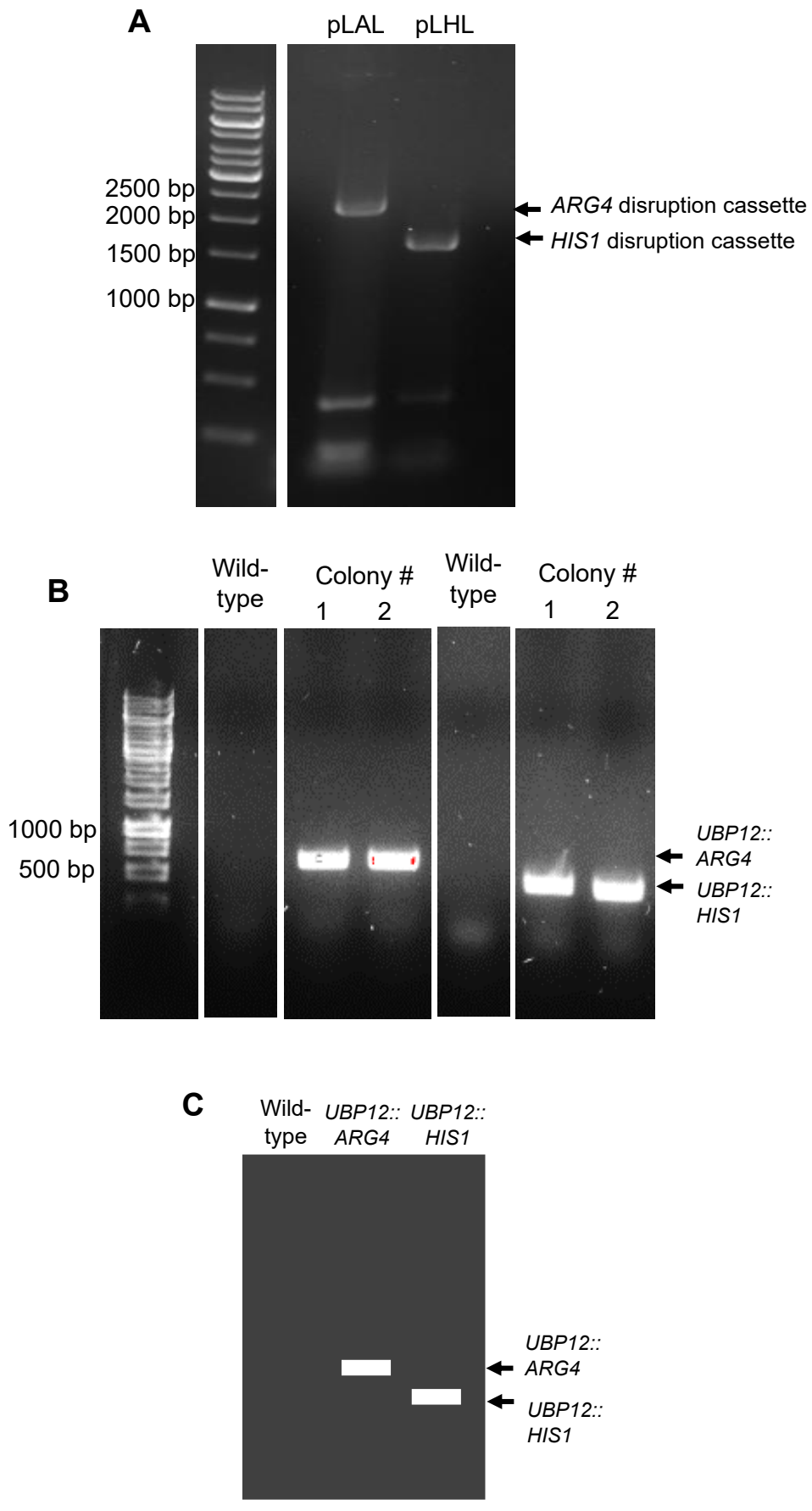
A
pLAL
pLHL
2500 bp
2000 bp
1500 bp
1000 bp
ARG4 disruption cassette
HIS1 disruption cassette
B
Wild-type
Colony #
1
2
Wild-type
Colony #
1
2
1000 bp
500 bp
UBP12::ARG4
UBP12::HIS1
C
Wild-type
UBP12::ARG4
UBP12::HIS1
UBP12::ARG4
UBP12::HIS1

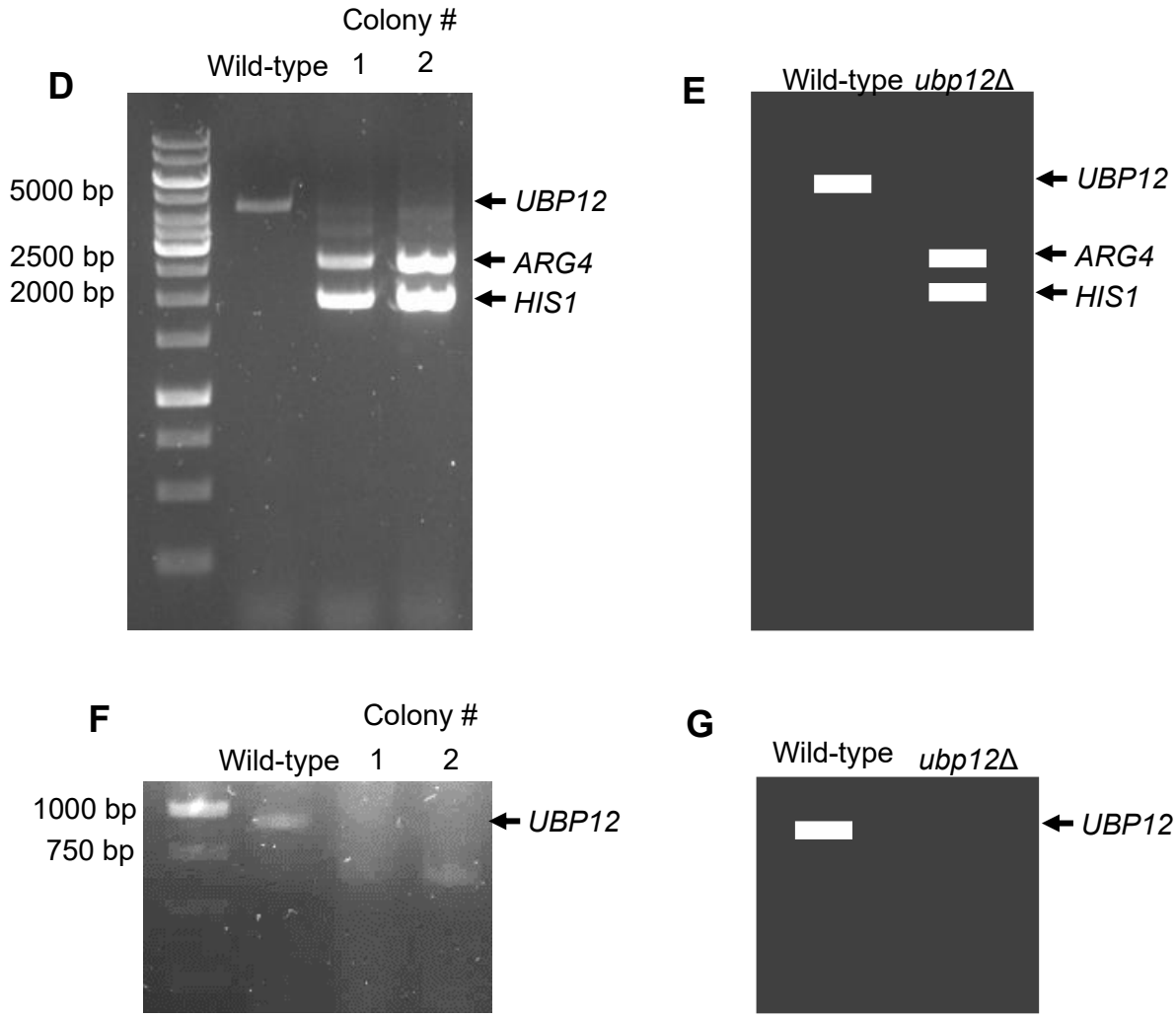

Figure 5.3. Both copies of *UBP12* were successfully deleted in *C. albicans*.

A) Agarose gel analysis of the Phusion PCR reactions (see section 2.3.1.1) to generate the *ARG4* and *HIS1* disruption cassettes, using plasmids pLAL (*ARG4* disruption cassette) and pLHL (*HIS1* disruption cassette) as templates. Both cassettes were generated using the Ubp12-Del-Fw-CA and Ubp12-Del-Rev-CA primers (see Appendix C, PCR conditions are detailed in section 2.3.1.1) Primers were designed as instructed in Dennison *et al.* (2005), using the sequences provided for plasmid homology (Dennison et al., 2005). The approximate predicted sizes of the *ARG4* and *HIS1* disruption cassettes are 2200 bp and 1700 bp respectively. B) Agarose gel analysis of wild-type (KA57) and the DreamTaq PCR reactions (see section 2.3.1.2) of 2 possible double disruptants (Arg+ and His+ transformants) to check the integration of the relevant selectable marker (*ARG4* or *HIS1*) at the *UBP12* gene locus on alternate chromosomes, using the external Ubp12-DelChk-Fw-CA primer and either the internal Arg4-Chk-EarlyRev-CA or the His1-Chk-EarlyRev-CA primers. The predicted sizes of the integration of *ARG4* and *HIS1* at the *UBP12* gene locus on alternate chromosomes is 511bp and 381bp respectively. C) Diagram of expected PCR for comparison to B). D) To confirm the absence of the wild type *UBP12* gene

and the replacement of each copy of the *UBP12* gene with either *ARG4* or *HIS1* DreamTaq PCR reactions were performed on the wild type strain (KA57) and the same two possible double gene disruptants as B), using the external Ubp12-DelChk-Fw-CA and Ubp12-DelChk-Rev-CA primers (DreamTaq PCR conditions are detailed in section 2.3.1.2). The presence of the wild-type *UBP12* gene was predicted to produce a band of size approximately 4500 bp, the *ARG4* marker to produce a band of size approximately 2500 bp and the *HIS1* marker to produce a band of size approximately 1900 bp on an agarose gel. E) Diagram of expected PCR products for comparison to D). F) A different DreamTaq PCR reaction to that described in D) was performed on the wild type strain (KA57) and two possible double gene disruptants (colony 1 and colony 2, as used in B) and D)) to confirm the absence of *UBP12*, using the internal Ubp12-check-fw-CA-internal and Ubp12-check-rev-CA-internal primers (DreamTaq reaction conditions are stated in section 2.3.1.2). If wild-type *UBP12* was present in either colony 1 or colony 2 a band of size approximately 960 bp present in the wild type control was expected on an agarose gel. G) Diagram of expected PCR products for comparison to F). GeneRuler 1 kb DNA Ladder (ThermoScientific) was used.

In particular, PCR amplification of the two disruption cassettes was successful (Figure 5.3A), and the integration of these cassettes into each copy of the *UBP12* genomic locus was confirmed in two independent colonies, colony 1 and colony 2 (Figure 5.3B and C). Furthermore, to confirm that no copies of the wild type *UBP12* gene remain in colony 1 and colony 2 primers which bind the genome were used in PCR reactions that were predicted to be able to produce PCR products with different sizes depending on whether the wild type *UBP12* gene is present (4500 bp) or if the *UBP12* gene has been replaced with either *ARG4* (2500 bp) or *HIS1* (1900 bp) (Figure 5.3D and E). As expected, both colony 1 and colony 2 contain the *ARG4* and *HIS1* markers in the correct position in the *UBP12* gene locus. However, some slower mobility bands were detected with some similarity in mobility to the PCR fragment corresponding to the presence of wild type *UBP12* (Figure 5.3D). It was possible that these were non-specific bands. However, to further confirm the absence of a wild-type copy of *UBP12* in colony 1 and/or colony 2, a further PCR reaction was performed using primers that bind within the *UBP12* gene and which were predicted to produce a PCR product of size approximately 960 bp if the wild type *UBP12* gene was present (Figure 5.3F and G, see wild-type control). In contrast to the wild-type control this PCR analysis of colony 1 and colony 2 did not produce a PCR product of approximately 960bp (Figure 5.3F). Hence, these data indicated that two independent strains had been successfully constructed where both copies of the *UBP12* gene had been replaced by either *ARG4*

or *HIS1*. To allow further studies of these newly constructed *ubp12Δ* strains, the colony 1 and colony 2 strains were next transformed with digested CIp10 to restore a functional *URA3* gene at the *RPS10* gene locus in both strains. *C. albicans* is auxotrophic for uridine, which can cause an attenuation in virulence and affect the abundance of other proteins in the cell; restoring *URA3* with integration of CIp10 rescues these uridine-linked effects (Brand et al., 2004). The colony 1 and colony 2 strains contain the wild type *URA3* gene and were named from here on as strains KA103 (colony 1) and KA108 (colony 2).

5.2.1.2 Epitope tagging

Given that Ubp12 in *S. cerevisiae* is oxidised in response to H_2O_2 it was also important to obtain reagents that would allow studies of the Ubp12 protein in *C. albicans*. Unfortunately, there are no antibodies available that can be used in studies of this DUB hence it was important to construct a *C. albicans* strain that expresses an epitope-tagged version of Ubp12. The strategy to construct this strain expressing epitope-tagged Ubp12 is detailed in Figure 5.4. Chromosomal gene tagging of *UBP12* in *C. albicans* was achieved using a cassette created by PCR amplification, which contained the *HIS1* selectable marker (Lavoie et al., 2008). Briefly, an epitope-tagging cassette (HA-*HIS1*) containing sequences encoding 3 x HA epitopes and the *HIS1* marker flanked by sequences of homology to the regions before the stop codon of Ubp12 and immediately after the stop codon of Ubp12 was generated by Phusion PCR, using the primers Ubp12-HA-F and Ubp12-HA-R (Appendix C). The pFA-HA-*HIS1* plasmid (Table 2.1) was used as template DNA (PCR conditions used are detailed in 2.3.1.1). This produced an epitope tagging cassette containing HA-*HIS1* with homology to either side of the stop codon of *UBP12*. This PCR was predicted to produce a HA-*HIS1* cassette of predicted size 1952 bp and indeed this was obtained (Figure 5.5A). The HA-*HIS1* cassette was purified from the agarose gel and then transformed into wild-type SN148 *C. albicans* cells and the cassette integrated by homologous recombination at the 3' end of one copy of the *UBP12* gene in the normal chromosomal locus. His+ colonies were obtained on appropriate selective media and integration at the correct genomic locus confirmed using DreamTaq PCR and Ubp12-HA-check-fw and HA-check-rev primers (Appendix C, for PCR conditions see 2.3.1.2). Significantly, a band of the correct size was detected (approximately 250 bp, Figure

5.5B), indicating that a strain had been constructed containing a copy of the HA-*HIS1* cassette integrated at the correct chromosomal location of one copy of *UBP12*. Hence this approach generated cells potentially expressing the wild type Ubp12 protein and the Ubp12-HA construct where Ubp12 is tagged with 3HA epitopes in-frame at the C-terminus of the protein. To complete the strain construction linearised CIp10 was transformed into the Ubp12-3HA *C. albicans* cells to restore a functional *URA3* gene for the reasons explained above. It is important to note that *C. albicans* is a diploid organism and hence successful integrants contain one copy of the wild-type *UBP12* gene and one copy of the modified *UBP12* gene expressing 3x HA epitope tagged Ubp12. This Ubp12-HA strain containing *URA3* was named KA69 from here on.

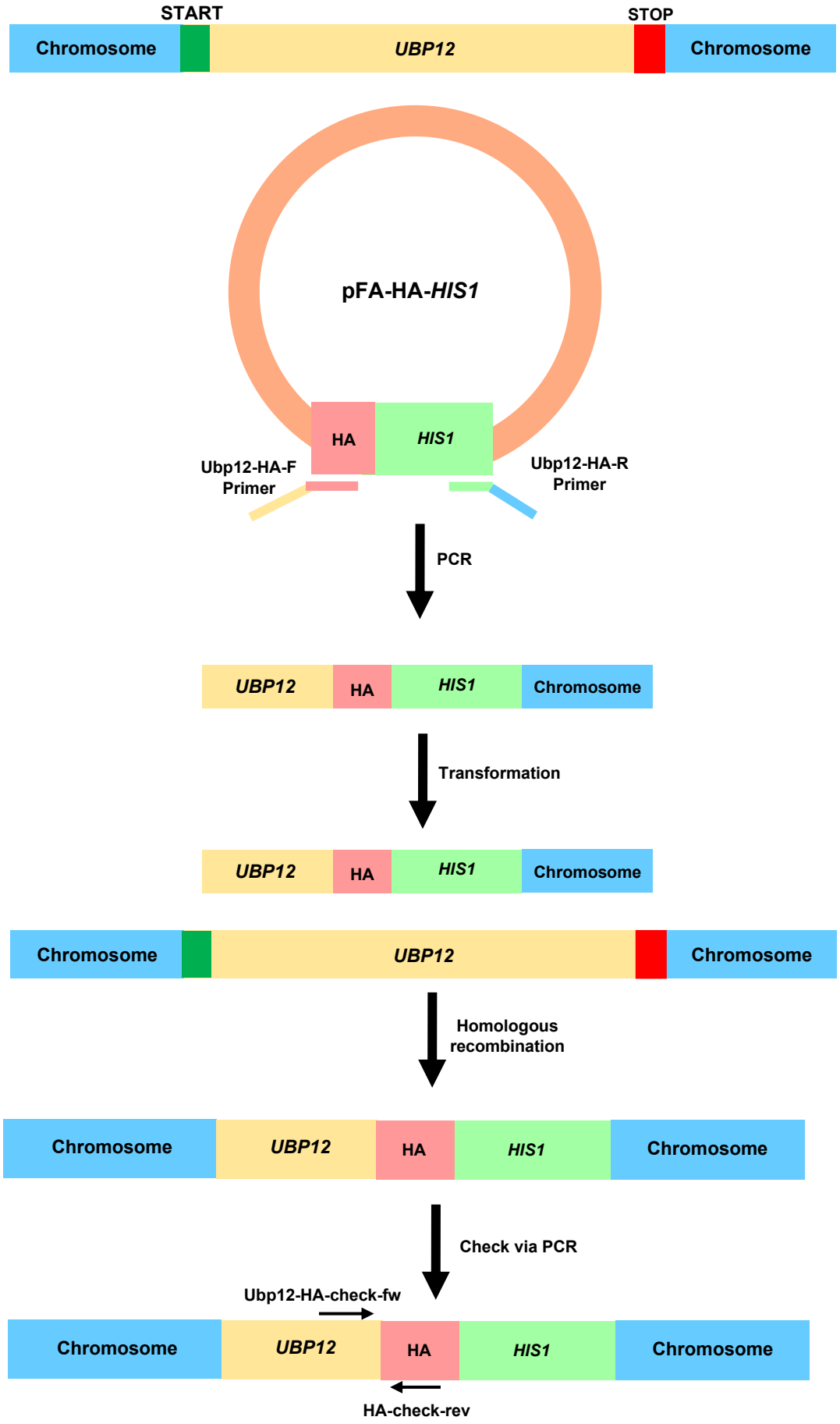
START
STOP
Chromosome
UBP12
Chromosome
pFA-HA-HIS1
HA
HIS1
Ubp12-HA-F Primer
Ubp12-HA-R Primer
PCR
UBP12
HA
HIS1
Chromosome
Transformation
UBP12
HA
HIS1
Chromosome
Chromosome
UBP12
Chromosome
Homologous recombination
Chromosome
UBP12
HA
HIS1
Chromosome
Check via PCR
Ubp12-HA-check-fw
Chromosome
UBP12
HA
HIS1
Chromosome
HA-check-rev

Figure 5.4. Strategy for epitope tagging Ubp12 in *C. albicans* expressed from the normal chromosomal locus.

The *UBP12* Tag F primer (Ubp12-HA-F) contains homology to the chromosome DNA sequence directly upstream of the stop codon of *UBP12* and homology to the pFA-HA-*HIS1* plasmid at the 5' end of the HA sequences. The *UBP12* Tag R primer (Ubp12-HA-R) contains homology to the 3' end of the selectable marker of the pFA-HA-*HIS1* plasmid and homology to the chromosome DNA sequences directly downstream of the stop codon of *UBP12*. The pFA-HA-*HIS1* plasmid was used as a template for PCR with the Ubp12-HA-F and Ubp12-HA-R primers to create a PCR product containing the sequences encoding 3x HA epitope tags, the *HIS1* selectable marker and homology to the chromosome either side of the stop codon of *UBP12*. The PCR product was transformed into wild-type *C. albicans* cells (KA57) and integrated into the genome via homologous recombination at the 3' end of *UBP12*, replacing the stop codon with the sequences encoding the 3x HA epitope tags and the *HIS1* gene. His+ colonies were obtained and checked by PCR using primers Ubp12-HA-check-fw and HA-check-rev. The DNA sequences of the modified *UBP12* gene were obtained to confirm correct integration with no errors in frame with the DNA sequences encoding the 3x HA epitope tags.

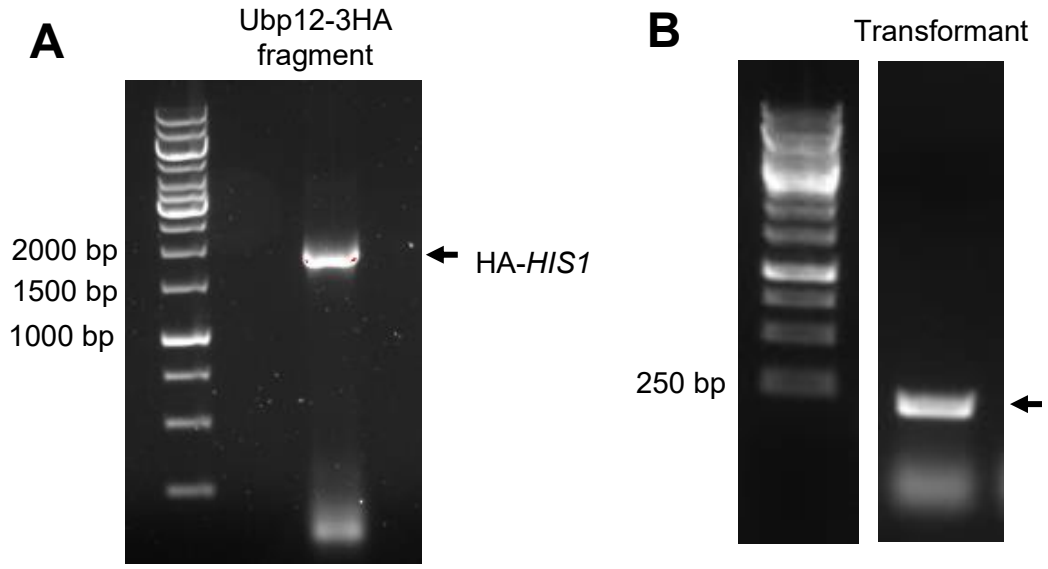

Figure 5.5. A *C. albicans UBP12-HA* strain was successfully constructed.

A) Analysis of the Phusion PCR reaction (see section 2.3.1.1) to generate the HA-*HIS1* cassette fragment using pFA-HA-HIS1 as template DNA (Table 2.1) and the Ubp12-HA-fw and Ubp12-HA-rev primers (Appendix C). A band of approximately 1952 bp was predicted on an agarose gel and is indicated. B) Analysis of a DreamTaq PCR reaction (see section 2.3.1.2) of a transformant colony to check the potential integration of the HA-*HIS1* cassette. The primers Ubp12-HA-check-fw and HA-check-rev were used to confirm integration (Appendix C). The presence of a band of the predicted size 200 bp (indicated by the arrow) on an agarose gel indicates that the cassette has been integrated at the correct location. GeneRuler 1 kb DNA Ladder (ThermoScientific) was used.

5.2.2 Analyses of the potential roles of Ubp12 in response to different oxidising agents in *C. albicans*

To begin to assess the potential roles of Ubp12 in oxidative stress responses in *C. albicans* the growth of the two independent *ubp12Δ* strains (KA103 and KA108) was examined after exposure to a range of oxidising agents. In addition, the growth of KA69 expressing 3HA epitope-tagged Ubp12 (Ubp12-3HA) was examined under the same conditions to explore whether the fusion of the epitopes to Ubp12 had altered the function of the protein. In particular, serial dilutions of wild-type (KA102), *ubp12Δ* (KA103 and KA108) and Ubp12-3HA (KA69) cells were spotted onto YPD plates at 30ºC containing various oxidising agents (Figure 5.6). In addition, the cells were also

exposed to hydroxyurea and UV light to examine whether Ubp12 has any role in response to DNA replication stress or DNA damage (Figure 5.6).

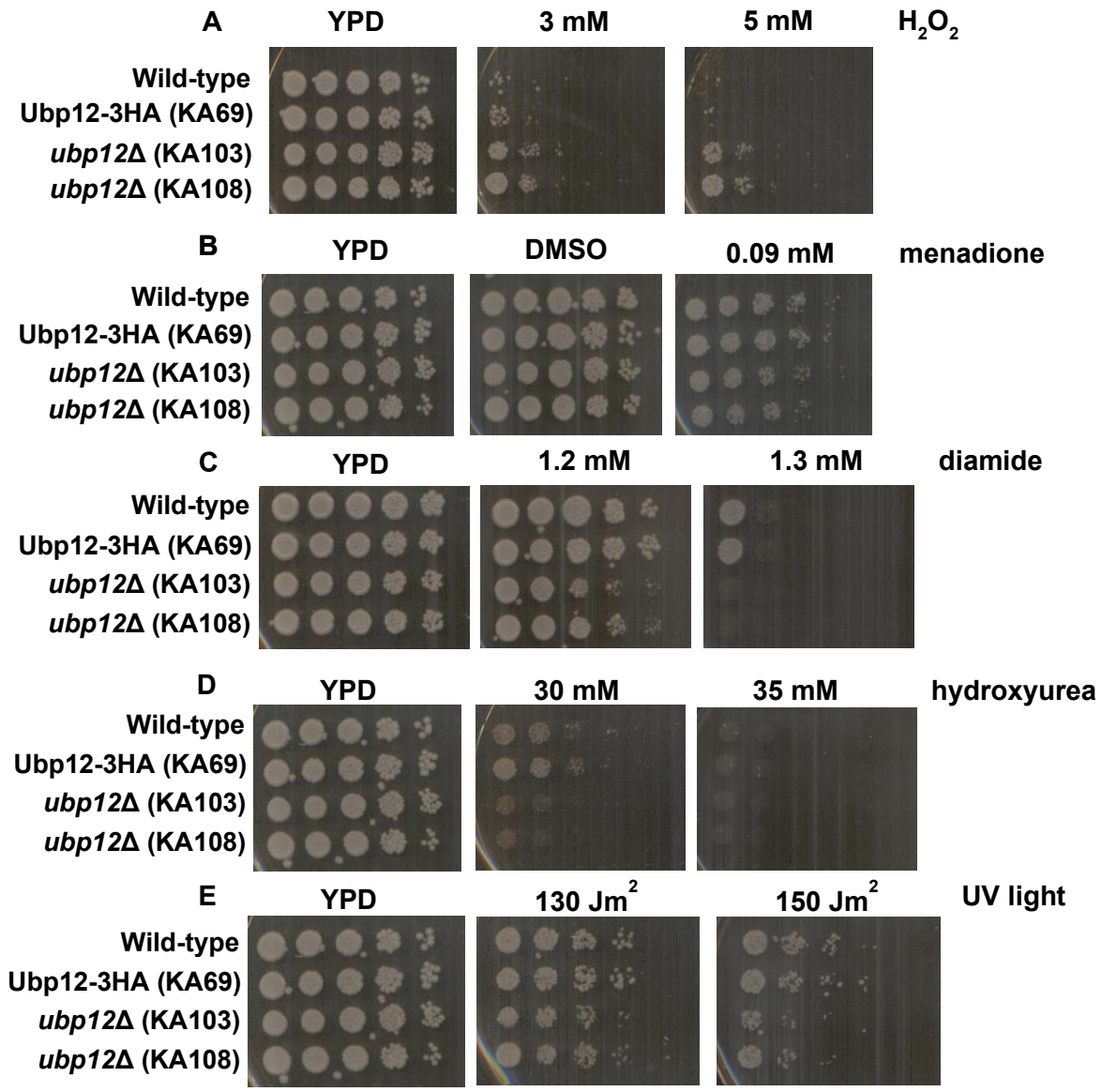

Figure 5.6. Ubp12 is involved in responses to oxidative stress, DNA replication stress and DNA damage.

(A – E) 5-fold serial dilutions of mid-log phase growing wild-type (KA102), Ubp12-3HA (KA69), and *ubp12Δ* (KA103 and KA108) cells were spotted onto YPD plates and exposed to the indicated stress condition. DMSO was included as an added control for treatment with menadione because the menadione stock solution was dissolved in DMSO. Plates were incubated at 30°C for 2 days before imaging. N=3.

Excitingly, analyses of the sensitivity tests revealed that Ubp12 is involved in responses to oxidative stress, DNA replication stress and DNA damage (Figure 5.6). Furthermore, it is also important to note that, unlike the *ubp12Δ* strains, the cells expressing Ubp12-3HA displayed similar sensitivity as wild-type cells to a range of different stress conditions, suggesting that the epitope tagging of Ubp12 has not altered the function of the DUB, at least as determined by these sensitivity tests (Figure 5.6).

Analyses of the sensitivity of the *ubp12Δ* strains to different oxidising agents revealed that Ubp12 is involved with responses to H_2O_2, diamide and the superoxide generating agent menadione (Figure 5.6A-C). Indeed, cells lacking Ubp12 displayed increased sensitivity to diamide compared to wild-type cells, indicating that Ubp12 function is required for resistance to this oxidising agent (Figure 5.6C). However, in contrast, *ubp12Δ* cells displayed increased resistance to H_2O_2 in comparison with wild-type cells (Figure 5.6A). This result suggests that Ubp12 activity is inhibitory to normal responses to H_2O_2 in *C. albicans*. Finally, menadione causes superoxide stress in *C. albicans* and *ubp12Δ* cells displayed slight, but reproducible, increased sensitivity to this oxidising agent compared to wild type cells (Figure 5.6B). Overall, these results are very interesting and suggest that Ubp12 function is involved in cell responses to a broad range of oxidising agents. Furthermore, the data suggest that Ubp12 may be linked to these cellular responses through different pathways. Although the underlying details of these different functions of Ubp12 are unclear it is tempting to speculate that perhaps these differences in function are linked to the regulation of ubiquitination of different substrates in response to each specific oxidising agent. Responses to oxidative stress are linked to the virulence of *C. albicans* (Warris and Ballou, 2019), through the ability of this pathogenic yeast to respond to ROS produced by host immune cells. Hence, these data raise the possibility that Ubp12 function influences the virulence of *C. albicans*.

The results of the sensitivity tests also revealed that Ubp12 function is required for responses to other stress conditions. In particular, in comparison to wild type control cells *ubp12Δ* cells were found to display increased sensitivity to hydroxyurea, a drug that induces DNA replication stress by decreasing dNTP levels in the cell (Singh and Xu, 2016), and to UV light, which causes DNA damage (Sinha and Häder, 2002) (Figure 5.6D,E). Although the functions of Ubp12 in these specific stress responses is

unknown these data have revealed that Ubp12 function is required for the responses of *C. albicans* cells to DNA replication stress and DNA damage caused by UV light.

Taken together, the results presented in this section have revealed that, similar to *S. cerevisiae*, Ubp12 is involved in responses to oxidative stress in *C. albicans*, although potentially the roles played by this DUB in these two yeasts are different. Furthermore, Ubp12 in *C. albicans* was found to be important for resistance to DNA replication stress and DNA damage.

5.2.3 Analyses of the Ubp12 protein in response to oxidative stress in *C. albicans*

As described above Ubp12 is clearly important for the resistance of C. albicans to several different oxidising agents (Figure 5.6). Moreover, studies of Ubp12 in *S. cerevisiae* revealed that the protein forms a HMW disulphide complex in response to H_2O_2 but not to menadione or diamide (Curtis, 2019) (Figure 3.2). Hence, these results raised the possibility that Ubp12 in *C. albicans* may also form a HMW disulphide complex in response to H_2O_2 and possibly other oxidising agents. To explore this possibility cells expressing Ubp12-3HA (KA69), which as shown above behave similarly to wild-type cells in responses to different oxidising agents (Figure 5.6), were exposed to either 5 mM H_2O_2 or 3 mM diamide for 0 or 10 minutes and protein extracts obtained under non-reducing conditions for analysis by western blot (Figure 5.7).

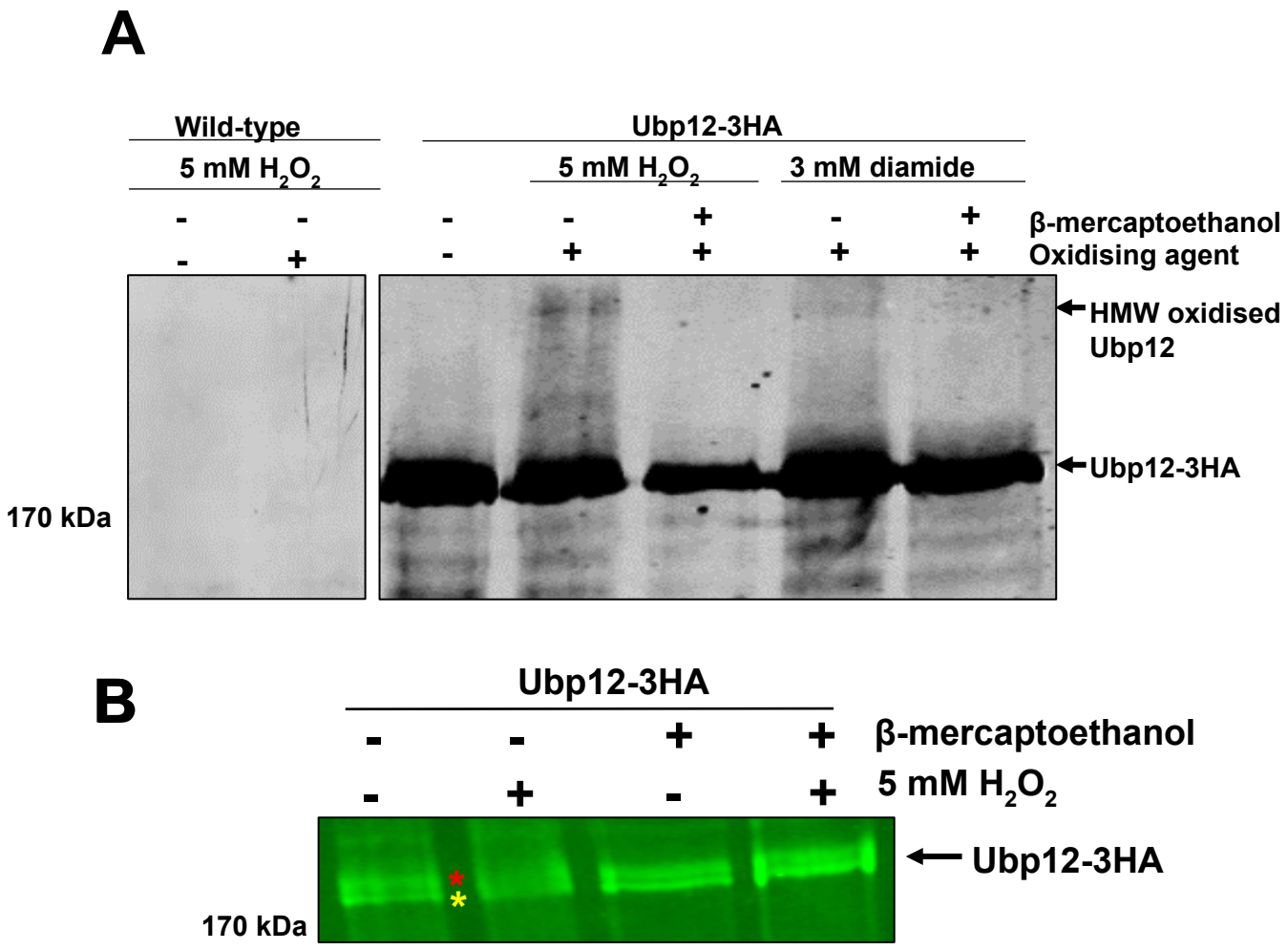

Figure 5.7. Ubp12 forms a HMW oxidised species in response to H_2O_2 and diamide and exists as a double band in *C. albicans*.

A) Western blot analysis of protein extracts isolated from mid-log phase growing *C. albicans* wild-type cells (KA102) and cells expressing one untagged copy of Ubp12 and one 3HA epitope-tagged copy of Ubp12 (Ubp12-3HA, KA69) in YPD media and treated with either 5 mM H_2O_2 or 3 mM diamide for 0 (-) or 10 (+) minutes. Protein extracts were prepared in either non-reducing or reducing conditions, separated by SDS-PAGE and proteins visualised using anti-HA antibodies. B) Western blot analysis of protein extracts isolated from mid-log phase growing *C. albicans* cells expressing one untagged copy of Ubp12 and one 3HA epitope-tagged copy of Ubp12 (Ubp12-3HA, KA69) in YPD media and treated with either 5 mM H_2O_2 for 0 (-) or 10 (+) minutes. Protein extracts were prepared in either non-reducing conditions (- β-mercaptoethanol) or reducing conditions (+ β-mercaptoethanol), separated by SDS-PAGE and proteins were visualised using anti-HA antibodies. The reduced form of Ubp12-3HA and the Ubp12 double band indicated (asterisks). PageRuler Prestained Protein Ladder (ThermoScientific) was used.

It was possible that the epitope-tagged Ubp12-3HA would not be detected, for example possibly because the tagged protein is unstable and/or expressed at a very low level. However, a specific band, not present in the untagged wild-type control lanes, of the predicted mobility, 175 kDa, for 3HA epitope-tagged Ubp12 was detected (Figure 5.7). Excitingly, similar to our observations in *S. cerevisiae*, Ubp12 was found to form HMW complexes of similar mobility to Ubp12 in *S. cerevisiae* (Figure 3.2) in response to H_2O_2 in *C. albicans* (Figure 5.7A). Furthermore, this HMW species was no longer detectable when the protein extracts were treated with β-mercaptoethanol indicating that these H_2O_2-induced Ubp12 HMW complexes were likely due to oxidation of Ubp12 (Figure 5.7, compare lanes 4 and 5). Interestingly, in contrast to Ubp12 in *S. cerevisiae*, Ubp12 in *C. albicans* was also found to form HMW complexes in response to diamide and these complex(es) are also not detectable when extracts were exposed to β-mercaptoethanol (Figure 5.7A, compare lanes 6 and 7). Hence, there are clearly similarities but also differences in the oxidation patterns of Ubp12 in *S. cerevisiae* compared with Ubp12 in *C. albicans* (Figure 5.7) (Curtis, 2019). Indeed, there are also other differences in the formation of Ubp12 HMW species in *C. albicans* when compared with *S. cerevisiae*. In particular, in *C. albicans* the relative abundance of H_2O_2-induced oxidised HMW complexes of Ubp12 formed compared to the Ubp12 protein that migrates at the expected size of reduced Ubp12 protein was much lower in comparison to the relative amount of Ubp12 found in HMW complexes when *S. cerevisiae* cells are exposed to H_2O_2. For example, approximately 40% of Ubp12 was detected in HMW disulphide complexes when *S. cerevisiae* W303 Ubp12-3HA cells (KA10) were exposed to H_2O_2 (see Figure 3.2). Although no quantification has been performed, a much smaller proportion of Ubp12 appears to be in HMW complexes when *C. albicans* cells were treated with H_2O_2 and diamide (compare Figures 3.2 and 5.7A). In addition to differences in relative abundance of the HMW complexes, the Ubp12 HMW complexes formed in *C. albicans* appear to be more diffuse in their migration profile on gels compared to the HMW complexes of Ubp12 from *S. cerevisiae* (compare Figures 3.2 and 5.7A). These observations will be discussed in more detail in the discussion section of the chapter. However, taken together with the findings that Ubp12 in *C. albicans* and *S. cerevisiae* appear to play both conserved and non-conserved roles in oxidative stress responses (Figures 4.1 and 5.6), these results support and extend a hypothesis where both the functions and the regulation of Ubp12 are linked to oxidative stress responses in these two yeasts. The formation

of the Ubp12 double band observed in *S. cerevisiae* (Figure 3.14) was also observed in *C. albicans* cells (Figure 5.7B), and consistent with findings in *S. cerevisiae*, was not sensitive to a reducing agent. Although the nature of this double band is unclear, evidence presented here suggests it is conserved and not a form of oxidation in *C. albicans* cells.

5.2.4 Analysis of the potential role of the thioredoxin system in the regulation of Ubp12 in *C. albicans*

As described previously in this thesis in Chapter 3, the thioredoxin antioxidant system influences the oxidation of Ubp12 in *S. cerevisiae*. Hence, having established that Ubp12 in *C. albicans* forms HMW oxidised complexes in response to H_2O_2 and diamide the next step was to begin to investigate whether, like *S. cerevisiae*, the thioredoxin system has any impact on the oxidation of this DUB. To assess whether the thioredoxin system influences the oxidation of Ubp12 in *C. albicans*, thioredoxin system mutant strains expressing Ubp12-3HA were generated using the strategy detailed in Figure 5.4. Briefly, an epitope-tagging cassette (HA-*URA3*) containing sequences encoding 3 x HA epitopes and the *URA3* marker flanked by sequences of homology to the regions before the stop codon of Ubp12 and immediately after the stop codon of Ubp12 was generated by PCR, using the primers Ubp12-HA-fw and Ubp12-HA-rev and plasmid pFA-HA-URA3 as template (as in Figure 5.4 but with the pFA-HA-URA3 plasmid). This PCR was predicted to produce a HA-*URA3* cassette of predicted size 1870 bp (Figure 5.8A). The HA-*URA3* cassette was purified from the agarose gel and then transformed into cells of the *C. albicans* thioredoxin system mutants *trx1*Δ (KA66), *tsa1*Δ (KA67) and *gpx3*Δ (KA68). Ura+ colonies were obtained on appropriate selective media and integration at the correct genomic locus confirmed using PCR (see Figure 5.4 for strategy to check correct integration). Significantly, a band of the correct size was detected (Figure 5.8B), indicating that all three strains had been constructed containing a copy of the HA-*URA3* cassette integrated at the correct location in one copy of the *UBP12* gene. Hence this approach generated *trx1*Δ Ubp12-3HA (KA71), *tsa1*Δ Ubp12-3HA (KA96) and *gpx3*Δ Ubp12-3HA (KA76) cells

potentially expressing the wild type Ubp12 protein and the Ubp12-HA construct where Ubp12 is tagged with 3HA epitopes in-frame at the C-terminus of the protein.

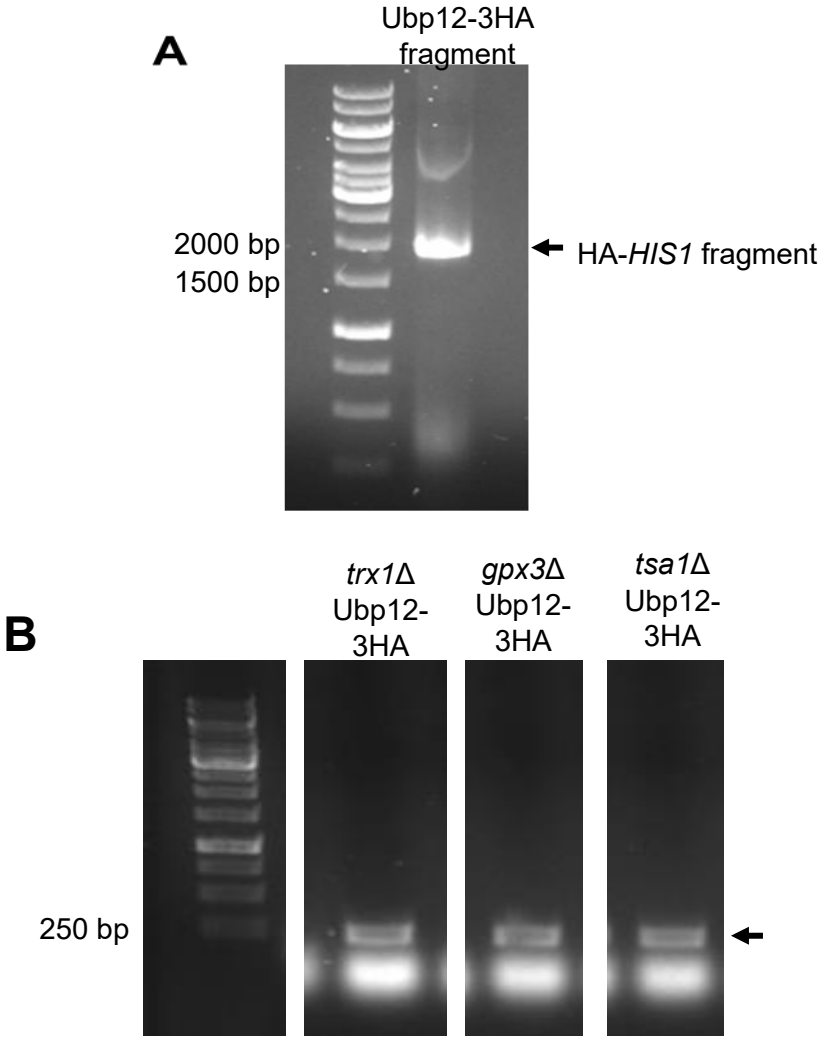

Figure 5.8. Construction of *C. albicans* thioredoxin system mutant strains containing the *UBP12-HA* cassette.

A) Analysis of the Phusion PCR reaction (see section 2.3.1.1) to generate the HA-*URA3* cassette fragment using pFA-HA-URA3 as template DNA (Table 2.1) and the primers Ubp12-HA-fw and Ubp12-HA-rev primers (PCR conditions are detailed in section 2.3.1.1). A band of approximately 1952 bp was predicted on an agarose gel and is indicated. B) Analysis of a DreamTaq PCR reaction (see section 2.3.1.2) of transformant colonies to check the potential integration of the HA-*URA3* cassette into the *trx1*Δ strain (KA66), the *gpx3*Δ strain (KA68), and the *tsa1*Δ strain (KA67). The primers Ubp12-HA-check-fw and HA-check-rev were used to confirm integration (PCR conditions are found in section 2.3.1.2). The presence of a band of predicted size 250 bp on an agarose gel (arrow) indicates that the cassette has been integrated at the correct location. GeneRuler 1 kb DNA Ladder (ThermoScientific) was used.

To examine whether any of the thioredoxin system proteins influence the oxidation of Ubp12 in *C. albicans* wild-type Ubp12-3HA (KA69), *trx1*Δ Ubp12-HA (KA71), *tsa1*Δ Ubp12-HA (KA96) and *gpx3*Δ (KA76) cells were exposed to 5 mM H_2O_2 for 0 or 10 minutes and protein extracts obtained under non reducing conditions for analysis by western blot (Figure 5.9). Significantly, a band of the predicted mobility, 175 kDa, for 3HA epitope-tagged Ubp12 was detected in extracts from *trx1*Δ Ubp12-HA (KA71), *tsa1*Δ Ubp12-HA (KA96) and *gpx3*Δ Ubp12-3HA (KA76) cells, indicating that the Ubp12-3HA cassette had integrated at the correct locus in the genome (Figure 5.9).

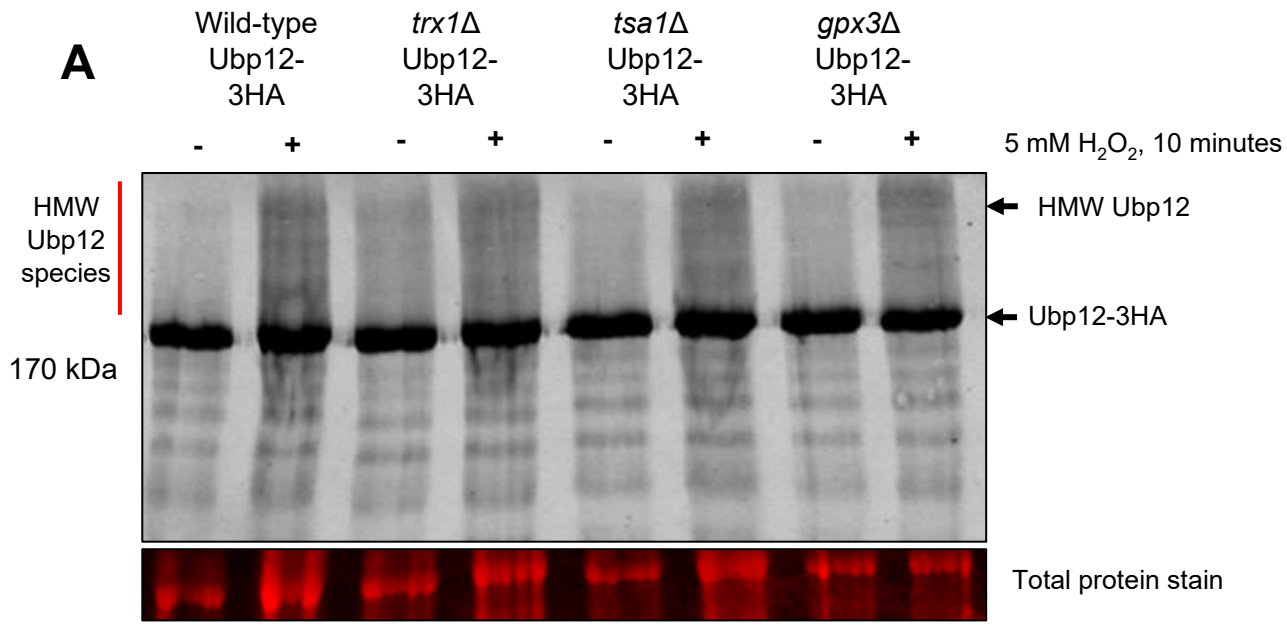
A
Wild-type Ubp12-3HA
trx1Δ Ubp12-3HA
tsa1Δ Ubp12-3HA
gpx3Δ Ubp12-3HA
- + - + - + - +
5 mM H2O2, 10 minutes
HMW Ubp12 species
170 kDa
HMW Ubp12
Ubp12-3HA
Total protein stain

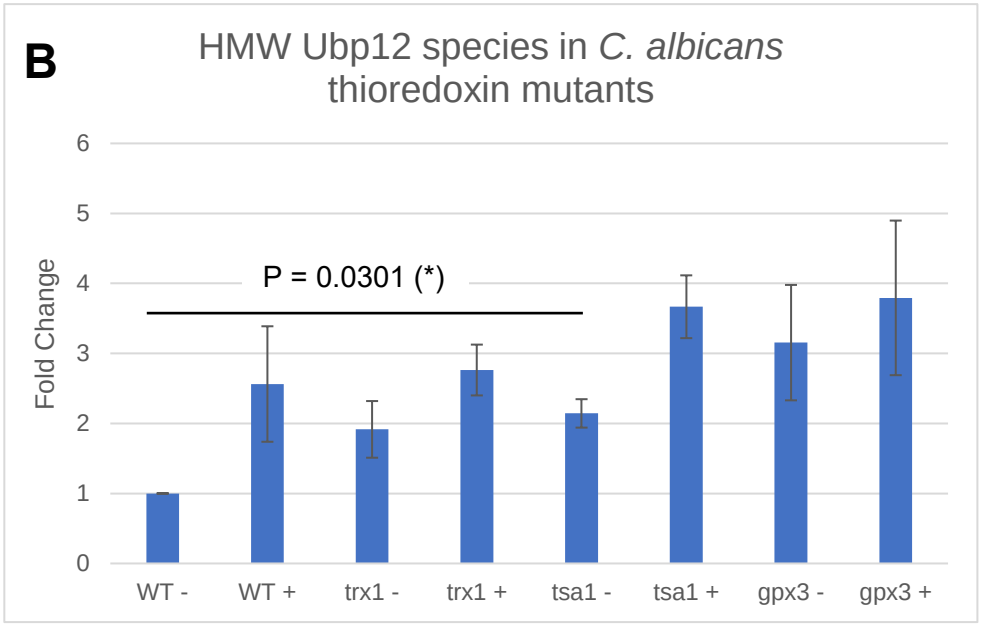
B
HMW Ubp12 species in C. albicans thioredoxin mutants
Fold Change
P = 0.0301 (*)
0
1
2
3
4
5
6
WT -
WT +
trx1 -
trx1 +
tsa1 -
tsa1 +
gpx3 -
gpx3 +

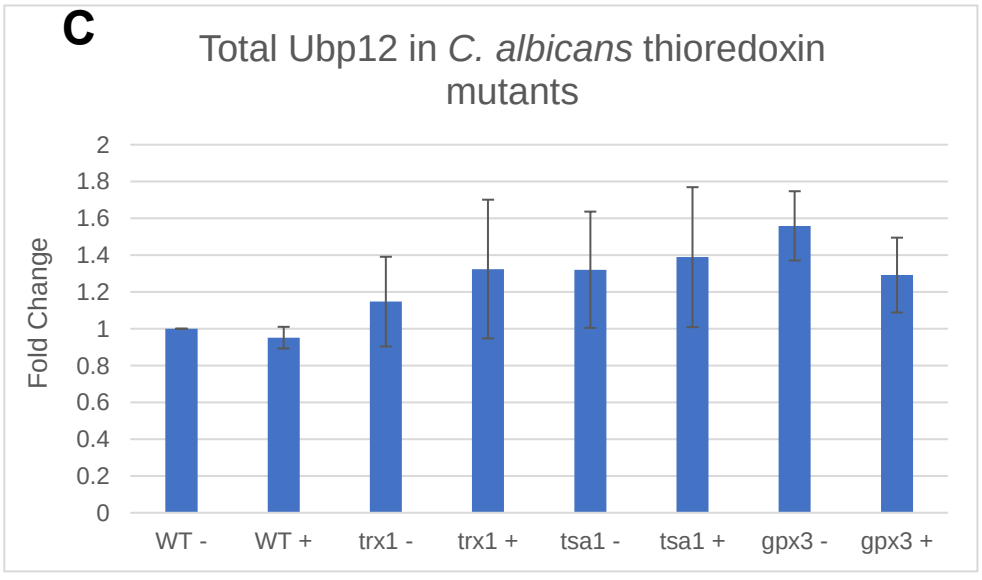
C
Total Ubp12 in C. albicans thioredoxin mutants
Fold Change
0
0.2
0.4
0.6
0.8
1
1.2
1.4
1.6
1.8
2
WT -
WT +
trx1 -
trx1 +
tsa1 -
tsa1 +
gpx3 -
gpx3 +

Figure 5.9. Ubp12 HMW complexes are influenced by the thioredoxin system in *C. albicans*.

A) Representative western blot analysis of protein extracts isolated from mid-log phase growing wild-type (KA102), *trx1*Δ (KA71), *tsa1*Δ (KA96) and *gpx3*Δ (KA76) cells expressing one untagged copy of Ubp12 and one 3HA epitope-tagged copy of Ubp12 (Ubp12-3HA) in YPD media and treated with 5 mM H_2O_2 for 0 (-) or 10 (+) minutes. Protein extracts were prepared in non-reducing conditions, separated by SDS-PAGE and proteins were visualised using anti-HA antibodies. N=3. B) The band intensities of detected HMW species of Ubp12 (as indicated by the red line) were quantified using ImageStudio and the total protein loaded in each lane. C) The band intensities of all Ubp12 species were quantified using ImageStudio and the total protein loaded in each lane. For quantification in (B) and (C) n =3 and error bars denote standard error of the mean. Fold change represents the comparison between the samples and the wild-type 0 minutes H_2O_2 which was set as 1. P values were calculated by T test analysis. Only significant P values are displayed. PageRuler Prestained Protein Ladder (ThermoScientific) was used.

Similar to the experiment described in Figure 5.7, the addition of 5 mM H_2O_2 resulted in the formation of oxidised HMW species of Ubp12 in the wild-type strain although this result was not significant using T test analysis (Figure 5.9A and B). Hence, more repeats would be required to support this conclusion. Interestingly, there appears to be an increased amount of HMW species detected prior to H_2O_2 treatment in each of the thioredoxin system mutants (Figure 5.9A and B). However, unpaired T test analyses of this data revealed that the only significant difference detected was between wild-type cells and *tsa1*Δ cells prior to H_2O_2 exposure (P = 0.0301) (Figure 5.9B). After H_2O_2 treatment, T test analyses did not reveal any significant differences between the amount of HMW Ubp12 species found in wild-type cells compared with all the thioredoxin mutant strains tested here. This contrasts with the results obtained using comparable thioredoxin system mutant strains of *S. cerevisiae* (Figure 3.2), although it is important to note that the quantification in *S. cerevisiae* was performed on specific HMW forms of Ubp12, not all HMW species as done in *C. albicans*. In *S. cerevisiae,* the formation of oxidised HMW Ubp12 complexes (including two unidentified forms of Ubp12 indicated by red asterisks) is increased in *trx1Δtrx2*Δ cells compared to wild-type cells following H_2O_2 exposure (Figures 3.2, 3.8, 3.9, 3.10). Additionally, formation of an oxidised Ubp12 species, intermediate in mobility between the unstressed, reduced form of Ubp12 and the HMW disulphide, was also observed in *trx1Δtrx2*Δ cells in *S. cerevisiae* regardless of H_2O_2 exposure, which is not readily detectable in any of the thioredoxin mutants in *C. albicans* (compare Figures 3.2 and

5.9). However, although mostly not significant by T test analyses, there could in fact be differences in the formation of the Ubp12 HMW complexes in response to H_2O_2 in various thioredoxin system mutants compared to wild-type cells in *C. albicans* (Figure 5.9B) but this would need further repeats of the western analysis to assess whether these possible differences are significant or not.

The studies of Ubp12 in *S. cerevisiae* described in Chapter 3 revealed that the abundance of Ubp12 is lower in specific thioredoxin system mutants when the abundance of Ubp12 was examined in non-reducing conditions (Figure 3.2). The basis for this effect was not clear but other experiments presented in Chapter 3 suggested that this effect of the thioredoxin system mutations could be due to altered oxidation of Ubp12 (see Chapter 3 section 3.2.1). Hence the abundance of Ubp12 was examined in wild type and thioredoxin system mutant *C. albicans* cells to assess whether the thioredoxin system and/or exposure of cells to H_2O_2 influences the amount of Ubp12 detectable in cells (Figure 5.9A and C). Interestingly, in contrast to the studies described in Chapter 3 in *S. cerevisiae*, T test analyses did not reveal any significant differences compared to unstressed wild type cells in abundance of Ubp12 in any of the thioredoxin system mutants or in response to H_2O_2 in either wild type cells or thioredoxin system mutant cells following exposure to H_2O_2 (Figure 5.9C). Hence, these analyses of abundance in the two yeast species suggests that the thioredoxin system possibly affects Ubp12 differently in *S. cerevisiae* and *C. albicans*.

5.2.5 Analysis of the role of Ubp12 in global ubiquitination in *C. albicans*

Global ubiquitination in *S. cerevisiae* is influenced by oxidative stress such as H_2O_2 (Finley, 2009, Shang and Taylor, 2011, Curtis, 2019). For example, previous work from our lab revealed that treatment of cells of the W303 and BY4741 strain backgrounds with H_2O_2 resulted in an increase in HMW poly-ubiquitin conjugates and a corresponding decrease in the levels of free ubiquitin (Curtis, 2019). The underlying mechanisms associated with these H_2O_2-induced changes in free ubiquitin/poly-ubiquitination are not well understood and there is no evidence for a role for Ubp12 in these mechanisms in *S. cerevisiae* (Curtis, 2019). However, as described above, Ubp12 in *S. cerevisiae* and *C. albicans* may play different roles in responses to

oxidative stress in these two yeast species and hence it was possible that Ubp12 in *C. albicans* may influence free ubiquitin/poly-ubiquitination. To begin to address whether Ubp12 has any global effects on ubiquitination wild type (KA102) and *ubp12*Δ (KA103 and KA108) cells were grown to mid-log phase and protein extracts obtained in non-reducing conditions. Global ubiquitination was then examined by western blot analysis, including analysis of the stacking gel to detect large HMW poly-ubiquitinated complexes (Seyfried et al., 2008) (Figure 5.10).

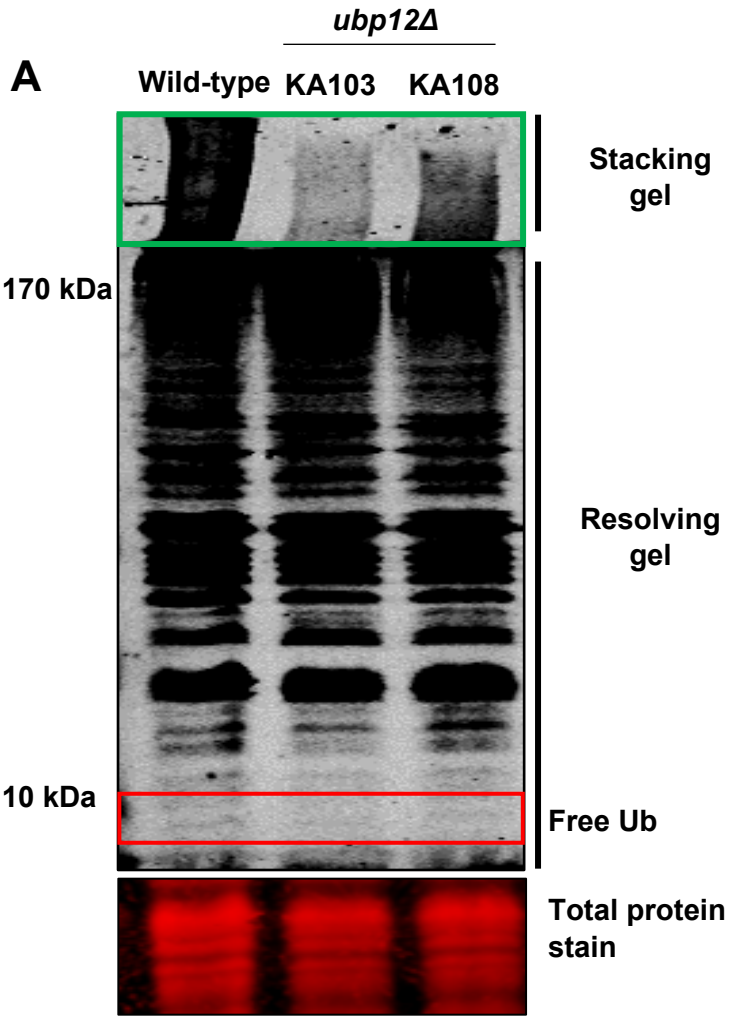
A
ubp12Δ
Wild-type
KA103
KA108
Stacking gel
170 kDa
Resolving gel
10 kDa
Free Ub
Total protein stain

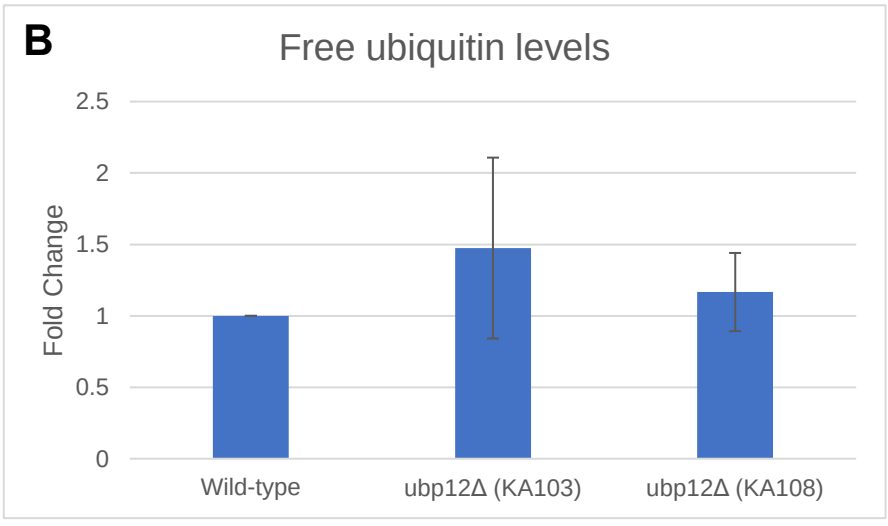
B
Free ubiquitin levels
Fold Change
2.5
2
1.5
1
0.5
0
Wild-type
ubp12Δ (KA103)
ubp12Δ (KA108)

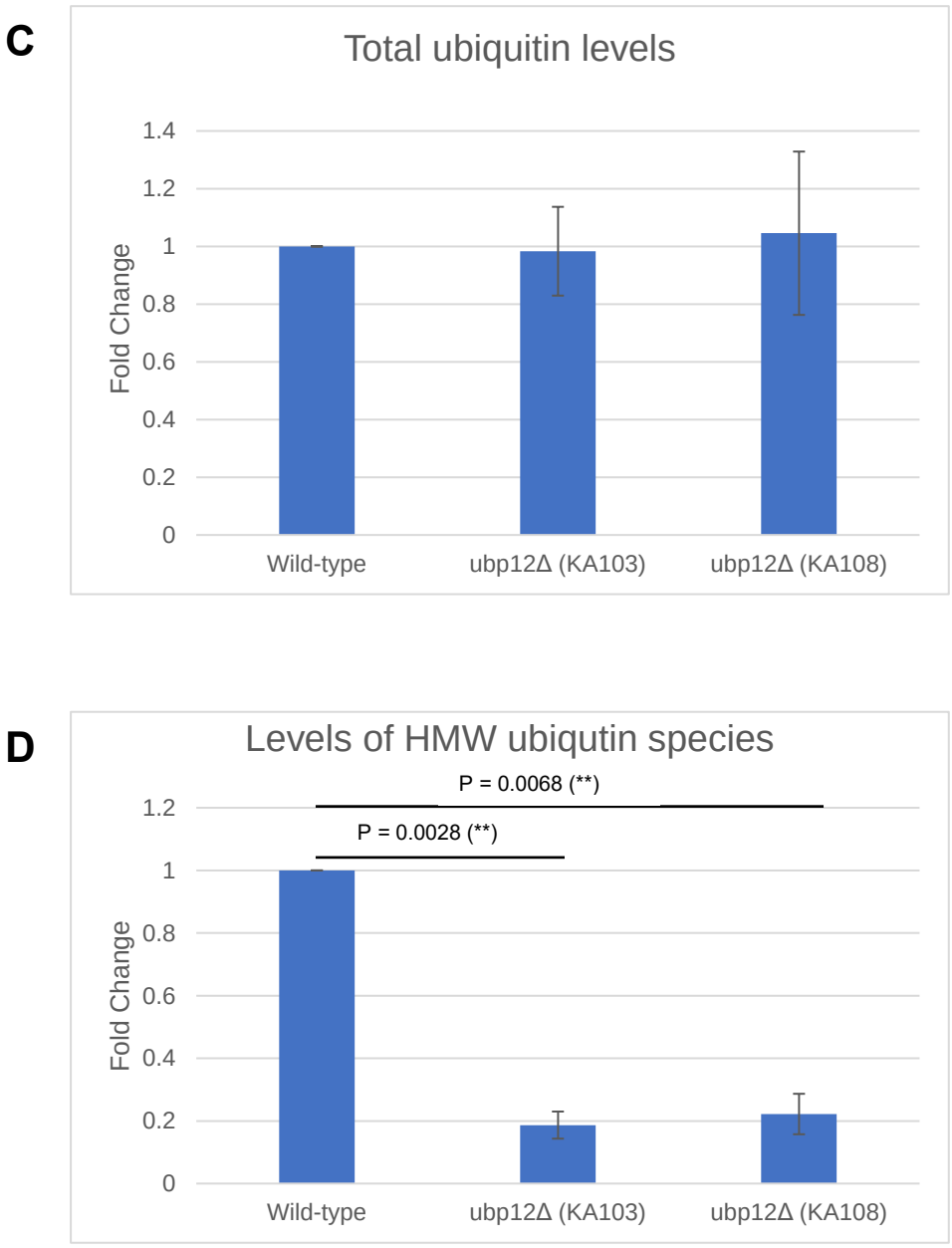

Figure 5.10. Ubp12 activity influences HMW poly-ubiquitinated proteins in *C. albicans.*

A) Western blot analysis of protein extracts prepared in non-reducing conditions from mid-log phase growing wild-type (KA102) cells and *ubp12*Δ cells (KA103 and KA108) cells in YPD media at 30ºC. Proteins were separated by SDS-PAGE and ubiquitin was visualised using anti-ubiquitin antibodies. Free ubiquitin is indicated (red box). B) The band intensities of free ubiquitin were quantified using ImageStudio and the total protein loaded in each lane. C) The band intensities of all ubiquitinated species (including free ubiquitin) were quantified using ImageStudio and the total protein loaded in each lane. D) The band intensities of the HMW poly-ubiquitinated species in

the stacking gel (green box) were quantified using ImageStudio and the total protein loaded in each lane. (B-D) For all quantification n =3 and error bars denote standard error of the mean. Fold change represents the comparison between the samples and the wild-type which was set as 1. P values were calculated by T test analysis. Only significant P values are displayed. PageRuler Prestained Protein Ladder (ThermoScientific) was used.

Similar to our previous studies in *S. cerevisiae* BY4741 and W303 strains (Curtis, 2019), loss of Ubp12 function in *C. albicans* did not have any detectable effect on either the levels of free ubiquitin or on the amount of total ubiquitin measured as the combination of levels of free ubiquitin and ubiquitin present in ubiquitinated substrates (Figure 5.10A-C). These results suggest that Ubp12 in both yeast species do not have major roles in these particular aspects of the ubiquitin cycle. However, unexpectedly, loss of Ubp12 was found to have an important role in the regulation of large poly ubiquitinated proteins in *C. albicans* (Figure 5.10A and D). In particular, a significant reduction in large poly ubiquitinated proteins in cell extracts isolated from both *ubp12*Δ strains, compared with extracts from wild-type cells, was detected in the stacking gel region (Figure 5.10A and D). Indeed, significance was indicated by T test analysis with P values of 0.0028(**) and 0.0068(**) obtained when KA103 and K108 *ubp12*Δ data were compared with wild-type data, respectively. Given that no significant differences in either free ubiquitin or total protein ubiquitination was detected in *ubp12*Δ cells compared with wild-type cells (Figure 5.10B and C), these data suggest that the lower levels of large poly ubiquitinated proteins detected in *ubp12*Δ cells may result in an increase in the levels of faster migrating poly ubiquitinated proteins in *ubp12*Δ cells. However, this could be difficult to detect given the very large amount of faster migrating ubiquitinated proteins present in wild-type and *ubp12*Δ cells (Figure 5.10A). It is also possible that the large poly ubiquitinated proteins are more sensitive to degradation in cells lacking Ubp12. Analyses of the ubiquitination status and stability of future identified Ubp12 substrates would be required to help resolve the potential explanations for these observations. However, in summary the observation that Ubp12 in *C. albicans*, but not *S. cerevisiae*, likely influences the poly ubiquitination of multiple proteins has revealed differences in the functions of this DUB in these two yeast species.

5.2.6 Analysis of the potential role of Ubp12 in the growth and morphology of *C. albicans*

As described above loss of Ubp12 function in *C. albicans* resulted in changes to global ubiquitination indicating that Ubp12 functions in normal growth conditions. Although no obvious differences in the growth of wild type and *ubp12*Δ cells was detected on the control (unstressed) plates in the sensitivity tests (Figure 5.6) it was possible that Ubp12 influenced the growth of *C. albicans* in unstressed conditions. To examine this possibility the growth of wild type (KA102) and *ubp12*Δ (KA103) cells was examined in liquid YPD media at 30ºC (Figure 5.11). Interestingly, consistent with the changes in global ubiquitination in cells lacking Ubp12 were found to have a slower growth rate than wild type cells (Figure 5.11). Furthermore, analyses of the data revealed that the doubling time of the wild type cells was 141.8 (+/-6) minutes versus a doubling time of 173.8 (+/-17) minutes for the *ubp12*Δ cells. This data was found to be non-significant (P = 0.073), however this could be due to the large error observed in the *ubp12*Δ strain (as a result of one repeat) and hence a further repeat would be necessary to validate any difference between the growth of the two strains. Although non-significant, the basis of the slower growth associated with loss of Ubp12 function in *C. albicans* is not known at this stage.

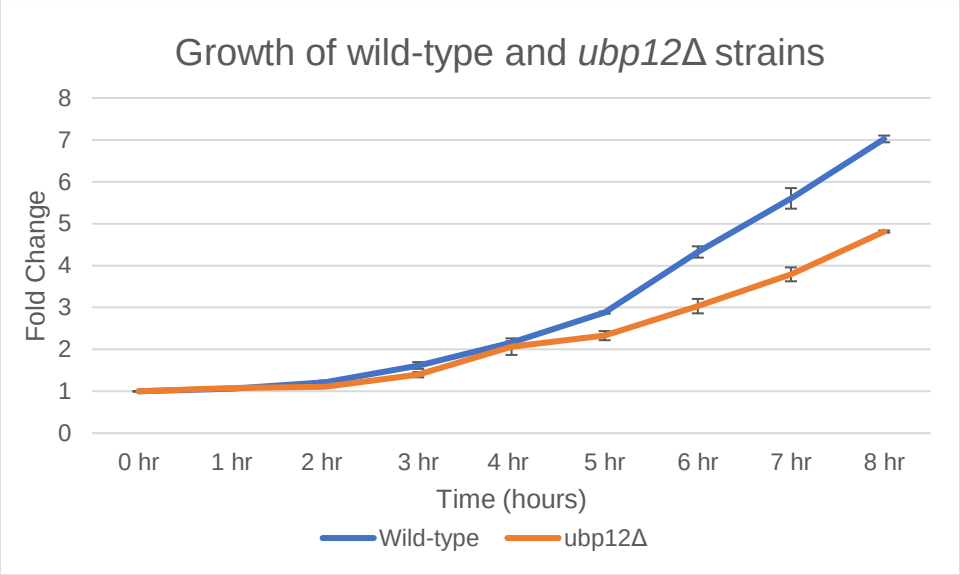

Figure 5.11. Growth curve of wild-type and *ubp12*Δ *C. albicans* cells.

Mid-log phase wild type (KA102) and *ubp12*Δ (KA103) cells were grown in YPD at 30°C for 8 hours and the OD_{660} of each culture measured every 60 minutes. The data was plotted as the fold change in OD at each time point compared with the Time 0 value which was set as 1. Error bars denote standard error of the mean, n = 3.

Having established that although non-significant, the growth of *ubp12*Δ cells is slightly slower than wild-type cells, the next step was to examine the cell morphology of cells lacking Ubp12 function in different growth conditions. Indeed, *C. albicans* can switch to different morphological forms dependent on environmental conditions (Figure 5.12). For example, *C. albicans* cells can grow and divide as a budding yeast or, in response to stress conditions such as hydroxyurea or H_2O_2, switch to a hyperpolarised bud morphology (da Silva Dantas et al., 2010, Bachewich et al., 2003). These different morphological forms can aid *C. albicans* response to the immune system. For example, hyphae are formed in response to phagocytosis to pierce the phagocyte and allow fungal escape (McKenzie et al., 2010). Interestingly, the hyperpolarised morphology is distinct from other filamentous forms of *C. albicans* such as the hyphal morphology or pseudohyphae which are stimulated by different conditions (Figure 5.12) (Whiteway and Bachewich, 2007). The role of the hyperpolarised growth in response to H_2O_2 is unclear, although it has been theorised that this may be an important defence mechanism of *C. albicans* when these cells encounter ROS-producing microorganisms (Dantas et al., 2015).

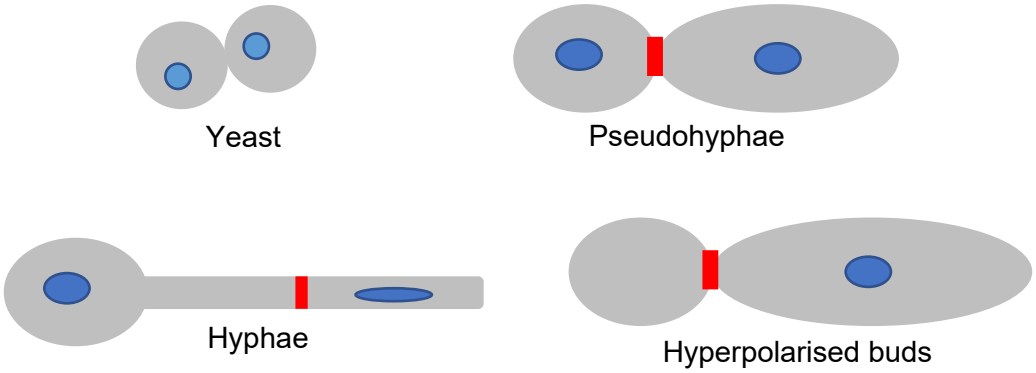

Figure 5.12. Different morphological forms of *C. albicans*.

C. albicans can exist as budding yeast, pseudohyphae, hyphae and hyperpolarised buds. Pseudohyphae area multicellular form of *C. albicans* characterised by constrictions at the point of septation of mother and daughter cells and are wider in diameter than hyphae. Hyphae are also multicellular, however are thinner in diameter than pseudohyphae, lack constrictions at the point of septation of mother and daughter cells and have parallel sides. Hyperpolarised buds are a single, elongated cells due to the presence of a single nucleus, found in the extended bud of the cell. They also have a constriction at the point of septation (Sudbery et al., 2004, Bachewich and Whiteway, 2005, da Silva Dantas et al., 2010).

Hence, given the results presented above, it was possible that Ubp12 may have a role in normal cell morphology under a range of different environmental conditions. To begin to investigate the potential role of Ubp12 in cell morphology and different cell growth mechanisms the first step was to test whether *ubp12*Δ cells show any morphological changes when growing in unstressed conditions in YPD at 30˚C. Cultures of wild-type (KA102) and *ubp12*Δ (KA103 and KA108) cells were grown to mid-log phase in YPD at 30˚C and the cells imaged (Figure 5.13).

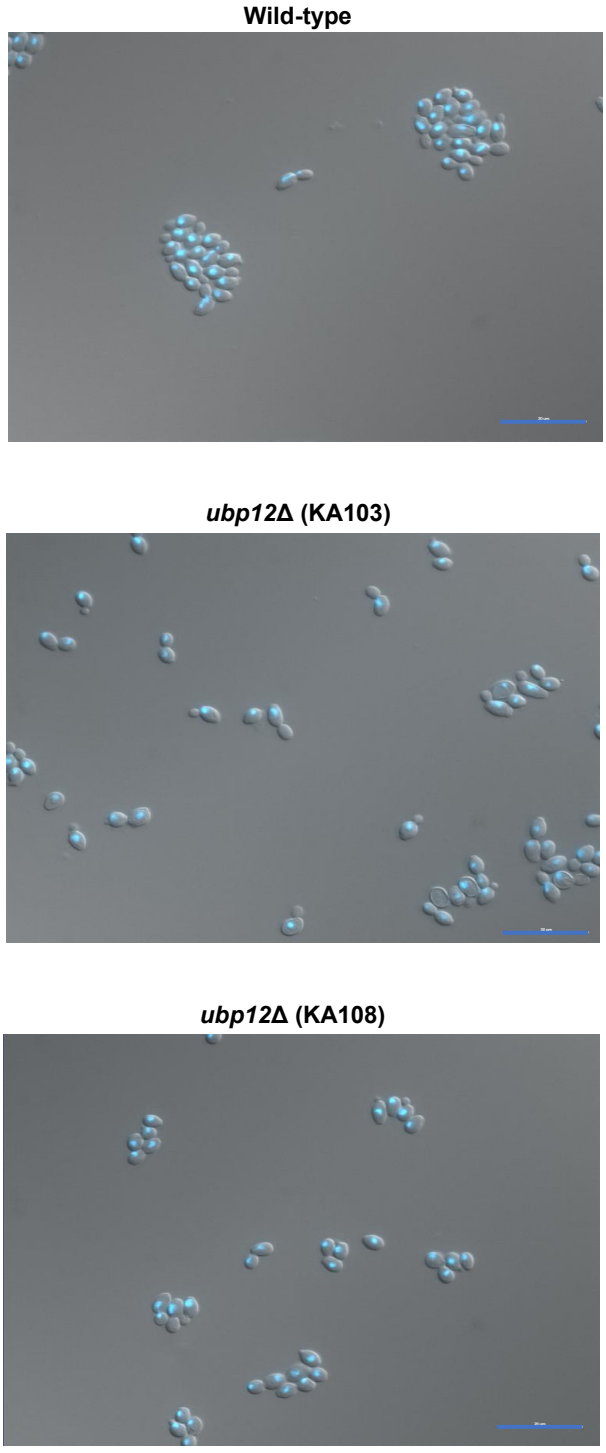

Figure 5.13. Loss of Ubp12 function does not affect cell morphology in unstressed growth conditions.

Wild-type (KA102), Ubp12-3HA (KA69) and *ubp12*Δ (KA103 and KA108) cells were grown to mid-log phase in YPD at 30°C, fixed and imaged by DIC using a fluorescence microscope with a 63X objective. Nuclear staining by DAPI is represented by the blue. Images are overlay images of DIC and DAPI fluorescence. Scale bars = 20 μm. N = 1.

Despite growing slower than wild-type cells, cell lacking Ubp12 appear very similar in size, shape and nuclear morphology/positioning compared with wild-type cells (Figure 5.13). Hence, this data raises the possibility that the metabolism of *ubp12*Δ cells may be lower than wild-type cells as the longer doubling time of *ubp12*Δ cells is not obviously reflected as larger cells. Alternatively, it is possible that the viability of cells within *ubp12*Δ cultures may be lower which would result in an apparent increase of the doubling time of the culture. Further experimentation would be required, together with FACS analyses, of *ubp12*Δ cultures to investigate these possibilities.

Next, the ability of *ubp12*Δ cells to induce the yeast to hyphae switch in morphology was examined. Wild-type (KA102) and *ubp12*Δ (KA103) cells were diluted 1:10 from stationary phase with YPD supplemented with 10% (v/v) serum to induce the yeast-hyphae switch (Taschdjian et al., 1960). Cells were grown at 37°C (which also induces hyphal growth) over a 3-hour period and the cells imaged (Figure 5.14). Interestingly, the budding yeast to hyphae switch was delayed in *ubp12*Δ cells compared to wild-type cells (Figure 5.14). For example, after 1 hour incubation with serum the wild-type cells, in contrast to *ubp12*Δ cells, began to form hyphae (Figure 5.14A).

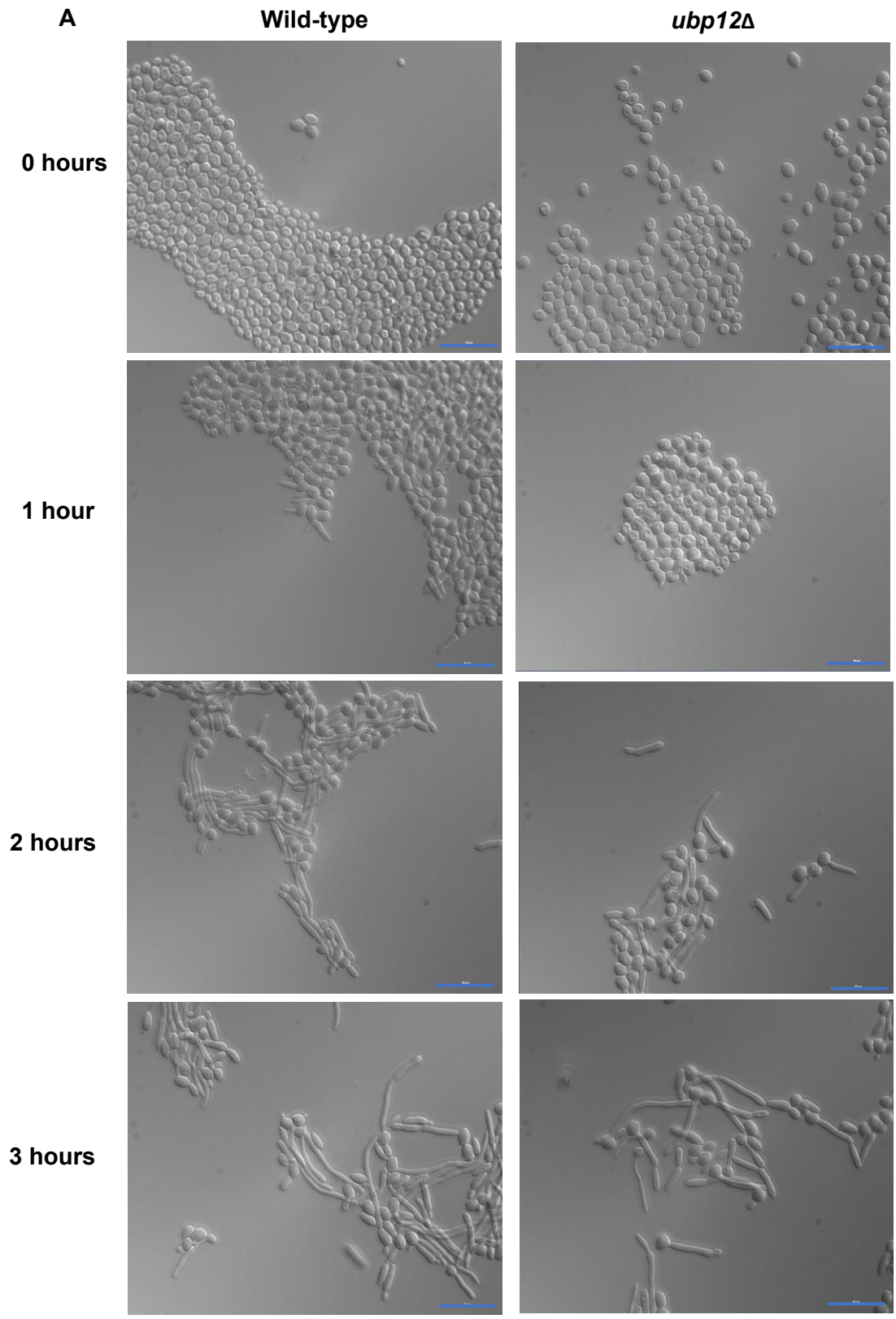
A
Wild-type
ubp12Δ
0 hours
1 hour
2 hours
3 hours

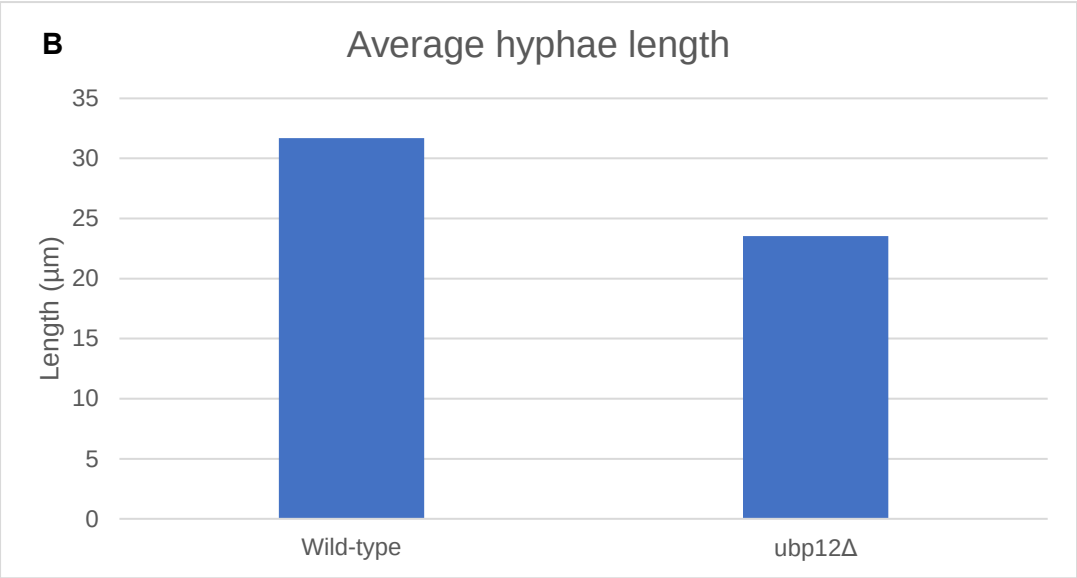

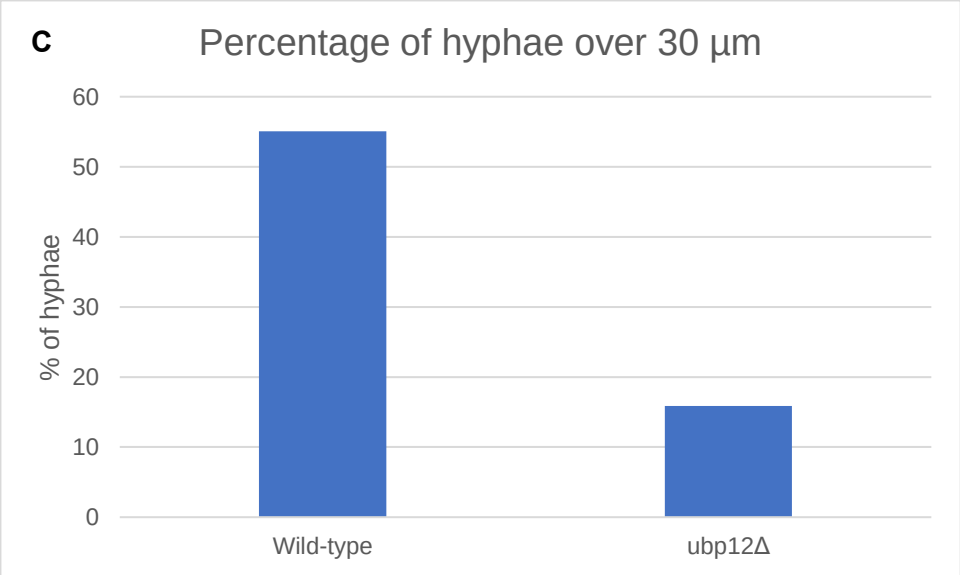

Figure 5.14. *ubp12*Δ cells display a delay in the budding yeast to hyphae switch.

A) Wild-type cells (KA102) and *ubp12*Δ cells (KA103) were grown to stationary phase in YPD, diluted 1:10 in YPD containing 10% (v/v) serum and grown for 3 hours at 37°C. Cells were collected at the indicated time points, fixed and DIC images obtained using a fluorescence microscope with a 63X objective. Scale bars = 20 µm. (B and C) The average length of hyphae (B) and the number of cells with hyphae greater than 30 µm (C) were calculated from 100 cells of each strain after 3 hours using the Graphics tool in Zen 2 (Blue Edition) Carl Zeiss imaging software. N = 1.

In addition, after 3 hours incubation with serum the average hyphae length of wild-type cells was 31.5 μm whilst in contrast the average hyphae length of *ubp12*Δ cells was 24.1 μm (Figure 5.14B). Furthermore, at the same time point only 19% of *ubp12*Δ hyphal cells were measured to be a length of 30 μm or over compared to 56% of hyphal cells in the wild-type strain (Figure 5.14C). However, this data has only been obtained from N=1 and hence further repeats would be required to confirm these conclusions. Nevertheless, this preliminary data suggests that Ubp12 function influences the budding yeast to hyphal switch. It is also worth noting that, although non-significant, *ubp12*Δ cells have a longer doubling time than wild-type cells and hence it is possible that loss of Ubp12 only indirectly affects this morphology change through the effect of the *ubp12*Δ mutation on cell division.

As described above *C. albicans* cells can also switch from budding yeast to a hyperpolarised bud morphology (Figure 5.12) in response to stress conditions such as hydroxyurea or H_2O_2 (da Silva Dantas et al., 2010). Cells lacking Ubp12 results in altered sensitivity/resistance to hydroxyurea and H_2O_2 (Figure 5.6) and hence the potential role of Ubp12 in the formation of hyperpolarised buds in response to hydroxyurea and H_2O_2 was examined. Mid-log phase wild-type (KA102) and *ubp12*Δ (KA103) cells growing in YPD media at 30˚C were treated with either 5 mM H_2O_2 or 40 mM hydroxyurea for 0 or 6 hours and the cells imaged (Figure 5.15).

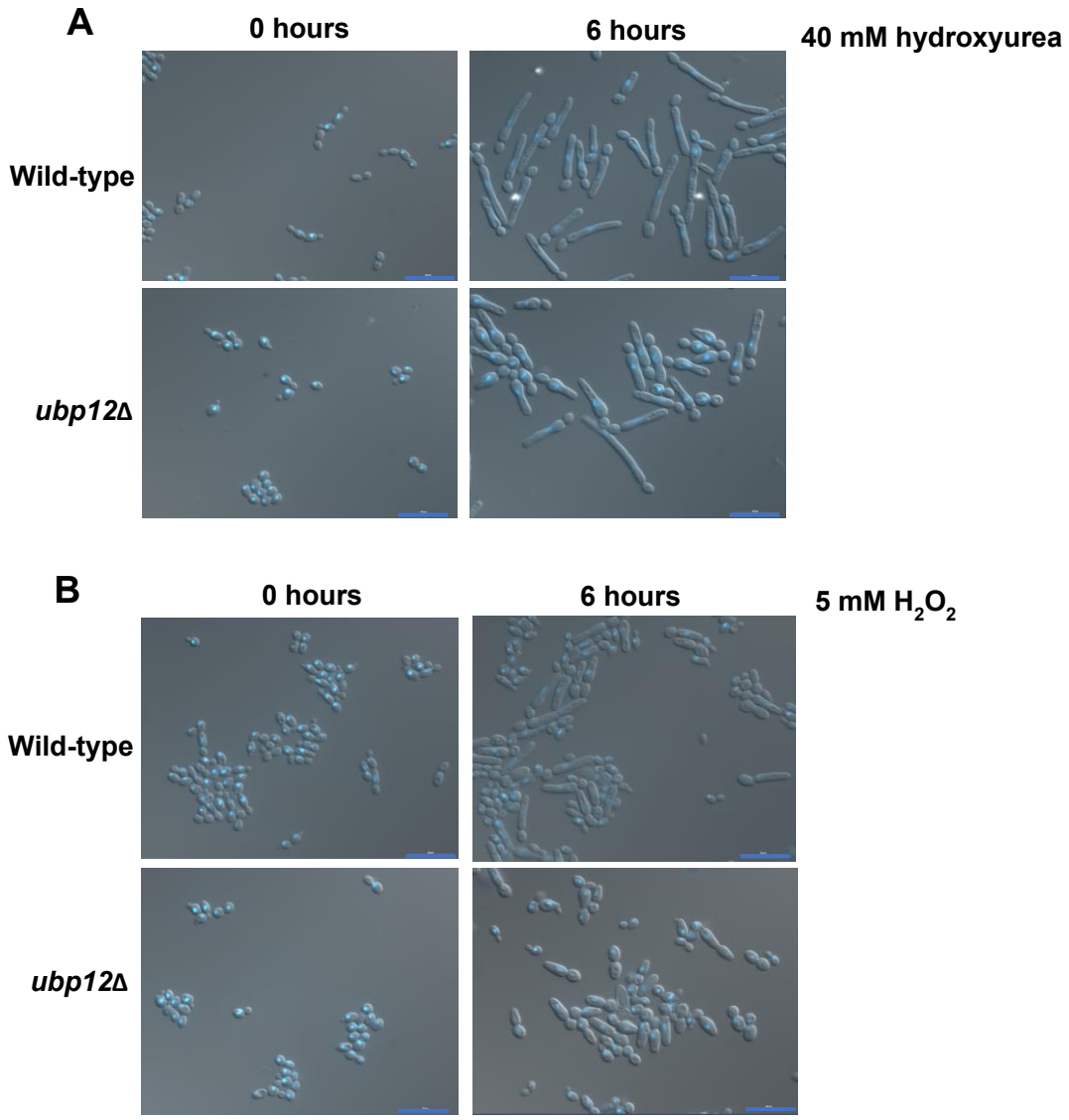

Figure 5.15. Ubp12 influences the formation of hyperpolarised buds.

(A and B) Wild-type cells (KA102) and *ubp12*Δ cells (KA103) were grown to mid-log phase in YPD at 30˚C and treated with either (A) hydroxyurea or (B) H_2O_2 at the indicated concentrations for 0 or 6 hours. Cells were fixed and DIC images obtained using a fluorescence microscope with a 63X objective. Nuclear staining by DAPI is represented by the blue. Images are overlay images of DIC and DAPI fluorescence. Scale bars = 20 µm. N = 1.

As expected, treatment of wild-type cells with either hydroxyurea or H_2O_2 resulted in the formation of well-defined hyperpolarised bud morphology (Figure 5.15) (da Silva Dantas et al., 2010). Qualitative observation of multiple images (data not shown) of the hyperpolarised buds formed in response to hydroxyurea in *ubp12*Δ cells suggest

that, although some cells look very similar in length to the wild-type cells, overall, the *ubp12*Δ cells are perhaps not quite as elongated as wild type cells in the same conditions (Figure 5.15A). However, this experiment has only been performed once and hence the experiment should be repeated with quantitative assessment of cell length.

Excitingly, a much more striking qualitative difference in cell morphology was observed when images of wild type and *ubp12*Δ cells treated with H_2O_2 were compared. In contrast to the perhaps subtle difference in the formation of hyperpolarised buds in the hydroxyurea treated wild-type and *ubp12*Δ cells, when treated with H_2O_2 there was a marked qualitative reduction in cell length, using multiple images, of the *ubp12*Δ cells in comparison with the wild-type cells (Figure 5.15B and data not shown). Again, this experiment has only been performed once and hence the experiment should be repeated with quantitative assessment of cell length. However, the data does suggest that, in contrast to hydroxyurea treated cells, there is significant inhibition of the formation of hyperpolarised buds in the *ubp12*Δ cells. Although it is possible that one or both effects (if repeated) of loss of Ubp12 function on the formation of hyperpolarised buds in response to hydroxyurea and H_2O_2 may be linked to the slow growth phenotype of *ubp12*Δ cells (Figure 5.11) the fact that the effect in response to H_2O_2 appears much greater than hydroxyurea suggests that Ubp12 may have a specific role to play in hyperpolarised bud formation in response to H_2O_2.

In summary, the data presented in this section suggests that Ubp12 may be important for different morphology transitions in *C. albicans*. It is not clear at this stage whether these effects are indirectly linked to the growth defect associated with loss of Ubp12 function. However, there is some evidence to suggest that Ubp12 may have specific function in morphology transitions in response to H_2O_2.

5.3 Discussion

Very little was known about the functions and regulation of the Ubp12 DUB in *C. albicans* prior to the research presented in this chapter, although interestingly polymorphisms in this DUB have been linked to fungal disease in patients (Zhang et al., 2009). As described elsewhere in this thesis Ubp12 in *S. cerevisiae* has been linked to oxidative stress responses. Excitingly, Ubp12 was found to be involved in oxidative stress responses and responses to other stress conditions in *C. albicans*

and, similar to Ubp12 in *S. cerevisiae*, Ubp12 in *C. albicans* is oxidised in response to specific oxidative stress conditions and the protein is influenced by the thioredoxin system. However, the roles and regulation of Ubp12 in oxidative stress responses in *C. albicans* also shows significant differences with *S. cerevisiae*. Furthermore, in contrast to *S. cerevisiae*, Ubp12 in *C. albicans* was found to have a significant role in maintaining global levels of poly-ubiquitination. Finally, initial studies of Ubp12 in *C. albicans* has suggested links to the regulation of growth programmes previously linked to virulence.

Given the results presented in Chapter 3 of thesis examining Ubp12 in oxidative stress responses, this chapter aimed to assess if these oxidative stress responses were conserved in *C. albicans*. Spot tests analysis revealed that *ubp12*Δ cells are slightly sensitive to menadione, sensitive to diamide and resistant to H_2O_2 compared to the wild-type strain (Figure 5.6). Interestingly, *C. albicans ubp12*Δ cells respond oppositely to *S. cerevisiae ubp12*Δ cells to diamide and H_2O_2 stress; treatment with H_2O_2 causes sensitivity in *S. cerevisiae ubp12*Δ cells yet resistance in *C. albicans ubp12*Δ cells, and diamide causes resistance in *S. cerevisiae ubp12*Δ cells yet sensitivity in *C. albicans ubp12*Δ cells (Figures 4.1 and 5.6). This suggests that the link between Ubp12 and oxidative stress responses is conserved but the precise roles may be different in response to H_2O_2 and diamide. However, it is also possible that the substrates of Ubp12 are conserved between these two yeast species but fulfil different cellular roles causing the phenotypic differences observed in Figure 5.6. Interestingly, sensitivity in *ubp12*Δ cells to menadione is conserved between *S. cerevisiae* and *C. albicans* (Figures 4.1 and 5.6), however, whether this is via the same mechanism requires further exploration.

To further characterise the role of Ubp12 in *C. albicans,* DNA damage responses (induced by UV light) and DNA replication stress responses (induced by hydroxyurea) were examined in *ubp12*Δ cells. Interestingly, in response to both agents, *ubp12*Δ cells displayed sensitivity, suggesting a possible for Ubp12 in DNA damage responses in *C. albicans* (Figure 5.6). This experiment was not performed in *S. cerevisiae* and so discussion on conservation is not possible, however it is interesting to note that in *S. cerevisiae* Ubp12 has been shown to deubiquitinate PCNA in order to regulate DNA damage responses (discussed in detail in 1.3.4.1) (Álvarez et al., 2019). In addition to this, Ubp12 in *S. pombe* regulates DNA replication during S phase via deubiquitination

events on PCNA (see 1.3.4.1) (Álvarez et al., 2016). PCNA ubiquitination in *C. albicans* has been documented, but the DUB(s) responsible for deubiquitination remains unknown (Zeng and Xiao, 2022). It is tempting to speculate that the sensitive phenotype observed in *ubp12*Δ cells in response to DNA damaging agents is due to a potential role for Ubp12 in PCNA deubiquitination given the conserved roles for Ubp12 in other yeast species in this process, although further experimentation is necessary to confirm this speculation. Thus, to fully understand the different sensitivities of *ubp12*Δ cells in both *C. albicans* and *S. cerevisiae* to oxidising agents and DNA stresses, identification of Ubp12 substrates is necessary.

Having established a link between Ubp12 in *C. albicans* and oxidative stress responses, the potential oxidation of Ubp12 was examined. In *S. cerevisiae*, Ubp12 forms a HMW intramolecular disulphide via its catalytic cysteine residue in response to H_2O_2 but not diamide (Curtis, 2019). Interestingly, chapter 3 of this thesis has revealed a role for the H_2O_2-specific thioredoxin system in regulating the oxidation of Ubp12 into various HMW forms. Data from this chapter has shown that Ubp12 in *C. albicans* also forms an oxidised, HMW complex(es) in response to H_2O_2 (Figure 5.7). However, in contrast to the data from *S. cerevisiae*, an oxidised HMW complex(es) was also induced in response to diamide (Figure 5.7). Some investigation into the role of the thioredoxin system on the H_2O_2-induced Ubp12 HMW complex(es) in *C. albicans* has been performed, revealing that there is more HMW Ubp12 species in thioredoxin mutants compared to wild-type cells, although this was found to be only significant for the *tsa1*Δ strain (Figure 5.9). Interestingly, analysis of thioredoxin system mutants in *S. cerevisiae* found that in *trx1*Δ*trx2*Δ and *trr1*Δ cells, unidentified oxidised HMW forms of Ubp12 were present, some of which were induced by H_2O_2 (Figures 3.2, 3.9, 3.10, 3.11). It is possible that this is true in *C. albicans* thioredoxin system mutants (Figure 5.9B), however the signals detected on the western blots are more diffuse and challenging to quantify. Chapter 3 also revealed a role for Trr1 in the regulation of Ubp12 oxidation in *S. cerevisiae*; Ubp12 abundance was significantly lower in *trr1*Δ cells under non-reducing conditions, which was restored under reducing conditions, suggesting Trr1 regulates various forms of oxidised Ubp12 that did not migrate with known species (Figures 3.2 and 3.3). *TRR1* is an essential gene in *C. albicans* and so this effect could not be investigated, however none of the thioredoxin system mutants analysed seem to regulate Ubp12 in this way (Figure 5.9). The

glutathione system was not analysed in this chapter, thus further experimentation using glutathione system mutants and BSO would be useful to clarify any role(s) for the glutathione system in regulating Ubp12 in *C. albicans*.

No evidence has been presented to suggest that the Ubp12 HMW complex(es) formed in response to H_2O_2 and diamide in *C. albicans* are the same complex(es) as formed in *S. cerevisiae*, thus analysis of cysteine residues involved in these complexes would begin to clarify their conservation. If the HMW Ubp12 complexes formed in *C. albicans* are found to involve the catalytic cysteine residue, it is interesting to note the different sensitivities *C. albicans ubp12*Δ cells to these two agents (Figure 5.6), although the time-frame of these two experiments is considerably different (western blot analysis 10 minutes exposure versus spot tests 2 days exposure). It is possible that formation of an inactivated, oxidised form of Ubp12 utilising the catalytic cysteine residue in *C. albicans* could fulfil different functions dependent upon the stress experienced. In response to H_2O_2, the HMW complex(es) formed may primarily fulfil an inhibitory role in *C. albicans*, preventing downstream deubiquitination events to aid cellular responses to H_2O_2, correlating with the resistance observed in *ubp12*Δ cells (Figure 5.6). Conversely, in response to diamide stress, the formation of Ubp12 HMW complex(es) utilising the catalytic cysteine residue in *C. albicans* may fulfil a protective role, preventing irreversible oxidation of Ubp12 thus allowing Ubp12 deubiquitination events to occur when levels of ROS are decreased, as hypothesised with the H_2O_2-induced Ubp12 disulphide in *S. cerevisiae*. If the catalytic cysteine is not involved in the formation of these Ubp12 HMW species in *C. albicans*, it is possible they could also fulfil an activating role for Ubp12, and that oxidation of Ubp12 is necessary for its catalytic function. Hence, mutagenic analysis of the cysteine residues of Ubp12 in *C. albicans* is essential to clarify the function of these HMW species. It is also important to assess if they are a form of dimerisation, either with another Ubp12 protein as a homodimer or with another protein as a heterodimer.

The signals of the Ubp12 HMW complexes are more diffuse and qualitatively, seem much lower, compared to the Ubp12 HMW complexes formed in *S. cerevisiae* (compare Figures 3.2 and 5.7). This could imply that the oxidised form of Ubp12 in *C. albicans* forms a different three-dimensional shape, altering migration in the gel, or perhaps that there are other oxidised forms of Ubp12 migrating at a similar molecular weight, giving the impression of a smear on the blot. However, this could also be

potentially due to the kinetics of the modification in *C. albicans* being slower, or the subcellular localization of Ubp12 and where it becomes oxidised. There has been no kinetic analysis of the formation of the Ubp12 HMW disulphide in *C. albicans* in this thesis or in the published literature, however it is possible that a higher, relative amount of ROS, or a longer exposure to ROS, is necessary to oxidise a comparable amount of the protein. In *S. cerevisiae* Ubp12 is found in the cytosol, nucleus and mitochondria but the subcellular localisation of Ubp12 in *C. albicans* has not yet been documented. It is possible that the subcellular location of Ubp12 in *C. albicans* is not the same as in *S. cerevisiae*, thus the amount of protein exposed to ROS may differ. Given that the subcellular location of Ubp12 in *C. albicans* has not yet been elucidated, it is possible that this affects the sensitivity of ROS-induced Ubp12 HMW species. Indeed, in *S. cerevisiae*, Ubp12 is an important regulator of mitochondrial morphology, thus will experience a high level of H_2O_2 (Anton et al., 2013). Thus, a large proportion (approximately 40%) of the protein is oxidised in response to H_2O_2 (Figure 3.2), potentially as a protective mechanism. Therefore, the location of Ubp12 within *C. albicans* cells could affect the levels (and types) of ROS experienced and the level of Ubp12 oxidation.

Previous studies of global ubiquitination found that H_2O_2 and not diamide induced the formation of HMW poly-ubiquitinated substrates in *S. cerevisiae*, but Ubp12 did not affect the levels of HMW polyubiquitinated proteins (Curtis, 2019). However, as described above, there are clearly differences in the roles of Ubp12 in *S. cerevisiae* and *C. albicans*, and so it was possible there was a role for Ubp12 in the regulation of polyubiquitin conjugates in *C. albicans*. Indeed, deletion of Ubp12 causes a decrease in the level of poly-ubiquitinated species in *C. albicans* but does not affect the levels of free ubiquitin (Figure 5.10). A decrease in polyubiquitinated substrates in *ubp12*Δ cells is counter-intuitive when considering the primary role of a DUB. It is possible that Ubp12 prevents the degradation of poly-ubiquitinated species, although this speculation requires further exploration into the substrates of Ubp12 in *C. albicans,* of which none are currently identified. Interestingly, in *S. cerevisiae,* known substrates of Ubp12 (Fzo1, Rad23 and Gpa1) are not destabilised in *ubp12*Δ cells, indicating a non-proteolytic role of this DUB which could be conserved in *C.* albicans (Simões et al., 2018, Gödderz et al., 2017, Wang et al., 2005). It is interesting that Ubp12 is important for regulating HMW polyubiquitin conjugates, but does not alter the levels of free

ubiquitin (Figure 5.10). In *S. cerevisiae,* H_2O_2 regulates the levels of HMW polyubiquitinated substrates but also the levels of free ubiquitin (Curtis, 2019). This data suggests that Ubp12 maybe functions as an endo-DUB in *C.* albicans cleaving whole ubiquitin chains, and has no role in recycling free ubiquitin. Conversely, in *S. cerevisiae*, Ubp12 can function as an endo-DUB, cleaving K48 and K63-linked chains, and an exo-DUB where it can cleave single ubiquitin monomers indiscriminately from polyubiquitin chains (Schaefer and Morgan, 2011, Simões et al., 2018). However, it is possible that Ubp12 functions redundantly with another DUB in *C. albicans* to cleave single ubiquitin monomers and so no alterations to free ubiquitin levels were detectable. Although the specificity of Ubp12 in *C. albicans* remains unclear, there is a clear role for Ubp12 in maintaining HMW-polyubiquitinated proteins, which was not observed in any strain background explored in *S. cerevisiae*. To further this work, assessing the global ubiquitination in *ubp12*Δ *C. albicans* cells under oxidative stress conditions would be useful to explore the roles, if any, of the Ubp12 HMW complexes in regulating global ubiquitination.

C. albicans has different growth forms, such as hyphae, pseudohyphae and hyperpolarised buds (Figure 5.12). These different morphologies are linked to the environment and influence the pathogenicity of *C. albicans*. For example, hyphal growth allows fungal escape from macrophages and hyperpolarised buds are theorised to be important in *C. albicans* response to H_2O_2-producing microorganisms (McKenzie et al., 2010, da Silva Dantas et al., 2010). Understanding the ways in which *C. albicans* regulate their morphology is therefore of high interest. Given the link between Ubp12 and oxidative stress in *C. albicans* explored in this chapter, the potential role of Ubp12 in the filamentous growth of *C. albicans* was explored. Although non-significant, *ubp12*Δ *C. albicans* cells were found to grow slower than wild-type cells in the yeast form and so that has to be considered when evaluating these results. Nevertheless, both experiments used to assess the role of Ubp12 in the formation of filamentous forms of *C. albicans* (the induction of hyphae using serum, Figure 5.14, and the induction of hyper-polarised buds using H_2O_2, Figure 5.15) suggest that deletion of Ubp12 causes a reduction in the ability of cells to form these filamentous forms. It is possible that the slower growing phenotype of *ubp12*Δ cells is also observed in the filamentous growth of *C. albicans ubp12*Δ cells. However, it is interesting to note that the percentage of hyphae over 30 µm observed in *ubp12*Δ cells

after 3 hours incubation with serum is 19%, compared to 56% in wild-type (Figure 5.14). Although hyphae formation may not have a linear relationship with cell doubling times, it is surprising that the percentage of hyphae over 30 μm is so much smaller in the *ubp12*Δ cells. However, the microscopy data is only representative of one repeat and hence repetition of this experiment is essential to confirm this phenotype. In addition, a longer incubation with serum would address whether there is simply a delay in the budding yeast to hyphal transition in *ubp12*Δ cells. The formation of hyper-polarised buds also seems to be stunted in *ubp12*Δ cells (Figure 5.15), particularly in response to H_2O_2. Again, these microscopy images are only representative of one repeat and hence further repeats and quantification would be necessary to validate this result. It is also possible that the slow-growing phenotype of *ubp12*Δ cells is affecting the growth of hyper-polarised buds and so longer time-frame images would be useful to assess if the effect on morphology is delayed or inhibited. However, it is important to note that hyper-polarised buds are induced due to a cell cycle arrest at the G1-S transition (Bachewich et al., 2005, Shi et al., 2007), and hence this process is unlikely to be affected by a slight growth defect. It is also possible that the impaired formation of hyper-polarised buds is linked to the H_2O_2 resistance of *ubp12*Δ cells (Figure 5.6). Previous studies of the formation of hyper-polarised buds in response to H_2O_2, identified Trx1 as a crucial protein in Rad53 activation, whereby H_2O_2 oxidises Trx1, allowing Rad23 activation and the formation of hyperpolarised buds (da Silva Dantas et al., 2010). Given that Ubp12 is known to be regulated by the thioredoxin system in *S. cerevisiae* (Chapter 3 of this thesis), and that there is a potential role for the thioredoxin system for regulating Ubp12 in *C. albicans* (Figure 5.9), there is a possibility the phenotype observed in *ubp12*Δ cells is linked to this regulation by the thioredoxin system. However, this is dependent on longer-time frame images suggesting that the deletion of Ubp12 inhibits, and not delays, the formation of hyperpolarised buds. The role of Ubp12 in *C. albicans* has not been well studied, however one paper has found that the *UBP12* gene is one of 23 genes where polymorphisms arise in particularly virulent strains (Zhang et al., 2009). It is possible that these polymorphisms may affect the potential role of Ubp12 in inducing filamentous growth in *C. albicans*, however more work into the specific functions and substrates of Ubp12 in *C. albicans* is necessary to further this speculation.

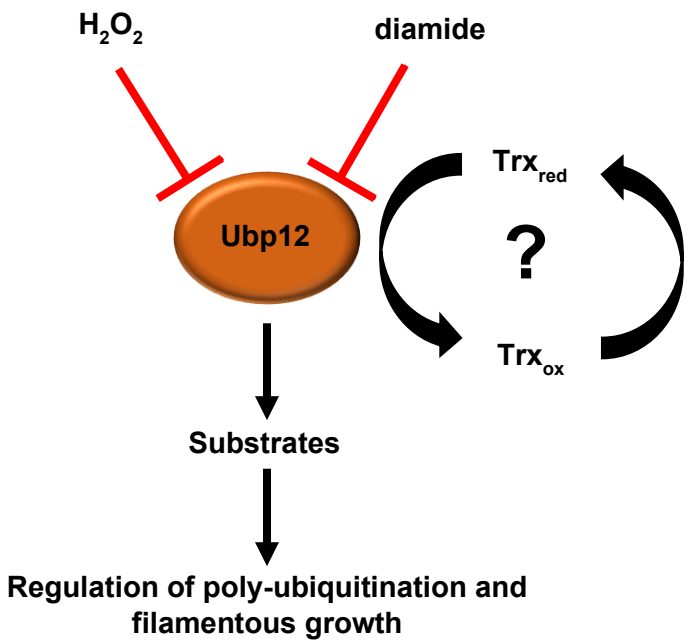

Figure 5.16. Model figure for the possible roles of Ubp12 in *C. albicans*.

It is hypothesised Ubp12 is inactivated (either to prevent its action or protect it from irreversible oxidation) by the formation of the HMW form detected in response to H_2O_2 and diamide, and that there is a potential role for the thioredoxin system in regulating Ubp12 in *C. albicans*. Ubp12 has been found to have roles in the regulation of HMW poly-ubiquitin conjugates and the formation of filamentous growth forms of *C. albicans*, specifically hyphae and hyper-polarised buds.

C. albicans is a major human fungal pathogen that exhibits resistance to many anti-fungal drugs making treatment of *C. albicans* infections challenging (Costa-de-Oliveira and Rodrigues, 2020). Oxidative stress responses are important in the pathogenicity of *C. albicans* so it can evade immune responses. Work in this chapter has identified that Ubp12 is involved in oxidative stress responses in *C. albicans* and possibly regulates filamentous growth (summarised in Figure 5.16), thus may be a potential drug target for treating *C. albicans* infections. To further this work, virulence assays assessing the role of Ubp12 would be useful. This chapter has also explored the levels of conservation of Ubp12 between *C. albicans* and the closely related yeast species *S. cerevisiae* in response to oxidative stress. Thus, this chapter may provide new angles for research into the more distantly related human homologue, USP15, a protein known to be involved in various cancers and neurodegenerative diseases.

Chapter Six: Final Discussion

The covalent attachment of ubiquitin to target proteins regulates many cellular processes and therefore its conjugation and deconjugation must be tightly regulated. Interestingly, many enzymes used in the conjugation and deconjugation of ubiquitin utilise catalytic cysteine residues, rendering them susceptible to oxidative regulation. Indeed, various studies have found that one mechanism utilised to regulate ubiquitination is the oxidation of the machinery involved in the addition and removal of ubiquitin at their catalytic cysteine residues (Doris et al., 2012, Cotto-Rios et al., 2012, Lee et al., 2013a). The addition of the UBL SUMO is regulated in this manner in human cells, where low levels of H_2O_2 initiate an inhibitory disulphide between conjugation enzymes, and high levels inactivate the deconjugation machinery (Bossis and Melchior, 2006, Xu et al., 2008). In *S. cerevisiae*, ubiquitination was found to also be regulated in this way, with H_2O_2 and diamide inducing an inhibitory disulphide between the conjugation enzymes Uba1 and Cdc34 (Doris et al., 2012). Interestingly, previous work from our lab assessing the majority of DUBs in *S. cerevisiae* identified one DUB Ubp12 that is regulated by oxidation (Curtis, 2019). Further work revealed that Ubp12 formed a H_2O_2-specific intramolecular disulphide, which was sensitive to H_2O_2 concentration and, furthermore, that the catalytic cysteine residue was essential for formation of this disulphide. Interestingly, preliminary work also demonstrated a potential role for the H_2O_2-specific cytoplasmic thioredoxin reductase in the regulation of Ubp12 however this was not further explored. Therefore, the main aim of this project was to explore the mechanisms underlying the oxidation and the regulation of Ubp12 in *S. cerevisiae*, focusing on the potential role of the thioredoxin system, and to investigate potential conservation of the role and regulation of the Ubp12 homologue in responses to oxidative stress in the closely related yeast species *C. albicans*, a fungal pathogen of humans.

6.1 Summary and discussion of key findings in this study

Chapter 3 of this thesis revealed that the thioredoxin system influences the regulation of Ubp12 in *S. cerevisiae*. The previous studies exploring the regulation of Ubp12 identified cytoplasmic Trr1 as an important regulator of Ubp12 abundance in non-reducing conditions in *S. cerevisiae* (Curtis, 2019). It was hypothesised that the

thioredoxin system could regulate Ubp12 by restoring the reduced form of the protein after H_2O_2 has been dealt with, or by oxidising Ubp12 in response to H_2O_2, which is often performed by peroxiredoxins, such as with the oxidation of the transcription factor Yap1 (Delaunay et al., 2002, Ross et al., 2000). Data in this thesis suggests that the thioredoxin system has a role in regulating the oxidation state of Ubp12, but no evidence was found that suggested a specific role for peroxiredoxins in the oxidation of Ubp12. Indeed, results presented in this thesis have found that Trr1 and Trx1 and/or Trx2 regulate the oxidation of Ubp12, as well as regulating its abundance. Indeed, in *trx1*Δ*trx2*Δ and *trr1*Δ cells, Ubp12 was found to form several, oxidised HMW forms in addition to the originally identified HMW intramolecular disulphide complex, suggesting that the cytosolic thioredoxin system determines the oxidation status of Ubp12. It was also found that the reversible formation of the Ubp12 HMW disulphide complex was maintained for longer time frames in *trx1*Δ*trx2*Δ cells, indicating a role for the thioredoxin system in the regulation of this complex. In addition to this, under reducing conditions, the abundance of Ubp12 is decreased in both the *trr1*Δ mutant and the *trx1*Δ*trx2*Δ mutant. Interestingly, in *trr1*Δ cells expressing the catalytic cysteine mutant version of Ubp12, unidentified HMW forms of Ubp12 similar in mobility to the new HMW species mentioned above were identified, suggesting that the catalytic cysteine may be involved in resolving these species. However, it is also possible that this is an alternate form of oxidation that occurs because the catalytic cysteine residue is missing. Together, these data suggest an important role for the cytosolic thioredoxin system in the regulation of Ubp12 and suggest that multiple, oxidised forms of Ubp12 are formed in response to H_2O_2. Excitingly, this is the first work that suggests the thioredoxin system has a role in regulating ubiquitin and UBL machinery in *S. cerevisiae*. Indeed, previous studies exploring the oxidation of ubiquitin and UBL machinery found that the glutathione system primarily regulates their oxidation. For example, the H_2O_2-induced intermolecular disulphide complex consisting of the sumoylation E1 enzyme Uba2 and E2 enzyme Ubc9 in human cells was reduced upon the addition of reduced glutathione and, moreover, treatment with BSO, a drug that reduces glutathione levels in the cell, significantly increased the levels and persistence of the H_2O_2-induced Uba2-Ubc9 disulphide complex (Bossis and Melchior, 2006). Furthermore, the disulphide formed between the ubiquitin pathway E1, Uba1, and the ubiquitin pathway E2, Cdc34 in *S. cerevisiae* was induced upon diamide treatment, a thiol-oxidising drug that oxidises glutathione but not thioredoxin in *S. cerevisiae*, and

BSO treatment, which inhibits glutathione synthesis (Doris et al., 2012). More recently, Uba1 has been found to also form a disulphide complex with Rad6, another E2 conjugating enzyme in *S. cerevisiae* in response to H_2O_2 (Simões et al., 2022). Treatment of cells with BSO and deletion of the gene encoding the glutathione reductase Glr1 caused a significant inhibition of the reduction of the H_2O_2-induced Uba1-Rad6 disulphide complex (Simões et al., 2022). Furthermore, mutations of thioredoxin system components had no effect on the Uba1-Rad6 disulphide complex suggesting that it is primarily the glutathione system that regulates this oxidation. Thus, the data presented in this thesis provide the first evidence establishing a role for the thioredoxin system in regulating the oxidation of ubiquitin/UBL pathway enzymes.

As mentioned, previous work from this lab revealed that Ubp12 forms a HMW intramolecular disulphide complex and, moreover, that the catalytic cysteine residue is essential for the formation of this complex (Curtis, 2019). Chapter 4 of this thesis examined whether other cysteines of Ubp12 were involved in the oxidation of Ubp12. Two groups of cysteines were chosen for mutagenesis (Group 1; C519, C536, C539, and Group 2; C967, C985, C988) on the basis that all but one (C519) were conserved residues in *S. cerevisiae, S pombe, C. albicans* and *H. sapiens*, and that both groups contained a CXXC motif, a motif known to have redox activity (Chivers et al., 1997). Interestingly, mutation of both groups of cysteine residues affected the formation of the Ubp12 HMW disulphide complex. No obvious signal was detectable in wild-type cells expressing either triple cysteine mutant, however analysis in the *trx1*Δ*trx2*Δ*ubp12*Δ strain revealed that a small amount of a Ubp12 species of comparable mobility to the HMW disulphide was present in cells expressing the Group 1 mutant. It is possible that there is a very faint signal detectable in extracts from wild-type cells expressing the Group 1 mutant, and it is possible that differences in protein loading may account for this. However, it is also possible that the signal is more readily detectable in the thioredoxin mutant as the thioredoxin system is involved in regulating this HMW disulphide. Thus, the cysteine residues mutated in Group 1 may not be essential for disulphide formation, but seem to influence the ability of cells to oxidise Ubp12 into the HMW disulphide. Analysis of cysteine residues in the predicted structure of Ubp12 suggested that neither the Group 1 or Group 2 cysteines could directly form a disulphide bond with the catalytic cysteine residue, suggesting that perhaps multiple disulphides utilising multiple cysteine residues are formed in

response to H_2O_2, before the final HMW disulphide is formed. This is consistent with data presented in Chapter 3, where unidentified oxidised forms of Ubp12 were formed in thioredoxin mutants, suggesting that the thioredoxin system is also involved in resolving these intermediate disulphides. For example, perhaps disulphide shuffling is involved in the formation of the HMW disulphide complex. Interestingly, both Group 1 and Group 2 sets of cysteine residues include a conserved CXXC motif, a motif which could have potential redox activity based on studies of CXXC motifs in various proteins such as thioredoxins (Schultz et al., 1999). Indeed, more recently, CXXC motifs have been shown to function as disulphide isomerases. For example, PDI (protein disulphide isomerase) uses two catalytic CXXC motifs, which form internal disulphides, when resolving disulphides in target proteins (Ali Khan and Mutus, 2014). It is therefore possible that the conserved CXXC motifs of Ubp12 function to shuffle disulphides within the protein, in order to form the final Ubp12 HMW disulphide complex in response to H_2O_2. Interestingly, studies of the mammalian homologue of Ubp12, USP15, has found that these equivalent conserved CXXC motifs are essential for coordinating a zinc ion, which is essential for catalysis (Ye et al., 2009). Although there is no evidence in the literature that Ubp12 binds zinc, it is possible that a zinc ion is coordinated by these CXXC motifs and that this may affect the formation of the HMW disulphide complex in some manner. Thus, further work analysing potential zinc binding with Ubp12 is essential to decipher the role of these CXXC motifs in Ubp12. Further analysis revealed that mutation of a single CXXC residue, C536, (the first cysteine of the Group 1 CXXC motif) appeared to promote formation of a HMW Ubp12 complex that migrated at a slower mobility compared to the Ubp12 HMW disulphide complex formed in wild-type cells. This is an interesting observation, particularly when considering the thioredoxin system mutant specific forms of Ubp12 observed in studies presented in Chapter 3. Hence, perhaps C536 is important for resolving these thioredoxin system mutant specific forms of Ubp12. However, further analysis is required to investigate the HMW complex observed in cells expressing the C536S mutated version of Ubp12. It is interesting to note that a HMW form of Ubp12 with similar mobility was also observed in the *trx1*Δ*trx2*Δ*ubp12*Δ mutant expressing the Group 1 mutant, further suggesting a connection with the Trx1 and Trx2 thioredoxins and a role for Group 1 cysteines in resolving this species. Together, data presented in Chapter 3 further supports the hypothesis that Ubp12 forms various disulphide complexes utilising numerous cysteine residues in response to H_2O_2 and, moreover,

that the thioredoxin system influences the formation and/or reduction of these complexes.

Work presented in Chapter 3 and Chapter 4 are summarised below in the current working model (Figure 6.1). In summary, the working hypothesis is that Ubp12 is oxidised specifically by H_2O_2, to form an initial disulphide bond between two cysteine residues. The thioredoxin system is then responsible for moving this disulphide bond within Ubp12, also termed disulphide shuffling, utilising various cysteine residues. Finally, the HMW disulphide is formed (the final disulphide), likely utilising the catalytic cysteine residue and another residue within the protein. The thioredoxin system is also responsible for reducing this protein back to the reduced form of Ubp12 (Figure 6.1).

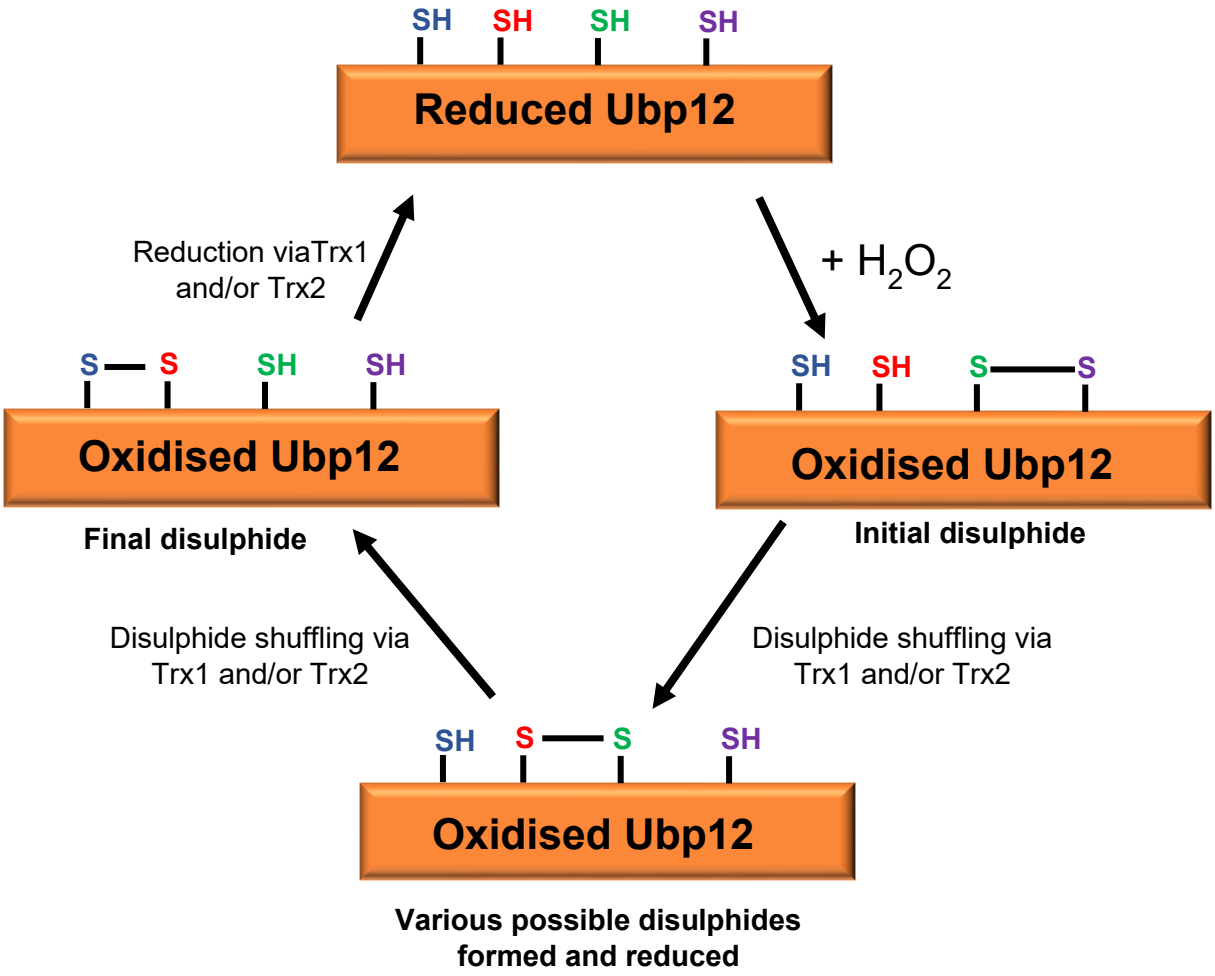

Figure 6.1. Current working model for Ubp12 oxidation and points of regulation by the thioredoxin system.

Reduced Ubp12 is oxidised by H_2O_2, forming an initial disulphide bond between two cysteines within the protein. This disulphide is then shuffled throughout Ubp12, utilising various cysteine residues, by the thioredoxin system. The final disulphide, presumably utilising the catalytic cysteine and another cysteine within the protein, is finally formed. Oxidised Ubp12 is then reduced, a process also regulated by the thioredoxin system.

Given the roles and regulation of Ubp12 in response to oxidative stress in *S. cerevisiae*, potential conservation of the roles and regulation of Ubp12 was explored in the closely related yeast species *C. albicans*, a fungal pathogen of humans. Ubp12 in *C. albicans* and *S. cerevisiae* have a conserved sequence identity of 34%, and 8 of the 19 cysteine residues in Ubp12 in *S. cerevisiae* are conserved in *C. albicans* Ubp12. In the current literature there is very little known about the role and regulation of Ubp12 in *C. albicans*, with one study finding that polymorphisms in Ubp12 in *C. albicans* was

linked to particularly virulent strains (Zhang et al., 2009). This link between Ubp12 and the pathogenicity of *C. albicans* highlights the importance of understanding the roles and regulation of this DUB in *C. albicans*. Excitingly, similarly to what was observed in *S. cerevisiae*, Ubp12 in *C. albicans* was also found to be essential for oxidative stress responses. However, in contrast to the findings in *S. cerevisiae*, deletion of the *UBP12* gene in *C. albicans* conferred increased resistance to H_2O_2 stress and increased sensitivity to diamide stress, suggesting different roles for Ubp12 in these two yeast species. Consistent with this, data suggests that Ubp12 has a role in DNA damage and DNA stress responses in *C. albicans*, with *ubp12*Δ cells displaying a sensitive phenotype to hydroxyurea and UV light exposure which was not observed in *S. cerevisiae* (Curtis, 2019). Interestingly, *C. albicans* Ubp12 was also found to form HMW oxidised complexes in response to H_2O_2, as observed in *S. cerevisiae*. However, in contrast to *S. cerevisiae*, treatment with diamide also induced the formation of oxidised HMW Ubp12 complexes in *C. albicans.* Hence, together these data indicate that Ubp12 is important in oxidative stress responses in both yeast species, but that they may fulfil different roles in response to H_2O_2 and diamide in the two yeasts. Interestingly, in contrast to *S. cerevisiae*, Ubp12 was also found to regulate the abundance of polyubiquitinated substrates in *C. albicans* (Curtis, 2019). Thus, Ubp12 seems to have different roles in the regulation of polyubiquitinated species in *S. cerevisiae* and *C. albicans*. The identification of all of the substrates of Ubp12 in both species, particularly in *C. albicans* where few studies have been performed, would underpin efforts to understand the different roles of Ubp12 in these two organisms. Ubp12 in *S. cerevisiae* has been linked to the regulation of mitochondrial dynamics and DNA damage responses through regulation of PCNA, two contexts where ROS are particularly relevant (Anton et al., 2013, Álvarez et al., 2019). In addition, Ubp12 in the more distantly related yeast, *S. pombe,* has also been shown to regulate PCNA (Álvarez et al., 2016), hence it would be interesting to assess the role of Ubp12 in *C. albicans* in these processes. It is also notable that some evidence was obtained suggesting that the thioredoxin system regulates the oxidation of Ubp12 in *C. albicans*, hence the regulatory mechanism of Ubp12 in response to oxidising agents may be conserved. Interestingly, results presented in Chapter 5 also suggested that Ubp12 may have some functions in the morphology of *C. albicans* cells. *C. albicans* can alter their morphology into more filamentous, virulent forms, such as hyphae and hyperpolarised buds, in response to various external stimuli (Whiteway and

Bachewich, 2007, Dantas et al., 2015). For example, hyphal growth can be induced in response to serum and a temperature of 37°C, and hyperpolarised buds can be induced in response to hydroxyurea and H_2O_2 (Whiteway and Bachewich, 2007, Dantas et al., 2015). Excitingly, initial studies revealed that deletion of Ubp12 in *C. albicans* cells caused a decrease in hyphae length, and a decrease in the length of hyperpolarised buds. Interestingly, the induction of hyperpolarised buds using hydroxyurea in *ubp12*Δ cells was not affected to the same extent cells as H_2O_2-induced hyperpolarised bud growth in the same strain. One study has shown that inactivation of the major thioredoxin in *C. albicans*, Trx1, by H_2O_2 is necessary to activate Rad53, a DNA checkpoint kinase (da Silva Dantas et al., 2010). Furthermore, this activation of Rad53 (a DNA checkpoint kinase) is essential for the formation of hyperpolarised buds in response to H_2O_2, and thus the formation of hyperpolarised buds is regulated indirectly by the thioredoxin system (da Silva Dantas et al., 2010). It is tempting to speculate that the roles for Ubp12 in oxidative stress responses and the possible role for the thioredoxin system in regulating Ubp12, are linked to the H_2O_2-induced, thioredoxin-regulated process of hyperpolarised bud formation. It is possible that Ubp12 is a key target of Trx1 in this process, which may explain the effect of deleting Ubp12 on hyperpolarised bud formation. It is also possible that Ubp12 is a substrate of Rad53, or that Rad53 is necessary for oxidation of Ubp12 in some way, however these hypotheses require extensive further investigation. Together, data presented in Chapter 5 of this thesis reveals previously unknown roles for Ubp12 in response to oxidative stress in *C. albicans*, and suggest possible roles for Ubp12 in the regulation of cell morphology.

6.2 Implications for mammalian cells

The human homologue of Ubp12, USP15, has been linked to the progression of various diseases, such as numerous types of cancer and neurodegenerative diseases (see Section 1.3.4.2) (Li et al., 2022). Hence, knowledge about the regulation and functions of Ubp12 in *S. cerevisiae* and *C. albicans* may aid the development of clinical treatments that target USP15. Interestingly, two potential inhibitors of USP15 have been developed. In acute myeloid leukaemia (AML) USP15 overexpression stabilises KEAP1, and this stabilisation of KEAP1 is linked with the progression of AML (Niederkorn et al., 2022). Normally KEAP1, an E3 ligase adaptor protein, binds and

inhibits the activity of NRF2, a transcription factor important for the regulation of various antioxidant genes (Suzuki et al., 2019). Upon ROS exposure, KEAP1 is inactivated by the formation of intramolecular disulphides, and so NRF2 is released and induces the transcription of various antioxidant genes, maintaining redox homeostasis (Baird and Yamamoto, 2020). Deletion of USP15 in mouse and human tissue AML models decreased the viability of progenitor cells and activates important antioxidant responses, as KEAP1 is no longer stabilised by USP15, hence NRF2 becomes active (Niederkorn et al., 2022). USP15-Inh is a small molecule inhibitor of USP15, and its addition causes phenotypic effects in AML cells consistent with deletion of USP15 and restores redox homeostasis (Niederkorn et al., 2022). USP15-Inh was found to target AML cells selectively, and provides evidence that USP15 is a druggable target (Niederkorn et al., 2022). Mitoxantrone is another inhibitor of USP15 and this drug binds to the S1 binding site (see 1.1.6.2.4) of USP15, potentially affecting proximal substrate binding and hence substrate specificity (Ward et al., 2018). However, this inhibition has only been studied *in vitro* and the study acknowledged that mitoxantrone is known to bind to several human proteins, suggesting it might not provide enough specificity to be a viable drug to specifically target USP15 (Ward et al., 2018). Thus, although the development of inhibitors of USP15 is underway, further understanding of the mechanisms that normally regulate USP15 may advance this research. Interestingly, the anti-cancer drug Curcusone D functions by increasing the levels of intracellular ROS to inhibit the action of DUBs and has displayed promising results in the treatment of several types of myelomas (Cao et al., 2014). Thus, gaining further understanding of the regulation of Ubp12 by ROS may aid the development of drugs to target USP15.

6.3 Implications for *C. albicans*

C. albicans is a polymorphic yeast that in most people exists as a harmless commensal (Romo and Kumamoto, 2020). However, several cell processes, such as the yeast-hyphae switch, promotes the ability of *C. albicans* to act as a human pathogen causing both superficial infections such as oral candiasis and systemic, life-threatening infections (Mayer et al., 2013). Hence, developing drugs to treat *C. albicans* infections is a research area of significant importance. Despite there being no known functions for Ubp12 in *C. albicans*, one paper has found that polymorphisms in the *UBP12* gene

are detected in particularly virulent strains (Zhang et al., 2009). Interestingly, Chapter 5 of this thesis revealed a role for Ubp12 in oxidative stress responses in *C. albicans*, and that Ubp12 may regulate the morphology of *C. albicans*, which is often directly linked to virulence. One pathogenic mechanism of *C. albicans* that is under investigation as a potential drug target is the yeast-hyphae switch. Indeed, studies have shown that inhibiting the yeast-hyphae switch in the early stages of infection significantly increased the survival of the host (Saville et al., 2006). Data presented in in this thesis uncovered a potential role for Ubp12 in the induction of hyphal growth, and hence further studies of this connection could provide a possible therapeutic route to modulate the yeast-hyphae switch. However, studies in several organisms have revealed that DUBs can have overlapping functions and hence drugs targeting Ubp12 directly may not cause the intended effects as perhaps another DUB can regulate cell morphology in its absence (Rossio et al., 2021, Schaefer and Morgan, 2011). Nevertheless, further characterising the role of Ubp12 in this process may gain new insights into a key pathogenic mechanism of *C. albicans*. In addition to morphological changes, *C. albicans* has developed a resistance to ROS to evade immune responses that utilise ROS to attack pathogens (Komalapriya et al., 2015). Indeed, numerous studies have shown that the inactivation of antioxidant genes attenuates the virulence of *C. albicans* and its ability to escape phagocytic killing (Brown et al., 2014). Thus, further understanding the ways that ROS regulate proteins, such as Ubp12, in *C. albicans* may extend the knowledge and understanding of this ROS resistance, potentially aiding the development of drugs that target ROS resistance mechanisms in *C. albicans*. Identification of Ubp12 substrates in *C. albicans* is an important next step in furthering this work, as it will establish physiological roles for this DUB, and may provide a potential route for drug development. Currently there are only three classes of anti-fungal drugs available and resistance to these anti-fungals is increasing, thus developing novel therapeutic routes to treat fungal infections is of high clinical relevance.

6.4 Outstanding questions

Data presented in this thesis has provided new insights about the mechanisms that regulate Ubp12 in *S. cerevisiae* in oxidative stress conditions. In addition, the studies have uncovered hitherto unknown knowledge regarding the regulation and functions

of Ubp12 in *C. albicans*. However, despite extensive investigations of the regulation of Ubp12 by the thioredoxin system (Chapter 3), there are some unanswered questions regarding this research:

- This study revealed that Ubp12 may have different roles and regulation in the BY4741 and W303 strain backgrounds – what is the nature of these strain-specific differences? It is already known that H_2O_2 signal transduction is different in these two strain backgrounds. The oxidation and activation of Yap1 is performed by Gpx3 and Ybp1 in BY4741 cells, yet Tsa1 performs this role in W303 (Ross et al., 2000, Delaunay et al., 2002). Hence, it is possible that the role and regulation of Ubp12 is also different between these two strain backgrounds. Work in this thesis examined the regulation of Ubp12 by the thioredoxin system in W303 cells and hence future studies should examine the role of the thioredoxin system in the regulation of Ubp12 in the BY4741 strain background to examine whether differences in roles is linked to altered regulation of the DUB.

- Analyses of the thioredoxin system mutants in W303 revealed several new oxidised HMW forms of Ubp12 which were not further explored in this study – what are these unidentified
- species? It would be interesting to use mass spectrometry to analyse the composition of these species, either as an intramolecular disulphide or an intermolecular disulphide. Following this, analysis of the cysteine residues involved in their formation would be interesting to further characterise these oxidation events.

- Finally, Chapter 3 identified a potential minor role for the glutathione system in the regulation of Ubp12 using BSO, however no further experimentation was performed. Hence, it would be interesting to analyse the effects, if any, of different glutathione pathway mutants on Ubp12 oxidation in both W303 and BY4741, and *C. albicans*, to further explore the specificity of the thioredoxin system in the regulation of Ubp12.

Chapter 4 revealed that oxidation of Ubp12 is more complex than first suspected, involving the formation of multiple disulphides and potentially that several cysteine

residues were important in their formation. This research has raised some interesting outstanding questions:

- For example, which are the specific cysteine residues (or other residues) involved directly in each disulphide complex? Creation of further single cysteine mutants and/or mass spectrometry analyses would help to characterise the H_2O_2-induced modifications of Ubp12.

- Another question that would be interesting to address is what is the function(s) of the formation of the Ubp12 HMW disulphide complex? Given the relevance of ROS in the contexts of some Ubp12 substrates (Fzo1 and mitochondrial dynamics, PCNA and DNA damage responses) (Anton et al., 2013, Álvarez et al., 2019), it would be interesting to assess their ubiquitination status and consequent regulation in cells treated with H_2O_2 to induce formation of the disulphide. Alternatively, the identification and mutation of the non-catalytic cysteine residue involved in the formation of the disulphide complex (assuming that the non-catalytic cysteine has no other key roles in Ubp12 function) could allow phenotypic analysis of the function of this disulphide, without hindering the normal activity of the protein. In addition, *in vitro* activity assays of Ubp12 that cannot form the disulphide complex with known substrates could explore a physiological role for this oxidation. These analyses could also address what the primary function of the disulphide is. Currently, two models have been proposed. The first is that the oxidation fulfils an inhibitory role, to inactivate the protein and modulate ubiquitination of substates in response to H_2O_2. The second model suggests oxidation fulfils a protective role, to protect Ubp12 from irreversible oxidation at its catalytic cysteine residue allowing the DUB to become active quickly when redox homeostasis is restored. Alternatively, both of these models could be true.
- Finally, it would be interesting to analyse the metal content of Ubp12 to clarify if the CXXC motifs present are involved in zinc binding, similar to USP15 in mammalian cells (Hetfeld et al., 2005).

Finally, Chapter 5 has revealed new insights regarding the functions and regulation of Ubp12 in *C. albicans*, however there remains many unanswered questions and suggested future directions for this work are as follows:

- Firstly, it would be important to generate a reconstituted *UBP12* strain, whereby wild-type Ubp12 is reintroduced into *ubp12*Δ cells to check if this rescues the phenotypes observed.

- In future investigations it would also be interesting to explore the composition of the H_2O_2-induced and diamide-induced HMW Ubp12 species, assessing if these complexes are also intramolecular disulphides.

- Following this, it would be particularly interesting to assess the role (if any) of the catalytic cysteine residue, together with other cysteines within the protein, on the oxidation of Ubp12. In addition, the examination of whether the oxidation of Ubp12 in *C. albicans* responds in a concentration–dependent manner could indicate roles for Ubp12 regulation in responses to different levels of ROS.

- There are currently no annotated substrates identified for Ubp12 in *C. albicans* and hence their identification would greatly support further studies of this DUB in oxidative stress responses and normal cell functions such as the yeast-hyphae switch and regulation of protein polyubiquitination.

- Finally, given the links of Ubp12 with cell morphology and oxidative stress responses in *C. albicans* it would obviously be very interesting to assess the potential role of Ubp12 in the virulence of *C. albicans*.

6.5 Concluding remarks

Recently, it has become clear that the modification of proteins by ubiquitin/UBLs is regulated by ROS. However, there is still much to learn in this growing area of research. Work presented here, together with previous work from this lab, has revealed that in *S. cerevisiae*, the Ubp12 DUB is specifically oxidised in response to H_2O_2 and, furthermore, that this oxidation is regulated by the thioredoxin system. As far as we are aware the connection between the thioredoxin system and the regulation of ubiquitin/UBL pathways has not previously been established and hence the present study has provided significant new knowledge. Furthermore, until this study, there was virtually nothing known about Ubp12 regulation or function(s) in *C. albicans*, thus the work presented in this thesis has provided significant insight into these areas. DUB dysregulation has been linked to the pathologies of several common human diseases and hence further understanding of the functions and regulation of DUBs has the

potential to provide new routes for the development of new drugs that specifically target DUBs for the benefit of human health. In addition, work presented here could also inform future research into antifungal drugs to treat *C. albicans* infections.

Appendix A

S. cerevisiae strains used in this study.

Strain ID	Strain background	Genotype	Reference
KA1	BY4741	*MATa his3Δ1, leu2Δ0, met15Δ0, ura3Δ0*	Lab stock
KA4	W303-1a	*MATa ade2-1 can1-100 his3-11,15 leu2-3,112 trp1-1 ura3-1*	Lab stock
KA5	W303-1b	*MATα ade2-1 can1-100 his3-11,15 leu2-3,112 trp1-1 ura3-1*	Lab stock
KA7	W303	*MATa ade2-1 can1-100 his3-11,15 leu2-3,112 trp1-1 ura3-1 ubp12::HIS3*	(Curtis, 2019)
KA10	W303	*MATa ade2-1 can1-100 his3-11,15 leu2-3,112 trp1-1 ura3-1 UBP12-3HA:KanMX*	(Curtis, 2019)
KA11	W303	*MATa ade2-1 can1-100 his3-11,15 leu2-3,112 trp1-1 ura3-1 trr1::HIS3*	Lab stock
KA24	BY4741	*MATa his3Δ1, leu2Δ0, met15Δ0, ura3Δ0 UBP12-TAP:KanMX*	Newcastle University High throughput service
KA26	W303	*MATa ade2-1 can1-100 his3-11,15 leu2-3,112 trp1-1 ura3-1 trr2::HIS3*	Gift from Chris Grant
KA32	W303	*MATα ade2-1 can1-100 his3-11,15 leu2-3,112 trp1-1 ura3-1 UBP12-3HA:KanMX*	(Curtis, 2019)
KA50	W303	*MAT? ade2-1 can1-100 his3-11,15 leu2-3,112 trp1-1 ura3-1 trr2::HIS3 UBP12-3HA:KanMX*	This study
KA60	W303	*MATα ade2-1 can1-100 his3-11,15 leu2-3,112 trp1-1 ura3-1 gpx3::HIS3 yap1::TRP1*	(Veal et al., 2003)

KA64	W303	*MAT? ade2-1 can1-100 his3-11,15 leu2-3,112 trp1-1 ura3-1 tsa2::LEU2 UBP12-3HA:KanMX*	This study
KA65	W303	*MAT? ade2-1 can1-100 his3-11,15 leu2-3,112 trp1-1 ura3-1 tsa1::HIS3 UBP12-3HA:KanMX*	This study
KA74	BY4741	*MATa his3Δ1, leu2Δ0, met15Δ0, ura3Δ0 ASH1-TAP:KanMX*	Newcastle University High throughput service
KA77	W303	*MATa ade2-1 can1-100 his3-11,15 leu2-3,112 trp1-1 ura3-1 trr1::HIS3 UBP12-3HA:KanMX*	(Curtis, 2019)
KA81	W303	*MAT? ade2-1 can1-100 his3-11,15 leu2-3,112 trp1-1 ura3-1 trx1::KanMX trx2::ura3^{-} UBP12-3HA:KanMX*	This study
KA91	BY4741	*MATa his3Δ1, leu2Δ0, met15Δ0, ura3Δ0 CDC48-TAP:KanMX*	Newcastle University High throughput service
KA95	BY4741	*MATa his3Δ1, leu2Δ0, met15Δ0, ura3Δ0 GPA1-TAP:KanMX*	Newcastle University High throughput service
KA107	BY4741	*MATa his3Δ1 leu2Δ0 met15Δ0 ura3Δ0 ubp12::KanMX*	Newcastle University High throughput service
KA113	BY4741	*MATa his3Δ1, leu2Δ0, met15Δ0,*	Newcastle

		ura3Δ0 RAD23-TAP:KanMX	University High throughput service
KA114	W303	*MAT? ade2-1 can1-100 his3-11,15 leu2-3,112 trp1-1 ura3-1 trx1::KanMX trx2::ura3⁻ gpx3::HIS3 UBP12-3HA:KanMX*	This study
KA116	W303	*MATa ade2-1 can1-100 his3-11,15 leu2-3,112 trp1-1 ura3-1 gpx3::HIS3 UBP12-3HA:KanMX*	This study
KA119	W303	*MAT? ade2-1 can1-100 his3-11,15 leu2-3,112 trp1-1 ura3-1 trx1::KanMX trx2::ura3⁻ ubp12::HIS3*	This study
SR9	W303	*MATa ade2-1 can1-100 his3-11,15 leu2-3,112 trp1-1 ura3-1 tsa1::HIS3*	(Ross et al., 2000)
SR48	W303	*MATa ade2-1 can1-100 his3-11,15 leu2-3,112 trp1-1 ura3-1 tsa2::LEU2*	Generated by Sarah Ross
KD467	W303	*MAT? ade2-1 can1-100 his3-11,15 leu2-3,112 trp1-1 ura3-1 trx1::KanMX trx2::ura3⁻*	Gift from Chris Grant

***S. cerevisiae* strains used in this study.**

MAT? Indicates unknown mating type.

Appendix B

C. albicans strains used in this study.

Strain ID	Strain background	Genotype	Reference
KA57	SN148	*arg4Δ/arg4Δ, leu2Δ/leu2Δ, his1Δ/his1Δ, ura3Δ::imm434/ura3Δ::imm434, iro1Δ::imm434/iro1Δ::imm434*	(Noble and Johnson, 2005)
KA66	SN148	*arg4Δ/arg4Δ, leu2Δ/leu2Δ, his1Δ/his1Δ, ura3Δ::imm434/ura3Δ::imm434, iro1Δ::imm434/iro1Δ::imm434 trx1::HIS1 trx1::ARG4*	(da Silva Dantas et al., 2010)
KA67	SN148	*arg4Δ/arg4Δ, leu2Δ/leu2Δ, his1Δ/his1Δ, ura3Δ::imm434/ura3Δ::imm434, iro1Δ::imm434/iro1Δ::imm434 tsa1::HIS1 tsa1::ARG4 tsa1::HisG tsa1::HisG*	(da Silva Dantas et al., 2010)
KA68	SN148	*arg4Δ/arg4Δ, leu2Δ/leu2Δ, his1Δ/his1Δ, ura3Δ::imm434/ura3Δ::imm434, iro1Δ::imm434/iro1Δ::imm434 gpx3::HIS1 gpx3::ARG4*	(Patterson et al., 2013)
KA69	SN148	*arg4Δ/arg4Δ, leu2Δ/leu2Δ, his1Δ/his1Δ, ura3Δ::imm434/ura3Δ::imm434, iro1Δ::imm434/iro1Δ::imm434 UBP12-3HA:HIS1, CIp10*	This study
KA71	SN148	*arg4Δ/arg4Δ, leu2Δ/leu2Δ, his1Δ/his1Δ, ura3Δ::imm434/ura3Δ::imm434, iro1Δ::imm434/iro1Δ::imm434*	This study

		trx1::HIS1 trx1::ARG4 UBP12-3HA:URA3	
KA76	SN148	*arg4Δ/arg4Δ, leu2Δ/leu2Δ, his1Δ/his1Δ, ura3Δ::imm434/ura3Δ::imm434, iro1Δ::imm434/iro1Δ::imm434 gpx3::HIS1 gpx3::ARG4 UBP12-3HA:URA3*	This study
KA96	SN148	*arg4Δ/arg4Δ, leu2Δ/leu2Δ, his1Δ/his1Δ, ura3Δ::imm434/ura3Δ::imm434, iro1Δ::imm434/iro1Δ::imm434 tsa1::HIS1 tsa1::ARG4 tsa1::HisG tsa1::HisG UBP12-3HA:URA3*	This study
KA102	SN148	*arg4Δ/arg4Δ, leu2Δ/leu2Δ, his1Δ/his1Δ, ura3Δ::imm434/ura3Δ::imm434, iro1Δ::imm434/iro1Δ::imm434, CIp10*	(da Silva Dantas et al., 2010)
KA103 (Transformant #1)	SN148	*arg4Δ/arg4Δ, leu2Δ/leu2Δ, his1Δ/his1Δ, ura3Δ::imm434/ura3Δ::imm434, iro1Δ::imm434/iro1Δ::imm434 ubp12::ARG4 ubp12::HIS1, CIp10*	This study
KA108 (Transformant #2)	SN148	*arg4Δ/arg4Δ, leu2Δ/leu2Δ, his1Δ/his1Δ, ura3Δ::imm434/ura3Δ::imm434, iro1Δ::imm434/iro1Δ::imm434 ubp12::ARG4 ubp12::HIS1, CIp10*	This study

***C. albicans* strains used in this study.**

Appendix C

Oligonucleotide primers used in this study.

Primer Name	Sequence (5' –> 3')
Trr2 Del Chk Fw	GTTAATTAATCACTCGATGG
Trr2 Del Chk Rev	GCCTATCTCTTTGTCTCTTC
Tsa1 Del Chk Fw	GTCCTTTAGGGATTTTTC
Tsa1 Del Chk Rev	CGATGATTGTTATTAGAACTG
Tsa2 Del Chk Fw	GAGTAATCAAGGATCAAC
Tsa2 Del Chk Rev	GTCTTCTGGATATAAAGATG
Trx1 Del Chk Fw	GTATATTCTTTTCGTTGGAAAAG
Trx1 Del Chk Rev	CCTCTTGTGTGAAAAATTAATTG
Trx2 Del Chk Fw	GATATCAGTATATAAGAAAGCCA
Trx2 Del Chk Rev	CATGACTGACATTTTATACATTC
Gpx3-Deletion Frag fw	CTGCATTATCGTTTTTAGCC
Gpx3-Deletion Frag rev	GCAATTTCTAAACCGTTTTG
M13F	GTAAAACGACGGCCAGTG
M13R	CAGGAAACAGCTATGACC
426-12-3HA-2-fw	GAAATTCTTCCGTTATAACGGATTTATTTGTCGGGATGTACAAATCAACGCTATATTCTCCCGAATCTCAAAATGTTTCTATAACGTT
426-12-3HA-1-rev	TTTTGAGATTCGGGAGAATATAGCGTTGATTTGTACATCCCGACAAATAAATCCGTTATAACGGAAGAATTTCTCTTTAAATGCATCT

426-12-3HA-3-fw	ACGATTCTCTCCAATTATTTTCCAAACCAGAAATACTAGGATTAACCGATTCGTGGTACTCTCCTACATCTAAGGAACATCGTCAGGCTAC
426-12-3HA-2-rev	TCCTTAGATGTAGGAGAGTACCACGAATCGGTTAATCCTAGTATTTCTGGTTTGGAAAATAATTGGAGAGAATCGTCCAAGGTTATGGTT
Ubp12-C536S-frag-1-rev	TTATAGAAACATTTTGACATTCGGGAGAATATAGCGTTGATTTGTACATCCCG
Ubp12-C536S-frag-2-fw	CGGGATGTACAAATCAACGCTATATTCTCCCGAATGTCAAAATGTTTCTATAA
ubp12ChkDelF	TATAATCAGGTATATTTCG
Ubp12 KA Fw 1	GTCCGTATCTGTCTATTG
Ubp12 Frag 2 Fw	GAACCAGCATCAGGTACTACTGGTTTGGTCAATTTG
Ubp12 KA Fw 2	CAATTTTTAACCTTGCAGG
Ubp12 Frag 3 Fw	GAAGAAGATGCAAGTACAGAGCCAGAATTAACAGATAAG
Ubp12 KA Fw 3	GATTAGGCAGCTCTAAAC
Ubp12 Rev 1	GTAATGTAGTCTGAAAAACC
Ubp12 Rev 2	GTTTTGAAACAACTTCTGAAC
Ubp12 Rev 3	CTTCATTGTCATTTGTTACTG
Ubp12 Rev 4	CTTTATTTTCTTCATCATCTC
Ubp12 Rev 5	GGATCATCTTTATAGACAAC
Ubp12 Rev 6	GTCACACCATTTTTTAAATTC
ubp12ChkTagR	TTGCTTCGTTTATGTAATT
Ubp12-HA-F	ATTGGTGCATATTAAAAGCAATGGTCGCCAAGAAGTCACTTCATCACCAGTACCAATTGAAACTGATGGTGACACTGATGTAACTGATTCCAATTCAACAGGTCGACGGATCCCCGGGTA

Ubp12-HA-R	CTTCTGATGTTTATTTTACGATTTATGGAGTGAGTGAGTGAA TAGGAGGGGGCAGGCAAATAATATTGCGACATTCTACGAC TGCTTGTTATATTGTCGTTCGATGAATTCGAGCTCGTT
Ubp12-HA-check-fw	GACCATTCGATGAACTCAAACC
HA-check-rev	CATGCATTTACTTATAATGGCGCGC
Ubp12-Del-Fw-CA	CTAAATACTAATAATTATAACAATAATTAATTGAATTATTCTA TAAACCACTGATATTTGATTTTATCTTTTTATTTTTGTTTGTT CCCATAATTGTGTCACGGCCAGTGAATTGTAATA
Ubp12-Del-Rev-CA	TACTTCAATTATATTTGGTAAATGTGTAAAGATGGCGTGTAC AGACGTTATATTTAATTTGACATTTCATTCATTCTTTTTATTG GGGTTAGTTTATTTATCGGAATTAACCCTCACTAA
Ubp12-DelChk-Fw-CA	TTACAACAGAGAAGAGACAAAG
Ubp12-DelChk-Rev-CA	CTGCAAAACGACATTATTTG
His1-Chk-EarlyRev-CA	CAATTGGCAAGTTTGTAG
Arg4-Chk-EarlyRev-CA	GTATGAATATCCTCATCACC
Ubp12-check-fw-CA-internal	GTTTATTACACGTTCCTG
Ubp12-check-rev-CA-internal	CTTCTTTATTCATCACCAC

Oligonucleotide primers used in this study.

The oligonucleotide primers were obtained from Sigma.

References

ABDUL REHMAN, S. A., ARMSTRONG, L. A., LANGE, S. M., KRISTARIYANTO, Y. A., GRÄWERT, T. W., KNEBEL, A., SVERGUN, D. I. & KULATHU, Y. 2021. Mechanism of activation and regulation of deubiquitinase activity in MINDY1 and MINDY2. *Mol Cell,* 81**,** 4176-4190.e6.

ABDUL REHMAN, S. A., KRISTARIYANTO, Y. A., CHOI, S.-Y., NKOSI, P. J., WEIDLICH, S., LABIB, K., HOFMANN, K. & KULATHU, Y. 2016. MINDY-1 Is a Member of an Evolutionarily Conserved and Structurally Distinct New Family of Deubiquitinating Enzymes. *Molecular cell,* 63**,** 146-155.

ADORNO, M., SIKANDAR, S., MITRA, S. S., KUO, A., NICOLIS DI ROBILANT, B., HARO-ACOSTA, V., OUADAH, Y., QUARTA, M., RODRIGUEZ, J., QIAN, D., REDDY, V. M., CHESHIER, S., GARNER, C. C. & CLARKE, M. F. 2013. Usp16 contributes to somatic stem-cell defects in Down's syndrome. *Nature,* 501**,** 380-4.

AKUTSU, M., DIKIC, I. & BREMM, A. 2016. Ubiquitin chain diversity at a glance. *J Cell Sci,* 129**,** 875-80.

AL-HAKIM, A. K., ZAGORSKA, A., CHAPMAN, L., DEAK, M., PEGGIE, M. & ALESSI, D. R. 2008. Control of AMPK-related kinases by USP9X and atypical Lys(29)/Lys(33)-linked polyubiquitin chains. *Biochem J,* 411**,** 249-60.

ALBUQUERQUE, C. P., SMOLKA, M. B., PAYNE, S. H., BAFNA, V., ENG, J. & ZHOU, H. 2008. A multidimensional chromatography technology for in-depth phosphoproteome analysis. *Mol Cell Proteomics,* 7**,** 1389-96.

ALEXOPOULOU, Z., LANG, J., PERRETT, R. M., ELSCHAMI, M., HURRY, M. E., KIM, H. T., MAZARAKI, D., SZABO, A., KESSLER, B. M., GOLDBERG, A. L., ANSORGE, O., FULGA, T. A. & TOFARIS, G. K. 2016. Deubiquitinase Usp8 regulates α-synuclein clearance and modifies its toxicity in Lewy body disease. *Proc Natl Acad Sci U S A,* 113**,** E4688-97.

ALI KHAN, H. & MUTUS, B. 2014. Protein disulfide isomerase a multifunctional protein with multiple physiological roles. *Front Chem,* 2**,** 70.

ALLEN, I. C., SCULL, M. A., MOORE, C. B., HOLL, E. K., MCELVANIA-TEKIPPE, E., TAXMAN, D. J., GUTHRIE, E. H., PICKLES, R. J. & TING, J. P. 2009. The NLRP3 inflammasome mediates in vivo innate immunity to influenza A virus through recognition of viral RNA. *Immunity,* 30**,** 556-65.

ÁLVAREZ, V., FRATTINI, C., SACRISTÁN, M. P., GALLEGO-SÁNCHEZ, A., BERMEJO, R. & BUENO, A. 2019. PCNA Deubiquitylases Control DNA Damage Bypass at Replication Forks. *Cell Rep,* 29**,** 1323-1335.e5.

ÁLVAREZ, V., VIÑAS, L., GALLEGO-SÁNCHEZ, A., ANDRÉS, S., SACRISTÁN, M. P. & BUENO, A. 2016. Orderly progression through S-phase requires dynamic ubiquitylation and deubiquitylation of PCNA. *Scientific Reports,* 6**,** 25513.

AMERIK, A., SWAMINATHAN, S., KRANTZ, B. A., WILKINSON, K. D. & HOCHSTRASSER, M. 1997. In vivo disassembly of free polyubiquitin chains by yeast Ubp14 modulates rates of protein degradation by the proteasome. *Embo j,* 16**,** 4826-38.

AMERIK, A. Y. & HOCHSTRASSER, M. 2004. Mechanism and function of deubiquitinating enzymes. *Biochim Biophys Acta,* 1695**,** 189-207.

ANG, J. S., DUFFY, S., SEGOVIA, R., STIRLING, P. C. & HIETER, P. 2016. Dosage Mutator Genes in Saccharomyces cerevisiae: A Novel Mutator Mode-of-Action of the Mph1 DNA Helicase. *Genetics,* 204**,** 975-986.

ANIK, M. I., MAHMUD, N., MASUD, A. A., KHAN, M. I., ISLAM, M. N., UDDIN, S. & HOSSAIN, M. K. 2022. Role of Reactive Oxygen Species in Aging and Age-Related Diseases: A Review. *ACS Applied Bio Materials,* 5**,** 4028-4054.

ANTON, F., DITTMAR, G., LANGER, T. & ESCOBAR-HENRIQUES, M. 2013. Two deubiquitylases act on mitofusin and regulate mitochondrial fusion along independent pathways. *Mol Cell,* 49**,** 487-98.

ARNÉR, E. S. & HOLMGREN, A. 2000. Physiological functions of thioredoxin and thioredoxin reductase. *Eur J Biochem,* 267**,** 6102-9.

ARNOLD, D. E. & HEIMALL, J. R. 2017. A Review of Chronic Granulomatous Disease. *Adv Ther,* 34**,** 2543-2557.

ARTAVANIS-TSAKONAS, K., MISAGHI, S., COMEAUX, C. A., CATIC, A., SPOONER, E., DURAISINGH, M. T. & PLOEGH, H. L. 2006. Identification by functional proteomics of a deubiquitinating/deNeddylating enzyme in Plasmodium falciparum. *Mol Microbiol,* 61**,** 1187-95.

ASLUND, F., EHN, B., MIRANDA-VIZUETE, A., PUEYO, C. & HOLMGREN, A. 1994. Two additional glutaredoxins exist in Escherichia coli: glutaredoxin 3 is a hydrogen donor for ribonucleotide reductase in a thioredoxin/glutaredoxin 1 double mutant. *Proc Natl Acad Sci U S A,* 91**,** 9813-7.

AUTEN, R. L. & DAVIS, J. M. 2009. Oxygen toxicity and reactive oxygen species: the devil is in the details. *Pediatr Res,* 66**,** 121-7.

AVERY, A. M. & AVERY, S. V. 2001. Saccharomyces cerevisiae expresses three phospholipid hydroperoxide glutathione peroxidases. *J Biol Chem,* 276**,** 33730-5.

AZEVEDO, D., TACNET, F., DELAUNAY, A., RODRIGUES-POUSADA, C. & TOLEDANO, M. B. 2003. Two redox centers within Yap1 for H2O2 and thiol-reactive chemicals signaling. *Free Radic Biol Med,* 35**,** 889-900.

BACHEWICH, C., NANTEL, A. & WHITEWAY, M. 2005. Cell cycle arrest during S or M phase generates polarized growth via distinct signals in Candida albicans. *Mol Microbiol,* 57**,** 942-59.

BACHEWICH, C., THOMAS, D. Y. & WHITEWAY, M. 2003. Depletion of a polo-like kinase in Candida albicans activates cyclase-dependent hyphal-like growth. *Mol Biol Cell,* 14**,** 2163-80.

BACHEWICH, C. & WHITEWAY, M. 2005. Cyclin Cln3p links G1 progression to hyphal and pseudohyphal development in Candida albicans. *Eukaryot Cell,* 4**,** 95-102.

BAE, Y. S., KANG, S. W., SEO, M. S., BAINES, I. C., TEKLE, E., CHOCK, P. B. & RHEE, S. G. 1997. Epidermal growth factor (EGF)-induced generation of hydrogen peroxide. Role in EGF receptor-mediated tyrosine phosphorylation. *J Biol Chem,* 272**,** 217-21.

BAEK, K. H., KIM, M. S., KIM, Y. S., SHIN, J. M. & CHOI, H. K. 2004. DUB-1A, a novel deubiquitinating enzyme subfamily member, is polyubiquitinated and cytokine-inducible in B-lymphocytes. *J Biol Chem,* 279**,** 2368-76.

BAIRD, L. & YAMAMOTO, M. 2020. The Molecular Mechanisms Regulating the KEAP1-NRF2 Pathway. *Mol Cell Biol,* 40.

BAKER, R. T., TOBIAS, J. W. & VARSHAVSKY, A. 1992. Ubiquitin-specific proteases of Saccharomyces cerevisiae. Cloning of UBP2 and UBP3, and functional analysis of the UBP gene family. *J Biol Chem,* 267**,** 23364-75.

BAKKER, B. M., OVERKAMP, K. M., VAN MARIS, A. J., KÖTTER, P., LUTTIK, M. A., VAN DIJKEN, J. P. & PRONK, J. T. 2001. Stoichiometry and compartmentation of NADH metabolism in Saccharomyces cerevisiae. *FEMS Microbiol Rev,* 25**,** 15-37.

BALABAN, R. S., NEMOTO, S. & FINKEL, T. 2005. Mitochondria, oxidants, and aging. *Cell,* 120**,** 483-95.

BECKMAN, K. B. & AMES, B. N. 1998. The free radical theory of aging matures. *Physiol Rev,* 78**,** 547-81.

BEDNASH, J. S. & MALLAMPALLI, R. K. 2016. Regulation of inflammasomes by ubiquitination. *Cell Mol Immunol,* 13**,** 722-728.

BEHREND, L., HENDERSON, G. & ZWACKA, R. M. 2003. Reactive oxygen species in oncogenic transformation. *Biochem Soc Trans,* 31**,** 1441-4.

BENSCHOP, J. J., BRABERS, N., VAN LEENEN, D., BAKKER, L. V., VAN DEUTEKOM, H. W., VAN BERKUM, N. L., APWEILER, E., LIJNZAAD, P., HOLSTEGE, F. C. & KEMMEREN, P. 2010. A consensus of core protein complex compositions for Saccharomyces cerevisiae. *Mol Cell,* 38**,** 916-28.

BERLETT, B. S. & STADTMAN, E. R. 1997. Protein oxidation in aging, disease, and oxidative stress. *J Biol Chem,* 272**,** 20313-6.

BERNIER-VILLAMOR, V., SAMPSON, D. A., MATUNIS, M. J. & LIMA, C. D. 2002. Structural basis for E2-mediated SUMO conjugation revealed by a complex between ubiquitin-conjugating enzyme Ubc9 and RanGAP1. *Cell,* 108**,** 345-56.

BERSWEILER, A., D'AUTRÉAUX, B., MAZON, H., KRIZNIK, A., BELLI, G., DELAUNAY-MOISAN, A., TOLEDANO, M. B. & RAHUEL-CLERMONT, S. 2017. A scaffold protein that chaperones a cysteine-sulfenic acid in H(2)O(2) signaling. *Nat Chem Biol,* 13**,** 909-915.

BIN, P., HUANG, R. & ZHOU, X. 2017. Oxidation Resistance of the Sulfur Amino Acids: Methionine and Cysteine. *Biomed Res Int,* 2017**,** 9584932.

BITEAU, B., LABARRE, J. & TOLEDANO, M. B. 2003. ATP-dependent reduction of cysteine-sulphinic acid by S. cerevisiae sulphiredoxin. *Nature,* 425**,** 980-4.

BLOOM, J., AMADOR, V., BARTOLINI, F., DEMARTINO, G. & PAGANO, M. 2003. Proteasome-mediated degradation of p21 via N-terminal ubiquitinylation. *Cell,* 115**,** 71-82.

BOHM, S., SZAKAL, B., HERKEN, B. W., SULLIVAN, M. R., MIHALEVIC, M. J., KABBINAVAR, F. F., BRANZEI, D., CLARK, N. L. & BERNSTEIN, K. A. 2016. The Budding Yeast Ubiquitin Protease Ubp7 Is a Novel Component Involved in S Phase Progression. *J Biol Chem,* 291**,** 4442-52.

BOLTON, J. L. & DUNLAP, T. 2017. Formation and Biological Targets of Quinones: Cytotoxic versus Cytoprotective Effects. *Chem Res Toxicol,* 30**,** 13-37.

BOLTON, J. L., TRUSH, M. A., PENNING, T. M., DRYHURST, G. & MONKS, T. J. 2000. Role of quinones in toxicology. *Chem Res Toxicol,* 13**,** 135-60.

BOSSIS, G. & MELCHIOR, F. 2006. Regulation of SUMOylation by reversible oxidation of SUMO conjugating enzymes. *Mol Cell,* 21**,** 349-57.

BOYD, S. D., CALVO, J. S., LIU, L., ULLRICH, M. S., SKOPP, A., MELONI, G. & WINKLER, D. D. 2019. The yeast copper chaperone for copper-zinc superoxide dismutase (CCS1) is a multifunctional chaperone promoting all levels of SOD1 maturation. *J Biol Chem,* 294**,** 1956-1966.

BRAND, A., MACCALLUM, D. M., BROWN, A. J., GOW, N. A. & ODDS, F. C. 2004. Ectopic expression of URA3 can influence the virulence phenotypes and proteome of Candida albicans but can be overcome by targeted reintegration of URA3 at the RPS10 locus. *Eukaryot Cell,* 3**,** 900-9.

BREMM, A., MONIZ, S., MADER, J., ROCHA, S. & KOMANDER, D. 2014. Cezanne (OTUD7B) regulates HIF-1alpha homeostasis in a proteasome-independent manner. *EMBO Rep,* 15**,** 1268-77.

BRIDGE, G., RASHID, S. & MARTIN, S. A. 2014. DNA mismatch repair and oxidative DNA damage: implications for cancer biology and treatment. *Cancers (Basel),* 6**,** 1597-614.

BRIEGER, K., SCHIAVONE, S., MILLER, F. J., JR. & KRAUSE, K. H. 2012. Reactive oxygen species: from health to disease. *Swiss Med Wkly,* 142**,** w13659.

BROWN, A. J., BUDGE, S., KALORITI, D., TILLMANN, A., JACOBSEN, M. D., YIN, Z., ENE, I. V., BOHOVYCH, I., SANDAI, D., KASTORA, S., POTRYKUS, J., BALLOU, E. R., CHILDERS, D. S., SHAHANA, S. & LEACH, M. D. 2014. Stress adaptation in a pathogenic fungus. *J Exp Biol,* 217**,** 144-55.

BROWN, J. L., NORTH, S. & BUSSEY, H. 1993. SKN7, a yeast multicopy suppressor of a mutation affecting cell wall beta-glucan assembly, encodes a product with domains homologous to prokaryotic two-component regulators and to heat shock transcription factors. *J Bacteriol,* 175**,** 6908-15.

BUETOW, L. & HUANG, D. T. 2016. Structural insights into the catalysis and regulation of E3 ubiquitin ligases. *Nature Reviews Molecular Cell Biology,* 17**,** 626-642.

BUETTNER, G. R. 1993. The pecking order of free radicals and antioxidants: lipid peroxidation, alpha-tocopherol, and ascorbate. *Arch Biochem Biophys,* 300**,** 535-43.

BURROUGHS, A. M., BALAJI, S., IYER, L. M. & ARAVIND, L. 2007. Small but versatile: the extraordinary functional and structural diversity of the β-grasp fold. *Biology Direct,* 2**,** 18.

CADWELL, K. & COSCOY, L. 2005. Ubiquitination on nonlysine residues by a viral E3 ubiquitin ligase. *Science,* 309**,** 127-30.

CAJEE, U. F., HULL, R. & NTWASA, M. 2012. Modification by ubiquitin-like proteins: significance in apoptosis and autophagy pathways. *Int J Mol Sci,* 13**,** 11804-11831.

CALVO, I. A., BORONAT, S., DOMÈNECH, A., GARCÍA-SANTAMARINA, S., AYTÉ, J. & HIDALGO, E. 2013. Dissection of a redox relay: H2O2-dependent activation of the transcription factor Pap1 through the peroxidatic Tpx1-thioredoxin cycle. *Cell Rep,* 5**,** 1413-24.

CANZONETTA, C., VERNARECCI, S., IULIANI, M., MARRACINO, C., BELLONI, C., BALLARIO, P. & FILETICI, P. 2015. SAGA DUB-Ubp8 Deubiquitylates Centromeric Histone Variant Cse4. *G3 (Bethesda, Md.),* 6**,** 287-298.

CAO, M. N., ZHOU, Y. B., GAO, A. H., CAO, J. Y., GAO, L. X., SHENG, L., XU, L., SU, M. B., CAO, X. C., HAN, M. M., WANG, M. K. & LI, J. 2014. Curcusone D, a novel ubiquitin-proteasome pathway inhibitor via ROS-induced DUB inhibition, is synergistic with bortezomib against multiple myeloma cell growth. *Biochim Biophys Acta,* 1840**,** 2004-13.

CAPPADOCIA, L. & LIMA, C. D. 2018. Ubiquitin-like Protein Conjugation: Structures, Chemistry, and Mechanism. *Chemical reviews,* 118**,** 889-918.

CAPUCCIATI, A., ZUCCA, F. A., MONZANI, E., ZECCA, L., CASELLA, L. & HOFER, T. 2021. Interaction of Neuromelanin with Xenobiotics and Consequences for Neurodegeneration; Promising Experimental Models. *Antioxidants (Basel),* 10.

CASSANDRI, M., SMIRNOV, A., NOVELLI, F., PITOLLI, C., AGOSTINI, M., MALEWICZ, M., MELINO, G. & RASCHELLÀ, G. 2017. Zinc-finger proteins in health and disease. *Cell Death Discov,* 3**,** 17071.

CEMERSKI, S., CANTAGREL, A., VAN MEERWIJK, J. P. & ROMAGNOLI, P. 2002. Reactive oxygen species differentially affect T cell receptor-signaling pathways. *J Biol Chem,* 277**,** 19585-93.

CHAE, H. Z., CHUNG, S. J. & RHEE, S. G. 1994. Thioredoxin-dependent peroxide reductase from yeast. *J Biol Chem,* 269**,** 27670-8.

CHANDRASEKARAN, A., IDELCHIK, M. & MELENDEZ, J. A. 2017. Redox control of senescence and age-related disease. *Redox Biol,* 11**,** 91-102.

CHARIZANIS, C., JUHNKE, H., KREMS, B. & ENTIAN, K. D. 1999. The mitochondrial cytochrome c peroxidase Ccp1 of Saccharomyces cerevisiae is involved in conveying an oxidative stress signal to the transcription factor Pos9 (Skn7). *Molecular and General Genetics MGG,* 262**,** 437-447.

CHAU, V., TOBIAS, J. W., BACHMAIR, A., MARRIOTT, D., ECKER, D. J., GONDA, D. K. & VARSHAVSKY, A. 1989. A multiubiquitin chain is confined to specific lysine in a targeted short-lived protein. *Science,* 243**,** 1576-83.

CHEESEMAN, K. H. & SLATER, T. F. 1993. An introduction to free radical biochemistry. *Br Med Bull,* 49**,** 481-93.

CHEN, D., TOONE, W. M., MATA, J., LYNE, R., BURNS, G., KIVINEN, K., BRAZMA, A., JONES, N. & BÄHLER, J. 2003. Global transcriptional responses of fission yeast to environmental stress. *Mol Biol Cell,* 14**,** 214-29.

CHIVERS, P. T., PREHODA, K. E. & RAINES, R. T. 1997. The CXXC motif: a rheostat in the active site. *Biochemistry,* 36**,** 4061-6.

CHOU, C.-K., CHANG, Y.-T., KORINEK, M., CHEN, Y.-T., YANG, Y.-T., LEU, S., LIN, I. L., TANG, C.-J. & CHIU, C.-C. 2017. The Regulations of Deubiquitinase USP15 and Its Pathophysiological Mechanisms in Diseases. *International journal of molecular sciences,* 18**,** 483.

CHOWDHURY, A., OGURA, T. & ESAKI, M. 2018. Two Cdc48 cofactors Ubp3 and Ubx2 regulate mitochondrial morphology and protein turnover. *J Biochem,* 164**,** 349-358.

CHUNG, K. W., KIM, D. H., PARK, M. H., CHOI, Y. J., KIM, N. D., LEE, J., YU, B. P. & CHUNG, H. Y. 2013. Recent advances in calorie restriction research on aging. *Exp Gerontol,* 48**,** 1049-53.

CIECHANOVER, A., HELLER, H., KATZ-ETZION, R. & HERSHKO, A. 1981. Activation of the heat-stable polypeptide of the ATP-dependent proteolytic system. *Proc Natl Acad Sci U S A,* 78**,** 761-5.

CLAGUE, M. J., BARSUKOV, I., COULSON, J. M., LIU, H., RIGDEN, D. J. & URBÉ, S. 2013. Deubiquitylases from genes to organism. *Physiol Rev,* 93**,** 1289-315.

CLAGUE, M. J. & URBE, S. 2006. Endocytosis: the DUB version. *Trends Cell Biol,* 16**,** 551-9.

CLEVERS, H. & NUSSE, R. 2012. Wnt/beta-catenin signaling and disease. *Cell,* 149**,** 1192-205.

COCKLIN, R., HEYEN, J., LARRY, T., TYERS, M. & GOEBL, M. 2011. New insight into the role of the Cdc34 ubiquitin-conjugating enzyme in cell cycle regulation via Ace2 and Sic1. *Genetics,* 187**,** 701-15.

COGHLAN, J., BENET, A., KUMARAN, P., FORD, M., VEALE, L., SKILTON, S. J., SAVELIEV, S. & SCHWENDEMAN, A. A. 2022. Streamlining the Characterization of Disulfide Bond Shuffling and

Protein Degradation in IgG1 Biopharmaceuticals Under Native and Stressed Conditions. *Frontiers in Bioengineering and Biotechnology,* 10.

COHEN, G., FESSL, F., TRACZYK, A., RYTKA, J. & RUIS, H. 1985. Isolation of the catalase A gene of Saccharomyces cerevisiae by complementation of the cta1 mutation. *Mol Gen Genet,* 200**,** 74-9.

COHEN, M., STUTZ, F., BELGAREH, N., HAGUENAUER-TSAPIS, R. & DARGEMONT, C. 2003. Ubp3 requires a cofactor, Bre5, to specifically de-ubiquitinate the COPII protein, Sec23. *Nat Cell Biol,* 5**,** 661-7.

COHN, M. A., KOWAL, P., YANG, K., HAAS, W., HUANG, T. T., GYGI, S. P. & D'ANDREA, A. D. 2007. A UAF1-containing multisubunit protein complex regulates the Fanconi anemia pathway. *Mol Cell,* 28**,** 786-97.

COLLINSON, L. P. & DAWES, I. W. 1992. Inducibility of the response of yeast cells to peroxide stress. *J Gen Microbiol,* 138**,** 329-335.

COLLINSON, L. P. & DAWES, I. W. 1995. Isolation, characterization and overexpression of the yeast gene, GLR1, encoding glutathione reductase. *Gene,* 156**,** 123-7.

CONKLIN, K. A. 2004. Chemotherapy-associated oxidative stress: impact on chemotherapeutic effectiveness. *Integr Cancer Ther,* 3**,** 294-300.

COPE, G. A. & DESHAIES, R. J. 2003. COP9 signalosome: a multifunctional regulator of SCF and other cullin-based ubiquitin ligases. *Cell,* 114**,** 663-71.

CORNELISSEN, T., HADDAD, D., WAUTERS, F., VAN HUMBEECK, C., MANDEMAKERS, W., KOENTJORO, B., SUE, C., GEVAERT, K., DE STROOPER, B., VERSTREKEN, P. & VANDENBERGHE, W. 2014. The deubiquitinase USP15 antagonizes Parkin-mediated mitochondrial ubiquitination and mitophagy. *Hum Mol Genet,* 23**,** 5227-42.

CORTI, O., LESAGE, S. & BRICE, A. 2011. What genetics tells us about the causes and mechanisms of Parkinson's disease. *Physiol Rev,* 91**,** 1161-218.

COSTA-DE-OLIVEIRA, S. & RODRIGUES, A. G. 2020. Candida albicans Antifungal Resistance and Tolerance in Bloodstream Infections: The Triad Yeast-Host-Antifungal. *Microorganisms,* 8.

COTTO-RIOS, X. M., BEKES, M., CHAPMAN, J., UEBERHEIDE, B. & HUANG, T. T. 2012. Deubiquitinases as a signaling target of oxidative stress. *Cell Rep,* 2**,** 1475-84.

CUI, F., MA, N., HAN, X., CHEN, N., XI, Y., YUAN, W., XU, Y., HAN, J., XU, X. & TU, Y. 2019. Effects of (60)Co γ Irradiation on the Reproductive Function of Caenorhabditis elegans. *Dose Response,* 17**,** 1559325818820981.

CURTIS, F. 2019. *The regulation of deubiquitinases by oxidative stress in Saccharomyces cerevisiae.* Newcastle University.

DA SILVA DANTAS, A., PATTERSON, M. J., SMITH, D. A., MACCALLUM, D. M., ERWIG, L. P., MORGAN, B. A. & QUINN, J. 2010. Thioredoxin regulates multiple hydrogen peroxide-induced signaling pathways in Candida albicans. *Mol Cell Biol,* 30**,** 4550-63.

DANTAS, A. D. S., DAY, A., IKEH, M., KOS, I., ACHAN, B. & QUINN, J. 2015. Oxidative stress responses in the human fungal pathogen, Candida albicans. *Biomolecules,* 5**,** 142-165.

DAS, T., KIM, E. E. & SONG, E. J. 2019a. Phosphorylation of USP15 and USP4 Regulates Localization and Spliceosomal Deubiquitination. *J Mol Biol,* 431**,** 3900-3912.

DAS, T., KIM, E. E. & SONG, E. J. 2019b. Phosphorylation of USP15 and USP4 Regulates Localization and Spliceosomal Deubiquitination. *Journal of Molecular Biology,* 431**,** 3900-3912.

DEBELYY, M. O., PLATTA, H. W., SAFFIAN, D., HENSEL, A., THOMS, S., MEYER, H. E., WARSCHEID, B., GIRZALSKY, W. & ERDMANN, R. 2011. Ubp15p, a ubiquitin hydrolase associated with the peroxisomal export machinery. *J Biol Chem,* 286**,** 28223-34.

DEISSEROTH, A. & DOUNCE, A. L. 1970. Catalase: Physical and chemical properties, mechanism of catalysis, and physiological role. *Physiol Rev,* 50**,** 319-75.

DELAUNAY, A., ISNARD, A. D. & TOLEDANO, M. B. 2000. H2O2 sensing through oxidation of the Yap1 transcription factor. *Embo j,* 19**,** 5157-66.

DELAUNAY, A., PFLIEGER, D., BARRAULT, M. B., VINH, J. & TOLEDANO, M. B. 2002. A thiol peroxidase is an H2O2 receptor and redox-transducer in gene activation. *Cell,* 111**,** 471-81.

DENNISON, P. M., RAMSDALE, M., MANSON, C. L. & BROWN, A. J. 2005. Gene disruption in Candida albicans using a synthetic, codon-optimised Cre-loxP system. *Fungal Genet Biol,* 42**,** 737-48.

DIAS, V., JUNN, E. & MOURADIAN, M. M. 2013. The role of oxidative stress in Parkinson's disease. *J Parkinsons Dis,* 3**,** 461-91.

DINAUER, M. C. 1993. The respiratory burst oxidase and the molecular genetics of chronic granulomatous disease. *Crit Rev Clin Lab Sci,* 30**,** 329-69.

DORIS, K. S., RUMSBY, E. L. & MORGAN, B. A. 2012. Oxidative stress responses involve oxidation of a conserved ubiquitin pathway enzyme. *Molecular and cellular biology,* 32**,** 4472-4481.

DRACULIC, T., DAWES, I. W. & GRANT, C. M. 2000. A single glutaredoxin or thioredoxin gene is essential for viability in the yeast Saccharomyces cerevisiae. *Mol Microbiol,* 36**,** 1167-74.

DRIVER, A. S., KODAVANTI, P. R. & MUNDY, W. R. 2000. Age-related changes in reactive oxygen species production in rat brain homogenates. *Neurotoxicol Teratol,* 22**,** 175-81.

DU, H., KIM, S., HUR, Y. S., LEE, M. S., LEE, S. H. & CHEON, C. I. 2015. A cytosolic thioredoxin acts as a molecular chaperone for peroxisome matrix proteins as well as antioxidant in peroxisome. *Mol Cells,* 38**,** 187-94.

DU, J., FU, L., SUI, Y. & ZHANG, L. 2020. The function and regulation of OTU deubiquitinases. *Front Med,* 14**,** 542-563.

DUPRE-CROCHET, S., ERARD, M. & NUBETAE, O. 2013. ROS production in phagocytes: why, when, and where? *J Leukoc Biol,* 94**,** 657-70.

DURCAN, T. M., TANG, M. Y., PÉRUSSE, J. R., DASHTI, E. A., AGUILETA, M. A., MCLELLAND, G. L., GROS, P., SHALER, T. A., FAUBERT, D., COULOMBE, B. & FON, E. A. 2014. USP8 regulates mitophagy by removing K6-linked ubiquitin conjugates from parkin. *Embo j,* 33**,** 2473-91.

EDDINS, M. J., VARADAN, R., FUSHMAN, D., PICKART, C. M. & WOLBERGER, C. 2007. Crystal structure and solution NMR studies of Lys48-linked tetraubiquitin at neutral pH. *J Mol Biol,* 367**,** 204-11.

EICHHORN, P. J., RODON, L., GONZALEZ-JUNCA, A., DIRAC, A., GILI, M., MARTINEZ-SAEZ, E., AURA, C., BARBA, I., PEG, V., PRAT, A., CUARTAS, I., JIMENEZ, J., GARCIA-DORADO, D., SAHUQUILLO, J., BERNARDS, R., BASELGA, J. & SEOANE, J. 2012. USP15 stabilizes TGF-beta receptor I and promotes oncogenesis through the activation of TGF-beta signaling in glioblastoma. *Nat Med,* 18**,** 429-35.

EMMERICH, C. H., ORDUREAU, A., STRICKSON, S., ARTHUR, J. S., PEDRIOLI, P. G., KOMANDER, D. & COHEN, P. 2013. Activation of the canonical IKK complex by K63/M1-linked hybrid ubiquitin chains. *Proc Natl Acad Sci U S A,* 110**,** 15247-52.

ENJALBERT, B., SMITH, D. A., CORNELL, M. J., ALAM, I., NICHOLLS, S., BROWN, A. J. & QUINN, J. 2006. Role of the Hog1 stress-activated protein kinase in the global transcriptional response to stress in the fungal pathogen Candida albicans. *Mol Biol Cell,* 17**,** 1018-32.

ERMAN, J. E. & VITELLO, L. B. 2002. Yeast cytochrome c peroxidase: mechanistic studies via protein engineering. *Biochim Biophys Acta,* 1597**,** 193-220.

FANG, J. & BEATTIE, D. S. 2003. External alternative NADH dehydrogenase of Saccharomyces cerevisiae: a potential source of superoxide. *Free Radic Biol Med,* 34**,** 478-88.

FANG, N. N., ZHU, M., ROSE, A., WU, K. P. & MAYOR, T. 2016. Deubiquitinase activity is required for the proteasomal degradation of misfolded cytosolic proteins upon heat-stress. *Nat Commun,* 7**,** 12907.

FEI, C., LI, Z., LI, C., CHEN, Y., CHEN, Z., HE, X., MAO, L., WANG, X., ZENG, R. & LI, L. 2013. Smurf1-mediated Lys29-linked nonproteolytic polyubiquitination of axin negatively regulates Wnt/beta-catenin signaling. *Mol Cell Biol,* 33**,** 4095-105.

FIELD, L. S., FURUKAWA, Y., O'HALLORAN, T. V. & CULOTTA, V. C. 2003. Factors controlling the uptake of yeast copper/zinc superoxide dismutase into mitochondria. *J Biol Chem,* 278**,** 28052-9.

FINKEL, T. 2011. Signal transduction by reactive oxygen species. *J Cell Biol,* 194**,** 7-15.

FINLEY, D. 2009. Recognition and processing of ubiquitin-protein conjugates by the proteasome. *Annu Rev Biochem,* 78**,** 477-513.

FINLEY, D., OZKAYNAK, E. & VARSHAVSKY, A. 1987. The yeast polyubiquitin gene is essential for resistance to high temperatures, starvation, and other stresses. *Cell,* 48**,** 1035-46.

FINLEY, D., ULRICH, H. D., SOMMER, T. & KAISER, P. 2012. The ubiquitin-proteasome system of Saccharomyces cerevisiae. *Genetics,* 192**,** 319-60.

FLICK, K., RAASI, S., ZHANG, H., YEN, J. L. & KAISER, P. 2006. A ubiquitin-interacting motif protects polyubiquitinated Met4 from degradation by the 26S proteasome. *Nat Cell Biol,* 8**,** 509-15.

FORMAN, H. J., FUKUTO, J. M. & TORRES, M. 2004. Redox signaling: thiol chemistry defines which reactive oxygen and nitrogen species can act as second messengers. *Am J Physiol Cell Physiol,* 287**,** C246-56.

FORMAN, H. J., ZHANG, H. & RINNA, A. 2009. Glutathione: overview of its protective roles, measurement, and biosynthesis. *Molecular aspects of medicine,* 30**,** 1-12.

FRAUER, C., ROTTACH, A., MEILINGER, D., BULTMANN, S., FELLINGER, K., HASENÖDER, S., WANG, M., QIN, W., SÖDING, J., SPADA, F. & LEONHARDT, H. 2011. Different binding properties and function of CXXC zinc finger domains in Dnmt1 and Tet1. *PloS one,* 6**,** e16627-e16627.

FRENCH, M. E., KOEHLER, C. F. & HUNTER, T. 2021. Emerging functions of branched ubiquitin chains. *Cell Discovery,* 7**,** 6.

GALLEGO-SÁNCHEZ, A., ANDRÉS, S., CONDE, F., SAN-SEGUNDO, P. A. & BUENO, A. 2012. Reversal of PCNA ubiquitylation by Ubp10 in Saccharomyces cerevisiae. *PLoS genetics,* 8**,** e1002826-e1002826.

GALLERY, M., BLANK, J. L., LIN, Y., GUTIERREZ, J. A., PULIDO, J. C., RAPPOLI, D., BADOLA, S., ROLFE, M. & MACBETH, K. J. 2007. The JAMM motif of human deubiquitinase Poh1 is essential for cell viability. *Mol Cancer Ther,* 6**,** 262-8.

GAREAU, J. R. & LIMA, C. D. 2010. The SUMO pathway: emerging mechanisms that shape specificity, conjugation and recognition. *Nat Rev Mol Cell Biol,* 11**,** 861-71.

GARIN, J., DIEZ, R., KIEFFER, S., DERMINE, J. F., DUCLOS, S., GAGNON, E., SADOUL, R., RONDEAU, C. & DESJARDINS, M. 2001. The phagosome proteome: insight into phagosome functions. *J Cell Biol,* 152**,** 165-80.

GARRIDO, E. O. & GRANT, C. M. 2002. Role of thioredoxins in the response of Saccharomyces cerevisiae to oxidative stress induced by hydroperoxides. *Mol Microbiol,* 43**,** 993-1003.

GARRISON, W. M. 1987. Reaction mechanisms in the radiolysis of peptides, polypeptides, and proteins. *Chemical Reviews,* 87**,** 381-398.

GASCH, A. P., SPELLMAN, P. T., KAO, C. M., CARMEL-HAREL, O., EISEN, M. B., STORZ, G., BOTSTEIN, D. & BROWN, P. O. 2000. Genomic expression programs in the response of yeast cells to environmental changes. *Mol Biol Cell,* 11**,** 4241-57.

GATTI, M., PINATO, S., MAIOLICA, A., ROCCHIO, F., PRATO, M. G., AEBERSOLD, R. & PENENGO, L. 2015. RNF168 promotes noncanonical K27 ubiquitination to signal DNA damage. *Cell Rep,* 10**,** 226-38.

GILMORE, T. D. 2006. Introduction to NF-kappaB: players, pathways, perspectives. *Oncogene,* 25**,** 6680-4.

GÖDDERZ, D., GIOVANNUCCI, T. A., LALÁKOVÁ, J., MENÉNDEZ-BENITO, V. & DANTUMA, N. P. 2017. The deubiquitylating enzyme Ubp12 regulates Rad23-dependent proteasomal degradation. *J Cell Sci,* 130**,** 3336-3346.

GOLDSTEIN, G., SCHEID, M., HAMMERLING, U., SCHLESINGER, D. H., NIALL, H. D. & BOYSE, E. A. 1975. Isolation of a polypeptide that has lymphocyte-differentiating properties and is probably represented universally in living cells. *Proceedings of the National Academy of Sciences of the United States of America,* 72**,** 11-15.

GONG, X., GUTALA, R. & JAISWAL, A. K. 2008. Quinone oxidoreductases and vitamin K metabolism. *Vitam Horm,* 78**,** 85-101.

GRALLA, E. B. & VALENTINE, J. S. 1991. Null mutants of Saccharomyces cerevisiae Cu,Zn superoxide dismutase: characterization and spontaneous mutation rates. *J Bacteriol,* 173**,** 5918-20.

GREETHAM, D. & GRANT, C. M. 2009. Antioxidant activity of the yeast mitochondrial one-Cys peroxiredoxin is dependent on thioredoxin reductase and glutathione in vivo. *Mol Cell Biol,* 29**,** 3229-40.

GROETTRUP, M., PELZER, C., SCHMIDTKE, G. & HOFMANN, K. 2008. Activating the ubiquitin family: UBA6 challenges the field. *Trends Biochem Sci,* 33**,** 230-7.

GUIDOT, D. M., MCCORD, J. M., WRIGHT, R. M. & REPINE, J. E. 1993. Absence of electron transport (Rho 0 state) restores growth of a manganese-superoxide dismutase-deficient Saccharomyces cerevisiae in hyperoxia. Evidence for electron transport as a major source of superoxide generation in vivo. *J Biol Chem,* 268**,** 26699-703.

HAAS, A. L. & ROSE, I. A. 1982. The mechanism of ubiquitin activating enzyme. A kinetic and equilibrium analysis. *J Biol Chem,* 257**,** 10329-37.

HAAS, A. L., WARMS, J. V., HERSHKO, A. & ROSE, I. A. 1982. Ubiquitin-activating enzyme. Mechanism and role in protein-ubiquitin conjugation. *J Biol Chem,* 257**,** 2543-8.

HAGLUND, K., SIGISMUND, S., POLO, S., SZYMKIEWICZ, I., DI FIORE, P. P. & DIKIC, I. 2003. Multiple monoubiquitination of RTKs is sufficient for their endocytosis and degradation. *Nat Cell Biol,* 5**,** 461-6.

HALLIWELL, B. 2006. Reactive species and antioxidants. Redox biology is a fundamental theme of aerobic life. *Plant Physiol,* 141**,** 312-22.

HANNA, J., HATHAWAY, N. A., TONE, Y., CROSAS, B., ELSASSER, S., KIRKPATRICK, D. S., LEGGETT, D. S., GYGI, S. P., KING, R. W. & FINLEY, D. 2006. Deubiquitinating enzyme Ubp6 functions noncatalytically to delay proteasomal degradation. *Cell,* 127**,** 99-111.

HARLAN, J. M., LEVINE, J. D., CALLAHAN, K. S., SCHWARTZ, B. R. & HARKER, L. A. 1984. Glutathione redox cycle protects cultured endothelial cells against lysis by extracellularly generated hydrogen peroxide. *J Clin Invest,* 73**,** 706-13.

HARRIGAN, J. A., JACQ, X., MARTIN, N. M. & JACKSON, S. P. 2018. Deubiquitylating enzymes and drug discovery: emerging opportunities. *Nat Rev Drug Discov,* 17**,** 57-78.

HARRIS, S. L. & LEVINE, A. J. 2005. The p53 pathway: positive and negative feedback loops. *Oncogene,* 24**,** 2899-908.

HASSAN, H. M. & SCHRUM, L. W. 1994. Roles of manganese and iron in the regulation of the biosynthesis of manganese-superoxide dismutase in Escherichia coli. *FEMS Microbiol Rev,* 14**,** 315-23.

HE, X. J. & FASSLER, J. S. 2005. Identification of novel Yap1p and Skn7p binding sites involved in the oxidative stress response of Saccharomyces cerevisiae. *Mol Microbiol,* 58**,** 1454-67.

HECK, D. E., VETRANO, A. M., MARIANO, T. M. & LASKIN, J. D. 2003. UVB light stimulates production of reactive oxygen species: unexpected role for catalase. *J Biol Chem,* 278**,** 22432-6.

HENRY, K. W., WYCE, A., LO, W. S., DUGGAN, L. J., EMRE, N. C., KAO, C. F., PILLUS, L., SHILATIFARD, A., OSLEY, M. A. & BERGER, S. L. 2003. Transcriptional activation via sequential histone H2B ubiquitylation and deubiquitylation, mediated by SAGA-associated Ubp8. *Genes Dev,* 17**,** 2648-63.

HERIDE, C., URBE, S. & CLAGUE, M. J. 2014. Ubiquitin code assembly and disassembly. *Curr Biol,* 24**,** R215-20.

HERNÁNDEZ-LÓPEZ, M. J., GARCÍA-MARQUÉS, S., RANDEZ-GIL, F. & PRIETO, J. A. 2011. Multicopy suppression screening of Saccharomyces cerevisiae Identifies the ubiquitination machinery as a main target for improving growth at low temperatures. *Applied and environmental microbiology,* 77**,** 7517-7525.

HERRERO, E. & DE LA TORRE-RUIZ, M. A. 2007. Monothiol glutaredoxins: a common domain for multiple functions. *Cell Mol Life Sci,* 64**,** 1518-30.

HERRERO, E., ROS, J., BELLI, G. & CABISCOL, E. 2008. Redox control and oxidative stress in yeast cells. *Biochim Biophys Acta,* 1780**,** 1217-35.

HERSHKO, A., HELLER, H., ELIAS, S. & CIECHANOVER, A. 1983. Components of ubiquitin-protein ligase system. Resolution, affinity purification, and role in protein breakdown. *J Biol Chem,* 258**,** 8206-14.

HETFELD, B. K., HELFRICH, A., KAPELARI, B., SCHEEL, H., HOFMANN, K., GUTERMAN, A., GLICKMAN, M., SCHADE, R., KLOETZEL, P. M. & DUBIEL, W. 2005. The zinc finger of the CSN-associated deubiquitinating enzyme USP15 is essential to rescue the E3 ligase Rbx1. *Curr Biol,* 15**,** 1217-21.

HICKE, L., SCHUBERT, H. L. & HILL, C. P. 2005. Ubiquitin-binding domains. *Nat Rev Mol Cell Biol,* 6**,** 610-21.

HIRST, J., KING, M. S. & PRYDE, K. R. 2008. The production of reactive oxygen species by complex I. *Biochem Soc Trans,* 36**,** 976-80.

HOCHSTRASSER, M. 2000. Evolution and function of ubiquitin-like protein-conjugation systems. *Nat Cell Biol,* 2**,** E153-7.

HOCHSTRASSER, M. 2009a. Origin and function of ubiquitin-like proteins. *Nature,* 458**,** 422-9.

HOCHSTRASSER, M. 2009b. Origin and function of ubiquitin-like proteins. *Nature,* 458**,** 422-429.

HOFER, T., MYHRE, O., PELTOLA-THIES, J. & HIRMANN, D. 2021. Analysis of elimination half-lives in MamTKDB 1.0 related to bioaccumulation: Requirement of repeated administration and blood plasma values underrepresent tissues. *Environ Int,* 155**,** 106592.

HOFFMANN, A., LEVCHENKO, A., SCOTT, M. L. & BALTIMORE, D. 2002. The IkappaB-NF-kappaB signaling module: temporal control and selective gene activation. *Science,* 298**,** 1241-5.

HÖRTNER, H., AMMERER, G., HARTTER, E., HAMILTON, B., RYTKA, J., BILINSKI, T. & RUIS, H. 1982. Regulation of synthesis of catalases and iso-1-cytochrome c in Saccharomyces cerevisiae by glucose, oxygen and heme. *Eur J Biochem,* 128**,** 179-84.

HU, M., LI, P., LI, M., LI, W., YAO, T., WU, J. W., GU, W., COHEN, R. E. & SHI, Y. 2002. Crystal structure of a UBP-family deubiquitinating enzyme in isolation and in complex with ubiquitin aldehyde. *Cell,* 111**,** 1041-54.

HUANG, D. T., WALDEN, H., DUDA, D. & SCHULMAN, B. A. 2004. Ubiquitin-like protein activation. *Oncogene,* 23**,** 1958-71.

HUANG, H., JEON, M. S., LIAO, L., YANG, C., ELLY, C., YATES, J. R., 3RD & LIU, Y. C. 2010. K33-linked polyubiquitination of T cell receptor-zeta regulates proteolysis-independent T cell signaling. *Immunity,* 33**,** 60-70.

HUANG, X., LANGELOTZ, C., HETFELD-PECHOC, B. K., SCHWENK, W. & DUBIEL, W. 2009. The COP9 signalosome mediates beta-catenin degradation by deneddylation and blocks adenomatous polyposis coli destruction via USP15. *J Mol Biol,* 391**,** 691-702.

HUBER-WUNDERLICH, M. & GLOCKSHUBER, R. 1998. A single dipeptide sequence modulates the redox properties of a whole enzyme family. *Fold Des,* 3**,** 161-71.

HUGUENIN-DEZOT, N., DE CESARE, V., PELTIER, J., KNEBEL, A., KRISTARYIANTO, Y. A., ROGERSON, D. T., KULATHU, Y., TROST, M. & CHIN, J. W. 2016. Synthesis of Isomeric Phosphoubiquitin Chains Reveals that Phosphorylation Controls Deubiquitinase Activity and Specificity. *Cell Rep,* 16**,** 1180-1193.

HUSEINOVIC, A., VAN DIJK, M., VERMEULEN, N. P. E., VAN LEEUWEN, F., KOOTER, J. M. & VOS, J. C. 2018. Drug toxicity profiling of a Saccharomyces cerevisiae deubiquitinase deletion panel shows that acetaminophen mimics tyrosine. *Toxicol In Vitro,* 47**,** 259-268.

HUTTI, J. E., TURK, B. E., ASARA, J. M., MA, A., CANTLEY, L. C. & ABBOTT, D. W. 2007. IkappaB kinase beta phosphorylates the K63 deubiquitinase A20 to cause feedback inhibition of the NF-kappaB pathway. *Mol Cell Biol,* 27**,** 7451-61.

IANNUZZI, C., ADROVER, M., PUGLISI, R., YAN, R., TEMUSSI, P. A. & PASTORE, A. 2014. The role of zinc in the stability of the marginally stable IscU scaffold protein. *Protein Sci,* 23**,** 1208-19.

INGVARSDOTTIR, K., KROGAN, N. J., EMRE, N. C. T., WYCE, A., THOMPSON, N. J., EMILI, A., HUGHES, T. R., GREENBLATT, J. F. & BERGER, S. L. 2005. H2B ubiquitin protease Ubp8 and Sgf11 constitute

a discrete functional module within the Saccharomyces cerevisiae SAGA complex. *Molecular and cellular biology,* 25**,** 1162-1172.

INN, K. S., GACK, M. U., TOKUNAGA, F., SHI, M., WONG, L. Y., IWAI, K. & JUNG, J. U. 2011. Linear ubiquitin assembly complex negatively regulates RIG-I- and TRIM25-mediated type I interferon induction. *Mol Cell,* 41**,** 354-65.

INOUE, Y., MATSUDA, T., SUGIYAMA, K., IZAWA, S. & KIMURA, A. 1999. Genetic analysis of glutathione peroxidase in oxidative stress response of Saccharomyces cerevisiae. *J Biol Chem,* 274**,** 27002-9.

ISOYAMA, T., MURAYAMA, A., NOMOTO, A. & KUGE, S. 2001. Nuclear import of the yeast AP-1-like transcription factor Yap1p is mediated by transport receptor Pse1p, and this import step is not affected by oxidative stress. *J Biol Chem,* 276**,** 21863-9.

IZAWA, S., INOUE, Y. & KIMURA, A. 1996. Importance of catalase in the adaptive response to hydrogen peroxide: analysis of acatalasaemic Saccharomyces cerevisiae. *Biochem J,* 320 (Pt 1)**,** 61-7.

IZAWA, S., MAEDA, K., SUGIYAMA, K., MANO, J., INOUE, Y. & KIMURA, A. 1999. Thioredoxin deficiency causes the constitutive activation of Yap1, an AP-1-like transcription factor in Saccharomyces cerevisiae. *J Biol Chem,* 274**,** 28459-65.

JAMIESON, D. J. 1998. Oxidative stress responses of the yeast Saccharomyces cerevisiae. *Yeast,* 14**,** 1511-27.

JANG, H. H., LEE, K. O., CHI, Y. H., JUNG, B. G., PARK, S. K., PARK, J. H., LEE, J. R., LEE, S. S., MOON, J. C., YUN, J. W., CHOI, Y. O., KIM, W. Y., KANG, J. S., CHEONG, G. W., YUN, D. J., RHEE, S. G., CHO, M. J. & LEE, S. Y. 2004. Two enzymes in one; two yeast peroxiredoxins display oxidative stress-dependent switching from a peroxidase to a molecular chaperone function. *Cell,* 117**,** 625-35.

JASTROCH, M., DIVAKARUNI, A. S., MOOKERJEE, S., TREBERG, J. R. & BRAND, M. D. 2010. Mitochondrial proton and electron leaks. *Essays Biochem,* 47**,** 53-67.

JENSEN, P. K. 1966. Antimycin-insensitive oxidation of succinate and reduced nicotinamide-adenine dinucleotide in electron-transport particles. I. pH dependency and hydrogen peroxide formation. *Biochim Biophys Acta,* 122**,** 157-66.

JENTSCH, S. & PYROWOLAKIS, G. 2000. Ubiquitin and its kin: how close are the family ties? *Trends Cell Biol,* 10**,** 335-42.

JEŽEK, J., COOPER, K. F. & STRICH, R. 2018. Reactive Oxygen Species and Mitochondrial Dynamics: The Yin and Yang of Mitochondrial Dysfunction and Cancer Progression. *Antioxidants (Basel),* 7.

JONES, M. J., COLNAGHI, L. & HUANG, T. T. 2012. Dysregulation of DNA polymerase κ recruitment to replication forks results in genomic instability. *Embo j,* 31**,** 908-18.

JUAN, C. A., PÉREZ DE LA LASTRA, J. M., PLOU, F. J. & PÉREZ-LEBEÑA, E. 2021. The Chemistry of Reactive Oxygen Species (ROS) Revisited: Outlining Their Role in Biological Macromolecules (DNA, Lipids and Proteins) and Induced Pathologies. *International Journal of Molecular Sciences* [Online], 22.

KAHANA, A. 2001. The deubiquitinating enzyme Dot4p is involved in regulating nutrient uptake. *Biochem Biophys Res Commun,* 282**,** 916-20.

KAHANA, A. & GOTTSCHLING, D. E. 1999. DOT4 links silencing and cell growth in Saccharomyces cerevisiae. *Mol Cell Biol,* 19**,** 6608-20.

KAISER, S. E., RILEY, B. E., SHALER, T. A., TREVINO, R. S., BECKER, C. H., SCHULMAN, H. & KOPITO, R. R. 2011. Protein standard absolute quantification (PSAQ) method for the measurement of cellular ubiquitin pools. *Nat Methods,* 8**,** 691-6.

KAMIYA, H., MIURA, K., ISHIKAWA, H., INOUE, H., NISHIMURA, S. & OHTSUKA, E. 1992. c-Ha-ras containing 8-hydroxyguanine at codon 12 induces point mutations at the modified and adjacent positions. *Cancer Res,* 52**,** 3483-5.

KANGA, S., BERNARD, D., MAGER-HECKEL, A. M., ERPAPAZOGLOU, Z., MATTIROLI, F., SIXMA, T. K., LEON, S., URBAN-GRIMAL, D., TARASSOV, I. & HAGUENAUER-TSAPIS, R. 2012. A deubiquitylating complex required for neosynthesis of a yeast mitochondrial ATP synthase subunit. *PLoS One,* 7**,** e38071.

KAR, S., SUBBARAM, S., CARRICO, P. M. & MELENDEZ, J. A. 2010. Redox-control of matrix metalloproteinase-1: a critical link between free radicals, matrix remodeling and degenerative disease. *Respir Physiol Neurobiol,* 174**,** 299-306.

KARIM, A. S., CURRAN, K. A. & ALPER, H. S. 2013. Characterization of plasmid burden and copy number in Saccharomyces cerevisiae for optimization of metabolic engineering applications. *FEMS Yeast Res,* 13**,** 107-16.

KAWANISHI, S. & OIKAWA, S. 2004. Mechanism of telomere shortening by oxidative stress. *Ann N Y Acad Sci,* 1019**,** 278-84.

KEE, Y., MUNOZ, W., LYON, N. & HUIBREGTSE, J. M. 2006. The deubiquitinating enzyme Ubp2 modulates Rsp5-dependent Lys63-linked polyubiquitin conjugates in Saccharomyces cerevisiae. *J Biol Chem,* 281**,** 36724-31.

KEHRER, J. P. 1993. Free radicals as mediators of tissue injury and disease. *Crit Rev Toxicol,* 23**,** 21-48.

KEHRER, J. P. 2000. The Haber-Weiss reaction and mechanisms of toxicity. *Toxicology,* 149**,** 43-50.

KERSCHER, O., FELBERBAUM, R. & HOCHSTRASSER, M. 2006. Modification of proteins by ubiquitin and ubiquitin-like proteins. *Annu Rev Cell Dev Biol,* 22**,** 159-80.

KHAN, A. A., RAHMANI, A. H., ALDEBASI, Y. H. & ALY, S. M. 2014. Biochemical and pathological studies on peroxidases -an updated review. *Glob J Health Sci,* 6**,** 87-98.

KIM, H. T., KIM, K. P., LLEDIAS, F., KISSELEV, A. F., SCAGLIONE, K. M., SKOWYRA, D., GYGI, S. P. & GOLDBERG, A. L. 2007. Certain pairs of ubiquitin-conjugating enzymes (E2s) and ubiquitin-protein ligases (E3s) synthesize nondegradable forked ubiquitin chains containing all possible isopeptide linkages. *J Biol Chem,* 282**,** 17375-86.

KIM, W., BENNETT, E. J., HUTTLIN, E. L., GUO, A., LI, J., POSSEMATO, A., SOWA, M. E., RAD, R., RUSH, J., COMB, M. J., HARPER, J. W. & GYGI, S. P. 2011. Systematic and quantitative assessment of the ubiquitin-modified proteome. *Mol Cell,* 44**,** 325-40.

KINNER, A. & KOLLING, R. 2003. The yeast deubiquitinating enzyme Ubp16 is anchored to the outer mitochondrial membrane. *FEBS Lett,* 549**,** 135-40.

KLEIN, T., VINER, R. I. & OVERALL, C. M. 2016. Quantitative proteomics and terminomics to elucidate the role of ubiquitination and proteolysis in adaptive immunity. *Philos Trans A Math Phys Eng Sci,* 374.

KLOTZ, L. O. & STEINBRENNER, H. 2017. Cellular adaptation to xenobiotics: Interplay between xenosensors, reactive oxygen species and FOXO transcription factors. *Redox Biol,* 13**,** 646-654.

KNIPSCHEER, P., FLOTHO, A., KLUG, H., OLSEN, J. V., VAN DIJK, W. J., FISH, A., JOHNSON, E. S., MANN, M., SIXMA, T. K. & PICHLER, A. 2008. Ubc9 sumoylation regulates SUMO target discrimination. *Mol Cell,* 31**,** 371-82.

KOHEN, R. & NYSKA, A. 2002. Oxidation of biological systems: oxidative stress phenomena, antioxidants, redox reactions, and methods for their quantification. *Toxicol Pathol,* 30**,** 620-50.

KOMALAPRIYA, C., KALORITI, D., TILLMANN, A. T., YIN, Z., HERRERO-DE-DIOS, C., JACOBSEN, M. D., BELMONTE, R. C., CAMERON, G., HAYNES, K., GREBOGI, C., DE MOURA, A. P., GOW, N. A., THIEL, M., QUINN, J., BROWN, A. J. & ROMANO, M. C. 2015. Integrative Model of Oxidative Stress Adaptation in the Fungal Pathogen Candida albicans. *PLoS One,* 10**,** e0137750.

KOMANDER, D. 2009. The emerging complexity of protein ubiquitination. *Biochem Soc Trans,* 37**,** 937-53.

KOMANDER, D. 2010. Mechanism, specificity and structure of the deubiquitinases. *Subcell Biochem,* 54**,** 69-87.

KOMANDER, D., LORD, C. J., SCHEEL, H., SWIFT, S., HOFMANN, K., ASHWORTH, A. & BARFORD, D. 2008. The structure of the CYLD USP domain explains its specificity for Lys63-linked polyubiquitin and reveals a B box module. *Mol Cell,* 29**,** 451-64.

KOMANDER, D. & RAPE, M. 2012. The ubiquitin code. *Annu Rev Biochem,* 81**,** 203-29.

KOMANDER, D., REYES-TURCU, F., LICCHESI, J. D., ODENWAELDER, P., WILKINSON, K. D. & BARFORD, D. 2009. Molecular discrimination of structurally equivalent Lys 63-linked and linear polyubiquitin chains. *EMBO Rep,* 10**,** 466-73.

KOSOWER, N. S. & KOSOWER, E. M. 1995. Diamide: an oxidant probe for thiols. *Methods Enzymol,* 251**,** 123-33.

KOULICH, E., LI, X. & DEMARTINO, G. N. 2008. Relative structural and functional roles of multiple deubiquitylating proteins associated with mammalian 26S proteasome. *Mol Biol Cell,* 19**,** 1072-82.

KRAFT, C., DEPLAZES, A., SOHRMANN, M. & PETER, M. 2008. Mature ribosomes are selectively degraded upon starvation by an autophagy pathway requiring the Ubp3p/Bre5p ubiquitin protease. *Nat Cell Biol,* 10**,** 602-10.

KREMS, B., CHARIZANIS, C. & ENTIAN, K. D. 1996. The response regulator-like protein Pos9/Skn7 of Saccharomyces cerevisiae is involved in oxidative stress resistance. *Curr Genet,* 29**,** 327-34.

KUGE, S. & JONES, N. 1994. YAP1 dependent activation of TRX2 is essential for the response of Saccharomyces cerevisiae to oxidative stress by hydroperoxides. *Embo j,* 13**,** 655-64.

KULATHU, Y. & KOMANDER, D. 2012. Atypical ubiquitylation - the unexplored world of polyubiquitin beyond Lys48 and Lys63 linkages. *Nat Rev Mol Cell Biol,* 13**,** 508-23.

KWASNA, D., ABDUL REHMAN, S. A., NATARAJAN, J., MATTHEWS, S., MADDEN, R., DE CESARE, V., WEIDLICH, S., VIRDEE, S., AHEL, I., GIBBS-SEYMOUR, I. & KULATHU, Y. 2018. Discovery and Characterization of ZUFSP/ZUP1, a Distinct Deubiquitinase Class Important for Genome Stability. *Mol Cell,* 70**,** 150-164.e6.

LAFONT, E., HARTWIG, T. & WALCZAK, H. 2018. Paving TRAIL's Path with Ubiquitin. *Trends Biochem Sci,* 43**,** 44-60.

LAI, K. P., CHEN, J. & TSE, W. K. F. 2020. Role of Deubiquitinases in Human Cancers: Potential Targeted Therapy. *Int J Mol Sci,* 21.

LAM, M. H., URBAN-GRIMAL, D., BUGNICOURT, A., GREENBLATT, J. F., HAGUENAUER-TSAPIS, R. & EMILI, A. 2009. Interaction of the deubiquitinating enzyme Ubp2 and the e3 ligase Rsp5 is required for transporter/receptor sorting in the multivesicular body pathway. *PLoS One,* 4**,** e4259.

LANGE, S. M., ARMSTRONG, L. A. & KULATHU, Y. 2022. Deubiquitinases: From mechanisms to their inhibition by small molecules. *Mol Cell,* 82**,** 15-29.

LANZ, M. C., YUGANDHAR, K., GUPTA, S., SANFORD, E. J., FAÇA, V. M., VEGA, S., JOINER, A. M. N., FROMME, J. C., YU, H. & SMOLKA, M. B. 2021. In-depth and 3-dimensional exploration of the budding yeast phosphoproteome. *EMBO Rep,* 22**,** e51121.

LAPINSKAS, P., RUIS, H. & CULOTTA, V. 1993. Regulation of Saccharomyces cerevisiae catalase gene expression by copper. *Curr Genet,* 24**,** 388-93.

LARSEN, C. N., KRANTZ, B. A. & WILKINSON, K. D. 1998. Substrate specificity of deubiquitinating enzymes: ubiquitin C-terminal hydrolases. *Biochemistry,* 37**,** 3358-68.

LAURENT, T. C., MOORE, E. C. & REICHARD, P. 1964. ENZYMATIC SYNTHESIS OF DEOXYRIBONUCLEOTIDES. IV. ISOLATION AND CHARACTERIZATION OF THIOREDOXIN, THE HYDROGEN DONOR FROM ESCHERICHIA COLI B. *J Biol Chem,* 239**,** 3436-44.

LAVOIE, H., SELLAM, A., ASKEW, C., NANTEL, A. & WHITEWAY, M. 2008. A toolbox for epitope-tagging and genome-wide location analysis in Candida albicans. *BMC genomics,* 9**,** 578-578.

LAWLESS, C., GREAVES, L., REEVE, A. K., TURNBULL, D. M. & VINCENT, A. E. 2020. The rise and rise of mitochondrial DNA mutations. *Open Biol,* 10**,** 200061.

LEE, J. G., BAEK, K., SOETANDYO, N. & YE, Y. 2013a. Reversible inactivation of deubiquitinases by reactive oxygen species in vitro and in cells. *Nat Commun,* 4**,** 1568.

LEE, J. R., LEE, S. S., JANG, H. H., LEE, Y. M., PARK, J. H., PARK, S. C., MOON, J. C., PARK, S. K., KIM, S. Y., LEE, S. Y., CHAE, H. B., JUNG, Y. J., KIM, W. Y., SHIN, M. R., CHEONG, G. W., KIM, M. G., KANG, K. R., LEE, K. O., YUN, D. J. & LEE, S. Y. 2009. Heat-shock dependent oligomeric status alters the function of a plant-specific thioredoxin-like protein, AtTDX. *Proc Natl Acad Sci U S A,* 106**,** 5978-83.

LEE, S., KIM, S. M. & LEE, R. T. 2013b. Thioredoxin and thioredoxin target proteins: from molecular mechanisms to functional significance. *Antioxid Redox Signal,* 18**,** 1165-207.

LEE, S. R., YANG, K. S., KWON, J., LEE, C., JEONG, W. & RHEE, S. G. 2002. Reversible inactivation of the tumor suppressor PTEN by H2O2. *J Biol Chem,* 277**,** 20336-42.

LEE, W. C., LEE, M., JUNG, J. W., KIM, K. P. & KIM, D. 2008. SCUD: Saccharomyces cerevisiae ubiquitination database. *BMC Genomics,* 9**,** 440.

LI, K., OSSAREH-NAZARI, B., LIU, X., DARGEMONT, C. & MARMORSTEIN, R. 2007. Molecular basis for bre5 cofactor recognition by the ubp3 deubiquitylating enzyme. *Journal of molecular biology,* 372**,** 194-204.

LI, M., CHEN, D., SHILOH, A., LUO, J., NIKOLAEV, A. Y., QIN, J. & GU, W. 2002. Deubiquitination of p53 by HAUSP is an important pathway for p53 stabilization. *Nature,* 416**,** 648-53.

LI, S. J. & HOCHSTRASSER, M. 1999. A new protease required for cell-cycle progression in yeast. *Nature,* 398**,** 246-51.

LI, W. & YE, Y. 2008. Polyubiquitin chains: functions, structures, and mechanisms. *Cell Mol Life Sci,* 65**,** 2397-406.

LI, Y. & REVERTER, D. 2021. Molecular Mechanisms of DUBs Regulation in Signaling and Disease. *Int J Mol Sci,* 22.

LI, Y. C., CAI, S. W., SHU, Y. B., CHEN, M. W. & SHI, Z. 2022. USP15 in Cancer and Other Diseases: From Diverse Functionsto Therapeutic Targets. *Biomedicines,* 10.

LIAKOPOULOS, D., DOENGES, G., MATUSCHEWSKI, K. & JENTSCH, S. 1998. A novel protein modification pathway related to the ubiquitin system. *Embo j,* 17**,** 2208-14.

LIGUORI, I., RUSSO, G., CURCIO, F., BULLI, G., ARAN, L., DELLA-MORTE, D., GARGIULO, G., TESTA, G., CACCIATORE, F., BONADUCE, D. & ABETE, P. 2018. Oxidative stress, aging, and diseases. *Clin Interv Aging,* 13**,** 757-772.

LIM, K.-H., JOO, J.-Y. & BAEK, K.-H. 2020. The potential roles of deubiquitinating enzymes in brain diseases. *Ageing Research Reviews,* 61**,** 101088.

LINGHU, B., CALLIS, J. & GOEBL, M. G. 2002. Rub1p processing by Yuh1p is required for wild-type levels of Rub1p conjugation to Cdc53p. *Eukaryotic cell,* 1**,** 491-494.

LIOU, G. Y. & STORZ, P. 2010. Reactive oxygen species in cancer. *Free Radic Res,* 44**,** 479-96.

LIVAK, K. J. & SCHMITTGEN, T. D. 2001. Analysis of relative gene expression data using real-time quantitative PCR and the 2(-Delta Delta C(T)) Method. *Methods,* 25**,** 402-8.

LOIS, L. M. & LIMA, C. D. 2005. Structures of the SUMO E1 provide mechanistic insights into SUMO activation and E2 recruitment to E1. *Embo j,* 24**,** 439-51.

LONGO, V. D., GRALLA, E. B. & VALENTINE, J. S. 1996. Superoxide dismutase activity is essential for stationary phase survival in Saccharomyces cerevisiae. Mitochondrial production of toxic oxygen species in vivo. *J Biol Chem,* 271**,** 12275-80.

LUIKENHUIS, S., PERRONE, G., DAWES, I. W. & GRANT, C. M. 1998. The yeast Saccharomyces cerevisiae contains two glutaredoxin genes that are required for protection against reactive oxygen species. *Mol Biol Cell,* 9**,** 1081-91.

LUK, E., YANG, M., JENSEN, L. T., BOURBONNAIS, Y. & CULOTTA, V. C. 2005. Manganese activation of superoxide dismutase 2 in the mitochondria of Saccharomyces cerevisiae. *J Biol Chem,* 280**,** 22715-20.

LUO, M., JIANG, Y. L., MA, X. X., TANG, Y. J., HE, Y. X., YU, J., ZHANG, R. G., CHEN, Y. & ZHOU, C. Z. 2010. Structural and biochemical characterization of yeast monothiol glutaredoxin Grx6. *J Mol Biol,* 398**,** 614-22.

LUO, S. & LEVINE, R. L. 2009. Methionine in proteins defends against oxidative stress. *Faseb j,* 23**,** 464-72.

MACDIARMID, C. W., TAGGART, J., KERDSOMBOON, K., KUBISIAK, M., PANASCHAROEN, S., SCHELBLE, K. & EIDE, D. J. 2013. Peroxiredoxin chaperone activity is critical for protein homeostasis in zinc-deficient yeast. *J Biol Chem,* 288**,** 31313-27.

MADIRAJU, C., NOVACK, J. P., REED, J. C. & MATSUZAWA, S. I. 2022. K63 ubiquitination in immune signaling. *Trends Immunol,* 43**,** 148-162.

MAKAROVA, K. S., ARAVIND, L. & KOONIN, E. V. 2000. A novel superfamily of predicted cysteine proteases from eukaryotes, viruses and Chlamydia pneumoniae. *Trends Biochem Sci,* 25**,** 50-2.
MANIATIS, T., FRITSCH, E.F., SAMBROOK, J., ENGEL, J. 1985. Molecular cloning–A laboratory manual. *Acta Biotechnologica,* 5**,** 104.
MARTIN, J. L. 1995. Thioredoxin —a fold for all reasons. *Structure,* 3**,** 245-250.
MARTINS, D. & ENGLISH, A. M. 2014. Catalase activity is stimulated by H(2)O(2) in rich culture medium and is required for H(2)O(2) resistance and adaptation in yeast. *Redox Biol,* 2**,** 308-13.
MATSUOKA, S., BALLIF, B. A., SMOGORZEWSKA, A., MCDONALD, E. R., 3RD, HUROV, K. E., LUO, J., BAKALARSKI, C. E., ZHAO, Z., SOLIMINI, N., LERENTHAL, Y., SHILOH, Y., GYGI, S. P. & ELLEDGE, S. J. 2007. ATM and ATR substrate analysis reveals extensive protein networks responsive to DNA damage. *Science,* 316**,** 1160-6.
MAYER, F. L., WILSON, D. & HUBE, B. 2013. Candida albicans pathogenicity mechanisms. *Virulence,* 4**,** 119-28.
MAYTAL-KIVITY, V., REIS, N., HOFMANN, K. & GLICKMAN, M. H. 2002. MPN+, a putative catalytic motif found in a subset of MPN domain proteins from eukaryotes and prokaryotes, is critical for Rpn11 function. *BMC Biochem,* 3**,** 28.
MCDOWELL, G. S. & PHILPOTT, A. 2013. Non-canonical ubiquitylation: mechanisms and consequences. *Int J Biochem Cell Biol,* 45**,** 1833-42.
MCKENZIE, C. G., KOSER, U., LEWIS, L. E., BAIN, J. M., MORA-MONTES, H. M., BARKER, R. N., GOW, N. A. & ERWIG, L. P. 2010. Contribution of Candida albicans cell wall components to recognition by and escape from murine macrophages. *Infect Immun,* 78**,** 1650-8.
MELOV, S., RAVENSCROFT, J., MALIK, S., GILL, M. S., WALKER, D. W., CLAYTON, P. E., WALLACE, D. C., MALFROY, B., DOCTROW, S. R. & LITHGOW, G. J. 2000. Extension of life-span with superoxide dismutase/catalase mimetics. *Science,* 289**,** 1567-9.
MESSICK, T. E., RUSSELL, N. S., IWATA, A. J., SARACHAN, K. L., SHIEKHATTAR, R., SHANKS, J. R., REYES-TURCU, F. E., WILKINSON, K. D. & MARMORSTEIN, R. 2008. Structural basis for ubiquitin recognition by the Otu1 ovarian tumor domain protein. *J Biol Chem,* 283**,** 11038-49.
METZGER, M. B., HRISTOVA, V. A. & WEISSMAN, A. M. 2012. HECT and RING finger families of E3 ubiquitin ligases at a glance. *J Cell Sci,* 125**,** 531-7.
MEULMEESTER, E., KUNZE, M., HSIAO, H. H., URLAUB, H. & MELCHIOR, F. 2008. Mechanism and consequences for paralog-specific sumoylation of ubiquitin-specific protease 25. *Mol Cell,* 30**,** 610-9.
MEVISSEN, T. E., HOSPENTHAL, M. K., GEURINK, P. P., ELLIOTT, P. R., AKUTSU, M., ARNAUDO, N., EKKEBUS, R., KULATHU, Y., WAUER, T., EL OUALID, F., FREUND, S. M., OVAA, H. & KOMANDER, D. 2013. OTU deubiquitinases reveal mechanisms of linkage specificity and enable ubiquitin chain restriction analysis. *Cell,* 154**,** 169-84.
MEVISSEN, T. E. T. & KOMANDER, D. 2017. Mechanisms of Deubiquitinase Specificity and Regulation. *Annu Rev Biochem,* 86**,** 159-192.
MEVISSEN, T. E. T., KULATHU, Y., MULDER, M. P. C., GEURINK, P. P., MASLEN, S. L., GERSCH, M., ELLIOTT, P. R., BURKE, J. E., VAN TOL, B. D. M., AKUTSU, M., OUALID, F. E., KAWASAKI, M., FREUND, S. M. V., OVAA, H. & KOMANDER, D. 2016. Molecular basis of Lys11-polyubiquitin specificity in the deubiquitinase Cezanne. *Nature,* 538**,** 402-405.
MITTLER, R. 2017. ROS Are Good. *Trends Plant Sci,* 22**,** 11-19.
MOAZED, D. & JOHNSON, D. 1996. A deubiquitinating enzyme interacts with SIR4 and regulates silencing in S. cerevisiae. *Cell,* 86**,** 667-77.
MOCCIARO, A. & RAPE, M. 2012. Emerging regulatory mechanisms in ubiquitin-dependent cell cycle control. *J Cell Sci,* 125**,** 255-63.
MOLDOVAN, G. L., PFANDER, B. & JENTSCH, S. 2007. PCNA, the maestro of the replication fork. *Cell,* 129**,** 665-79.
MONIZ, S., BANDARRA, D., BIDDLESTONE, J., CAMPBELL, K. J., KOMANDER, D., BREMM, A. & ROCHA, S. 2015. Cezanne regulates E2F1-dependent HIF2alpha expression. *J Cell Sci,* 128**,** 3082-93.

MORGAN, B. A., BOUQUIN, N., MERRILL, G. F. & JOHNSTON, L. H. 1995. A yeast transcription factor bypassing the requirement for SBF and DSC1/MBF in budding yeast has homology to bacterial signal transduction proteins. *Embo j,* 14**,** 5679-89.

MORGAN, M. T., HAJ-YAHYA, M., RINGEL, A. E., BANDI, P., BRIK, A. & WOLBERGER, C. 2016. Structural basis for histone H2B deubiquitination by the SAGA DUB module. *Science,* 351**,** 725-8.

MORRIS, J. R. & SOLOMON, E. 2004. BRCA1 : BARD1 induces the formation of conjugated ubiquitin structures, dependent on K6 of ubiquitin, in cells during DNA replication and repair. *Hum Mol Genet,* 13**,** 807-17.

MUELLER, T. D., KAMIONKA, M. & FEIGON, J. 2004. Specificity of the interaction between ubiquitin-associated domains and ubiquitin. *J Biol Chem,* 279**,** 11926-36.

MULFORD, K. E. & FASSLER, J. S. 2011. Association of the Skn7 and Yap1 transcription factors in the Saccharomyces cerevisiae oxidative stress response. *Eukaryot Cell,* 10**,** 761-9.

MULLER, E. G. 1991. Thioredoxin deficiency in yeast prolongs S phase and shortens the G1 interval of the cell cycle. *J Biol Chem,* 266**,** 9194-202.

MURPHY, J. W. 1991. Mechanisms of natural resistance to human pathogenic fungi. *Annu Rev Microbiol,* 45**,** 509-38.

MYTHRI, R. B., VALI, S. & BHARATH, M. M. S. 2013. Oxidative Stress, Protein Damage. *In:* DUBITZKY, W., WOLKENHAUER, O., CHO, K.-H. & YOKOTA, H. (eds.) *Encyclopedia of Systems Biology.* New York, NY: Springer New York.

NAGARAJAN, N., OKA, S. & SADOSHIMA, J. 2017. Modulation of signaling mechanisms in the heart by thioredoxin 1. *Free radical biology & medicine,* 109**,** 125-131.

NAKABEPPU, Y. 2014. Cellular levels of 8-oxoguanine in either DNA or the nucleotide pool play pivotal roles in carcinogenesis and survival of cancer cells. *Int J Mol Sci,* 15**,** 12543-57.

NAKABEPPU, Y., SAKUMI, K., SAKAMOTO, K., TSUCHIMOTO, D., TSUZUKI, T. & NAKATSU, Y. 2006. Mutagenesis and carcinogenesis caused by the oxidation of nucleic acids. *Biol Chem,* 387**,** 373-9.

NAKAGAWA, T. & NAKAYAMA, K. 2015. Protein monoubiquitylation: targets and diverse functions. *Genes Cells,* 20**,** 543-62.

NAKAYAMA, K. I. & NAKAYAMA, K. 2006. Ubiquitin ligases: cell-cycle control and cancer. *Nat Rev Cancer,* 6**,** 369-81.

NANAO, M. H., TCHERNIUK, S. O., CHROBOCZEK, J., DIDEBERG, O., DESSEN, A. & BALAKIREV, M. Y. 2004. Crystal structure of human otubain 2. *EMBO Rep,* 5**,** 783-8.

NANDI, A., YAN, L. J., JANA, C. K. & DAS, N. 2019. Role of Catalase in Oxidative Stress- and Age-Associated Degenerative Diseases. *Oxid Med Cell Longev,* 2019**,** 9613090.

NASUTION, O., SRINIVASA, K., KIM, M., KIM, Y. J., KIM, W., JEONG, W. & CHOI, W. 2008. Hydrogen peroxide induces hyphal differentiation in Candida albicans. *Eukaryot Cell,* 7**,** 2008-11.

NAYAK, A. & MÜLLER, S. 2014. SUMO-specific proteases/isopeptidases: SENPs and beyond. *Genome Biology,* 15**,** 422.

NAZIO, F., STRAPPAZZON, F., ANTONIOLI, M., BIELLI, P., CIANFANELLI, V., BORDI, M., GRETZMEIER, C., DENGJEL, J., PIACENTINI, M., FIMIA, G. M. & CECCONI, F. 2013. mTOR inhibits autophagy by controlling ULK1 ubiquitylation, self-association and function through AMBRA1 and TRAF6. *Nat Cell Biol,* 15**,** 406-16.

NETTO, L. E. & ANTUNES, F. 2016. The Roles of Peroxiredoxin and Thioredoxin in Hydrogen Peroxide Sensing and in Signal Transduction. *Mol Cells,* 39**,** 65-71.

NI, G., KONNO, H. & BARBER, G. N. 2017. Ubiquitination of STING at lysine 224 controls IRF3 activation. *Sci Immunol,* 2.

NI, X., KOU, W., GU, J., WEI, P., WU, X., PENG, H., TAO, J., YAN, W., YANG, X., LEBID, A., PARK, B. V., CHEN, Z., TIAN, Y., FU, J., NEWMAN, S., WANG, X., SHEN, H., LI, B., BLAZAR, B. R., WANG, X., BARBI, J., PAN, F. & LU, L. 2019. TRAF6 directs FOXP3 localization and facilitates regulatory T-cell function through K63-linked ubiquitination. *Embo j,* 38.

NIEDERKORN, M., ISHIKAWA, C., K, M. H., BARTRAM, J., STEPANCHICK, E., J, R. B., A, E. C.-C., BOLANOS, L. C., UIBLE, E., CHOI, K., WUNDERLICH, M., PERENTESIS, J. P., T, M. C., FILIPPI, M. D. & STARCZYNOWSKI, D. T. 2022. The deubiquitinase USP15 modulates cellular redox and is a therapeutic target in acute myeloid leukemia. *Leukemia,* 36**,** 438-451.

NIJMAN, S. M., LUNA-VARGAS, M. P., VELDS, A., BRUMMELKAMP, T. R., DIRAC, A. M., SIXMA, T. K. & BERNARDS, R. 2005. A genomic and functional inventory of deubiquitinating enzymes. *Cell,* 123**,** 773-86.

NIKKO, E. & ANDRE, B. 2007. Evidence for a direct role of the Doa4 deubiquitinating enzyme in protein sorting into the MVB pathway. *Traffic,* 8**,** 566-81.

NOBLE, S. M. & JOHNSON, A. D. 2005. Strains and strategies for large-scale gene deletion studies of the diploid human fungal pathogen Candida albicans. *Eukaryot Cell,* 4**,** 298-309.

NOH, Y. H., BAEK, J. Y., JEONG, W., RHEE, S. G. & CHANG, T. S. 2009. Sulfiredoxin Translocation into Mitochondria Plays a Crucial Role in Reducing Hyperoxidized Peroxiredoxin III. *J Biol Chem,* 284**,** 8470-7.

NOVATCHKOVA, M., TOMANOV, K., HOFMANN, K., STUIBLE, H. P. & BACHMAIR, A. 2012. Update on sumoylation: defining core components of the plant SUMO conjugation system by phylogenetic comparison. *New Phytol,* 195**,** 23-31.

OECKINGHAUS, A. & GHOSH, S. 2009. The NF-kappaB family of transcription factors and its regulation. *Cold Spring Harb Perspect Biol,* 1**,** a000034.

OGATA, F. T., BRANCO, V., VALE, F. F. & COPPO, L. 2021. Glutaredoxin: Discovery, redox defense and much more. *Redox Biology,* 43**,** 101975.

OGUNJIMI, A. A., BRIANT, D. J., PECE-BARBARA, N., LE ROY, C., DI GUGLIELMO, G. M., KAVSAK, P., RASMUSSEN, R. K., SEET, B. T., SICHERI, F. & WRANA, J. L. 2005. Regulation of Smurf2 ubiquitin ligase activity by anchoring the E2 to the HECT domain. *Mol Cell,* 19**,** 297-308.

OHDATE, T., KITA, K. & INOUE, Y. 2010. Kinetics and redox regulation of Gpx1, an atypical 2-Cys peroxiredoxin, in Saccharomyces cerevisiae. *FEMS Yeast Res,* 10**,** 787-90.

OLDENBURG, K. R., VO, K. T., MICHAELIS, S. & PADDON, C. 1997. Recombination-mediated PCR-directed plasmid construction in vivo in yeast. *Nucleic Acids Res,* 25**,** 451-2.

ORDUREAU, A., HEO, J. M., DUDA, D. M., PAULO, J. A., OLSZEWSKI, J. L., YANISHEVSKI, D., RINEHART, J., SCHULMAN, B. A. & HARPER, J. W. 2015. Defining roles of PARKIN and ubiquitin phosphorylation by PINK1 in mitochondrial quality control using a ubiquitin replacement strategy. *Proc Natl Acad Sci U S A,* 112**,** 6637-42.

ORDUREAU, A., SARRAF, S. A., DUDA, D. M., HEO, J. M., JEDRYCHOWSKI, M. P., SVIDERSKIY, V. O., OLSZEWSKI, J. L., KOERBER, J. T., XIE, T., BEAUSOLEIL, S. A., WELLS, J. A., GYGI, S. P., SCHULMAN, B. A. & HARPER, J. W. 2014. Quantitative proteomics reveal a feedforward mechanism for mitochondrial PARKIN translocation and ubiquitin chain synthesis. *Mol Cell,* 56**,** 360-75.

OSTAPENKO, D., BURTON, J. L. & SOLOMON, M. J. 2015. The Ubp15 deubiquitinase promotes timely entry into S phase in Saccharomyces cerevisiae. *Molecular biology of the cell,* 26**,** 2205-2216.

OZKAN, E., YU, H. & DEISENHOFER, J. 2005. Mechanistic insight into the allosteric activation of a ubiquitin-conjugating enzyme by RING-type ubiquitin ligases. *Proc Natl Acad Sci U S A,* 102**,** 18890-5.

OZKAYNAK, E., FINLEY, D., SOLOMON, M. J. & VARSHAVSKY, A. 1987. The yeast ubiquitin genes: a family of natural gene fusions. *Embo j,* 6**,** 1429-39.

PALM-ESPLING, M. E., NIEMIEC, M. S. & WITTUNG-STAFSHEDE, P. 2012. Role of metal in folding and stability of copper proteins in vitro. *Biochim Biophys Acta,* 1823**,** 1594-603.

PAN, X., WU, S., WEI, W., CHEN, Z., WU, Y. & GONG, K. 2022. Structural and Functional Basis of JAMM Deubiquitinating Enzymes in Disease. *Biomolecules,* 12.

PARK, M. H. & HONG, J. T. 2016. Roles of NF-κB in Cancer and Inflammatory Diseases and Their Therapeutic Approaches. *Cells,* 5.

PATTERSON, M. J., MCKENZIE, C. G., SMITH, D. A., DA SILVA DANTAS, A., SHERSTON, S., VEAL, E. A., MORGAN, B. A., MACCALLUM, D. M., ERWIG, L. P. & QUINN, J. 2013. Ybp1 and Gpx3 signaling

in Candida albicans govern hydrogen peroxide-induced oxidation of the Cap1 transcription factor and macrophage escape. *Antioxid Redox Signal,* 19**,** 2244-60.

PEDRAJAS, J. R., KOSMIDOU, E., MIRANDA-VIZUETE, A., GUSTAFSSON, J. A., WRIGHT, A. P. & SPYROU, G. 1999. Identification and functional characterization of a novel mitochondrial thioredoxin system in Saccharomyces cerevisiae. *J Biol Chem,* 274**,** 6366-73.

PENG, J., SCHWARTZ, D., ELIAS, J. E., THOREEN, C. C., CHENG, D., MARSISCHKY, G., ROELOFS, J., FINLEY, D. & GYGI, S. P. 2003. A proteomics approach to understanding protein ubiquitination. *Nat Biotechnol,* 21**,** 921-6.

PENNINCKX, M. J. 2002. An overview on glutathione in Saccharomyces versus non-conventional yeasts. *FEMS Yeast Res,* 2**,** 295-305.

PICHLMAIR, A., SCHULZ, O., TAN, C. P., NÄSLUND, T. I., LILJESTRÖM, P., WEBER, F. & REIS E SOUSA, C. 2006. RIG-I-mediated antiviral responses to single-stranded RNA bearing 5'-phosphates. *Science,* 314**,** 997-1001.

PICKART, C. M. 2001. Mechanisms underlying ubiquitination. *Annu Rev Biochem,* 70**,** 503-33.

PICKART, C. M. 2004. Back to the future with ubiquitin. *Cell,* 116**,** 181-90.

PICKART, C. M., KASPEREK, E. M., BEAL, R. & KIM, A. 1994. Substrate properties of site-specific mutant ubiquitin protein (G76A) reveal unexpected mechanistic features of ubiquitin-activating enzyme (E1). *J Biol Chem,* 269**,** 7115-23.

POOLE, L. B. 2007. The catalytic mechanism of peroxiredoxins. *Subcell Biochem,* 44**,** 61-81.

POPOVIC, D., VUCIC, D. & DIKIC, I. 2014. Ubiquitination in disease pathogenesis and treatment. *Nat Med,* 20**,** 1242-53.

PRUNEDA, J. N., DURKIN, C. H., GEURINK, P. P., OVAA, H., SANTHANAM, B., HOLDEN, D. W. & KOMANDER, D. 2016. The Molecular Basis for Ubiquitin and Ubiquitin-like Specificities in Bacterial Effector Proteases. *Mol Cell,* 63**,** 261-276.

QI, L., WU, X. C. & ZHENG, D. Q. 2019. Hydrogen peroxide, a potent inducer of global genomic instability. *Curr Genet,* 65**,** 913-917.

QUAN, S., SCHNEIDER, I., PAN, J., VON HACHT, A. & BARDWELL, J. C. A. 2007. The CXXC motif is more than a redox rheostat. *J Biol Chem,* 282**,** 28823-28833.

QUINN, J., FINDLAY, V. J., DAWSON, K., MILLAR, J. B., JONES, N., MORGAN, B. A. & TOONE, W. M. 2002. Distinct regulatory proteins control the graded transcriptional response to increasing H(2)O(2) levels in fission yeast Schizosaccharomyces pombe. *Mol Biol Cell,* 13**,** 805-16.

RAASI, S., VARADAN, R., FUSHMAN, D. & PICKART, C. M. 2005. Diverse polyubiquitin interaction properties of ubiquitin-associated domains. *Nat Struct Mol Biol,* 12**,** 708-14.

RAGU, S., DARDALHON, M., SHARMA, S., IRAQUI, I., BUHAGIAR-LABARCHÈDE, G., GRONDIN, V., KIENDA, G., VERNIS, L., CHANET, R., KOLODNER, R. D., HUANG, M. E. & FAYE, G. 2014. Loss of the thioredoxin reductase Trr1 suppresses the genomic instability of peroxiredoxin tsa1 mutants. *PLoS One,* 9**,** e108123.

RAND, J. D. & GRANT, C. M. 2006. The thioredoxin system protects ribosomes against stress-induced aggregation. *Mol Biol Cell,* 17**,** 387-401.

RATTANAWONG, K., KERDSOMBOON, K. & AUESUKAREE, C. 2015. Cu/Zn-superoxide dismutase and glutathione are involved in response to oxidative stress induced by protein denaturing effect of alachlor in Saccharomyces cerevisiae. *Free Radic Biol Med,* 89**,** 963-71.

RAVICHANDRAN, K. E., KADUHR, L., SKUPIEN-RABIAN, B., SHVETSOVA, E., SOKOŁOWSKI, M., KRUTYHOŁOWA, R. C., KWASNA, D., BRACHMANN, C., LIN, S., GUZMAN PEREZ, S., WILK, P., KÖSTERS, M., GRUDNIK, P., JANKOWSKA, U., LEIDEL, S. A., SCHAFFRATH, R. & GLATT, S. 2022. E2/E3-independent ubiquitin-like protein conjugation by Urm1 is directly coupled to cysteine persulfidation. *Embo j,* 41**,** e111318.

REGELMANN, J., SCHULE, T., JOSUPEIT, F. S., HORAK, J., ROSE, M., ENTIAN, K. D., THUMM, M. & WOLF, D. H. 2003. Catabolite degradation of fructose-1,6-bisphosphatase in the yeast Saccharomyces cerevisiae: a genome-wide screen identifies eight novel GID genes and indicates the existence of two degradation pathways. *Mol Biol Cell,* 14**,** 1652-63.

REICHERT, C. O., DE FREITAS, F. A., SAMPAIO-SILVA, J., ROKITA-ROSA, L., BARROS, P. L., LEVY, D. & BYDLOWSKI, S. P. 2020. Ferroptosis Mechanisms Involved in Neurodegenerative Diseases. *Int J Mol Sci,* 21.

REINDLE, A., BELICHENKO, I., BYLEBYL, G. R., CHEN, X. L., GANDHI, N. & JOHNSON, E. S. 2006. Multiple domains in Siz SUMO ligases contribute to substrate selectivity. *J Cell Sci,* 119**,** 4749-57.

REYES-TURCU, F. E., HORTON, J. R., MULLALLY, J. E., HEROUX, A., CHENG, X. & WILKINSON, K. D. 2006. The ubiquitin binding domain ZnF UBP recognizes the C-terminal diglycine motif of unanchored ubiquitin. *Cell,* 124**,** 1197-208.

REYES-TURCU, F. E., VENTII, K. H. & WILKINSON, K. D. 2009. Regulation and cellular roles of ubiquitin-specific deubiquitinating enzymes. *Annu Rev Biochem,* 78**,** 363-97.

RHEE, S. G. 2016. Overview on Peroxiredoxin. *Mol Cells,* 39**,** 1-5.

RHEE, S. G., CHAE, H. Z. & KIM, K. 2005. Peroxiredoxins: a historical overview and speculative preview of novel mechanisms and emerging concepts in cell signaling. *Free Radic Biol Med,* 38**,** 1543-52.

RICHARDSON, L. A., REED, B. J., CHARETTE, J. M., FREED, E. F., FREDRICKSON, E. K., LOCKE, M. N., BASERGA, S. J. & GARDNER, R. G. 2012. A conserved deubiquitinating enzyme controls cell growth by regulating RNA polymerase I stability. *Cell Rep,* 2**,** 372-85.

RICHTER, C., PARK, J. W. & AMES, B. N. 1988. Normal oxidative damage to mitochondrial and nuclear DNA is extensive. *Proc Natl Acad Sci U S A,* 85**,** 6465-7.

ROBZYK, K. & KASSIR, Y. 1992. A simple and highly efficient procedure for rescuing autonomous plasmids from yeast. *Nucleic Acids Res,* 20**,** 3790.

ROBZYK, K., RECHT, J. & OSLEY, M. A. 2000. Rad6-dependent ubiquitination of histone H2B in yeast. *Science,* 287**,** 501-4.

RODRIGUES-POUSADA, C., DEVAUX, F., CAETANO, S. M., PIMENTEL, C., DA SILVA, S., CORDEIRO, A. C. & AMARAL, C. 2019. Yeast AP-1 like transcription factors (Yap) and stress response: a current overview. *Microb Cell,* 6**,** 267-285.

RODRÍGUEZ-MANZANEQUE, M. T., ROS, J., CABISCOL, E., SORRIBAS, A. & HERRERO, E. 1999. Grx5 glutaredoxin plays a central role in protection against protein oxidative damage in Saccharomyces cerevisiae. *Mol Cell Biol,* 19**,** 8180-90.

ROMO, J. A. & KUMAMOTO, C. A. 2020. On Commensalism of Candida. *J Fungi (Basel),* 6.

RONAU, J. A., BECKMANN, J. F. & HOCHSTRASSER, M. 2016. Substrate specificity of the ubiquitin and Ubl proteases. *Cell Res,* 26**,** 441-56.

ROSS, S. J., FINDLAY, V. J., MALAKASI, P. & MORGAN, B. A. 2000. Thioredoxin peroxidase is required for the transcriptional response to oxidative stress in budding yeast. *Molecular biology of the cell,* 11**,** 2631-2642.

ROSSIO, V., PAULO, J. A., CHICK, J., BRASHER, B., GYGI, S. P. & KING, R. W. 2021. Proteomics of broad deubiquitylase inhibition unmasks redundant enzyme function to reveal substrates and assess enzyme specificity. *Cell Chem Biol,* 28**,** 487-502.e5.

ROUAULT, T. A. & TONG, W. H. 2008. Iron-sulfur cluster biogenesis and human disease. *Trends Genet,* 24**,** 398-407.

RUDNICKA, A. & YAMAUCHI, Y. 2016. Ubiquitin in Influenza Virus Entry and Innate Immunity. *Viruses,* 8.

SANTOS, A. L., SINHA, S. & LINDNER, A. B. 2018. The Good, the Bad, and the Ugly of ROS: New Insights on Aging and Aging-Related Diseases from Eukaryotic and Prokaryotic Model Organisms. *Oxid Med Cell Longev,* 2018**,** 1941285.

SANZ-BARRIO, R., FERNÁNDEZ-SAN MILLÁN, A., CARBALLEDA, J., CORRAL-MARTÍNEZ, P., SEGUÍ-SIMARRO, J. M. & FARRAN, I. 2012. Chaperone-like properties of tobacco plastid thioredoxins f and m. *J Exp Bot,* 63**,** 365-79.

SAVILLE, S. P., LAZZELL, A. L., BRYANT, A. P., FRETZEN, A., MONREAL, A., SOLBERG, E. O., MONTEAGUDO, C., LOPEZ-RIBOT, J. L. & MILNE, G. T. 2006. Inhibition of filamentation can be used to treat disseminated candidiasis. *Antimicrob Agents Chemother,* 50**,** 3312-6.

SCHAEFER, J. B. & MORGAN, D. O. 2011. Protein-linked ubiquitin chain structure restricts activity of deubiquitinating enzymes. *J Biol Chem,* 286**,** 45186-96.
SCHIEBER, M. & CHANDEL, N. S. 2014. ROS function in redox signaling and oxidative stress. *Current biology : CB,* 24**,** R453-R462.
SCHIESTL, R. H. & GIETZ, R. D. 1989. High efficiency transformation of intact yeast cells using single stranded nucleic acids as a carrier. *Current Genetics,* 16**,** 339-346.
SCHMITZ, C., KINNER, A. & KOLLING, R. 2005. The deubiquitinating enzyme Ubp1 affects sorting of the ATP-binding cassette-transporter Ste6 in the endocytic pathway. *Mol Biol Cell,* 16**,** 1319-29.
SCHRÖDINGER 2015. The PyMOL Molecular Graphics System, Version 2.1, Schrödinger, LLC.
SCHULMAN, B. A. & HARPER, J. W. 2009. Ubiquitin-like protein activation by E1 enzymes: the apex for downstream signalling pathways. *Nat Rev Mol Cell Biol,* 10**,** 319-31.
SCHULTZ, L. W., CHIVERS, P. T. & RAINES, R. T. 1999. The CXXC motif: crystal structure of an active-site variant of Escherichia coli thioredoxin. *Acta Crystallogr D Biol Crystallogr,* 55**,** 1533-8.
SCHULZE, J. M., HENTRICH, T., NAKANISHI, S., GUPTA, A., EMBERLY, E., SHILATIFARD, A. & KOBOR, M. S. 2011. Splitting the task: Ubp8 and Ubp10 deubiquitinate different cellular pools of H2BK123. *Genes Dev,* 25**,** 2242-7.
SCHWEITZER, K., BOZKO, P. M., DUBIEL, W. & NAUMANN, M. 2007. CSN controls NF-kappaB by deubiquitinylation of IkappaBalpha. *Embo j,* 26**,** 1532-41.
SCHWOB, E., BÖHM, T., MENDENHALL, M. D. & NASMYTH, K. 1994. The B-type cyclin kinase inhibitor p40SIC1 controls the G1 to S transition in S. cerevisiae. *Cell,* 79**,** 233-44.
SCIALÒ, F., SRIRAM, A., FERNÁNDEZ-AYALA, D., GUBINA, N., LÕHMUS, M., NELSON, G., LOGAN, A., COOPER, H. M., NAVAS, P., ENRÍQUEZ, J. A., MURPHY, M. P. & SANZ, A. 2016. Mitochondrial ROS Produced via Reverse Electron Transport Extend Animal Lifespan. *Cell Metab,* 23**,** 725-34.
SEYFRIED, N. T., XU, P., DUONG, D. M., CHENG, D., HANFELT, J. & PENG, J. 2008. Systematic approach for validating the ubiquitinated proteome. *Anal Chem,* 80**,** 4161-9.
SHA, W., HU, F. & BU, S. 2020. Mitochondrial dysfunction and pancreatic islet β-cell failure (Review). *Exp Ther Med,* 20**,** 266.
SHAHANA, S., CHILDERS, D. S., BALLOU, E. R., BOHOVYCH, I., ODDS, F. C., GOW, N. A. & BROWN, A. J. 2014. New Clox Systems for rapid and efficient gene disruption in Candida albicans. *PLoS One,* 9**,** e100390.
SHANG, F. & TAYLOR, A. 2011. Ubiquitin-proteasome pathway and cellular responses to oxidative stress. *Free Radic Biol Med,* 51**,** 5-16.
SHI, Q. M., WANG, Y. M., ZHENG, X. D., LEE, R. T. & WANG, Y. 2007. Critical role of DNA checkpoints in mediating genotoxic-stress-induced filamentous growth in Candida albicans. *Mol Biol Cell,* 18**,** 815-26.
SHIKAMA, K. 2006. Nature of the FeO2 bonding in myoglobin and hemoglobin: A new molecular paradigm. *Prog Biophys Mol Biol,* 91**,** 83-162.
SHRESTHA, R. K., RONAU, J. A., DAVIES, C. W., GUENETTE, R. G., STRIETER, E. R., PAUL, L. N. & DAS, C. 2014. Insights into the mechanism of deubiquitination by JAMM deubiquitinases from cocrystal structures of the enzyme with the substrate and product. *Biochemistry,* 53**,** 3199-217.
SIEVERS, F., WILM, A., DINEEN, D., GIBSON, T. J., KARPLUS, K., LI, W., LOPEZ, R., MCWILLIAM, H., REMMERT, M., SÖDING, J., THOMPSON, J. D. & HIGGINS, D. G. 2011. Fast, scalable generation of high-quality protein multiple sequence alignments using Clustal Omega. *Mol Syst Biol,* 7**,** 539.
SILVA, G. M., FINLEY, D. & VOGEL, C. 2015. K63 polyubiquitination is a new modulator of the oxidative stress response. *Nat Struct Mol Biol,* 22**,** 116-23.
SIMÕES, T., SCHUSTER, R., DEN BRAVE, F. & ESCOBAR-HENRIQUES, M. 2018. Cdc48 regulates a deubiquitylase cascade critical for mitochondrial fusion. *Elife,* 7.

SIMÕES, V., CIZUBU, B. K., HARLEY, L., ZHOU, Y., PAJAK, J., SNYDER, N. A., BOUVETTE, J., BORGNIA, M. J., ARYA, G., BARTESAGHI, A. & SILVA, G. M. 2022. Redox-sensitive E2 Rad6 controls cellular response to oxidative stress via K63-linked ubiquitination of ribosomes. *Cell Rep,* 39**,** 110860.

SINGH, A. & XU, Y. J. 2016. The Cell Killing Mechanisms of Hydroxyurea. *Genes (Basel),* 7.

SINHA, R. P. & HÄDER, D. P. 2002. UV-induced DNA damage and repair: a review. *Photochem Photobiol Sci,* 1**,** 225-36.

SKAUG, B., CHEN, J., DU, F., HE, J., MA, A. & CHEN, Z. J. 2011. Direct, noncatalytic mechanism of IKK inhibition by A20. *Mol Cell,* 44**,** 559-71.

SKONECZNY, M. & RYTKA, J. 2000. Oxygen and haem regulate the synthesis of peroxisomal proteins: catalase A, acyl-CoA oxidase and Pex1p in the yeast Saccharomyces cerevisiae; the regulation of these proteins by oxygen is not mediated by haem. *Biochem J,* 350 Pt 1**,** 313-9.

SLAUCH, J. M. 2011. How does the oxidative burst of macrophages kill bacteria? Still an open question. *Mol Microbiol,* 80**,** 580-3.

STADTMAN, E. R. 2006. Protein oxidation and aging. *Free Radic Res,* 40**,** 1250-8.

STANKOVIC-VALENTIN, N., DRZEWICKA, K., KÖNIG, C., SCHIEBEL, E. & MELCHIOR, F. 2016. Redox regulation of SUMO enzymes is required for ATM activity and survival in oxidative stress. *The EMBO journal,* 35**,** 1312-1329.

STEFFENSEN, I. L., DIRVEN, H., COUDERQ, S., DAVID, A., D'CRUZ, S. C., FERNÁNDEZ, M. F., MUSTIELES, V., RODRÍGUEZ-CARRILLO, A. & HOFER, T. 2020. Bisphenols and Oxidative Stress Biomarkers-Associations Found in Human Studies, Evaluation of Methods Used, and Strengths and Weaknesses of the Biomarkers. *Int J Environ Res Public Health,* 17.

STEIN, A., RUGGIANO, A., CARVALHO, P. & RAPOPORT, T. A. 2014. Key steps in ERAD of luminal ER proteins reconstituted with purified components. *Cell,* 158**,** 1375-1388.

STEPHEN, D. W. & JAMIESON, D. J. 1996. Glutathione is an important antioxidant molecule in the yeast Saccharomyces cerevisiae. *FEMS Microbiol Lett,* 141**,** 207-12.

STEWART, M. D., RITTERHOFF, T., KLEVIT, R. E. & BRZOVIC, P. S. 2016. E2 enzymes: more than just middle men. *Cell research,* 26**,** 423-440.

STOHS, S. J. 1995. The role of free radicals in toxicity and disease. *J Basic Clin Physiol Pharmacol,* 6**,** 205-28.

STORER, A. C. & MENARD, R. 1994. Catalytic mechanism in papain family of cysteine peptidases. *Methods Enzymol,* 244**,** 486-500.

STORZ, P. 2005. Reactive oxygen species in tumor progression. *Front Biosci,* 10**,** 1881-96.

STREICH, F. C., JR. & LIMA, C. D. 2014. Structural and functional insights to ubiquitin-like protein conjugation. *Annu Rev Biophys,* 43**,** 357-79.

STURTZ, L. A., DIEKERT, K., JENSEN, L. T., LILL, R. & CULOTTA, V. C. 2001. A fraction of yeast Cu,Zn-superoxide dismutase and its metallochaperone, CCS, localize to the intermembrane space of mitochondria. A physiological role for SOD1 in guarding against mitochondrial oxidative damage. *J Biol Chem,* 276**,** 38084-9.

SUDBERY, P., GOW, N. & BERMAN, J. 2004. The distinct morphogenic states of Candida albicans. *Trends Microbiol,* 12**,** 317-24.

SUN, L. & CHEN, Z. J. 2004. The novel functions of ubiquitination in signaling. *Curr Opin Cell Biol,* 16**,** 119-26.

SUN, L., XING, Y., CHEN, X., ZHENG, Y., YANG, Y., NICHOLS, D. B., CLEMENTZ, M. A., BANACH, B. S., LI, K., BAKER, S. C. & CHEN, Z. 2012. Coronavirus papain-like proteases negatively regulate antiviral innate immune response through disruption of STING-mediated signaling. *PLoS One,* 7**,** e30802.

SURESH, B., LEE, J., KIM, K. S. & RAMAKRISHNA, S. 2016. The Importance of Ubiquitination and Deubiquitination in Cellular Reprogramming. *Stem Cells Int,* 2016**,** 6705927.

SUZUKI, T. & KAMIYA, H. 2016. Mutations induced by 8-hydroxyguanine (8-oxo-7,8-dihydroguanine), a representative oxidized base, in mammalian cells. *Genes and Environment,* 39**,** 2.

SUZUKI, T., MURAMATSU, A., SAITO, R., ISO, T., SHIBATA, T., KUWATA, K., KAWAGUCHI, S. I., IWAWAKI, T., ADACHI, S., SUDA, H., MORITA, M., UCHIDA, K., BAIRD, L. & YAMAMOTO, M. 2019. Molecular Mechanism of Cellular Oxidative Stress Sensing by Keap1. *Cell Rep,* 28**,** 746-758.e4.

SWAMINATHAN, S., AMERIK, A. Y. & HOCHSTRASSER, M. 1999. The Doa4 deubiquitinating enzyme is required for ubiquitin homeostasis in yeast. *Mol Biol Cell,* 10**,** 2583-94.

SWATEK, K. N. & KOMANDER, D. 2016. Ubiquitin modifications. *Cell Res,* 26**,** 399-422.

TAHARA, E. B., NAVARETE, F. D. & KOWALTOWSKI, A. J. 2009. Tissue-, substrate-, and site-specific characteristics of mitochondrial reactive oxygen species generation. *Free Radic Biol Med,* 46**,** 1283-97.

TAN, K., FEIZI, H., LUO, C., FAN, S. H., RAVASI, T. & IDEKER, T. G. 2008. A systems approach to delineate functions of paralogous transcription factors: role of the Yap family in the DNA damage response. *Proc Natl Acad Sci U S A,* 105**,** 2934-9.

TANAKA, T., IZAWA, S. & INOUE, Y. 2005. GPX2, encoding a phospholipid hydroperoxide glutathione peroxidase homologue, codes for an atypical 2-Cys peroxiredoxin in Saccharomyces cerevisiae. *J Biol Chem,* 280**,** 42078-87.

TANG, L., WANG, W., ZHOU, W., CHENG, K., YANG, Y., LIU, M., CHENG, K. & WANG, W. 2015. Three-pathway combination for glutathione biosynthesis in Saccharomyces cerevisiae. *Microb Cell Fact,* 14**,** 139.

TASCHDJIAN, C. L., BURCHALL, J. J. & KOZINN, P. J. 1960. Rapid identification of Candida albicans by filamentation on serum and serum substitutes. *AMA J Dis Child,* 99**,** 212-5.

TAYMAZ-NIKEREL, H., CANKORUR-CETINKAYA, A. & KIRDAR, B. 2016. Genome-Wide Transcriptional Response of Saccharomyces cerevisiae to Stress-Induced Perturbations. *Frontiers in bioengineering and biotechnology,* 4**,** 17-17.

THROWER, J. S., HOFFMAN, L., RECHSTEINER, M. & PICKART, C. M. 2000. Recognition of the polyubiquitin proteolytic signal. *Embo j,* 19**,** 94-102.

TIRICHEN, H., YAIGOUB, H., XU, W., WU, C., LI, R. & LI, Y. 2021. Mitochondrial Reactive Oxygen Species and Their Contribution in Chronic Kidney Disease Progression Through Oxidative Stress. *Front Physiol,* 12**,** 627837.

TOLEDANO, M. B., DELAUNAY-MOISAN, A., OUTTEN, C. E. & IGBARIA, A. 2013. Functions and cellular compartmentation of the thioredoxin and glutathione pathways in yeast. *Antioxid Redox Signal,* 18**,** 1699-711.

TRACZ, M. & BIALEK, W. 2021. Beyond K48 and K63: non-canonical protein ubiquitination. *Cellular & Molecular Biology Letters,* 26**,** 1.

TRACZYK, A., BILIŃSKI, T., LITWIŃSKA, J., SKONECZNY, M. & RYTKA, J. 1985. Catalase T deficient mutants of Saccharomyces cerevisiae. *Acta Microbiol Pol,* 34**,** 231-41.

TRAN, H. J., ALLEN, M. D., LOWE, J. & BYCROFT, M. 2003. Structure of the Jab1/MPN domain and its implications for proteasome function. *Biochemistry,* 42**,** 11460-5.

TROTTER, E. W. & GRANT, C. M. 2005. Overlapping roles of the cytoplasmic and mitochondrial redox regulatory systems in the yeast Saccharomyces cerevisiae. *Eukaryotic cell,* 4**,** 392-400.

URESHINO, R. P., ROCHA, K. K., LOPES, G. S., BINCOLETTO, C. & SMAILI, S. S. 2014. Calcium signaling alterations, oxidative stress, and autophagy in aging. *Antioxid Redox Signal,* 21**,** 123-37.

VAN DER VEEN, A. G. & PLOEGH, H. L. 2012. Ubiquitin-like proteins. *Annu Rev Biochem,* 81**,** 323-57.

VAN LOON, A. P., PESOLD-HURT, B. & SCHATZ, G. 1986. A yeast mutant lacking mitochondrial manganese-superoxide dismutase is hypersensitive to oxygen. *Proc Natl Acad Sci U S A,* 83**,** 3820-4.

VEAL, E. A., ROSS, S. J., MALAKASI, P., PEACOCK, E. & MORGAN, B. A. 2003. Ybp1 is required for the hydrogen peroxide-induced oxidation of the Yap1 transcription factor. *J Biol Chem,* 278**,** 30896-904.

VENTII, K. H. & WILKINSON, K. D. 2008. Protein partners of deubiquitinating enzymes. *Biochem J,* 414**,** 161-75.

VERDECIA, M. A., JOAZEIRO, C. A., WELLS, N. J., FERRER, J. L., BOWMAN, M. E., HUNTER, T. & NOEL, J. P. 2003. Conformational flexibility underlies ubiquitin ligation mediated by the WWP1 HECT domain E3 ligase. *Mol Cell,* 11**,** 249-59.

VON ZGLINICKI, T. 2000. Role of oxidative stress in telomere length regulation and replicative senescence. *Ann N Y Acad Sci,* 908**,** 99-110.

VOS, R. M., ALTREUTER, J., WHITE, E. A. & HOWLEY, P. M. 2009. The ubiquitin-specific peptidase USP15 regulates human papillomavirus type 16 E6 protein stability. *J Virol,* 83**,** 8885-92.

WADA, K. & KAMITANI, T. 2006. UnpEL/Usp4 is ubiquitinated by Ro52 and deubiquitinated by itself. *Biochem Biophys Res Commun,* 342**,** 253-8.

WANG, H., SCHOEBEL, S., SCHMITZ, F., DONG, H. & HEDFALK, K. 2020a. Characterization of aquaporin-driven hydrogen peroxide transport. *Biochimica et Biophysica Acta (BBA) - Biomembranes,* 1862**,** 183065.

WANG, Q., LIU, X., CUI, Y., TANG, Y., CHEN, W., LI, S., YU, H., PAN, Y. & WANG, C. 2014. The E3 ubiquitin ligase AMFR and INSIG1 bridge the activation of TBK1 kinase by modifying the adaptor STING. *Immunity,* 41**,** 919-33.

WANG, W., LI, M., PONNUSAMY, S., CHI, Y., XUE, J., FAHMY, B., FAN, M., MIRANDA-CARBONI, G. A., NARAYANAN, R., WU, J. & WU, Z. H. 2020b. ABL1-dependent OTULIN phosphorylation promotes genotoxic Wnt/β-catenin activation to enhance drug resistance in breast cancers. *Nat Commun,* 11**,** 3965.

WANG, X., HERR, R. A., CHUA, W. J., LYBARGER, L., WIERTZ, E. J. & HANSEN, T. H. 2007. Ubiquitination of serine, threonine, or lysine residues on the cytoplasmic tail can induce ERAD of MHC-I by viral E3 ligase mK3. *J Cell Biol,* 177**,** 613-24.

WANG, Y., MAROTTI, L. A., JR., LEE, M. J. & DOHLMAN, H. G. 2005. Differential regulation of G protein alpha subunit trafficking by mono- and polyubiquitination. *J Biol Chem,* 280**,** 284-91.

WANG, Y. & WANG, F. 2021. Post-Translational Modifications of Deubiquitinating Enzymes: Expanding the Ubiquitin Code. *Front Pharmacol,* 12**,** 685011.

WARD, S. J., GRATTON, H. E., INDRAYUDHA, P., MICHAVILA, C., MUKHOPADHYAY, R., MAURER, S. K., CAULTON, S. G., EMSLEY, J. & DREVENY, I. 2018. The structure of the deubiquitinase USP15 reveals a misaligned catalytic triad and an open ubiquitin-binding channel. *J Biol Chem,* 293**,** 17362-17374.

WARRIS, A. & BALLOU, E. R. 2019. Oxidative responses and fungal infection biology. *Seminars in Cell & Developmental Biology,* 89**,** 34-46.

WAUER, T., SWATEK, K. N., WAGSTAFF, J. L., GLADKOVA, C., PRUNEDA, J. N., MICHEL, M. A., GERSCH, M., JOHNSON, C. M., FREUND, S. M. & KOMANDER, D. 2015. Ubiquitin Ser65 phosphorylation affects ubiquitin structure, chain assembly and hydrolysis. *Embo j,* 34**,** 307-25.

WEE, S., GEYER, R. K., TODA, T. & WOLF, D. A. 2005. CSN facilitates Cullin–RING ubiquitin ligase function by counteracting autocatalytic adapter instability. *Nature Cell Biology,* 7**,** 387-391.

WENG, S. L., HUANG, K. Y., KAUNANG, F. J., HUANG, C. H., KAO, H. J., CHANG, T. H., WANG, H. Y., LU, J. J. & LEE, T. Y. 2017. Investigation and identification of protein carbonylation sites based on position-specific amino acid composition and physicochemical features. *BMC Bioinformatics,* 18**,** 66.

WENK, J., BRENNEISEN, P., WLASCHEK, M., POSWIG, A., BRIVIBA, K., OBERLEY, T. D. & SCHARFFETTER-KOCHANEK, K. 1999. Stable overexpression of manganese superoxide dismutase in mitochondria identifies hydrogen peroxide as a major oxidant in the AP-1-mediated induction of matrix-degrading metalloprotease-1. *J Biol Chem,* 274**,** 25869-76.

WENZEL, D. M., LISSOUNOV, A., BRZOVIC, P. S. & KLEVIT, R. E. 2011. UBCH7 reactivity profile reveals parkin and HHARI to be RING/HECT hybrids. *Nature,* 474**,** 105-108.

WERTZ, I. E., O'ROURKE, K. M., ZHOU, H., EBY, M., ARAVIND, L., SESHAGIRI, S., WU, P., WIESMANN, C., BAKER, R., BOONE, D. L., MA, A., KOONIN, E. V. & DIXIT, V. M. 2004. De-ubiquitination and ubiquitin ligase domains of A20 downregulate NF-kappaB signalling. *Nature,* 430**,** 694-9.

WHEELER, G. L., TROTTER, E. W., DAWES, I. W. & GRANT, C. M. 2003. Coupling of the transcriptional regulation of glutathione biosynthesis to the availability of glutathione and methionine via the Met4 and Yap1 transcription factors. *J Biol Chem,* 278**,** 49920-8.

WHITEWAY, M. & BACHEWICH, C. 2007. Morphogenesis in Candida albicans. *Annu Rev Microbiol,* 61**,** 529-53.

WHITTAKER, M. M. & WHITTAKER, J. W. 2012. Metallation state of human manganese superoxide dismutase expressed in Saccharomyces cerevisiae. *Arch Biochem Biophys,* 523**,** 191-7.

WIENER, R., DIBELLO, A. T., LOMBARDI, P. M., GUZZO, C. M., ZHANG, X., MATUNIS, M. J. & WOLBERGER, C. 2013. E2 ubiquitin-conjugating enzymes regulate the deubiquitinating activity of OTUB1. *Nat Struct Mol Biol,* 20**,** 1033-9.

WILKINSON, K. A. & HENLEY, J. M. 2010. Mechanisms, regulation and consequences of protein SUMOylation. *Biochem J,* 428**,** 133-45.

WILLEMS, A. R., SCHWAB, M. & TYERS, M. 2004. A hitchhiker's guide to the cullin ubiquitin ligases: SCF and its kin. *Biochim Biophys Acta,* 1695**,** 133-70.

WINTERBOURN, C. C. 1995. Toxicity of iron and hydrogen peroxide: the Fenton reaction. *Toxicol Lett,* 82-83**,** 969-74.

WOLTERS, N. & AMERIK, A. 2015. The N-terminal domains determine cellular localization and functions of the Doa4 and Ubp5 deubiquitinating enzymes. *Biochem Biophys Res Commun,* 467**,** 570-6.

WONG, C. M., SIU, K. L. & JIN, D. Y. 2004. Peroxiredoxin-null yeast cells are hypersensitive to oxidative stress and are genomically unstable. *J Biol Chem,* 279**,** 23207-13.

WONG, C. M., ZHOU, Y., NG, R. W., KUNG HF, H. F. & JIN, D. Y. 2002. Cooperation of yeast peroxiredoxins Tsa1p and Tsa2p in the cellular defense against oxidative and nitrosative stress. *J Biol Chem,* 277**,** 5385-94.

WOOD, M. J., ANDRADE, E. C. & STORZ, G. 2003. The redox domain of the Yap1p transcription factor contains two disulfide bonds. *Biochemistry,* 42**,** 11982-91.

XIONG, Y., UYS, J. D., TEW, K. D. & TOWNSEND, D. M. 2011. S-glutathionylation: from molecular mechanisms to health outcomes. *Antioxid Redox Signal,* 15**,** 233-70.

XU, P., DUONG, D. M., SEYFRIED, N. T., CHENG, D., XIE, Y., ROBERT, J., RUSH, J., HOCHSTRASSER, M., FINLEY, D. & PENG, J. 2009. Quantitative proteomics reveals the function of unconventional ubiquitin chains in proteasomal degradation. *Cell,* 137**,** 133-145.

XU, Z., LAM, L. S., LAM, L. H., CHAU, S. F., NG, T. B. & AU, S. W. 2008. Molecular basis of the redox regulation of SUMO proteases: a protective mechanism of intermolecular disulfide linkage against irreversible sulfhydryl oxidation. *Faseb j,* 22**,** 127-37.

YADAV, D. K., KUMAR, S., CHOI, E. H., CHAUDHARY, S. & KIM, M. H. 2019. Molecular dynamic simulations of oxidized skin lipid bilayer and permeability of reactive oxygen species. *Sci Rep,* 9**,** 4496.

YAMAMOTO, M., OKAMOTO, T., TAKEDA, K., SATO, S., SANJO, H., UEMATSU, S., SAITOH, T., YAMAMOTO, N., SAKURAI, H., ISHII, K. J., YAMAOKA, S., KAWAI, T., MATSUURA, Y., TAKEUCHI, O. & AKIRA, S. 2006a. Key function for the Ubc13 E2 ubiquitin-conjugating enzyme in immune receptor signaling. *Nat Immunol,* 7**,** 962-70.

YAMAMOTO, M., SATO, S., SAITOH, T., SAKURAI, H., UEMATSU, S., KAWAI, T., ISHII, K. J., TAKEUCHI, O. & AKIRA, S. 2006b. Cutting Edge: Pivotal function of Ubc13 in thymocyte TCR signaling. *J Immunol,* 177**,** 7520-4.

YAN, C., LEE, L. H. & DAVIS, L. I. 1998. Crm1p mediates regulated nuclear export of a yeast AP-1-like transcription factor. *The EMBO journal,* 17**,** 7416-7429.

YAU, R. & RAPE, M. 2016. The increasing complexity of the ubiquitin code. *Nature Cell Biology,* 18**,** 579-586.

YE, Y., AKUTSU, M., REYES-TURCU, F., ENCHEV, R. I., WILKINSON, K. D. & KOMANDER, D. 2011. Polyubiquitin binding and cross-reactivity in the USP domain deubiquitinase USP21. *EMBO Rep,* 12**,** 350-7.

YE, Y., SCHEEL, H., HOFMANN, K. & KOMANDER, D. 2009. Dissection of USP catalytic domains reveals five common insertion points. *Mol Biosyst,* 5**,** 1797-808.

YIN, Z., YANG, L., WU, F., FAN, J., XU, J., JIN, Y. & YANG, G. 2019. Reactive Oxygen Species-Mediated Cezanne Inactivation by Oxidation of its Catalytic Cysteine Residue in Hepatocellular Carcinoma. *Oncol Res,* 27**,** 1069-1077.

YOSHIDA, S., HONG, S., SUZUKI, T., NADA, S., MANNAN, A. M., WANG, J., OKADA, M., GUAN, K. L. & INOKI, K. 2011. Redox regulates mammalian target of rapamycin complex 1 (mTORC1) activity by modulating the TSC1/TSC2-Rheb GTPase pathway. *J Biol Chem,* 286**,** 32651-60.

YOUNUS, H. 2018. Therapeutic potentials of superoxide dismutase. *Int J Health Sci (Qassim),* 12**,** 88-93.

YUAN, J., LUO, K., ZHANG, L., CHEVILLE, J. C. & LOU, Z. 2010. USP10 regulates p53 localization and stability by deubiquitinating p53. *Cell,* 140**,** 384-96.

YUAN, W. C., LEE, Y. R., LIN, S. Y., CHANG, L. Y., TAN, Y. P., HUNG, C. C., KUO, J. C., LIU, C. H., LIN, M. Y., XU, M., CHEN, Z. J. & CHEN, R. H. 2014. K33-Linked Polyubiquitination of Coronin 7 by Cul3-KLHL20 Ubiquitin E3 Ligase Regulates Protein Trafficking. *Mol Cell,* 54**,** 586-600.

ZENG, C. & XIAO, W. 2022. Molecular cloning and functional characterization of UBC13 and MMS2 from Candida albicans. *Gene,* 816**,** 146163.

ZHANG, N., UPRITCHARD, J. E., HOLLAND, B. R., FENTON, L. E., FERGUSON, M. M., CANNON, R. D. & SCHMID, J. 2009. Distribution of mutations distinguishing the most prevalent disease-causing Candida albicans genotype from other genotypes. *Infect Genet Evol,* 9**,** 493-500.

ZHANG, X. S., WANG, T., LIN, X. W., DENLINGER, D. L. & XU, W. H. 2017. Reactive oxygen species extend insect life span using components of the insulin-signaling pathway. *Proc Natl Acad Sci U S A,* 114**,** E7832-e7840.

ZHOU, C., WEE, S., RHEE, E., NAUMANN, M., DUBIEL, W. & WOLF, D. A. 2003. Fission yeast COP9/signalosome suppresses cullin activity through recruitment of the deubiquitylating enzyme Ubp12p. *Mol Cell,* 11**,** 927-38.

ZHOU, X., LI, W., LIU, Y. & AMON, A. 2021. Cross-compartment signal propagation in the mitotic exit network. *Elife,* 10.

ZHU, H., SANTO, A. & LI, Y. 2012. The antioxidant enzyme peroxiredoxin and its protective role in neurological disorders. *Exp Biol Med (Maywood),* 237**,** 143-9.

ZONCU, R., EFEYAN, A. & SABATINI, D. M. 2011. mTOR: from growth signal integration to cancer, diabetes and ageing. *Nat Rev Mol Cell Biol,* 12**,** 21-35.

ZOU, Q., JIN, J., HU, H., LI, H. S., ROMANO, S., XIAO, Y., NAKAYA, M., ZHOU, X., CHENG, X., YANG, P., LOZANO, G., ZHU, C., WATOWICH, S. S., ULLRICH, S. E. & SUN, S. C. 2014. USP15 stabilizes MDM2 to mediate cancer-cell survival and inhibit antitumor T cell responses. *Nat Immunol,* 15**,** 562-70.